Control and Estimation Oriented Model Order Reduction for Linear and Nonlinear Systems

by

Richard B. Choroszucha

A dissertation submitted in partial fulfillment
of the requirements for the degree of
Doctor of Philosophy
(Naval Architecture and Marine Engineering)
in the University of Michigan
2017

Doctoral Committee:

Professor Jing Sun, Chair
Doctor Kenneth Roy Butts, Toyota Technical Center
Professor Ryan Michael Eustice
Professor Ilya Vladimir Kolmanovsky

Richard Bogdan Choroszucha

riboch@umich.edu

ORCID iD: 0000-0002-3637-0244

To all the educators and scientists that had a positive impact on my work.

Acknowledgements

I would like to thank Prof. Divakar Viswanath for his course on nonlinear ordinary differential equations. Prof. Viswanath answered my questions, provided insight, further references, and opportunities that led me to pursue a lifetime of research.

Next, a thank you is in order to the Flat Panel Imager Group in the Physics Division of the School of Medicine's Department of Radiation Oncology, particularly: Prof. Larry Antonuk, Dr. Youcef El-Mohri, Dr. Qihua Zhao, Martin Koniczek, John MacDonald, and Dr. Hao Jiang for the discussions, patience, and all the knowledge that was imparted.

On the Toyota-side of my work: Prashant Ramachandra, Masato Ehara, Jason Rodgers, Sandesh Kirolkar, Dominic Liao-McPherson, Dr. Kevin Zaseck, and Dr. Hayato Nakada. A massive thank you to Dr. Mike Huang for bailing me out on more than one occasion with his Simulink diesel airpath model and controller.

On the University-side of my research: the entirety of the Real-Time Adaptive Control Engineering Lab (RACELab) and visiting scholars, particularly: Macheng Shen, Jun Hou, Hao Wang, Kai Wu, Dr. Zeng (Connie) Qiu, Dr. David Reed, Dr. Caihao Weng, and Dr. Hyeongjun Park for reviewing my papers and sitting through my mind numbing, math-filled presentations.

Thank you to Prof. Huei Peng for the battery project, and Prof. Heath Hofmann and his lab for the electric machine models and experiments.

I am deeply indebted to each member of my committee for having such a profound impact on me professionally and academically. Prof. Ilya Kolmanovsky helped cultivate me, introduced me to Prof. Sun and Dr. Butts, and inspired me through our discussions. Prof. Ryan Eustice taught a Mobile Robotics course, giving me a robotics 'itch,' and led to a number of other professional opportunities. Dr. Ken Butts provided the initial problem

and project funding, recommended me to the Toyota Co-op program, showed a continued interest in my work, and provided many fruitful discussions. Finally, Prof. Jing Sun has my gratitude for her mentorship.

Contents

List of Figures

List of Tables

List of Algorithms

List of Appendices

List of Abbreviations

Abbreviation:	**Meaning**
ADI:	Alternating Direction Implicit
ALE:	Algebraic Lyapunov Equation
ARE:	Algebraic Riccati Equation
cALE:	Continuous Algebraic Lyapunov Equation
CARE:	Control ARE
CF-ADI:	Cholesky Factor ADI
dALE:	Discrete Algebraic Lyapunov Equation
DAP:	Diesel Airpath
DEIM:	Discrete Empirical Interpolated MOR
ECU:	Engine Control Unit
EG:	Empirical Gramian
EGR:	Exhaust Gas Recirculation
EKF:	Extended Kalman Filter
EM:	Electric Machine
eMPC:	Explicit MPC
ERSV:	Empirical Riccati Singular Value
EVV:	Eigenvalue/vector
EVV-LR-ADI:	Eigenvalue/vector LR-ADI
FARE:	Filter ARE
FEA:	Finite Element Analysis
GB:	Gigabyte
gcALE:	Generalized Continuous ALE
gdALE:	Generalized Discrete ALE
HJB:	Hamilton-Jacobi-Bellman
HSVs:	Hankel Singular Values
LBT:	Lyapunov Balanced Truncation
LDLT:	Lower/Diagonal/Lower Transpose
LG:	Linear Gramian
LQE:	Linear Quadratic Estimation
LQG:	Linear Quadratic Gaussian
LQGBT:	Linear Quadratic Gaussian Balanced Truncation
LQR:	Linear Quadratic Regulator
LMPC:	Linear MPC
LR-ADI:	Low-Rank ADI

Abbreviation:	**Meaning**
MHE:	Moving Horizon Estimator
MIMO:	Single Input, Single Output
MOR:	Model Order Reduction
MPC:	Model Predictive Control
NEDC:	New European Drive Cycle
NMPC:	Nonlinear MPC
ODE:	Ordinary Differential Equation
PDE:	Partial Differential Equation
POD:	Proper Orthogonal Decomposition
PWA:	Piecewise Affine
RAM:	Random Access Memory
RBT:	Riccati Balanced Truncation
ROOFMPC:	Reduced Order Output Feedback MPC
RPI:	Robust Positive Invariant
RSV:	Riccati Singular Value
SISO:	Single Input, Single Output
SQP:	Sequential Quadratic Programming
SVD:	Singular Value Decomposition
UADC:	Urban Assault Drive Cycle
VGT:	Variable Geometry Turbo

Abstract

Optimization based controls are advantageous in meeting stringent performance requirements and accommodating constraints. Although computers are becoming more powerful, solving optimization problems in real-time remains an obstacle because of associated computational complexity. Research efforts to address real-time optimization with limited computational power have intensified over the last decade, and one direction that has shown some success is model order reduction.

This dissertation contains a collection of results relating to open- and closed-loop reduction techniques for large scale unconstrained linear descriptor systems, constrained linear systems, and nonlinear systems.

For unconstrained linear descriptor systems, this dissertation develops novel gramian and Riccati solution approximation techniques. The gramian approximation is used for an open-loop reduction technique following that of balanced truncation proposed by (Moore, 1981) for ordinary linear systems and (Stykel, 2004) for linear descriptor systems. The Riccati solution is used to generalize the Linear Quadratic Gaussian balanced truncation (LQGBT) of (Verriest, 1981) and (Jonckheere and Silverman, 1983). These are applied to an electric machine model to reduce the number of states from >100000 to 8 while improving accuracy over the state-of-the-art modal truncation of (Zhou, 2015) for the purpose of condition monitoring. Furthermore, a link between unconstrained model predictive control (MPC) with a terminal penalty and LQG of a linear system is noted, suggesting an LQGBT reduced model as a natural model for reduced MPC design. The efficacy of such a reduced controller is demonstrated by the real-time control of a diesel airpath.

Model reduction generally introduces modeling errors, and controlling a constrained plant subject to modeling errors falls squarely into robust control. A standard assumption of

robust control is that inputs/states/outputs are constrained by convex sets, and these sets are "tightened" for robust constraint satisfaction. However, robust control is often overly conservative, and resulting control strategies cannot take advantage of the true admissible sets. A new reduction problem is proposed that considers the reduced order model accuracy and constraint conservativeness. A constant tube methodology for reduced order constrained MPC is presented, and the proposed reduced order model is found to decrease the constraint conservativeness of the reduced order MPC law compared to reduced order models obtained by gramian and LQG reductions.

For nonlinear systems, a reformulation of the empirical gramians of (Lall et al., 1999) and (Hahn et al., 2003) into simpler, yet more general forms is provided. The modified definitions are used in the balanced truncation of a nonlinear diesel airpath model, and the reduced order model is used to design a reduced MPC law for tracking control. Further exploiting the link between the gramian and Riccati solution for linear systems, the new empirical gramian formulation is extended to obtain empirical Riccati covariance matrices used for closed-loop model order reduction of a nonlinear system. Balanced truncation using the empirical Riccati covariance matrices is demonstrated to result in a closer-to-optimal nonlinear compensator than the previous balanced truncation techniques discussed in the dissertation.

Chapter 1

Introduction

Models of processes open up a variety of avenues for analysis, simulation, and control. However, given a process with fast responses and limited computational resources, accurate real-time simulation [1], condition monitoring [2], control, and/or estimation[1] [3] present several challenges.

The first challenge is computational complexity. To do simulation and condition monitoring of a process, a model is necessary; however, models of processes tend to be complex [1, 4] and cannot be used in real-time. Often, the loss of model accuracy is traded for decreased computational complexity. This brings about the next challenge: accuracy of the model. There are a variety of ways to perform this trade-off: reduced order modeling, model identification, and model order reduction, etc. [5].

Reduced order modeling has several connotations, for the purpose of distinction from model order reduction, it will be defined as the development of first principles models using simplifying assumptions that reduce the number of states. Model identification requires selecting a parametrization of the model, and identifying the parameters that minimize some objective function [6, 7, 8]. Then there is model order reduction, which starts with a high dimensional model, and systematically removes states to meet some objective [9, 10, 11, 12].

A general model reduction problem is to approximate a state-space model in descriptor

[1]Combined control and estimation will be referred to as a compensator.

form

$$\Sigma : \begin{cases} 0 &= F(\dot{x}, x, u), \\ y &= h(x, u), \end{cases} \tag{1.1}$$

with $u \in \mathbb{R}^m$, $x \in \mathbb{R}^n$, and $y \in \mathbb{R}^p$, by a lower order model

$$\Sigma_r : \begin{cases} 0 &= F_r(\dot{x}_r, x_r, u), \\ y_r &= h_r(x_r, u), \end{cases} \tag{1.2}$$

with $x_r \in \mathbb{R}^r$, with $r < n$, that achieves some objective and is obtained via a systematic procedure.

For many real-time applications (simulation, control, etc.), reduced order/reduced complexity models are the only implementable solution. In this dissertation, three forms of F will be addressed for the various applications:

1. continuous (discrete) ordinary linear systems: $F = \dot{x} - Ax - Bu$ ($F = x_{t+1} - Ax_t - Bu_t$), $h = Cx + Du$;

2. continuous linear descriptor systems: $F = E\dot{x} - Ax - Bu$, $h = Cx + Du$; and

3. continuous nonlinear systems: $F = \dot{x} - f(x, u)$.

While reduction techniques exist for many different types of systems and applications: linear time invariant [13], linear time varying [14], linear parameter-varying [15], nonlinear [16], only a brief review of techniques that are often used to reduce the selected forms are provided in the next section. The chapter is concluded with the contributions of this dissertation.

1.1 Review of Model Reduction and Research Gaps

While there are many possible ways to classify reduction algorithms, one pertinent classification for reduced compensator design is open- versus closed-loop model order reduction. Closed-loop techniques consider how the compensator interacts with the system, while open-loop techniques only consider the input-to-output behavior.

1.1.1 Model Order Reduction for Open- and Closed-Loop Linear Systems

The way that many reduction methods work is by obtaining a transformation that places the state space representation into a canonical form, and then removing states. One type of representation that appears often in the model reduction literature is the notion of a balanced representation. Balanced representations are state space representations that satisfy selected properties, e.g. Lyapunov balanced representation yield equal and diagonal solutions (with diagonal entries in decreasing order) to the dual algebraic Lyapunov equations [13]. Typical ways to remove the states are truncation (i.e., the neglecting of dynamics) and residualization (i.e., using singular perturbations to remove states while ensuring the DC-gain of the full and reduced models match [17]). Methods such as this are popular because they typically remove states that do not contribute much to the selected objective while retaining properties such as stability.

Linear systems have seen a wide variety of reduction techniques and the following are not an exhaustive list. On the open-loop side, there are: modal/eigenvalue truncation [18], Lyapunov balanced truncation [13], frequency weighted model reduction [19, 20, 21, 22], normalized co-prime factorization [23, 24], moment matching [25], optimal Hankel approximations [26], Karhunen-Loève (proper orthogonal decomposition (POD)) [27], etc.

In the case of Lyapunov balanced truncation, which is used later in the dissertation, the state space representation is put into the specified balanced form, and the $n - r$ states and dynamics are simply removed. The removed states correspond to states that do not pass much "energy" from the input-to-output, and hence result in small output errors for the same input.

Most open-loop reduction methods can be recast as controller reduction methods, but errors incurred by such approaches can destabilize the closed-loop model comprised of the model and reduced controller [9]. Instead, closed-loop model reduction may be employed to provide compensators that are more robust to the error between the full and reduced model. Examples of closed-loop reduction techniques include: H_∞/linear quadratic Gaussian balanced truncation (LQGBT) [3, 28, 29], closed-loop gramian balanced truncation

[30], frequency weighted model reduction [31], normalized co-prime factorization [32], etc. For closed-loop reduction techniques, typically states that do not contribute much to an associated cost function are removed.

Closed-loop model reduction are available only for limited control methods. Many new controller methodologies, such as model predictive control (MPC), do not have the corresponding closed-loop model reduction framework. MPC has become well known for its ability to optimally control multi-input, multi-output (MIMO) systems with constraints. However, few works have addressed MPC with reduced order models [33] or even reduced compensators with constraints. Some works have provided ways to address model-based control of constrained systems using reduced order models; however, to the author's knowledge, no work has been presented on how to obtain a reduced order model that simultaneously considers the compensator and constraints [34, 35, 36, 37, 38].

1.1.2 Model Order Reduction of Large Scale and Linear Descriptor Systems

It is often necessary to simplify models governed by partial differential equations (PDEs) to a system of differential equations. Using techniques such as finite element analysis, these systems often are provided in a large scale, but sparse descriptor system form. Given current commercial computing power and size of random access memory (RAM), large scale systems are presently defined to be greater than about 10000 states.

Despite the sparseness, model reduction techniques for linear systems often become intractable for models with high dimensional state spaces due to associated computational and storage complexity. The calculation involved in deriving transformations required by most of the standard model reduction methods are generally dense [11, 39, 40]. For example, to exactly calculate Lyapunov or Riccati solutions, storage complexity of $O(n^2)$ and computational complexity of $O(n^3)$ are required [39].

There are a variety of ways to address such complexities: POD, Krylov subspace methods, modal/eigenvalue truncation, and approximate balanced truncation. Reviews of Krylov subspace methods and POD for large scale systems may be found in [2, 11, 40]. However,

POD, Krylov methods, and modal truncation are all dependent upon the designer selected points/inputs/snapshots/modes, respectively, and can yield poor approximations outside the selected regime.

Approximate balanced truncation, however, seeks to provide a good reduced order model that captures all dominant characteristics. For the purpose of input-to-output accuracy, often used in the simulations of PDEs, a great deal of attention has been paid to approximate Lyapunov balanced truncation.

Approximate Lyapunov balanced truncation uses gramians and direct truncation. Instead of calculating a similarity transformation and its inverse, direct balanced truncation uses economic matrix factorizations of the gramian to yield left (submersion) and right (immersion) transformations that immediately yield a reduced order model [41, 42]. The economic matrix factorization limit the computational and storage complexity, but leave the challenging problem of calculating a gramian.

Restricting to the case of asymptotically stable systems (systems where $x \to 0$, if $u \to 0$), gramians are generally dense, symmetric, and positive definite. As such, there exist a variety of low-rank approximations. One common approximation is the low-rank matrix square root factor calculated by low-rank alternating direction implicit (LR-ADI) methods.

LR-ADI methods are iterative and work like a control problem: scalar shifts are selected to make the columns of a low-rank matrix square root factor iteration converge to 0, for excellent overviews, see [43, 44, 45]. Because LR-ADI methods are iterative, the accuracy of the low-rank matrix square root factors is strongly dependent on how fast the iteration converges. This opens many avenues for research, such as how to select shifts and/or keep the low-rank factor sufficiently small in RAM.

1.1.3 Model Order Reduction for Nonlinear Systems

Many nonlinear reduction techniques have been developed that exploit the structure of the nonlinear systems, the "strength" and type of the nonlinearity, and the objective of the reduction [15, 16, 46, 47, 48, 49, 50, 51, 52, 53, 54, 55].

Model reduction of affine input nonlinear systems has perhaps the most comprehensive theory [16, 56]. Define an affine input nonlinear system to be the system in local coordinates,

$f(x,u) = f_1(x) + g_1(x)u$, where $f_1 \in \mathbb{R}^n$, $g_1 \in \mathbb{R}^{n\times m}$ [57]. Using linear systems theory as a guide, the affine input nature often enables extensions of linear results to nonlinear systems [58, 59]. Open and closed-loop reduction techniques include: Lyapunov balancing, normalized co-prime factors/H_∞, and moment matching reduction [16, 25, 60, 61, 62, 63, 64, 65].

Despite such a wealth of mathematical results, two assumptions often restrict the applicability of these methods to academic examples: sufficiently smooth f_1 and g_1, and the existence of a smooth energy function (a solution to a nonlinear PDE), [66, 67]. Instead empirical/POD based methods often end up being used to define a transformation from an approximate gramian obtained using response data. Identical to linear systems, snapshots are used, a transformation is derived, and truncation is performed for a reduced order nonlinear model [27].

On one extreme end of the POD based methods is that of empirical gramians/covariance matrices [68]. POD uses snapshots of "nominal operation" of the model, to contrast this empirical gramians probe all directions of the state and input space to build up statistical information about the input-to-output characteristics [46, 69, 70]. The empirical gramians are used to define a balancing transformation for model order reduction. However, there has been no development of empirical gramians where the compensator is considered.

1.2 Contributions and Organization of the Dissertation

This dissertation is divided into two parts: model reduction for linear systems (Chapters 2 through 4) and nonlinear systems (Chapters 5 and 6). Then in Chapter 7 the work is recapped and open problems are presented. The specific contributions and organization are contained in the remaining sections of the chapter.

1.2.1 Chapter 2: Lyapunov Balanced Truncation of Large Scale Linear Descriptor Systems

Chapter 2 presents a suite of tools to aid in the calculation of low-rank matrix square roots by LR-ADI methods. The contributions of the chapter include the following:

1. Bilinear discretizations of descriptor systems are defined, and their eigenvalues/eigenvectors are employed in a novel way for LR-ADI shift selection.

2. An approximate up/downdate algorithm is proposed and a suite of tools are developed for:

   (a) parallelization of gramian approximations of MIMO systems by breaking the problem up into gramian "elements,"

   (b) condensing and restarting the low-rank matrix square root factor of the gramian elements, and

   (c) a posteriori weighting of the gramian elements.

3. Using approximate balanced truncation calculated from the proposed methods, reducing a combined electric machine model with >100000 states to just 8 states for the purpose of condition monitoring.

1.2.2 Chapter 3: Riccati Balanced Truncation of Linear Systems

This chapter contains the work of [71] as well as extensions to large scale systems, and experimental results. The contributions of Chapter 3 are:

1. A generalization of the Linear Quadratic Gaussian (LQG) balanced truncation of [3, 28, 29] to include direct feedthrough, control and output weights (including the cross terms, e.g. $y^\top Su$), and cross term/non-normalized noise for estimation.

2. Using the low-rank matrix square root approximation framework from Chapter 2 with a Newton-Kleinman iteration, low-rank matrix square root approximations of the Riccati

solutions are found, and used to perform approximate LQG balanced truncation of the combined electric machine model.

3. The infinite time linear quadratic regulator is closely related to unconstrained model predictive control with a linear quadratic cost and properly chosen terminal penalty. This relationship is exploited to yield a reduced order model suited for model predictive control design.

4. Efficacy of model order reduction with the generalized LQG balanced truncation method in different MPC frameworks is demonstrated on 8th order linear and nonlinear diesel engine airpath models, as well as an experimental diesel engine.

1.2.3 Chapter 4: Model Order Reduction for Constrained Linear MPC

In Chapter 4, obtaining a reduced order model for control/estimation of a constrained system is formulated as an optimization problem. The three main contributions of the chapter are:

1. A tracking result for reduced order output feedback robust model predictive control with a reduced order model obtained by residualization.

2. The definition of a set conservativeness function, and the formulation of a general model order reduction problem for constrained systems.

3. Using a selected control methodology and constraint conservativeness function, a model order reduction problem for constrained systems is formulated, a solution proposed, and a numerical example demonstrating efficacy of the proposed solution along with different facets of the problem.

1.2.4 Chapter 5: Empirical Gramian Balanced Truncation for Nonlinear Systems

Chapter 5 contains the work of [72], and delves into nonlinear model order reduction by balanced truncation using empirical gramians. The two contributions of this chapter are:

1. A modified definition of empirical gramians/covariance matrices that:
   (a) potentially decreases the number of experiments required, and
   (b) includes input and output weightings.
2. Using the modified definition, a 9 state diesel airpath model is reduced by balanced truncation and used to calculate a tracking reduced model predictive control law. Improvements over selected linear model reduction methods are demonstrated.

1.2.5 Chapter 6: Empirical Riccati Covariance Balanced Truncation for Nonlinear Control and Estimation

The work of [73] is presented in Chapter 6. The key contributions of the chapter are:

1. The development of the empirical Riccati covariance matrices.
2. The extension of closed-loop gramian reduction (a further generalization of LQG balanced truncation) to nonlinear systems using empirically obtained quantities.
3. Efficacy of the proposed approach to the MPC/extended Kalman filter compensation of a spatially discretized catalytic rod model.

Chapter 2

Model Order Reduction of Large Scale Descriptor Systems

Control and estimation of a plant governed by linear partial differential equations (PDEs, or distributed parameter systems) may be handled analytically for simple geometries and possibly even in real-time using closed-form solutions. However, for more complicated geometries, closed-form solutions may not exist and approximations of either the system or the solution must be used [74].

A popular technique to approximate a PDE is to use finite element analysis (FEA). FEA uses bases (or elements) to "spatially discretize" the PDE into a model comprised of n time dependent differential equations (a.k.a. a lumped parameter model) [75]. For an accurate approximation of the dynamics, a large number of differential equations/states ($n > 10000$) are often required [11], moreover, linear FEA often results in the linear descriptor systems representation

$$E\dot{x} = Ax + Bu. \tag{2.1}$$

When $E = I$, the identity, (2.1) is referred to as an ordinary linear system model [76].

Linear FEA models often lead to sparse matrices E and A. The sparseness of the matrices in (2.1) may be exploited to reduce computational complexity, and it is often the only way a system can be feasibly represented in the random access memory (RAM) of a computer and be quickly manipulated. Consider the case of a non-singular E, where both E and A

are sparse and fit in the RAM of a computer. Under these conditions, E is invertible, and $E^{-1}A$ is defined. However, $E^{-1}A$ is in general not sparse [76], and therefore may not be containable in a computer's RAM. Therefore, it is often desirable in design and evaluation to keep the system in the form of (2.1) to leverage numerical advantages.

Despite efficient sparse operations and solvers, one of the key limitations to using these linear FEA models for real-time simulation, condition monitoring, control, and/or estimation of a plant, is still the computational complexity. To meet the real-time requirement, a reduced order model is often pursued.

One of the first approaches for systematic model order reduction in the control literature is that of [13]. For ordinary linear systems, [13] exploits the notion of Lyapunov (or gramian) balanced representation, which ranks subspaces by an input-to-output energy, through Hankel Singular Values (HSVs). The subspaces associated with small HSVs do not contribute much to input-to-output energy, and may be neglected. Lyapunov balanced truncation (LBT) is performed by removing the subspaces and dynamics that correspond to small HSVs. To calculate the HSVs of the system and the similarity transformation to place the system into the balanced representation, gramians are required.

Gramians, however, are generally dense, require $O(n^3)$ operations to find, and cannot be reasonably computed for large n [39]. Gramians do exhibit exploitable properties, such as if the system is controllable (observable) the controllability (observability) gramian is positive semidefinite, meaning that the gramian can be represented by matrix square root factors [40], which can be used instead to define the balancing transformation [77].

While matrix square root factors are still dense factorizations, linear FEA problems have been known to exhibit rapid degeneration of the HSVs [78]. This means that for a given positive semi-definite or definite matrix, P, with a matrix square root factor $\tilde{K}_P$, there exists a K_P of rank $q \ll n$ such that $\tilde{K}_P\tilde{K}_P^\top \approx K_P K_P^\top$. K_P may be used to define an approximate balancing transformation for model order reduction [41, 43, 79]. This shifts the problem of obtaining a gramian to that of calculating an approximate low-rank matrix square root factor of a gramian.

There are several techniques and challenges to calculating a low-rank matrix square root factor of a gramian. Practical algorithms for calculating the low-rank matrix square root

factors use an iteration scheme [80]. Because a low-rank approximation is being found via an iteration, key problems to address are the accuracy and the rate of convergence. The rate of convergence dictates the computational and storage complexity as well as the accuracy [81].

In this chapter, the notion of bilinear discretizations of a descriptor system is developed. The eigenvalues/eigenvectors of the discretized models are used to develop a novel algorithm to find low-rank matrix square root factors of gramians for approximate model order reduction of non-singular E linear descriptor systems, with a note included on how to extend it to general descriptor systems with singular E. For large scale problems, the low-rank matrix square root factors may not converge fast enough in the case of limited RAM. Modifications to the singular value decomposition (SVD) update rule of [81] are proposed: a way to restart and condense the low-rank matrix square root calculation, up/downdate the low-rank matrix square root factors as information is added or removed, and a way to do a posteriori weighted LBT. The techniques are then demonstrated and compared on a variety of example systems, including a combined electric machine thermal conduction model with more than 100,000 states.

The chapter is organized as: Section 2.1 provides pertinent background on linear descriptor systems, gramians, low-rank matrix square root factors for gramian approximation, and approximate Lyapunov Balanced Truncation (LBT). Section 2.2 extends the concept of a bilinear discretization to descriptor systems and contains the novel algorithms to calculate low-rank matrix square root factors of the gramian. Section 2.3 discusses up/downdating, restarted low-rank approximations, and the exploitation of gramian linearity to provide a posteriori weighted low-rank matrix square root factors of gramians. Section 2.4 goes through the performance of the algorithms and presents an application to approximate model order reduction of large dense systems, and a sparse system given by the finite element model of an electric machine. Finally, Section 2.5 concludes the chapter with a recapitulation of the results.

2.1 Background

2.1.1 Descriptor Systems

Descriptor systems are a form of differential algebraic equation and for linear systems they are best characterized by the addition of a "mass" matrix, E, multiplying the derivative term of a system:

$$\Sigma : \begin{cases} E\dot{x} &= Ax + Bu, \\ y &= Cx + Du, \end{cases} \tag{2.2}$$

where $E,\ A \in \mathbb{R}^{n\times n}$, $B \in \mathbb{R}^{n\times m}$, $C \in \mathbb{R}^{p\times n}$, $D \in \mathbb{R}^{p\times m}$, and the natural assumption that $p,\ m \ll n$. The transfer function of Σ is given as

$$G(s) = C(sE - A)^{-1}B + D. \tag{2.3}$$

Descriptor systems, however, do require additional technical machinery for solutions when E is not the identity, and even more technical machinery when E is singular (i.e. $\det(E) = 0$) [82, 83]. If E is singular, but $\det(\lambda E - A) \neq 0$ for almost all $\lambda \in \mathbb{C}$, then it is said to be *regular*. If E is non-singular, $\lambda E - A$ is always regular.

Remark 2.1.1. *For the remainder of the work, it will be assumed that E is non-singular ($\det(E) \neq 0$), and hence regular, to avoid excessive technicalities. When they are known to exist, generalizations to the case of singular E will be noted.*

There are many notions of stability, controllability, stabilizability, observability, and detectability for descriptor systems. The interested reader is recommended to read [45] for a concise overview.

Of particular interest to this work is stability of the matrix pencil $\lambda E - A$, r-controllability, and r-observability. To aid in the definition of stability, the eigenvalues and eigenvectors of a matrix pencil are necessary:

Definition 2.1.1 (Eigenvalue/Eigenvector of a Matrix Pencil)**.** *For a matrix pencil $\lambda E - A$, the right and left eigenvalue (λ)/eigenvector (v), ($\lambda_{right}, v_{right}$) and ($\lambda_{left}, v_{left}$), solve the*

root finding problems

$$(\lambda_{right}E - A)v_{right} = 0, \tag{2.4a}$$

$$v_{left}^{\top}(\lambda_{left}E - A) = 0, \tag{2.4b}$$

where $v_{right},\ v_{left} \in \mathbb{C}^{n\times 1}$ *and are assumed to not be zero, and* $\lambda_{right},\ \lambda_{left} \in \mathbb{C}$.

This is also known as the generalized eigenvalue problem. Unless explicitly noted, only right eigenvalue/eigenvectors will be used in this dissertation.

For admissible initial conditions, stability dictates whether the homogeneous solutions ($u = 0$) of Σ converge to 0, as $t \to \infty$. Stability of descriptor systems may be defined using the eigenvalues of the pencil $\lambda E - A$:

Definition 2.1.2 (Stability)**.** *For a non-singular* E*, the matrix pencil is said to be stable if all the eigenvalues of* $\lambda E - A$ *exist on the open left half plane,* $\mathbb{C}_- = \{\lambda \in \mathbb{C} |\ Re\{\lambda\} < 0\}$.

Assume E and $E^{\top}$ have full rank, then r-controllability and r-observability are defined as:

Definition 2.1.3 (R-Controllable)**.** *A system is said to be r-controllable if*

$$\text{rank}([\lambda E - A, B]) = n$$

for all $\lambda \in \mathbb{C}$ *[45].*

R-observability is defined dual to r-controllability:

Definition 2.1.4 (R-Observable)**.** *A system is said to be r-observable if*

$$\text{rank}([\lambda E^{\top} - A^{\top}, C^{\top}]) = n$$

for all $\lambda \in \mathbb{C}$ *[45].*

When a system is stable, regular, r-controllable and r-observable, there exist symmetric positive definite matrices known as gramians [84], these provide one way to systematically reduce the order of Σ in the form of (2.2) from n to r states.

2.1.2 Gramians and Hankel Singular Values

In control theory, gramians have many uses. The so-called controllability and observability gramians may be used to determine controllability/observability, the controllable/unobservable subspaces, the energy transmitted from input-to-state and state-to-output, respectively, and Hankel singular values [26]. Two common ways to define gramians are through improper integrals for continuous systems and algebraic equations [42].

In continuous time, the controllability, P, and observability, Π, gramians are the solutions to generalized continuous algebraic Lyapunov equations (gcALEs)

$$APE^\top + EPA^\top + BB^\top = 0, \tag{2.5a}$$

$$A^\top \Pi E + E^\top \Pi A + C^\top C = 0. \tag{2.5b}$$

The Hankel singular values (HSVs) are given by the following definition.

Definition 2.1.5 (Hankel singular values)**.** *Given a system, Σ, and solutions to* (2.5a) *and* (2.5b)*, the Hankel singular values, σ_i, are defined as*

$$\sigma_i = \sqrt{\lambda_i(PE^\top \Pi E)}, \tag{2.6}$$

where λ_i denotes the i-th eigenvalue.

HSVs are associated with input-to-output properties of a system, and they are invariant under state space transformations. Further, they characterize the energy a subspace passes from input-to-output. Subspaces that contribute little to the input-to-output behavior, those corresponding to small HSVs, can be thought of as unimportant and removing them will have little or no impact [13, 26]. This gives rise to the concept of Lyapunov Balanced Truncation (LBT) for model order reduction.

2.1.3 Lyapunov Balanced Truncation of Descriptor Systems

LBT was popularized in the control literature by [13]. The original idea sought to match the impulse response of a high order model with that of a reduced order model, this naturally led to using gramians and Hankel singular values to define a balanced representation, which was then truncated.

To reveal what subspaces contribute little to the input-to-output behavior, the Lyapunov balanced representation is used.

Definition 2.1.6 (Balanced Representation)**.** *A representation is said to be internally balanced if the controllability and observability gramians are equal, diagonal, and comprised of the HSVs in descending order along the diagonal [13].*

Truncation, projection truncation, or Galerkin truncation is one of the easiest methods to remove states. Consider a general linear descriptor system (and its partitioning) defined by

$$\Sigma : (E, A, B, C, D) = \left(\begin{bmatrix} E_{11} & E_{12} \\ E_{21} & E_{22} \end{bmatrix}, \begin{bmatrix} A_{11} & A_{12} \\ A_{21} & A_{22} \end{bmatrix}, \begin{bmatrix} B_1 \\ B_2 \end{bmatrix}, \begin{bmatrix} C_1 & C_2 \end{bmatrix}, D \right) \tag{2.7}$$

where n is the order, and $E,\ A \in \mathbb{R}^{n\times n}$, $B \in \mathbb{R}^{n\times m}$, $C \in \mathbb{R}^{p\times n}$, and $D \in \mathbb{R}^{p\times m}$. The truncation of a model is obtained by removing any term with a 2 in its subscript, i.e.,

$$\Sigma : (E, A, B, C, D) \mapsto \Sigma_r : (E_{11}, A_{11}, B_1, C_1, D),$$

where r is the reduced order, and $E_{11},\ A_{11} \in \mathbb{R}^{r\times r}$, $B_1 \in \mathbb{R}^{r\times m}$, $C_1 \in \mathbb{R}^{p\times r}$, and $D_1 \in \mathbb{R}^{p\times m}$.

Typically, balanced truncation is performed with a single similarity transformation,

$$\mathscr{T} : (E, A, B, C, D) \to (\mathscr{T}^{-1}E\mathscr{T}, \mathscr{T}^{-1}A\mathscr{T}, \mathscr{T}^{-1}B, C\mathscr{T}, D);$$

however, for large scale systems $\mathscr{T}$ is generally dense and should not be explicitly formed or inverted. Instead Algorithm 2.1 provides the method of [42] to directly calculate left and right transformations for the balanced truncation of a descriptor system.

Algorithm 2.1 Lyapunov balanced truncation for descriptor systems.

1: **procedure** LBTDESCRIPTOR($\Sigma : (E, A, B, C, D), r$)

Require: $\lambda E - A$ stable.

2: Solve (2.5a) and (2.5b) for the generalized controllability, P, and observability gramian, Π, respectively.

3: Compute the full rank Cholesky factors $\tilde{K}_P$ and $\tilde{K}_\Pi$ of the gramians, such that $P = \tilde{K}_P \tilde{K}_P^\top$ and $\Pi = \tilde{K}_\Pi \tilde{K}_\Pi^\top$.

4: Perform the singular value decomposition

$$\tilde{K}_P^\top E \tilde{K}_\Pi = [U_1, U_2]\mathrm{diag}(\Sigma_1, \Sigma_2)[V_1, V_2]^\top,$$

where $[U_1, U_2]$ and $[V_1, V_2]$ have orthonormal columns, $\Sigma_1 = \mathrm{diag}(\sigma_1, \ldots, \sigma_r)$, $\Sigma_2 = \mathrm{diag}(\sigma_{r+1}, \ldots \sigma_n) > 0$.

5: Compute the left and right transformations

$$\mathscr{T}_L = \tilde{K}_\Pi U_1 \Sigma_1^{-1/2} \tag{2.8}$$

$$\mathscr{T}_R = \tilde{K}_P V_1 \Sigma_1^{-1/2}. \tag{2.9}$$

6: Apply $\mathscr{T}_L$ and $\mathscr{T}_R$ to obtain the truncation

$$\Sigma_r : \ (E_r, A_r, B_r, C_r, D_r) = (\mathscr{T}_L^\top E \mathscr{T}_R, \mathscr{T}_L^\top A \mathscr{T}_R, \mathscr{T}_L^\top B, C \mathscr{T}_R, D) \tag{2.10}$$

return $\Sigma_r : \ (E_r, A_r, B_r, C_r, D_r)$

7: **end procedure**

Remark 2.1.2. *Balancing transformations may also be defined for singular systems, the generalization can be found in [42, 45].*

Provided with transfer functions, G_c and $G_{r,c}$, of Σ and Σ_r, respectively, in continuous time, truncation ensures that $G_c(\infty) = G_{r,c}(\infty)$ (where the c subscript denotes continuous). The equality at infinite frequency ensures that the initial response matches arbitrarily well. However, for discrete time systems, no such relationship holds generally [12].

The descriptor system LBT of [42] enjoys the same "twice the sum of the tail" error bounds of [13]. Given the transfer functions of the full order system from (2.3), $G(s) = G_c(s)$, and the reduced order system

$$G_{r,c}(s) = C_r(sE_r - A_r)^{-1}B_r + D_r, \tag{2.11}$$

the H_∞ error between the full and reduced order model is

$$||G_c(s) - G_{r,c}(s)||_\infty = 2 \sum_{i=r+1}^{n} \sigma_i. \tag{2.12}$$

Algorithm 2.1 is challenging to execute for large scale systems: solving (2.5a) and (2.5b) are known to have $O(n^3)$ complexity using the standard generalized Bartels-Stewart method [39], and the solutions are generally dense (so storage is $O(n^2)$) [4, 80]. Additionally, the complexity and storage are multiplied by the number of matrix factorizations and transformations required to find a balancing transformation.

To get around the storage and computational limitation for large systems, a way to approximately compute $\mathscr{T}_L^\top$ and $\mathscr{T}_R$ is employed. These quantities are obtained using approximations of the gramians, and are found with low-rank alternating direction implicit (LR-ADI) methods [80].

2.1.4 Low-Rank Cholesky Factors and Approximate Lyapunov Balanced Truncation

To follow the common terminology of the literature, a matrix square root factor will be called a Cholesky factor, despite not being required to be lower triangular [45]. Further, for the rest of this chapter, focus will be placed on the solution, P, of the controllability gcALE, (2.5a). Using duality, the solution to the observability gcALE may be found using the same framework.

Several facts allowing accurate approximations of the solutions to (2.5a) and (2.5b) are noted as follows:

1. the eigenvalues of P tend to decay faster as the number of states increases [78];
2. the solutions to (2.5a) and (2.5b) for stable, r-controllable systems are symmetric, positive definite and unique [84]; and
3. a symmetric positive semidefinite matrix exhibits a non-unique Cholesky factor of the

form $P = \tilde{K}_P \tilde{K}_P^{\top 1}$.

The eigenvalue decay of P (and dual Π) leads to rapid HSV decay [78]. This gives rise to two expected results: a reduced order model of order $r \ll n$, recall small HSVs get truncated and rapid decay ensures an accurate approximation by (2.12); and P may be well approximated by $K_P K_P^\top$, where K_P has rank $q \ll n$. The other two facts are exploited by [43] to develop a computationally efficient algorithm for the calculation of low-rank Cholesky factors.

The low-rank Cholesky factors, generated by LR-ADI or Cholesky factor ADI (CF-ADI) [80], use a variation on the Smith iterator [85] called the cyclic Smith(l) iterator of [43]. The Smith iterator uses a sequence of bilinear matrix transformations, defined using a set of l shifts, $\{\tau_i\}_{i=0}^{l-1}$, and iterations to build a full rank solution (storage $O(n^2)$) to the controllability gcALE. The cyclic Smith(l) iterator, on the other hand, iterates a vector and appends it to the low-rank Cholesky factor; after q iterations, this would require storage $O(nmq)$. One issue identified with these methods is that if the iteration is slow to converge, then many columns could be necessary for an accurate approximation; however, if the iterations converge quickly, $mq \ll n$ and the low-rank Cholesky factor is more practical in terms of storage.

Algorithm 2.1 is modified to use the economic SVD [40], and the low-rank Cholesky factors are used in place of the full-rank Cholesky factors to generate $W\mathscr{T}_L^\top$ and $\mathscr{T}_R V$ directly. This becomes known as approximate LBT because an approximation of the full rank Cholesky factor is used.

Algorithm 2.2 provides the real cyclic Smith(l) iterator of [43] using the notation and generalization to non-singular descriptor systems of [45]. With the algorithm, there come three questions: what is the complexity, how should the shifts be generated, and is the resulting approximate balanced reduced order model stable?

[1]As examples: a real P exhibits a singular value decomposition $P = U\tilde{\Sigma}V^\top$, $U,\ V$ unitary, $\tilde{\Sigma}$ diagonal, with $V = U$, so $P = U\tilde{\Sigma}U^\top$, and therefore $\tilde{K}_P = U\tilde{\Sigma}^{1/2}$. When $\tilde{K}_P$ has the lower diagonal form, the decomposition is the classical Cholesky factorization [40].

Algorithm 2.2 Real Smith(l) iterator for low-rank Cholesky factors of the controllability gramian.

procedure SMITH(l)($E, A, B, \{\tau_i\}_{i=0}^{l-1}$)
Require: $\lambda E - A$ stable, $\tau_i \in \mathbb{R}_-$
  $W_0 = B$, $K = [\,]$, $k = 1$
  while $(||W_{k-1}^\top W_{k-1}||/||W_0^\top W_0|| > \varepsilon \; and \; k < k_{max})$ **do**
    $i = k \mod l$
    $\tilde{V}_k = (E + \tau_i A)^{-1} W_{k-1}$
    $W_k = W_{k-1} - 2\tau_i A \tilde{V}_k$
    $K = [K \; \sqrt{-2\tau_i}\tilde{V}_k]$
    $k = k + 1$
  end while
  return K
end procedure

It is seen that the computational complexity of all Smith iterator techniques are dependent upon how $(E + \tau_i A)^{-1}$ is handled [43]. For large systems, $(E + \tau_i A)^{-1}$ should never be explicitly formed, instead matrix factorizations or Gaussian elimination should be used. Depending on the properties of the pencil $E + \tau_i A$, the complexity could range from $O(n)$ to $O(n^3)$, potentially making LR-ADI more feasible than exact solutions found with the generalized Bartels-Stewart method [86].

The shifts, τ_i, determine the rate of convergence and hence the accuracy of the low-rank Cholesky factor, and they are calculated using one of two paradigms: static shifts or self generating shifts. For the optimal set of l static shifts, it is known that the minimax problem

$$\{\hat{\tau}_1, \ldots, \hat{\tau}_l\} = arg \min_{\tau_1,\ldots,\tau_l \in \mathbb{R}_-} \max_{t \in Sp(E,A)} \frac{|1 - \tau_1 t| \cdots |1 - \tau_l t|}{|1 + \tau_1 t| \cdots |1 + \tau_l t|}$$

must be solved, where $Sp(E, A)$ denotes the spectrum, or eigenvalues, of the matrix pencil $\lambda E - A$ [87]. However, this optimization requires knowledge of all the eigenvalues, potentially unattainable for large systems. Instead, it has been noted that replacing $Sp(E, A)$ with a small set of the largest and smallest in magnitude eigenvalues yields good results in practice [45], using these shifts and the Smith(l) iterator comprises sub-optimal LR-ADI.

Nevertheless, these eigenvalue approaches do not consider how the input matrix B interacts with the dynamics (E, A). To account for this, the self generating shifts are employed

by selecting τ_k on-the-fly instead of from a static set. Many techniques have been proposed, for an overview of popular shift selection strategies, see [44, Chapter 5].

Then there is the question of stability, unlike Lyapunov balanced truncation, a reduced order model obtained by approximate truncation is not guaranteed to be stable. However, it has been noted that in practice the approximate Lyapunov balanced truncation of a stable model will yield a stable reduced order model [80].

In the following sections, bilinear discretizations of descriptor systems will be built up and their eigenvalue/vector information will be exploited for a new way to calculate shifts online. Various algorithms will be developed to aid in the calculation of low-rank Cholesky factors of gramians; and demonstrations of speed and accuracy, as well as a reduced order model of an electric machine obtained using these methods will be provided and compared.

2.2 Bilinear Discretization of Descriptor Systems

In complex analysis, one definition of a single parameter bilinear (Möbius) transformation is [88]:

$$s = \alpha \frac{z-1}{z+1}. \tag{2.13}$$

For the purpose of discretization, the bilinear transformation maps the transfer function from continuous (s) to the discrete (z) domain by (2.13) with

$$\alpha = \frac{2}{T_s}, \tag{2.14}$$

where $T_s > 0$ is the sample time.

There are four classes of bilinear discretizations for linear systems, however, for ordinary linear systems, $\Sigma_O : (\tilde{A}, \tilde{B}, \tilde{C}, \tilde{D})$, two classes degenerate into one to yield three unique classes. The three classes of bilinear discretizations are differentiated by how the input and

output matrices are discretized [89, Lemma 7.2.1]:

$$\begin{aligned}
\tilde{A}_d &= (\alpha I_{n\times n} + \tilde{A})(\alpha I_{n\times n} - \tilde{A})^{-1}, && (2.15a)\\
\tilde{B}_d &= \eta_1(\alpha I_{n\times n} - \tilde{A})^{-1}\tilde{B}, && (2.15b)\\
\tilde{C}_d &= \eta_2 C(\alpha I_{n\times n} - \tilde{A})^{-1}, && (2.15c)\\
\tilde{D}_d &= \tilde{C}(\alpha I_{n\times n} - \tilde{A})^{-1}\tilde{B} + \tilde{D}, && (2.15d)
\end{aligned}$$

$$\begin{aligned}
\tilde{A}_d &= (\alpha I_{n\times n} + \tilde{A})(\alpha I_{n\times n} - \tilde{A})^{-1}, && (2.16a)\\
\tilde{B}_d &= \eta_1(\alpha I_{n\times n} - \tilde{A})^{-2}\tilde{B}, && (2.16b)\\
\tilde{C}_d &= \eta_2 C, && (2.16c)\\
\tilde{D}_d &= \tilde{C}(\alpha I_{n\times n} - \tilde{A})^{-1}\tilde{B} + \tilde{D}, && (2.16d)
\end{aligned}$$

$$\begin{aligned}
\tilde{A}_d &= (\alpha I_{n\times n} + \tilde{A})(\alpha I_{n\times n} - \tilde{A})^{-1}, && (2.17a)\\
\tilde{B}_d &= \eta_1\tilde{B}, && (2.17b)\\
\tilde{C}_d &= \eta_2 C(\alpha I_{n\times n} - \tilde{A})^{-2}, && (2.17c)\\
\tilde{D}_d &= \tilde{C}(\alpha I_{n\times n} - \tilde{A})^{-1}\tilde{B} + \tilde{D}, && (2.17d)
\end{aligned}$$

where $I_{n\times n}$ is the $n \times n$ identity matrix, and the product $\eta_1\eta_2 = 2\alpha$.

When the discretization of (2.15) is selected and $\eta_1 = \eta_2 = \sqrt{2\alpha}$, it is found that the solutions to the continuous and discrete controllability and observability ALEs are equal. That is, given Σ_O and its discretization, the solutions $\tilde{P}$ and $\tilde{P}_d$ of the continuous and discrete controllability ALEs are equal ($\tilde{P} = \tilde{P}_d$):

$$\begin{aligned}
\tilde{A}\tilde{P} + \tilde{P}\tilde{A}^\top + \tilde{B}\tilde{B}^\top &= 0, && (2.18a)\\
\tilde{A}_d\tilde{P}_d\tilde{A}_d^\top - \tilde{P}_d + \tilde{B}_d\tilde{B}_d^\top &= 0. && (2.18b)
\end{aligned}$$

Likewise, $\tilde{\Pi}$ and $\tilde{\Pi}_d$ are the solutions of

$$\tilde{A}^\top \tilde{\Pi} + \tilde{\Pi}\tilde{A} + \tilde{C}^\top \tilde{C} = 0, \tag{2.19a}$$

$$\tilde{A}_d^\top \tilde{\Pi}_d \tilde{A}_d - \tilde{\Pi}_d + \tilde{C}_d^\top \tilde{C}_d = 0, \tag{2.19b}$$

and are equal, i.e., $\tilde{\Pi} = \tilde{\Pi}_d$ [26].

Assuming an asymptotically stable Σ_O, there are two ways to obtain the controllability gramian: solve (2.18a) or calculate the integral of the product of matrix exponentials:

$$\tilde{P} = \int_0^\infty e^{\tilde{A}t} \tilde{B}\tilde{B}^\top e^{\tilde{A}^\top t} dt. \tag{2.20}$$

Whereas for the discrete time controllability gramian, (2.18b) gets solved, or an infinite sum is calculated:

$$\tilde{P}_d = \sum_{i=0}^{\infty} \tilde{A}_d^i \tilde{B}_d \tilde{B}_d^\top (\tilde{A}_d^i)^\top = \begin{bmatrix} \tilde{B}_d & \tilde{A}_d\tilde{B}_d & \tilde{A}_d^2\tilde{B}_d & \dots \end{bmatrix} \begin{bmatrix} \tilde{B}_d & \tilde{A}_d\tilde{B}_d & \tilde{A}_d^2\tilde{B}_d & \dots \end{bmatrix}^\top. \tag{2.21}$$

Each technique has its advantages and disadvantages, but for the purpose of low-rank Cholesky factors, it is seen that the discrete case already yields a Cholesky factor using the Krylov matrix $\tilde{K}_P = \begin{bmatrix} \tilde{B}_d & \tilde{A}_d\tilde{B}_d & \tilde{A}_d^2\tilde{B}_d & \dots \end{bmatrix}$, which can be truncated to be "low-rank."

For regular descriptor systems, however, it is found that different discretizations are necessary for equality of the continuous and discrete controllability and observability gramians. In Section 2.2.1 and 2.2.2, the discretizations that yield the equality of the continuous and discrete controllability and observability gramians are derived, respectively. These two discretizations are related back to the LR-ADI for calculating low-rank Cholesky factors, and in Section 2.2.3 eigenvalue/vector information of the discretizations are used to select shifts in a computationally efficient manner.

2.2.1 Control Sided Bilinear Discretization

Using the stability and regularity assumption, i.e. $\alpha E - A$ can be inverted, (2.13) is substituted into (2.3), to yield the transfer function:

$$\begin{aligned} G(z) &= G\left(\alpha\frac{z-1}{z+1}\right) = C\left(\alpha\frac{z-1}{z+1}E - A\right)^{-1}B + D, \\ &= (z+1)C((\alpha E - A)z - (\alpha E + A))^{-1}B + D. \end{aligned} \tag{2.22}$$

Defining

$$\begin{aligned} A_d &= (\alpha E - A)^{-1}(\alpha E + A), \\ B_d &= (\alpha E - A)^{-1}B, \end{aligned}$$

yields

$$G(z) = zC(zI_{n\times n} - A_d)^{-1}B_d + C(zI_{n\times n} - A_d)^{-1}B_d + D. \tag{2.23}$$

Note that

$$\begin{aligned} zC(zI_{n\times n} - A_d)^{-1}B_d &= C(zI_{n\times n} - A_d + A_d)(zI_{n\times n} - A_d)^{-1}B_d, \\ &= CA_d(zI_{n\times n} - A_d)^{-1}B_d + CB_d. \end{aligned}$$

Substituting the result for $zC(zI_{n\times n} - A_d)^{-1}B_d$ back into (2.23) results in

$$\begin{aligned} G(z) &= CA_d(zI_{n\times n} - A_d)^{-1}B_d + C(zI_{n\times n} - A_d)^{-1}B_d + (CB_d + D), \\ &= C(A_d + I_{n\times n})(zI_{n\times n} - A_d)^{-1}B_d + (CB_d + D). \end{aligned}$$

In this form, it is found that

$$\begin{aligned} C_d &= C(A_d + I_{n\times n}). \\ D_d &= CB_d + D, \end{aligned}$$

resulting in an ordinary discrete time system.

While the above derivation provides a class of bilinear discretization, the discrete controllability gramian found using (A_d, B_d) is a scalar multiple of the continuous controllability gramian found using (E, A, B). To make the discrete and continuous controllability gramians equal, the scalar multiple of 2α arising in C_d is distributed amongst the input and output

by $\sqrt{2\alpha}$ as in (2.24):

$$\begin{aligned} A_{dc} &= (\alpha E - A)^{-1}(\alpha E + A), && \text{(2.24a)} \\ B_{dc} &= \sqrt{2\alpha}(\alpha E - A)^{-1}B, && \text{(2.24b)} \\ C_{dc} &= \frac{1}{\sqrt{2\alpha}}C(A_d + I_{n\times n}) = \sqrt{2\alpha}C(\alpha E - A)^{-1}E, && \text{(2.24c)} \\ D_{dc} &= C(\alpha E - A)^{-1}B + D. && \text{(2.24d)} \end{aligned}$$

Theorem 2.2.1. *Given a non-singular, stable, r-controllable Σ, the continuous controllability gramian, P (that solves* (2.5a) *with (E, A, B)), and the discrete controllability gramian, P_d (that solves* (2.18b) *with (A_{dc}, B_{dc})), are equal, unique, and positive definite.*

Proof. See Appendix A.1.1 for the proof. □

Theorem 2.2.2. *Given a continuous time, regular descriptor system $\Sigma : (E, A, B, C, D)$ with eigenvalues $\lambda_{c,i}$ and corresponding right eigenvectors $V_{c,i}$ of the matrix pencil $\lambda E - A$, for $i = 1, \ldots, n$, the bilinear discretization $A_{dc} = (\alpha E - A)^{-1}(\alpha E + A)$ has eigenvalues*

$$\lambda_{dc,i} = \frac{\alpha + \lambda_{c,i}}{\alpha - \lambda_{c,i}}, \tag{2.25}$$

and eigenvectors

$$V_{dc,i} = V_{c,i}, \tag{2.26}$$

for all $\alpha \neq \lambda_{c,i}$.

Proof. See Appendix A.1.2 for the proof. □

2.2.2 Observer Sided Bilinear Discretization

As noted previously: for ordinary systems, only a single bilinear discretization is necessary to yield the equality of the continuous gramians and the respective discrete gramians. This is not the case for descriptor systems. Using the discretization given by (2.24a)-(2.24d), the

discrete observability ALE is:

$$A_{dc}^{\top}\Pi_d A_{dc} - \Pi_d + C_{dc}^{\top}C_{dc} = 0.$$

Substituting and factoring out $(\alpha E + A)$ and its transpose like in the proof of Theorem 2.2.1, it is found that

$$\begin{aligned}(\alpha E + A)^{\top}((\alpha E - A)^{-\top}\Pi_d(\alpha E - A)^{-1} - (\alpha E + A)^{-\top}\Pi_d(\alpha E + A)^{-1} \\ -2\alpha(\alpha E + A)^{-\top}E^{\top}(\alpha E - A)^{-\top}C^{\top}C(\alpha E - A)^{-1}E(\alpha E + A)^{-1})(\alpha E + A) = 0.\end{aligned}$$

Immediately, three problems arise: there are additional $E^{\top}$ and E on the $C^{\top}C$ term, the equation cannot be simplified into a known form, and Π_d cannot be shown to satisfy (2.5b). Therefore, a different discretization is required for equality of the observability gramians.

Following a similar derivation to that of the control sided bilinear discretization of a descriptor system, the observer sided bilinear discretization is found using $(\alpha E + A)(\alpha E - A)^{-1}$ in (2.22) and the transfer function of the dual system, $\Sigma^* : (E^{\top}, A^{\top}, C^{\top}, B^{\top}, D^{\top})$:

$$\begin{aligned} A_{do} &= (\alpha E + A)(\alpha E - A)^{-1}, && \text{(2.27a)} \\ B_{do} &= \frac{1}{\sqrt{2\alpha}}(A_d + I)B = \sqrt{2\alpha}E(\alpha E - A)^{-1}B, && \text{(2.27b)} \\ C_{do} &= \sqrt{2\alpha}C(\alpha E - A)^{-1}, && \text{(2.27c)} \\ D_{do} &= C(\alpha E - A)^{-1}B + D. && \text{(2.27d)} \end{aligned}$$

Remark 2.2.1. *When Σ is an ordinary system, i.e. $E = I_{n\times n}$, $A_{dc} = A_{do}$ and the control and observer sided discretizations are equal, resulting in three classes of bilinear discretization. However, for descriptor systems, $A_{dc} \neq A_{do}$ in general, meaning there are four classes of bilinear discretization. To find the remaining two classes, the same derivation technique is used with: 1) $A_{dc} = (\alpha E - A)^{-1}(\alpha E + A)$ and the dual system $\Sigma^* : (E^{\top}, A^{\top}, C^{\top}, B^{\top}, D^{\top})$, and 2) $A_{do} = (\alpha E + A)(\alpha E - A)^{-1}$ and Σ.*

Theorem 2.2.3. *Given a non-singular, stable, r-observable Σ, the continuous observability*

gramian, Π *(that solves* (2.5b) *with* (E, A, C)*), and the discrete observability gramian,* Π_d *(that solves* (2.19b) *with* (A_{do}, B_{do})*), are equal, unique, and positive definite.*

Proof. The proof follows that of Theorem 2.2.1, and can be found in Appendix A.1.1. □

Theorem 2.2.4. *Given a continuous time, regular descriptor system* $\Sigma : (E, A, B, C, D)$ *with eigenvalues* $\lambda_{c,i}$ *and corresponding right eigenvectors* $V_{c,i}$ *of the matrix pencil* $\lambda E - A$*, for* $i = 1, \ldots, n$*, the bilinear discretization* $A_{do} = (\alpha E + A)(\alpha E - A)^{-1}$ *has eigenvalues*

$$\lambda_{do,i} = \frac{\alpha + \lambda_{c,i}}{\alpha - \lambda_{c,i}}, \tag{2.28}$$

and eigenvectors

$$V_{do,i} = EV_{c,i}, \tag{2.29}$$

for all $\alpha \neq \lambda_{c,i}$*.*

Proof. See Appendix A.1.4 for the proof. □

Corollary 2.2.1. *The left eigenvalues/vectors of the control sided bilinear discretization,* A_{dc}*, are the right eigenvalues/vectors of the observer sided bilinear discretization, and vice-versa.*

Then there are the important systems properties of stability, controllability, and observability covered by Theorem 2.2.5.

Theorem 2.2.5. *If* $\Sigma : (E, A, B, C, D)$ *is stable, then the discrete systems given by* (2.24a)-(2.24d) *and* (2.27a)-(2.27d) *are stable. If* $\Sigma : (E, A, B, C, D)$ *is r-controllable (r-observable) then* $\Sigma_{dc} : (A_{dc}, B_{dc}, C_{dc}, D_{dc})$ *(*$\Sigma_{do} : (A_{do}, B_{do}, C_{do}, D_{do})$*) with the system matrices specified in* (2.24a)-(2.24d) *(*(2.27a)-(2.27d)*) is controllable (observable).*

Proof. See Appendix A.1.5 for the proof. □

Theorem 2 of [79] is used to connect LR-ADI and the calculation of the discrete gramians from a bilinearly discretized system through the column span of a Krylov matrix. While eigenvalues of the bilinearly discretized Σ have been well known [44], the eigenvectors of the discretizations open new avenues for determining shift selection and improve the approximation of P by $K_P K_P^\top$ using fewer iterations.

2.2.3 LR-ADI with Eigenvalue Information

There are two main paradigms for using the Smith(l) iterator: static shifts and self generating shifts. As noted in [44], precomputed sub-optimal LR-ADI shifts do not consider how B interacts with the dynamics, and may not accurately capture the dominant input-output behavior, which potentially inhibits convergence and requires more memory to store the low-rank Cholesky factor. As such, there has been a move towards self generating shifts. In the context of controls, self generating shifts are a nonlinear control problem to regulate W_k in Algorithm 2.2 through "input" τ_k, but such shifts can be expensive to compute on-the-fly for large problems. For a more in depth review, see [44, Chapter 5].

With the potential for slow convergence of static shifts or a high computational cost for self generating shifts, a middle ground is proposed: select a shift from a static set of shifts to meet some objective during an iteration in a computationally efficient manner, akin to input space discretization in dynamic programming [90] but without completely discretizing the space. Expanding upon sub-optimal LR-ADI, eigenvalue information will be used, but now in conjunction with the discrete eigenvectors of Theorem 2.2.2 and 2.2.4.

For large systems, the largest and smallest eigenvalue/vector information of matrix pencils are readily computable using Lanczos, Krylov, or Arnoldi iterations [91, Chapter 10]. This information may be used to guide the calculation of the low-rank Cholesky factor. To see how, the geometry of lines and sets mapped by the bilinear transform is crucial.

Fig. 2.1 shows how the bilinear transform of (2.13) maps the open left half plane to an open unit ball (green line separates the left and right half planes). This means that stable continuous eigenvalues get mapped to stable discrete eigenvalues. Consider Fig. 2.1(a) and continuous eigenvalues contained within the dashed lines, Fig. 2.1(b)-2.1(c) show the dependence of the discrete eigenvalue positions on α. Particularly, Fig. 2.1(b) shows how the real part of the continuous eigenvalues may be zeroed, and Fig. 2.1(c) shows how the spectal radius of the discrete eigenvalues can be minimized.

This dependence is employed to manipulate $(\alpha E - A)^{-1}$ (the $(E + \tau_k A)^{-1} W_{k-1}$ step of Algorithm 2.2) and mitigate the largest contributor of W_{k-1} to the next iteration.

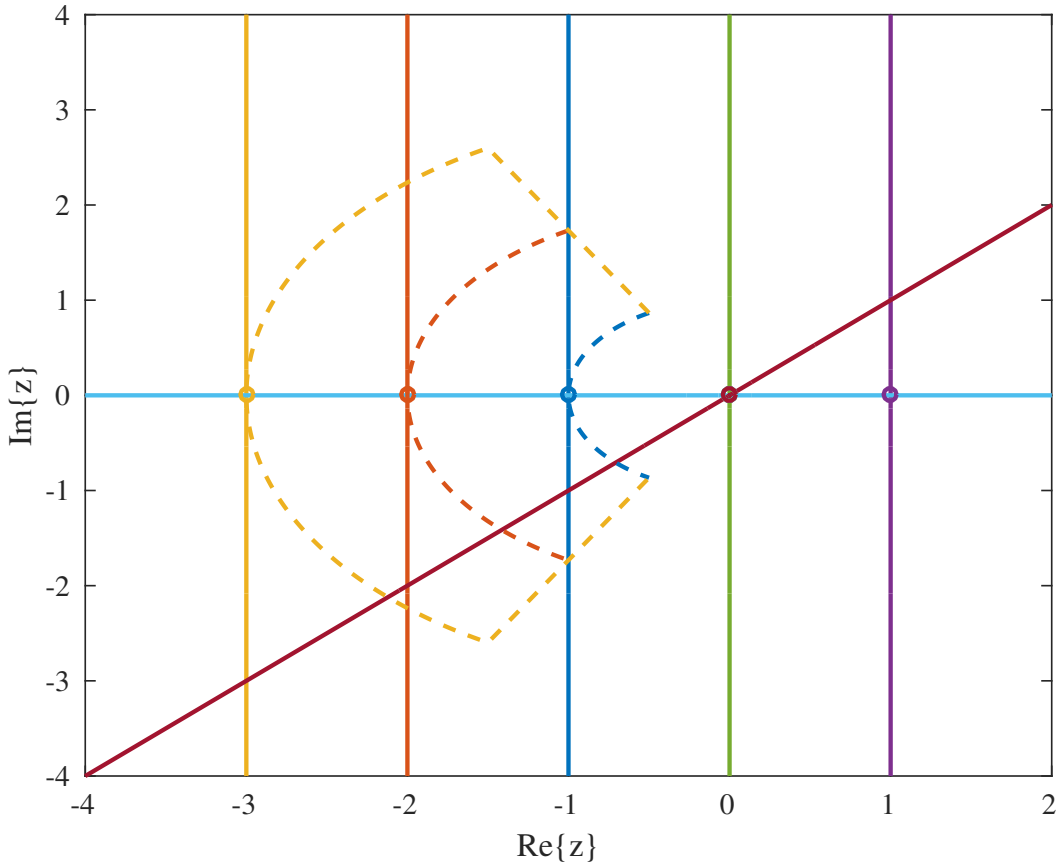

(a) Continuous eigenvalues bounded by dashed region.

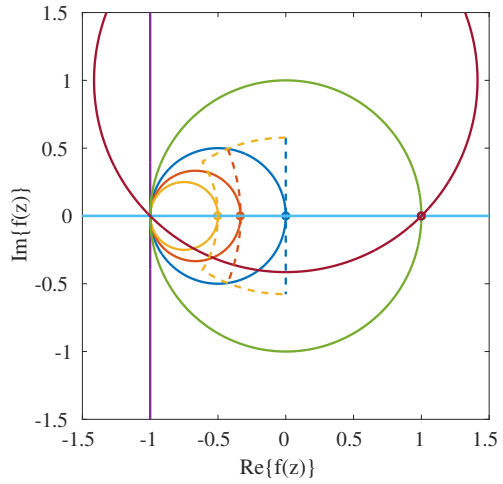

(b) Mobius transform of continuous eigenvalue bounds, $\alpha = 2$. Transforms the continuous eigenvalue of -1 to the discrete eigenvalue 0.

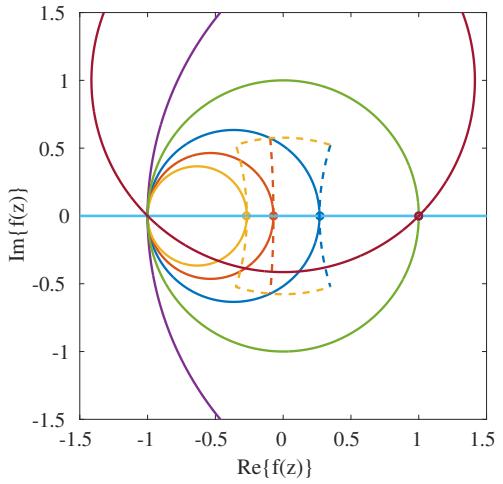

(c) Optimal Mobius transform of continuous eigenvalue bounds, $\alpha = \sqrt{3}$. Minimizes the discrete pencil's real spectral radius.

Figure 2.1: Bilinear transform mapping of sectors and lines to demonstrate the mapping of stable continuous eigenvalues to stable discrete eigenvalues.

Given any continuous time matrix pencil, $\lambda E - A$, select Λ_c to denote the set of all eigenvalues arranged according to their magnitude from largest to smallest:

$$\Lambda_c = \{\lambda_{c,1}, \lambda_{c,2}, \ldots, \lambda_{c,n-1}, \lambda_{c,n}\}.$$

Select Λ_c^s to be the s largest in magnitude, and s smallest in magnitude continuous eigenvalues from Λ_c,

$$\Lambda_c^s = \{ \underbrace{\lambda_{c,1}, \ldots, \lambda_{c,s}}_{\text{Largest Magnitude}} , \underbrace{\lambda_{c,n-s}, \ldots, \lambda_{c,n}}_{\text{Smallest Magnitude}}\}, \tag{2.30}$$

and let V_d^s contain the corresponding normalized discrete eigenvectors

$$V_d^s = \begin{bmatrix} V_{dc,1} & \ldots & V_{dc,s} & V_{dc,n-s} & V_{dc,n} \end{bmatrix}. \tag{2.31}$$

Using the notion that the discrete eigenvalue may be placed to remove the contribution of the eigenvector to the low-rank Cholesky factor, a new shift selection criteria is proposed.

Let W_{k-1} be approximated with the vectors of V_d

$$W_{k-1} \approx \xi_1 V_{dc,1} + \cdots + \xi_s V_{dc,s} + \xi_{n-s} V_{dc,n-s} + \ldots + \xi_n V_{dc,n} = \tilde{V}. \tag{2.32}$$

For Algorithm 2.2 to converge rapidly, $||(\alpha E - A)^{-1}(\alpha E + A)\tilde{V}||$ must be minimized at each step. While $\alpha > 0$ could be used to achieve this goal, for computational simplicity it is assumed that $(\alpha E - A)^{-1}(\alpha E + A)\tilde{V}$ is dominated by the eigenvector with the largest ξ_{k^*}. The bilinear discretization is then used to move λ_{d,k^*} so that it has zero real part, removing the largest contributor to W_k.

In the event that W_{k-1} is not well approximated by colspan(V_d^s), α is selected to minimize the spectral radius of the unknown (or uncalculated) discrete eigenvalues bounded by $|\lambda_{d,s}| \leq |\lambda_{d,unknown}| \leq |\lambda_{d,n-s}|$. A straightforward calculation reveals that

$$T_s^\star = \left| \sqrt{\frac{4}{\lambda_{c,s}\lambda_{c,n-s}}} \right|$$

minimizes the spectral radius of the unknown discrete eigenvalues by making $|\lambda_{d,s}| = |\lambda_{d,n-s}|$.

Algorithm 2.3 captures the proposed approach but returns the shift, $\tau = -\frac{1}{\alpha}$, for use in the Smith(l) iterator given in Algorithm 2.2, the eigenvalue/vector LR-ADI (EVV-LR-ADI) to calculate the low-rank Cholesky factor of the controllability gramian of Σ is given by Algorithm 2.4. In Algorithm 2.4, $K_{\{\gamma\}}$ denotes the γ-th column of K, and $K_{\{\gamma:\delta\}}$ denote the γ to δ columns of the low-rank Cholesky factor, K.

Algorithm 2.3 Eigenvalue placement/residual spectrum minimization shift selection.

procedure τ_SELECTION(W, V_d^s, Λ_c^s)
  if $||W^\top V_d^s|| > \varepsilon$ **then**
    $k^* = \arg \max_{k \in \{1,\ldots,s,n-s,\ldots,s\}} ||W^\top V_{d,k}||$
    $T_s^\star = \left| \frac{2}{\lambda_{c,k^*}} \right|$
  else
    $T_s^\star = \left| \sqrt{\frac{4}{\lambda_{c,s}\lambda_{c,n-s}}} \right|$
  end if
  $\tau = -\frac{T_s^\star}{2}$
  return τ
end procedure

Algorithm 2.4 EVV-LR-ADI low-rank controllability gramian Cholesky factor.

procedure EVVLRADI$(E, A, B, V_d^s, \Lambda_c^s, q)$
Require: $\lambda E - A$ stable, $B \in \mathbb{R}^{n \times 1}$
  $W_0 = B$, $K_{\{0\}} = [\,]$, $k = 1$
  while $(||W_{k-1}^\top W_{k-1}||/||W_0^\top W_0|| > \varepsilon$ *and* $k < q)$ **do**
    $\tau = \tau$_Selection$(W_{k-1}, V_d^s, \Lambda_c^s)$
    $\tilde{V}_k = (E + \tau A)^{-1} W_{k-1}$
    $W_k = W_{k-1} - 2\tau A \tilde{V}_k$
    $K = [K_{\{1:(k-1)\}}\ \sqrt{-2\tau}\tilde{V}_k]$
    $k = k + 1$
  end while
  return K
end procedure

Remark 2.2.2. *The requirement that $B \in \mathbb{R}^{n \times 1}$ comes from the linear dependence of the controllability gramian on $BB^\top$, and will be further highlighted in Section 2.3.3.*

Finally, Algorithm 2.4 may be extended in a variety of ways:

1. to find the observability gramian, the dual system may be used;

2. a generalized Cayley transformation and LR-ADI with complex shifts [44] can be used to increase the rate of convergence (such an approach is valuable when oscillatory dynamics dominate the state (i.e., the eigenvalues are almost pure imaginary)); and

3. using the work of [42], the EVV-LR-ADI may be extended to singular systems.

2.3 Exploiting Linearity and Numerical Linear Algebra

For large n and a slowly converging LR-ADI iteration, the number of columns in the low-rank Cholesky factor, K, may grow too large to fit in memory [81]. To keep $\tilde{K}$, the low-rank Cholesky factor, to at most q columns, both [81, 92] have proposed to recalculate the low-rank Cholesky factor by updating an SVD and truncating singular values below a specified threshold, or condensing the low-rank Cholesky factor.

In this section, a similar idea is proposed to address: condensing and restarting a slowly converging LR-ADI, parallelization, and a posteriori weighting.

2.3.1 Approximate Updating and Downdating

A common problem when dealing with matrix factorizations is modifying the factorization efficiently when new information is presented or ignored [91, 93, 94, 95]. For low-rank Cholesky factors, this can manifest in two ways: updating and downdating.

Assume the following are known: symmetric, positive semidefinite matrices X, $X_1 \in \mathbb{R}^{n\times n}$, low-rank Cholesky factors K_0 of X and K_1 of X_1, with column rank q_0 and q_1, respectively. The approximate update problem is to incorporate K_0, K_1 into a condensed low-rank Cholesky factor $\tilde{K}$ with smaller column rank $q \leq q_0 + q_1$ such that

$$X_u = X + X_1 = K_0 K_0^\top + K_1 K_1^\top \approx \tilde{K}\tilde{K}^\top. \tag{2.33}$$

Using the SVD, $K_0 K_0^\top + K_1 K_1^\top$ may be optimally approximated in the induced matrix 2-norm by $\tilde{K}\tilde{K}^\top$, with column rank q, using the low-rank SVD approximation [40].

Likewise, the downdate problem seeks to remove the additional information:

$$X_d = X - X_1 = K_0 K_0^\top - K_1 K_1^\top \approx \tilde{K}\tilde{K}^\top. \tag{2.34}$$

For the downdate problem, it must be assumed that $X_d \geq 0$ for a real Cholesky factor to exist. There are many up/downdating techniques available for various factorizations [96], yet most require full rank of K_0 for Cholesky factors [91], or for the existence of a hyperbolic rotation (for the case of the Hyperbolic SVD, which calculates the LDLT decomposition, or equivalent SVD, of a positive definite $AA^\top - BB^\top$) [97].

Algorithm 2.5 presents a technique that captures both multiple-rank updating and downdating of the low-rank Cholesky factor K_0 by K_1 to rank q (absent of thresholding). ν is the sign of the $K_1 K_1^\top$ term: positive for updating, negative for downdating.

Algorithm 2.5 Up/Downdated Low-Rank Cholesky Factorization

1: **procedure** UpDowndatedLRCholesky(K_0,K_1,q,ν)

Require: $\nu \in \{1, -1\}$

2: Calculate the economic singular value decompositions (SVDs)

$$[U_0, \Sigma_0, V_0] = \text{svd}(K_0), \tag{2.35a}$$
$$[U_1, \Sigma_1, V_1] = \text{svd}(K_1) \tag{2.35b}$$

3: Combine U_0, U_1, Σ_0^2, and $\nu\Sigma_1^2$ to form portions of $X + \nu X_1 = K_0 K_0^\top + \nu K_1 K_1^\top$:

$$\begin{aligned}
&\left[\ U_0\Sigma_0V_0^\top \ \middle|\ \nu U_1\Sigma_1V_1^\top\ \right]\left[\ U_0\Sigma_0V_0^\top \ \middle|\ U_1\Sigma_1V_1^\top\ \right]^\top \\
&\quad= \begin{bmatrix} U_0^\top \\ U_1^\top \end{bmatrix}^\top \begin{bmatrix} \Sigma_0 & 0 \\ 0 & \nu\Sigma_1 \end{bmatrix} \begin{bmatrix} V_0^\top & 0 \\ 0 & V_1^\top \end{bmatrix} \begin{bmatrix} V_0 & 0 \\ 0 & V_1 \end{bmatrix} \begin{bmatrix} \Sigma_0 & 0 \\ 0 & \Sigma_1 \end{bmatrix} \begin{bmatrix} U_0^\top \\ U_1^\top \end{bmatrix} \\
&\quad= \begin{bmatrix} U_0 & U_1 \end{bmatrix} \begin{bmatrix} \Sigma_0^2 & 0 \\ 0 & \nu\Sigma_1^2 \end{bmatrix} \begin{bmatrix} U_0^\top \\ U_1^\top \end{bmatrix}
\end{aligned}$$

4: Calculate the economic QR factorization of $\begin{bmatrix} U_0 & U_1 \end{bmatrix}$:

$$[Q, R] = \text{qr}\left(\begin{bmatrix} U_0 & U_1 \end{bmatrix}\right). \tag{2.36}$$

5: Calculate the SVD of $R(\Sigma_0^2 \oplus \nu\Sigma_1^2)R^\top$ to expose the singular values as well as the economic SVD of $X + \nu X_1 = (QU)\Sigma^2(QV)^\top$:

$$\begin{bmatrix} U, \Sigma^2, V \end{bmatrix} = \text{svd}\left(R \begin{bmatrix} \Sigma_0^2 & 0 \\ 0 & \nu\Sigma_1^2 \end{bmatrix} R^\top\right). \tag{2.37}$$

6: Form rank q approximations

$$Z = QU \begin{bmatrix} I_{q\times q} & 0 \end{bmatrix}^\top, \tag{2.38a}$$
$$\Sigma_q = \begin{bmatrix} I_{q\times q} & 0 \end{bmatrix} \Sigma \begin{bmatrix} I_{q\times q} & 0 \end{bmatrix}^\top. \tag{2.38b}$$

7: $\tilde{K} \leftarrow Z\Sigma_q$

return $\tilde{K}$

8: **end procedure**

Remark 2.3.1. *For repeated applications of Algorithm 2.5, it would be more efficient to return Z, Σ_q and accept it in place of K_0 at each iteration to avoid redundant calculations of* (2.35a).

Remark 2.3.2. *Algorithm 2.5 is non-associative in general. To check computationally, take three low-rank Cholesky factors of appropriate size: K_0, K_1, K_2, with minimum rank q_{min}, select q such that $0 < q < q_{min}$, and let $K_0 \star K_1 = UpDowndatedLRCholesky(K_0, K_1, q, 1)$.*

Perform $K_0 \star (K_1 \star K_2)$ *and* $(K_0 \star K_1) \star K_2$*, and in general* $K_0 \star (K_1 \star K_2) \neq (K_0 \star K_1) \star K_2$*.*

Remark 2.3.3. *In Algorithm 2.5, it is assumed that* $X + \nu X_1 \geq 0$*, which would result in* $U = V$ *[40]. However, when downdating is performed* ($\nu = -1$) *on* K_0 *that does not have full column rank, the colspan*(K_1)$\not\subseteq$*colspan*(K_0)*, resulting in an indefinite* $X + \nu X_1$ *and* $U \neq V$*. Nevertheless, caution only need be exercised in practice when* $U \begin{bmatrix} I_{r\times r} & 0 \end{bmatrix}^\top \neq V \begin{bmatrix} I_{r\times r} & 0 \end{bmatrix}^\top$ *(when* $Z\Sigma_q$ *is not a low-rank Cholesky factor), where* $r \ll q$ *is the reduced order. There are at least two ways to handle this seemingly rare case: decrease* r *(which may result in decreased reduced order model performance), or increase the rank of* K_0*.*

2.3.2 Condensing and Restarted Low-Rank Approximations

Algorithm 2.4 may be iterated by "popping" the last column of K_0 off, $K_{\{q\}}$, and feeding $W_0 = K_{\{q\}}$ back into Algorithm 2.4, restarting the calculation, to yield a K_1 and the approximation to the controllability gramian

$$P \approx K_0 K_0^\top + K_1 K_1^\top. \tag{2.39}$$

The approximation of $K_0 K_0^\top + K_1 K_1^\top$ by a single factor is cast as an update problem in the framework of Algorithm 2.5. Algorithm 2.6 provides how to restart and condense in the event that an LR-ADI iteration is slow to converge.

Algorithm 2.6 Condense and Restart

procedure CondenseAndRestart($E, A, B, q, V_d^s, \Lambda_c^s$)
  $W_0 = B$
  $\tilde{K} = 0_{n\times q}$
  while ($||W_0||/||B|| > \varepsilon$ and $c_0 <$Max Iteration) **do**
    $K = EVVLRADI(E, A, W_0, q, V_d^s, \Lambda_c^s)$
    $\tilde{K} = UpDowndatedLRCholesky(\tilde{K}, K_{\{1:q-1\}}, q, 1)$
    $W_0 = K_{\{q\}}$, $c_0 = c_0 + 1$
  end while
  return $\tilde{K}$
end procedure

The following theorem provides the error bounds of repeated application of Algorithm 2.6.

Theorem 2.3.1. *Assume updating ($\nu = 1$) of Algorithm 2.5 is repeatedly applied. Let $\sigma_{q+1,s}$ be the largest truncated singular value at the s-th application of Algorithm 2.5, and let $\tilde{K}_s$ be the result of the $s-1$-th application of Algorithm 2.6. Then*

$$\left\| \tilde{K}_s \tilde{K}_s^\top - \sum_{i=0}^{s} K_i K_i^\top \right\|_2 \leq \sum_{i=1}^{s} \sigma_{q+1,i}^2. \tag{2.40}$$

Proof. The proof may be found in Appendix A.1.6. □

2.3.3 Linearity of the Lyapunov Solution, Parallelization, and A Posteriori Weighting

Assume that $B \in \mathbb{R}^{n\times m}$, (E, A, B) is r-controllable, and $BB^\top$ in (2.18a) is weighted by a symmetric, positive definite Q, à la $BQB^\top$, such that $(E, A, BQ^{1/2})$ is also r-controllable. Then the gramians are linear with respect to $B_j B_j^\top$ and $B_i B_j^\top + B_j B_i^\top$ (the outer product of columns of B). For the generalized cALE (2.5a), the gramian may be separated into P_{jj} and P_{ij} that solve:

$$AP_{jj}E^\top + EP_{jj}A^\top + B_j B_j^\top = 0, \tag{2.41a}$$

$$AP_{ij}E^\top + EP_{ij}A^\top + B_i B_j^\top + B_j B_i^\top = 0. \tag{2.41b}$$

By appropriately weighting P_{jj} and P_{ij} with the elements of Q, and adding (2.41a) and (2.41b), the solution to a weighted generalized cALE (or the weighted controllability gramian) is found:

$$APE^\top + EPA^\top + BQB^\top = 0, \tag{2.42}$$

where $P > 0$ since $\lambda E - A$ is stable and regular, and $BQ^{1/2}$ is assumed to be r-controllable [84].

For the portion of P corresponding to the diagonal terms P_{jj} that solve (2.41a), the diagonally weighted part is obtained by repeated application of updating using Algorithm

2.5:

$$\sum_{j=1}^{m} P_{jj} = \sum_{j=1}^{m} K_{jj} K_{jj}^{\top}.$$

The cross terms $B_i B_j^{\top} + B_j B_i^{\top}$ pose a problem for the proposed LR-ADI framework because

$$B_i B_j^{\top} + B_j B_i^{\top} = \begin{bmatrix} B_i & B_j \end{bmatrix} \begin{bmatrix} B_j^{\top} \\ B_i^{\top} \end{bmatrix} = \begin{bmatrix} B_i & B_j \end{bmatrix} \begin{bmatrix} 0 & 1 \\ 1 & 0 \end{bmatrix} \begin{bmatrix} B_i & B_j \end{bmatrix}^{\top}, \tag{2.43}$$

has rank 2, is not positive semidefinite, and therefore P_{ij} is not guaranteed to be positive semidefinite. Nevertheless, this can be side stepped by using a polarization/parallelogram combination of B_i and B_j:

$$\bar{B}_{ij,1} = \frac{\sqrt{2}}{2}(B_i + B_j) \tag{2.44a}$$

$$\bar{B}_{ij,2} = \frac{\sqrt{2}}{2}(B_i - B_j). \tag{2.44b}$$

Assuming that $(E, A, \bar{B}_{ij,k})$, $k = 1, 2$, are r-controllable, then positive definite solutions $\bar{P}_{ij,k}$ corresponding to $\bar{B}_{ij,k}\bar{B}_{ij,k}^{\top}$ may be found. The solutions may then be combined as

$$P_{ij} = \bar{P}_{ij,1} - \bar{P}_{ij,2} \approx \bar{K}_{ij,1}\bar{K}_{ij,1}^{\top} - \bar{K}_{ij,2}\bar{K}_{ij,2}^{\top}, \tag{2.45}$$

which may be approximated using the downdating of $\bar{K}_{ij,1}$ and $\bar{K}_{ij,2}$ by Algorithm 2.5.

In total, the weighted controllability gramian may be separated into the computation of the m^2, single input/output, low-rank Cholesky factors: K_{jj}, $\bar{K}_{ij,1}$, and $\bar{K}_{ij,2}$, resulting in a massively parallel problem. Further, K_{jj}, $\bar{K}_{ij,1}$, and $\bar{K}_{ij,2}$ may be stored and weighted in an a posteriori fashion, resulting in the gramians needing to be calculated only once. The additional weightings open up a new design paradigm for Lyapunov balanced truncation of non-SISO systems: balanced truncation of constant weighted controllability and observability gramians which may result in a more accurate reduced order model [19].

Algorithm 2.7 provides a way to combine the individual computed low-rank Cholesky factors: K_{jj}, $\bar{K}_{ij,1}$, and $\bar{K}_{ij,2}$, given the Q weighting by updating the factors corresponding to the diagonal weights first, then up/downdating or down/updating the factors corresponding

to the cross term weights.

Algorithm 2.7 A posteriori weighting and combination of low-rank factors.

procedure APOSTERIORIWEIGHTING($\{K_{jj}, \bar{K}_{ij,1}, \bar{K}_{ij,2}\}$,$q$,$Q$)
  $\tilde{K} = 0_{n\times q}$
  for $j = 1, \ldots, m$ **do** ▷ Q Diagonal Elements
    $\tilde{K} = UpDowndatedLRCholesky(\tilde{K}, \sqrt{|Q_{jj}|}K_{jj}, q, \text{sgn}(Q_{jj}))$
  end for
  for $j = 1, \ldots, m$ **do** ▷ Q Cross Term Elements
    for $i = j + 1, \ldots, m$ **do**
      $\tilde{K} = UpDowndatedLRCholesky(\tilde{K}, \sqrt{|Q_{ij}|}\bar{K}_{ij,1}, q, \text{sgn}(Q_{ij}))$
      $\tilde{K} = UpDowndatedLRCholesky(\tilde{K}, \sqrt{|Q_{ij}|}\bar{K}_{ij,2}, q, -\text{sgn}(Q_{ij}))$
    end for
  end for
  return $\tilde{K}$
end procedure

In practice, Algorithm 2.7 performs well, but may not provide the "best" low-rank Cholesky factor of the gramian. For example, assume $Q = I_{m\times m}$, changing the diagonal loop of Algorithm 2.7 from $j = \{1, \ldots, m\}$ to $j = \{m, m-1, \ldots, 1\}$ may result in a better approximation and/or smaller error bounds from the fact that Algorithm 2.5 is non-associative (Remark 2.3.2) and Theorem 2.3.1. There are between $m!$ (m-factorial) and $\frac{m(m+1)}{2}!$ ways that $\tilde{K}$ can be calculated (Q diagonal and fully populated, respectively). The ordering of the up/downdating to obtain $\tilde{K}$ of Algorithm 2.7 to obtain the "best" low-rank Cholesky factor remains an open problem.

2.4 Examples

For all the following calculations and simulations, an Intel Xeon CPU E7-8860 with 12 GB RAM was used; all implementations were created using MATLAB's built in functions, and the $(E + \tau A)^{-1}W_{k-1}$ step is performed with MATLAB's "backslash" operator.

2.4.1 Evaluation of Speed and Accuracy Using Randomly Generated Systems

To capture the general behavior of the different low-rank Cholesky factorizations, random, dense, non-symmetric, asymptotically stable single-input, single-output (SISO) systems of varying size were used to calculate the controllability gramian, (2.18a). Algorithm 2.8 provides the snippet of MATLAB code used to generate the random systems.

For lower rank systems ($n < 1250$), MATLAB's `lyap` is used. `lyap` is an implementation of the generalized Bartels-Stewart algorithm [39], and has computational and storage complexity $O(n^3)$ and $O(n^2)$, respectively, making its use for high dimensional problems infeasible [4, 80].

Algorithm 2.8 MATLAB code snippet used to generate random systems.

```
state_num=[2 5 10 20 25 35 round(logspace(log10(50),log10(1250),100))];
for a1=1:numel(state_num)
    n=state_num(a1);      %State Dimension
    m=1;                  %Input Dimension

    rng(5);               %Use the same random seed each time
    A=sprandn(n,n,0.25);
    A=A/(max(svds(A))+1);          %Non-symmetric
    A=(A-A')/2-n*diag(rand(n,1));%Non-symmetric
    E=randn(n,n)+n/2*eye(n,n);
    B=randn(n,m);
end
```

Two aspects of low-rank Cholesky factor computation are of immediate consequence: the time it takes to calculate the factor and its accuracy. Through the lenses of complexity, it is expected that the LR-ADI approaches will be dominated by the $(E+\tau A)^{-1}W_{k-1}$ step, which results in a storage complexity of $O(nq)$, but whose computational complexity is subject to the solution method chosen. For example, if the structure of E and A can be exploited (e.g. banding, sparsity, symmetry), the complexity of the q backsolves could be as little as $O(nq)$ [98]. Therefore, approximations appear to be the only feasible way to calculate and store approximate solutions to gramians of large systems.

Fig. 2.2 shows the "wall time," t_w, for `lyap`, the sub-optimal ADI parameters defined

using the spectrum of $\lambda E - A$ [45], and the unweighted proposed EVV-LR-ADI for different sized systems (n), number of shifts or eigenvalues, and column rank of the approximation (q). The expected trend that the `lyap` time increases as $O(n^3)$ is seen, but that around $n = 500$ and $t_w = 2.5$ s, the approximations become cheaper to compute. Fig. 2.2 demonstrates that the approximation computation time increases at about $O(n^{1.7})$, much less than $O(n^3)$ of the Bartels-Stewart algorithm.

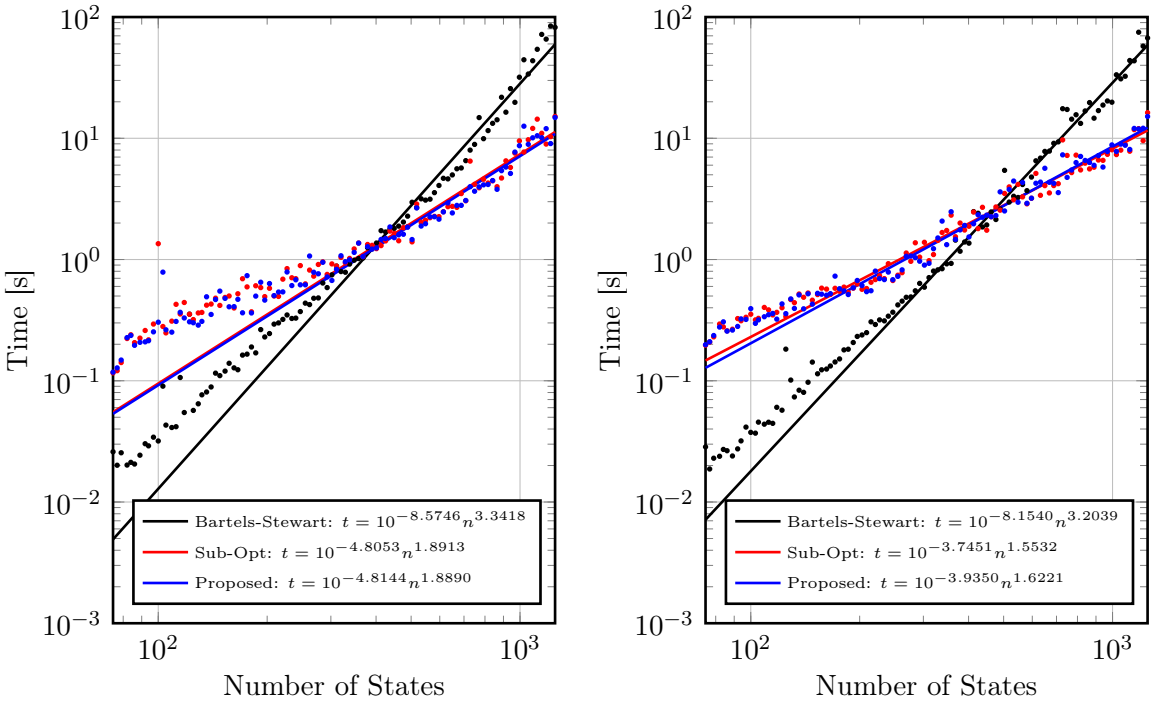

(a) 10 Shifts, 75 Columns

(b) 10 Shifts, 100 Columns

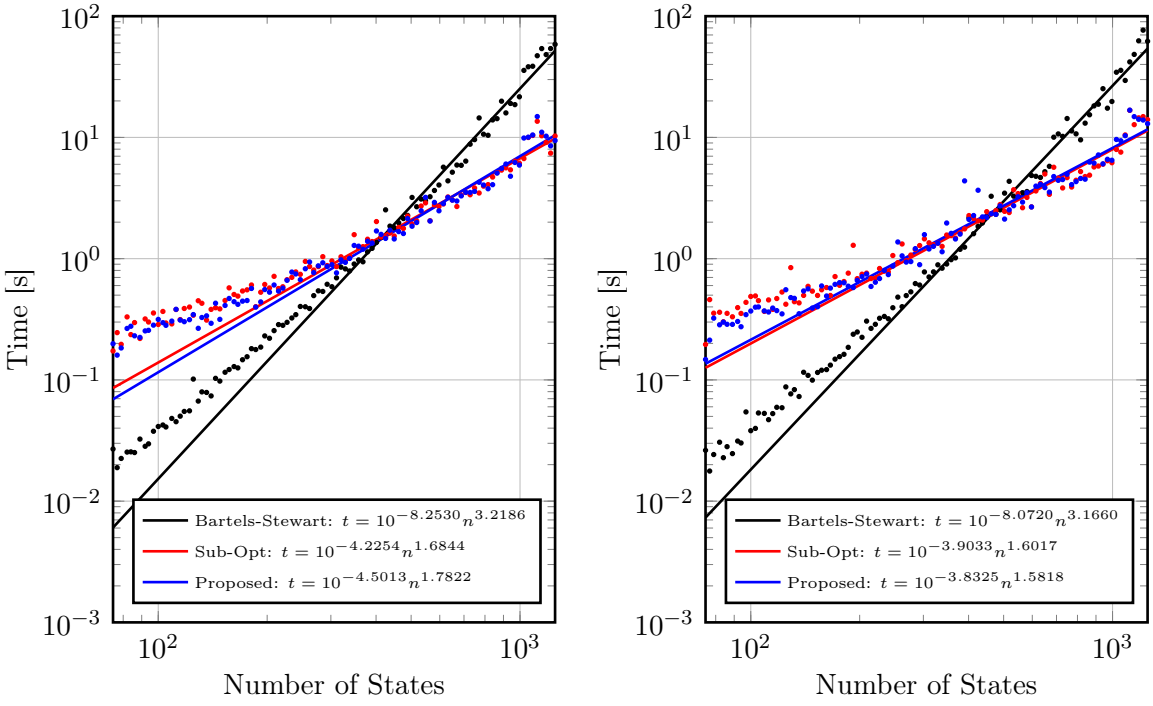

(c) 20 Shifts, 75 Columns

(d) 20 Shifts, 100 Columns

Figure 2.2: Wall time and log-regressions of the various methods for different number of shifts (or eigenvalues), columns, and number of states.

The selected measure of accuracy of the low-rank approximation is the Frobenius norm of the weighted controllability Lyapunov operator

$$\mathcal{L}_Q(P) = APE^\top + EPA^\top + BQB^\top, \tag{2.46}$$

because $||\mathcal{L}_Q(P)||_2 \leq ||\mathcal{L}_Q(P)||_F$, by Cauchy-Schwarz, and is less expensive to compute. The Frobenius norm is defined as

$$||\mathcal{L}_Q(P)||_F = \sqrt{\sum_{i=1}^{n}\sum_{j=1}^{n} |[\mathcal{L}_Q(P)]_{ij}|^2}, \tag{2.47}$$

where $[\cdot]_{ij}$ denotes the element in the i-th row and the j-th column.

Fig. 2.3 shows the accuracy in the Frobenius norm of $\mathcal{L}_I(P)$, where $I = 1$ and P is the solution given by `lyap`, the sub-optimal LR-ADI Cholesky factor, or the unweighted EVV-LR-ADI Cholesky factor.

Starting from 10 shifts and 75 columns of Fig. 2.3(a), and increasing the total number of columns to 100, Fig. 2.3(b), or increasing the number of shifts, Fig. 2.3(c), an improvement in accuracy of the approximate Cholesky factors are seen. However, as the number of states increase, the sub-optimal LR-ADI can grow inaccurate (suggesting that either more columns or shifts are necessary). Whereas, the proposed EVV-LR-ADI, while not being as accurate as the sub-optimal LR-ADI approximation for all number of states, overall retains accuracy better than MATLAB's `lyap` as columns or shifts are added and the sub-optimal LR-ADI as the order of the system increases. As shown in Fig. 2.3(d), for 20 shifts and 100 columns, EVV-LR-ADI is more accurate than `lyap` for all tests.

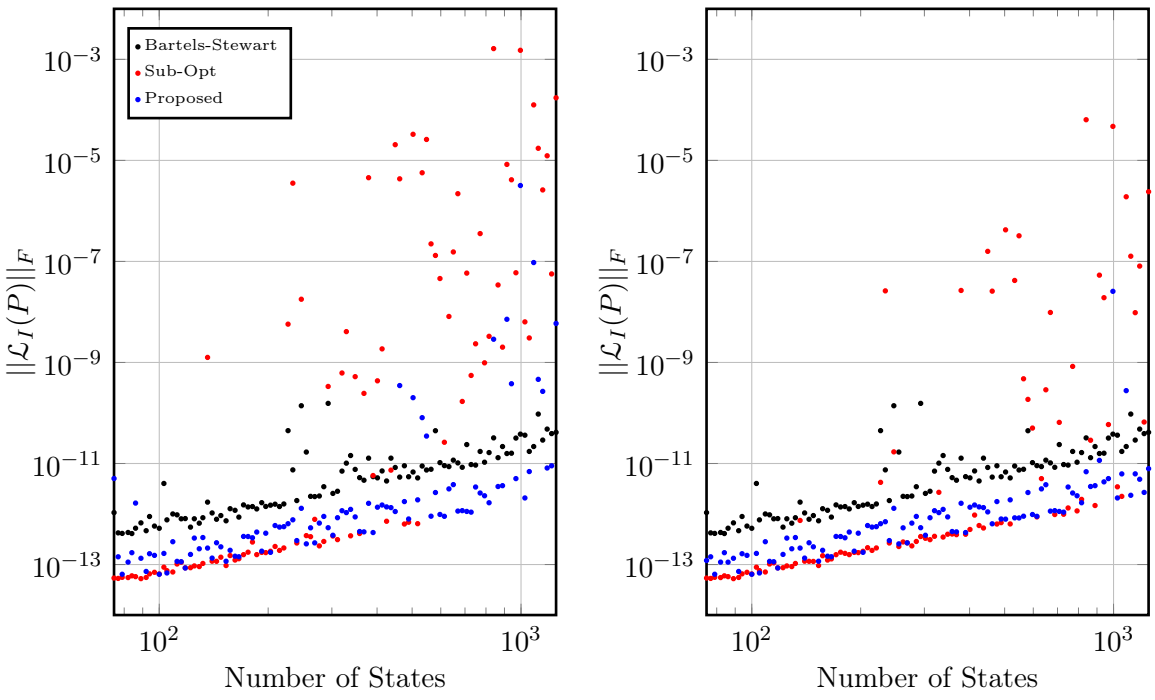

(a) 10 Shifts, 75 Columns

(b) 10 Shifts, 100 Columns

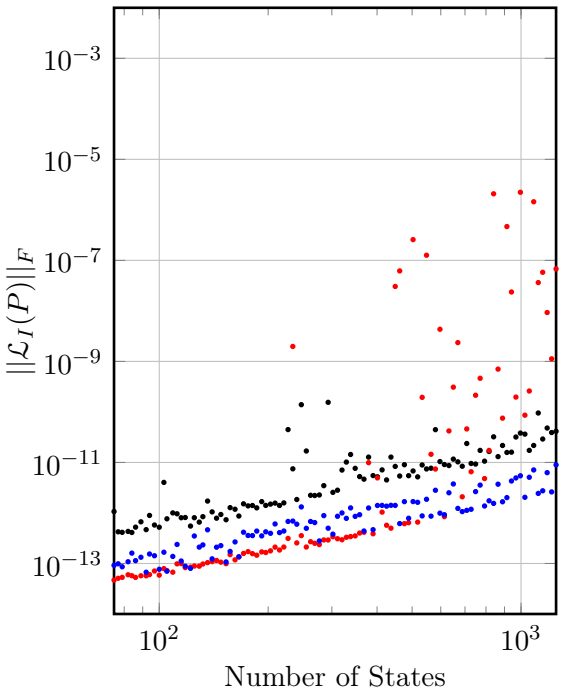

(c) 20 Shifts, 75 Columns

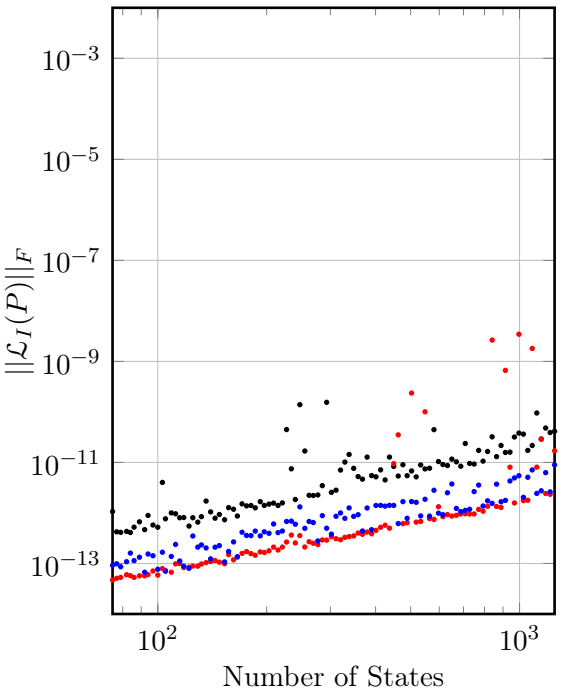

(d) 20 Shifts, 100 Columns

Figure 2.3: Frobenius error of the unweighted Lyapunov solution using the two methods for different number of shifts (or eigenvalues), columns, and number of states compared to MATLAB's `lyap`.

2.4.2 Weighted Gramian Approximation Accuracy

The accuracy of the a posteriori weighting by low-rank up/downdating of Algorithm 2.7 with EVV-LR-ADI is demonstrated. The code of Algorithm 2.8 is modified slightly by making $m = 2$. The selected weighting is

$$Q = \begin{bmatrix} 10 & -1.75 \\ -1.75 & 2 \end{bmatrix}, \tag{2.48}$$

and is chosen to accentuate the first input (providing comparison to Fig. 2.3) and cross terms. The same error methodology of the previous section is applied, and similar results are obtained.

Fig. 2.4 provides the Frobenius norm of the weighted controllability Lyapunov operator for various numbers of states, shifts, and number of columns in the approximation. The same general trends are seen as in Fig. 2.3, but error is multiplied by the weightings. Nevertheless, for 20 shifts (eigenvalues), the EVV-LR-ADI a posteriori weighted approximation is generally still more accurate than `lyap`.

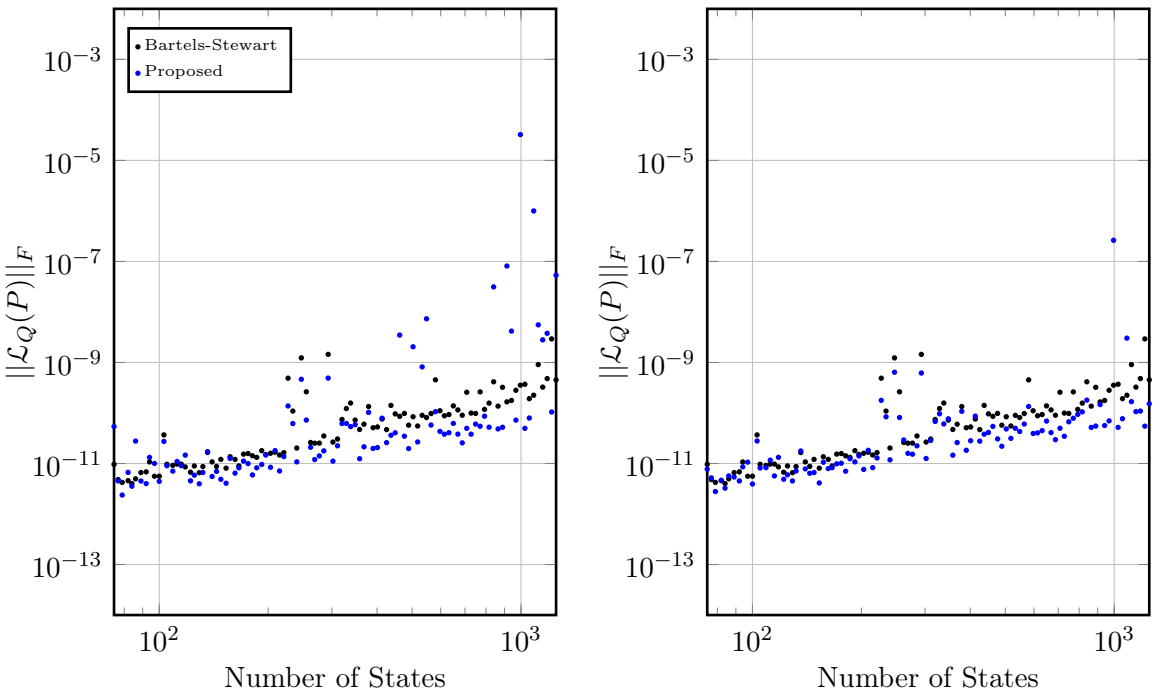

(a) 10 Shifts, 75 Columns

(b) 10 Shifts, 100 Columns

(c) 20 Shifts, 75 Columns

(d) 20 Shifts, 100 Columns

Figure 2.4: Frobenius error of the weighted Lyapunov solution of the proposed EVV-LR-ADI for different number of shifts (or eigenvalues), columns, and number of states compared to MATLAB's `lyap`.

2.4.3 Reduction of an Electric Machine Thermal Model

In this subsection, the proposed algorithms are applied to a problem of practical interest and importance.

Electric machines play an integral role in transportation and energy generation. For the purpose of simulating an integrated design of an electric machine in a vehicle powertrain or electric grid, fast and accurate simulation of various components, and their scalings [99], are necessary [2, 100]. However, the dynamics of many of the components are governed by PDEs which must be approximated by an FEA model in order to simulate. These FEA approximations are often computationally impractical for simulation due to the number of states required for accuracy to the true solution.

One important aspect to determining electric machine efficiency, and maintaining a safe operating condition, is the temperature of the rotor and stator of the electric machine [100]. The temperature model is governed by the parabolic heat equation:

$$\frac{\partial T}{\partial t} - c\nabla^2 T = f \tag{2.49}$$

where T, f are functions of time and the spatial coordinates, ∇^2 is the Laplace operator, and c is the thermal diffusivity [101].

For this work, a thermal conduction model is used with 11 loss inputs and 2 temperature outputs. The loss inputs are spatially distributed and are detailed in [2], while the outputs are points (denoted by purple rings in Fig. 2.5(a)). The PDE model is meshed and FEA coefficients are derived from the mesh (Fig. 2.5(b)), resulting in two linear descriptor system of the form (2.2), with more than 50,000 states and a sparsity of 0.99972 each (or only 0.027% of the entries are non-zero). To store a dense matrix of this size in double precision floating point numbers (8 bytes), e.g. the gramian or balancing transformations, it would require 20 GB of storage per model.

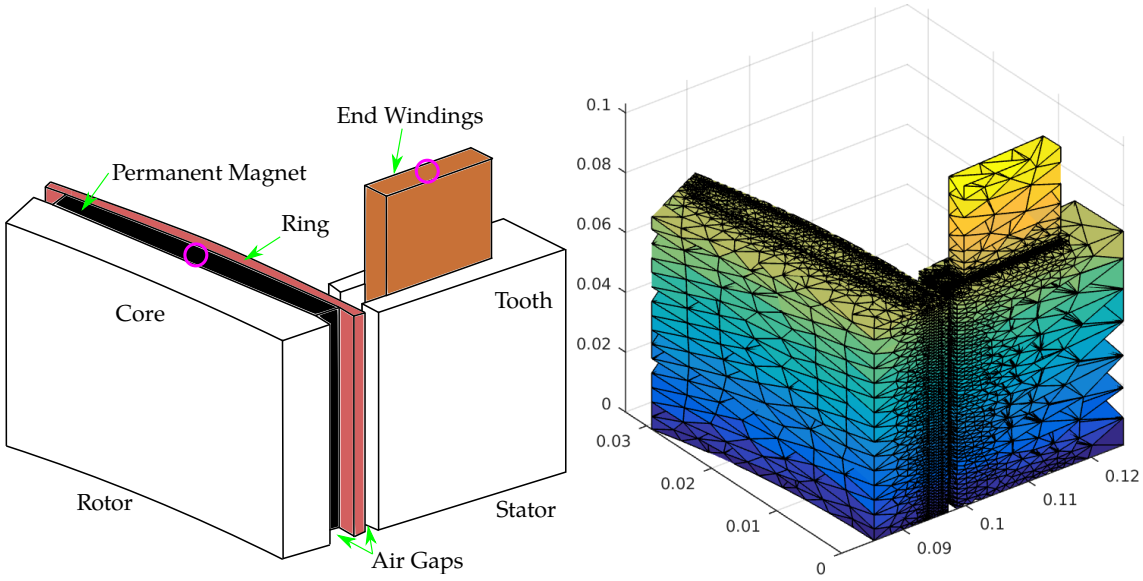

(a) Electric Machine (b) Meshing

Figure 2.5: Isometric view and mesh of the electric machine.

Model order reduction is performed to overcome the limitations of the FEA model. For the usefulness of the model in predicting the temperature, it is required that outputs of the reduced order model have less than 1°C of error from the full order model response in both the stator and rotor when the Urban Assault Drive Cycle [102] is used. Prior work of [2] used the eigenvalue/eigenvector modal truncation of [103] and found that 11 states (7 stator, 4 rotor) were necessary to meet the accuracy requirements. Modal truncation has the benefit that it is often much cheaper to compute since only a small number of the smallest in magnitude eigenvalues/vectors need to be computed, however, this technique is limited to systems and inputs with responses characterized well by the slow eigenmodes. LBT (and approximate LBT) considers the dominant input-to-output behavior, and is expected to yield a more accurate reduced order model in general.

The Algorithms 2.4, 2.6, and 2.7 are used to yield two approximate balancing transformations: unweighted and weighted for both the stator and rotor models. 50 eigenvalue/vector pairs are used for the unweighted EVV-LR-ADI, the gramian calculations are split up to exploit linearity as in Section 2.3.3, and a $q = 500$ columns are used to approximate the 4 controllability and observability gramians of the rotor and stator model. The input and output weightings used are denoted with subscripts c and o for controllability and observability,

respectively, and *rot* and *sta* for rotor and stator, respectively:

$$Q_{c,rot} = \begin{bmatrix} 1 & 0 & 0 & 0 & 0 \\ 0 & 1000 & 0.9 & 0 & 0 \\ 0 & 0.9 & 1 & 0 & 0 \\ 0 & 0 & 0 & 1 & 0 \\ 0 & 0 & 0 & 0 & 1 \end{bmatrix}, \; Q_{c,sta} = \begin{bmatrix} 1 & 0 & 0 & 0 & 0 & 0 \\ 0 & 1 & 0 & 0 & 0 & 0 \\ 0 & 0 & 1 & 0 & 0 & 0 \\ 0 & 0 & 0 & 0.875 & 0 & 0 \\ 0 & 0 & 0 & 0 & 1 & 0 \\ 0 & 0 & 0 & 0 & 0 & 1 \end{bmatrix},$$

$$Q_{o,rot} = 50, \text{ and } Q_{o,sta} = 100.$$

Approximate LBT is used to obtain a reduced order models of 8 states (4 stator, 4 rotor). Sub-optimal LR-ADI using 50 shifts resulted in slow convergence and large errors, and is not shown.

For proper complexity and performance comparisons, a modally truncated model with 8 states (4 stator, 4 rotor) is used, and the reduction technique of [103] used in [2] is employed for all reduced order models. The models are simulated using a backward Euler integration scheme [104] with a discretization of 1 second.

Fig. 2.6(a) shows the corresponding "Full" and reduced responses for a locked rotor test using the demanded drive cycle current [2]. The "Full" order response is obscured by the reduced order model response, and the reduced order model obtained by modal truncation has errors far greater than the 1°C specification in the stator. The output from the model obtained by the proposed unweighted EVV-LR-ADI shows a stator response with much better error performance, shown in Fig. 2.6(b), almost a 10× improvement, but in Fig. 2.6(c), the rotor response error of the unweighted EVV-LR-ADI model is greater than the modal-based reduction. Regardless, unweighted EVV-LR-ADI satisfies the error criteria. It is hypothesized that the anomalous result of the reduced order modal rotor modal performing better than the EVV-LR-ADI model is due to the almost perfect excitation of slow modes.

The weighted EVV-LR-ADI results show the stator performance is marginally better than unweighted EVV-LR-ADI; moreover, the rotor performance is better than even the modal model. Table 2.1 provides the maximum, root-mean-squared (RMS), and max relative error

of the reduced model responses to the full order responses, as well as the wall time to calculate the output. The table demonstrates the approximate balanced truncation models not only satisfy the error criteria, but can be made to perform better than the modal truncation model.

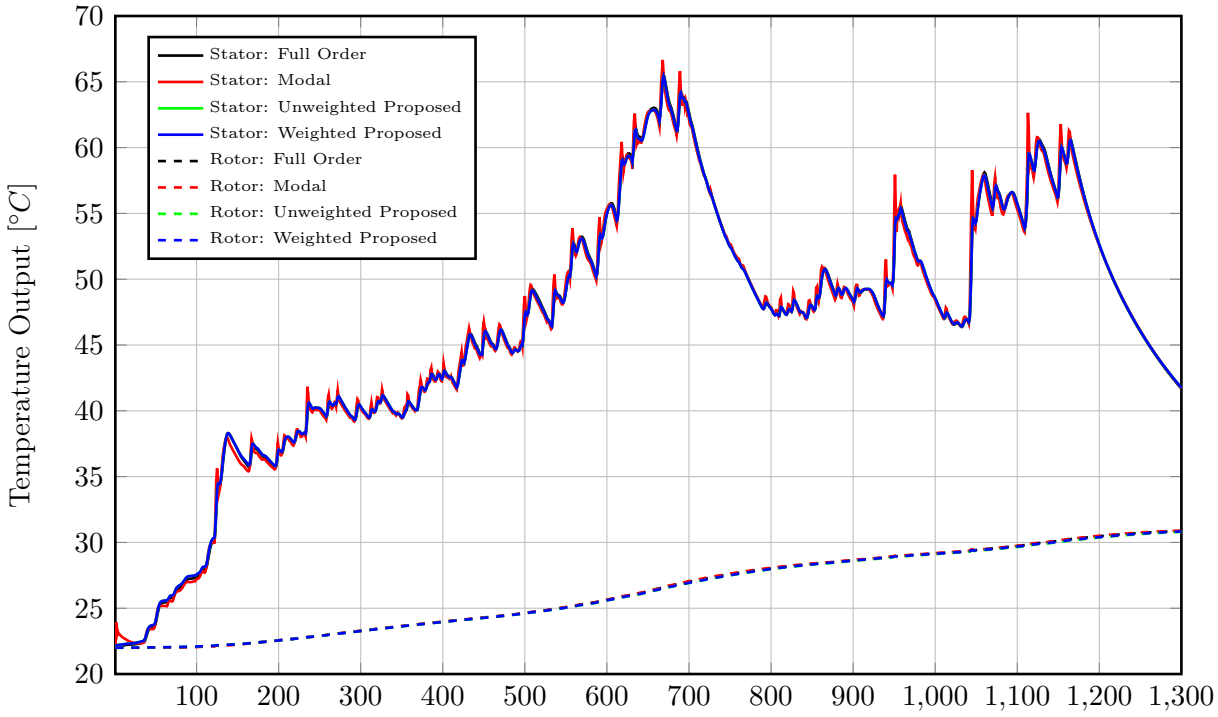

(a) Output

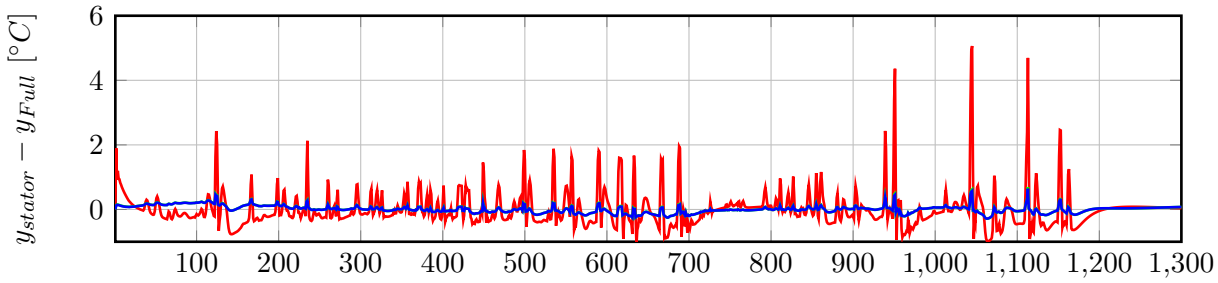

(b) Stator Error

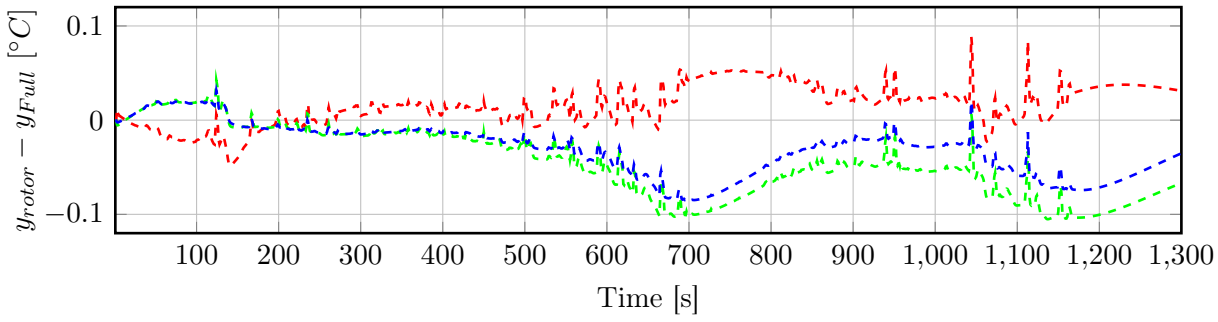

(c) Rotor Error

Figure 2.6: Outputs of the various models, and the errors between the full and 4th order reduced models for the locked rotor test.

The "Full" order model takes ≈2000 seconds to simulate a 1300 second drive cycle at 1 second sampling, resulting in a >99.99% reduction in simulation time, and allowing the model to be used for the purpose of on-line condition monitoring.

Table 2.1: Reduced order model output error comparisons of locked rotor test ($\omega = 0$ RPM).

	Stator Max.	Rotor Max.	Stator Rel.	Rotor Rel.	Stator RMS	Rotor RMS	Wall Time [s]
Modal	5.062265	0.088559	0.097305	0.003014	0.560488	0.026249	0.138920
Unweighted Proposed	0.695048	0.105179	0.015733	0.003834	0.114579	0.057626	0.129309
Weighted Proposed	0.643097	0.085055	0.014763	0.003158	0.111175	0.040979	0.137602

Remark 2.4.1. *Assuming that the same mesh is used, and components of the electric machine (e.g., physical dimensions) are scaled as in [99], then Algorithm 2.7 may be used to generate the gramians and reduction of the scaled electric machine from the original individual electric machine gramians.*

2.5 Conclusions

In this chapter, bilinear discretizations for descriptor systems were developed, eigenvalues of a discretization were found, and exploited to find low-rank matrix square root factors (Cholesky factors) of the controllability and observability gramian using an eigenvalue/vector-based low-rank alternating direction implicit (EVV-LR-ADI) method. A new singular valued decomposition-based low-rank updating and downdating algorithm is proposed and used to restart the low-rank Cholesky factorization algorithm if the factor gets too large, and error bounds are derived. Using the same updating and downdating algorithm, linearity of the gramians (relative to the input and output matrices) are exploited to parallelize the low-rank approximation calculation, and a more accurate reduced order model is obtained by a posteriori weighting and without recalculating gramian components.

The efficacy of the proposed techniques were then demonstrated on random dense stable descriptor systems of varying sizes and a combined stator and rotor electric machine thermal model with over 100,000 states. Using the randomly generated stable descriptor systems, the Cholesky factors obtained by the EVV-LR-ADI and well researched sub-optimal LR-ADI algorithm were compared against each other and relative to the generalized Bartels-Stewart solution in the Frobenius norm. It is found that the proposed EVV-LR-ADI algorithm, using

only 75 iterations on random systems, is often as accurate as the Bartels-Stewart solution, while the sub-optimal LR-ADI can be less accurate as the order of the system increases. The same methodology is applied to show the accuracy of the low-rank up/downdating algorithm coupled with the EVV-LR-ADI Cholesky factors, and it is found that the solution is again accurate.

Finally, the techniques are applied to a stator and rotor thermal model of an electric machine (EM) with 11 inputs and 2 outputs, and a combined order of more than 100000. Using the Urban Assault Drive Cycle, it is shown the EM model can be reduced to just 8 states, while maintaining less than 1°C error, and provides a more accurate model than that derived by the current state-of-the-art modal truncation.

Chapter 3

Riccati Balanced Truncation

Linear model order reduction (MOR) in its most popular form of "balanced realization and truncation" was introduced in Moore's seminal paper [13], and is a form of open-loop model order reduction. Open-loop model order reduction techniques focus on matching the open loop responses of the original and reduced order models without considering the effect of feedback control on the output. Many other model order reduction techniques, some explicitly accounting for closed-loop behavior, have since been developed by the controls community [86]. Unlike open-loop model order reduction, which can lead to destabilizing reduced order compensator even when the open-loop behavior is matched arbitrarily well [105], the closed-loop model order reduction emphasizes matching the behavior of the closed-loop system, thereby overcoming the non-robust drawback of the open-loop approaches.

Closed-loop model order reduction for normalized linear quadratic Gaussian (LQG) and H_∞ design has been addressed in [28], [3], and [29]. In these three references, dual Riccati based balanced realization and truncation was proposed to perform model-order reduction and achieve closed-loop stability for strictly proper systems. [30] and [106] addresses the case when the LQ weights are not normalized, but the systems to be treated have strictly proper transfer functions, or there is no direct throughput in the state space realization.

In this chapter, closed-loop model order reduction following [3] is pursued and applied to the electric machine problem and the DAP problem by extending the results to the case of direct feedthrough inclusion, non-normalized weightings, and cross term weighting. The proposed technique will be referred to as Riccati balanced truncation (RBT).

The proposed RBT technique is applied to design a compensator for the diesel engine airpath (DAP) with reduced complexity. The efficacy of a RBT-based compensator is demonstrated relative to a compensator designed with a reduced order model obtained using the more popular Lyapunov Balanced Truncation (LBT) of [13]. The two reduced compensators will be compared on a linearized model, a Toyota proprietary engine model, and on an experimental 3 liter, 4 cylinder diesel Toyota KD engine.

The chapter is structured as follows: Section 3.1 presents the background of LQG balanced truncation and the generalization to direct feedthrough inclusion, non-normalized weightings, and cross term weighting. Section 3.2 develops the algorithm for computing low-rank matrix square root factors of Riccati solutions for large scale descriptor systems and performance is compared on the electric machine model of Chapter 2. Section 3.3 provides a link between LQG and conventional MPC/Kalman filters, and the use of robust RBT reduced models in a rate-based MPC framework. Section 3.4 applies a rate-based MPC law designed using linear models to a nonlinear diesel airpath problem for the purpose of real-time control.

For the remainder of this chapter, a controller, estimator, or compensator designed using a reduced order model will be referred to as a reduced controller, estimator, or compensator, respectively.

3.1 LQG and Riccati Balanced Truncation

3.1.1 LQG Balanced Truncation

In continuous time, assume the linear model $\Sigma : (A, B, C, D)$ with process and measurement noises $v(t)$ and $w(t)$, has the following form:

$$\Sigma : \left\{ \begin{array}{rcl} \dot{x}(t) & = & Ax(t) + B(u(t) + v(t)), \\ y(t) & = & Cx(t) + D(u(t) + v(t)) + w(t), \end{array} \right. \tag{3.1}$$

where $A \in \mathbb{R}^{n\times n}$, $B \in \mathbb{R}^{n\times m}$, $C \in \mathbb{R}^{p\times n}$, $D \in \mathbb{R}^{p\times m}$, and $v(t)$ and $w(t)$ are zero-mean, Gaussian noises with covariance Γ, and Λ, respectively.

The LQG compensator is a very well known and understood problem [107], it consists of optimally controlling a system and estimating its state subject to zero mean additive Gaussian process and measurement noises, $v(t)$ and $w(t)$. In continuous-time, the LQG regulator problem is defined as

$$\min_{u(\cdot)} \mathbb{E}\left[\lim_{t\to\infty} \frac{1}{t}\int_0^t y(\tau)^\top Q y(\tau) + u(\tau)^\top R u(\tau) d\tau\right] \quad \text{subject to (3.1)} \tag{3.2}$$

where $\mathbb{E}$ is the expectation. When $D = 0$, the LQG problem has a guaranteed stabilizing solution if (A, B) is stabilizable, $(Q^{1/2}C, A)$ is detectable, $C^\top QC$ is positive semi-definite, and R is positive definite [108]. It is also well known that the compensator design can be separated into a linear quadratic regulator (LQR) and linear quadratic estimator (LQE) problem to obtain a controller and estimator, respectively.

When $D = 0$, $Q = I_{p\times p}$, $R = I_{m\times m}$, $\Lambda = I_{p\times p}$, $\Gamma = I_{m\times m}$, (3.2) becomes the "normalized LQG problem" and the Riccati equations associated with the solution of LQR and LQE are dual:

$$A^\top P_0 + P_0 A + C^\top C - P_0 B B^\top P_0 = 0, \tag{3.3a}$$

$$A\Pi_0 + \Pi_0 A^\top + B B^\top - \Pi_0 C^\top C \Pi_0 = 0, \tag{3.3b}$$

The optimal LQG compensator takes the form

$$\dot{\hat{x}}(t) = A\hat{x}(t) + Bu(t) + \Pi_0 C^\top (y - C\hat{x}(t)), \tag{3.4a}$$

$$u(t) = -B^\top P_0 \hat{x}(t). \tag{3.4b}$$

LQG balanced truncation (LQGBT) can be applied to the normalized problem to derive a balanced realization and perform truncation, resulting in a reduced order LQG compensator. The reduced order compensator is then designed and applied to the plant, as in Fig. 3.1.

LQGBT may be interpreted as removing subspaces that are easy to control and easy to estimate while keeping subspaces that contribute more to the cost functional in designing a reduced order compensator to optimize (3.2).

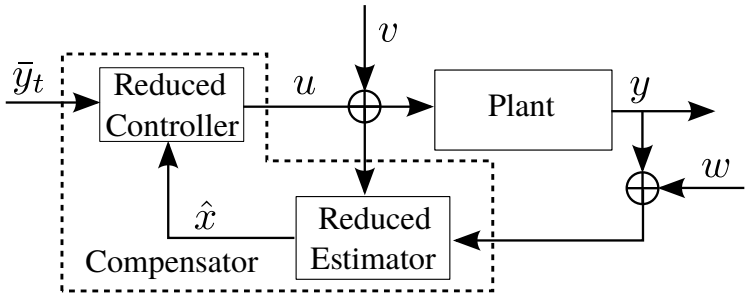

Figure 3.1: Block diagram of the plant with reduced compensator.

The measure of how easy it is to control and estimate a subspace is given by the Riccati singular values (RSVs) and follows that of [3].

Definition 3.1.1. *Given the solutions P_0, Π_0 to the dual algebraic Riccati equations* (3.3a), (3.3b)*, respectively, the RSVs are defined as $\mu_j = \sqrt{\lambda_j(P_0\Pi_0)}$. $\lambda_j(\cdot)$ denotes the eigenvalues of the matrix ordered from the largest to the smallest.*

RSVs are an invariant under state similarity transformations and a small RSV corresponds to a subspace that is easy to control and estimate, thereby having little impact on the cost [109].

Just like in Definition 2.1.6, balanced representations may be defined in terms of the Riccati solutions:

Definition 3.1.2. *(A, B, C, D) is said to be input normal when $P_0 = I_{n\times n}$, $\Pi_0 = M^2$, output normal when $P_0 = M^2$, $\Pi_0 = I_{n\times n}$, and internally balanced when $P_0 = \Pi_0 = M$. I denotes the identity matrix, $M = \mathrm{diag}(\mu_1, \ldots, \mu_n)$ with $\mu_1 \geq \mu_2 \geq \ldots \geq \mu_n$, where n is the order of the system.*

After obtaining a balancing transformation $\mathscr{T}$, balanced truncation or residualization (Algorithms 3.2 and 4.1, respectively) may be applied to obtain a reduced order model, $\Sigma_r : (A_r, B_r, C_r, D_r)$. The reduced LQG compensator is designed using Σ_r and the transformed LQG problem:

$$\dot{\hat{x}}_r(t) = A_r\hat{x}_r(t) + B_r u(t) + M_1 C_r^\top (y - C_r\hat{x}_r) \tag{3.5a}$$

$$u(t) = -B_r^\top M_1 \hat{x}_r, \tag{3.5b}$$

where $M_1 = \text{diag}(\mu_1, \ldots, \mu_r)$.

3.1.2 LQG Solution for Systems with Non-zero D

When the weights and noises are not normalized, and $D \neq 0$, the quadratic cost of (3.2) will consist of a cross term $2x^\top C^\top QDu$, when expressed in terms of x and u. This fundamentally alters the structure of the solution to the optimization problem; nevertheless, a separation principle is maintained and the problem can again be separated into LQR and LQE.

The LQR solution is given by

$$u(t) = -\underbrace{\tilde{R}^{-1}(B^\top P + D^\top QC)}_{K} x(t), \tag{3.6}$$

where P solves the continuous control algebraic Riccati equation (CARE)

$$\tilde{A}^\top P + P\tilde{A} + \tilde{Q} - PB\tilde{R}^{-1}B^\top P = 0 \tag{3.7}$$

with

$$\tilde{R} = D^\top QD + R, \tag{3.8a}$$

$$\tilde{A} = A - B\tilde{R}^{-1}D^\top QC, \tag{3.8b}$$

$$\tilde{Q} = C^\top QC - C^\top QD\tilde{R}^{-1}D^\top QC, \tag{3.8c}$$

where $\tilde{Q} \geq 0$. In LQG control, the $x(t)$ of (3.6) is replaced by the estimate $\hat{x}(t)$ that is obtained by solving the LQE problem.

The optimal LQE solution takes the form:

$$\dot{\hat{x}}(t) = A\hat{x}(t) + Bu(t) + L(y(t) - (C\hat{x}(t) + Du(t))). \tag{3.9}$$

Because of the direct feedthrough noise, $Dv(t)$, the noise covariances and dynamics must be

modified as in the LQR case to get

$$\hat{\Lambda} = D\Gamma D^\top + \Lambda, \tag{3.10a}$$

$$\hat{A} = A - B\Gamma D^\top \hat{\Lambda}^{-1} C, \tag{3.10b}$$

$$\hat{\Gamma} = B\Gamma B^\top - B\Gamma D^\top \hat{\Lambda}^{-1} D\Gamma B^\top, \tag{3.10c}$$

where $\hat{\Gamma} \geq 0$. The filter algebraic Riccati equation (FARE) becomes

$$\hat{A}\Pi + \Pi\hat{A}^\top + \hat{\Gamma} - \Pi C^\top \hat{\Lambda}^{-1} C\Pi = 0, \tag{3.11}$$

and the optimal gain used in (3.9) is

$$L = (\Pi C^\top + B\Gamma D^\top)\hat{\Lambda}^{-1}. \tag{3.12}$$

3.1.3 Riccati Balanced Truncation (RBT)

In this section, the LQG balanced truncation is extended to the case of a non-normalized cost with direct feedthrough, and the extension will be referred to as the Riccati balanced truncation (RBT).

To perform Riccati balanced truncation, there are two steps: finding a transformation that balances the solutions to (3.7) and (3.11), and then transforming, partitioning, and truncating the resulting internally balanced system before designing a reduced order compensator.

Under the stabilizability and detectability assumptions, positive definite solutions to (3.7) and (3.11) are guaranteed to exist [108], and the procedure outlined in [77] is modified to calculate the Riccati solution balancing transformation of Algorithm 3.1.

Algorithm 3.1 Riccati balancing transformation.

1: **procedure** RICCATIBALTRANS($\Sigma : (A, B, C, D), Q, R, \Gamma, \Lambda$)
2: Solve (3.7) and (3.11) for positive definite P and Π, respectively.
3: Calculate the Cholesky factors of $P = XX^\top$, $\Pi = YY^\top$.
4: Calculate the singular value decomposition (SVD) of $Y^\top X = UMV^\top$, where M is a positive definite diagonal matrix and U and V are orthogonal matrices.
5: Form the balancing transformation

$$\mathscr{T} = M^{1/2}U^\top Y^{-1}. \tag{3.13}$$

($\mathscr{T} = MU^\top Y^{-1}$ or $\mathscr{T} = U^\top Y^{-1}$, places the realization in output or input normal form, respectively.)
6: Define the contragredient transformation for the ARE solutions for the transformed system:

$$\bar{P} = \mathscr{T}^{-\top} P \mathscr{T}^{-1}, \tag{3.14}$$

$$\text{and } \bar{\Pi} = \mathscr{T} \Pi \mathscr{T}^\top. \tag{3.15}$$

return $\mathscr{T}$
7: **end procedure**

Theorem 3.1.1. *After applying* (3.13) *to* Σ*, the solutions of* (3.7) *and* (3.11) *are equal and balanced* ($\bar{P} = \bar{\Pi} = M$).

Proof. See appendix A.2.1 for the proof. □

To obtain the reduced order model Σ_r, the balancing transformation, $\mathscr{T}$, is found using Algorithm 3.1 and (3.1) is truncated using Algorithm 3.2 to an order r. Σ_r is used to design the reduced control and estimator, respectively.

Algorithm 3.2 Truncation of an ordinary linear system.

1: **procedure** LINEAR_TRUNCATION($\mathscr{T}, \Sigma : (A, B, C, D), x_0, r$)
2: Define the submersion and immersion matrices

$$W = \begin{bmatrix} I_{r\times r} & 0 \end{bmatrix}, \tag{3.16a}$$

$$V = \begin{bmatrix} I_{r\times r} \\ 0 \end{bmatrix}. \tag{3.16b}$$

3: Apply the similarity transformation $\mathscr{T}$

$$\Sigma_r : (A_r, B_r, C_r, D_r) = (W\mathscr{T}^{-1}A\mathscr{T}V, W\mathscr{T}^{-1}B, C\mathscr{T}V, D), \tag{3.17a}$$

$$x_r(0) = W\mathscr{T}^{-1}x_0. \tag{3.17b}$$

return $\Sigma_r : (A_r, B_r, C_r, D_r), x_r(0)$
4: **end procedure**

Denote P_r and Π_r to be the solution of (3.7) and (3.11) subject to Σ_r and the selected weights. Using the property that $M_1 = P_r = \Pi_r$, the reduced compensator gains, (K_r, L_r), are obtained by removing the $n - r$ columns from K and rows from L of the internally balanced system, and is demonstrated below:

$$\begin{aligned}
M_2 &= \operatorname{diag}(\mu_{r+1}, \ldots, \mu_n) \\
K &= \tilde{R}^{-1}\left(\begin{bmatrix} B_r \\ B_2 \end{bmatrix}^\top \begin{bmatrix} M_1 & 0 \\ 0 & M_2 \end{bmatrix} + D^\top Q \begin{bmatrix} C_r & C_2 \end{bmatrix}\right), \\
K_r &= \tilde{R}^{-1}\left(B_r^\top M_1 + D^\top Q C_r\right), \qquad (3.18a) \\
L &= \left(\begin{bmatrix} M_1 & 0 \\ 0 & M_2 \end{bmatrix} \begin{bmatrix} C_r & C_2 \end{bmatrix}^\top + \begin{bmatrix} B_r \\ B_2 \end{bmatrix} \Gamma D^\top\right) \hat{\Lambda}^{-1}, \\
L_r &= \left(M_1 C_r^\top + B_r \Gamma D^\top\right) \hat{\Lambda}^{-1}. \qquad (3.18b)
\end{aligned}$$

This means that in continuous time, the reduced compensator may be designed directly from the balanced full or reduced order model, just as in the LQGBT case [3].

For an internally balanced system in continuous-time, $M_1 = P_r = \Pi_r$. However, in discrete-time, this relation no longer holds. Instead, discrete analogs of P_r and Π_r satisfy

an analogous result for a truncated ARE to the results presented in [110] for a truncated Lyapunov solution. Additionally, more care is required in the reduced compensator design.

Remark 3.1.1. *RBT can be further generalized to handle arbitrary cross terms in the cost function* (3.2)*,* $2y^\top Su$*, through a straightforward modification of the feedback gain and* (3.8)*. After a similar modification of the FARE and observer gain, correlated process/measurement noise may also be handled.*

Remark 3.1.2. *If one were to redefine the output to be*

$$\tilde{y} = y - Du, \tag{3.19}$$

then in the design of the estimator, D *is taken to be zero, and different reduced order models are used for controller and estimator portions of the compensator design. For discrete time, this is presented in [71].*

3.2 LQG of Large Scale Descriptor Systems and Approximate Riccati Balanced Truncation

In this section, and only in this section, the linear system will be assumed to be a non-singular linear descriptor system of the form (2.2). LQGBT has seen a great number of applications for the reduced compensation of large scale and infinite dimensional (PDE) systems [111, 112, 113, 114].

Like gramians, Riccati solutions are generally dense and have a computational and storage complexity of $O(n^3)$ and $O(n^2)$ to obtain a solution [115, 116], respectively. This poses a problem for the calculation of balancing transformations for large scale systems, as well as descriptor systems. However, Riccati solutions also enjoy rapid decay of singular values [117], and can be found using a Newton iterated LR-ADI framework, making approximate Riccati balanced truncation plausible.

3.2.1 LQG and Riccati Solutions of a Descriptor System

Consider the generalized LQG problem of obtaining a compensator that minimizes (3.2), but subject to the linear descriptor system (2.2). This can be separated in LQR and LQE problems, but now using generalized algebraic Riccati solutions and LQ gains.

Let S and N be the cross terms of LQR and LQE cost functions, then the generalized continuous control and filter algebraic Riccati equations are defined, respectively, as [118]

$$E^\top PA + A^\top PE + C^\top QC - (B^\top PE + S^\top C)^\top R^{-1}(B^\top PE + S^\top C) = 0, \quad (3.20a)$$

$$E\Pi A^\top + A\Pi E^\top + B\Gamma B^\top - (C\Pi E^\top + NB^\top)\Lambda^{-1}(C\Pi E^\top + NB^\top)^\top = 0. \quad (3.20b)$$

With the solutions, P and Π, the generalized LQR and LQE gains are, respectively:

$$K = -R^{-1}(B^\top PE + S^\top C), \quad (3.21a)$$

$$L = -\Lambda^{-1}(C\Pi E^\top + NB^\top), \quad (3.21b)$$

and the LQE compensator may be formed.

Using the above gains, the generalized algebraic Riccati equations can be factored into:

$$E^\top P(A + BK) + (A + BK)^\top PE = -C^\top QC - K^\top RK + SK + K^\top S^\top, \quad (3.22a)$$

$$E\Pi(A + LC)^\top + (A + LC)\Pi E^\top = -B\Gamma B^\top - L\Lambda L^\top + LN^\top + NL^\top, \quad (3.22b)$$

which are in the form of Lyapunov equations, whose solutions are known as closed-loop gramians [30].

Focusing on the generalized control algebraic Riccati equation, the discrete time LQR gain is found by solving the generalized discrete control algebraic Riccati equation

$$E_d^\top P_d E_d = C_d^\top QC_d + A_d^\top P_d A_d - (A_d^\top P_d B_d + C_d^\top S_d)(R_d + B_d^\top P_d B_d)^{-1}(A_d^\top P_d B_d + C_d^\top S_d)^\top, \quad (3.23)$$

and the gain is

$$K_d = -(R_d + B_d^\top P_d B_d)^{-1}(B_d^\top P_d A_d + S_d^\top C_d), \quad (3.24)$$

where the subscript d denotes a discretization, $S_d = QD_d + S$, and $R_d = R + S^\top D_d + D_d^\top S + D_d^\top Q D_d$ are used. The result of [119] is readily extended to descriptor systems with the observer sided discretization defined by (2.27) to show that $P = P_d$ with $E_d = I_{n\times n}$. Likewise, the solution to the generalized discrete filter algebraic Riccati equation, $\Pi_d = \Pi$, the solution to (3.22b), when the control sided discretization defined by (2.24) is used with $E_d = I_{n\times n}$.

With this in mind, and the assumption that the continuous K is known, the solution of the control algebraic Riccati equation may be approximated using the LR-ADI framework developed in Chapter 2. However, the assumption that K is known is unrealistic and the LR-ADI framework must be iterated using the Newton-Kleinman iteration. The Newton-Kleinman iteration is implemented by guessing a solution P_0, forming the gain K_0 with (3.21a) using P_0 (which is assumed to stabilize the continuous system), obtaining a closed-loop gramian P, calculating a new stabilizing gain K, and repeating until it converges [118, Chapter 11].

Given an initial guess, Z_{-1} of P, the Riccati solution is found using the Newton-Kleinman iteration implementation in Algorithm 3.3. Eigenvalues of $A - BK$ are not easily obtained because BK is in general dense, hence Algorithm 3.3 uses a single shift LR-ADI or Smith(1) iterator. Further, some changes are necessary to make for efficient computations, these include: factoring the right hand sides of (3.22) for parallelization and then using Algorithm 2.2 and 2.7, and handling of the low-rank factors to not form a dense BK.

Remark 3.2.1. *In practice, a good initial guess for Z_{-1} is the low-rank Cholesky factor of the observability gramian of (E, A, B, C, D).*

Algorithm 3.3 Smith Iterator - Approximate Generalized Algebraic Control Riccati Solution (Newton-Kleinman Iteration)

procedure RICCATISMITHITERATOR($E, A, B, C, D, \alpha, Q, R, S, Z_{-1}$)
  Define $K = -R^{-1}((B^\top Z_{-1})(Z_{-1}^\top E) + S^\top C)$
Require: $\lambda E - (A + BK)$ stable.
  $Z_0 = \infty$
  while $||Z_0 - Z_{-1}|| > \varepsilon$ **do**
    $B_d = \sqrt{2\alpha}E(\alpha E - A)^{-1}B$ ▷ $(\alpha E - A)^{-1}$ should never be formed
    $C_d = \sqrt{2\alpha}C(\alpha E - A)^{-1}$
    $D_d = C(\alpha E - A)^{-1}B + D$
    $R_d = R + S^\top D_d + D_d^\top S + D_d^\top Q D_d$
    $S_d = QD_d + S$
    $K_d = (R_d + (B_d^\top Z_{-1})(B_d^\top Z_{-1})^\top)^{-1}((B_d^\top Z_{-1})(Z_{-1}(\alpha E + A)(\alpha E - A)^{-1}) + S_d^\top C_d)$
    $\hat{Q} = \begin{bmatrix} Q & -S_d^\top \\ -S_d & R_d \end{bmatrix} = XX^\top$
    $\hat{C} = \begin{bmatrix} C_d^\top & K_d^\top \end{bmatrix} X$ ▷ Use the columns of $\hat{C}$ to exploit linearity of the Gramian for parallelization
    $W_0 = \hat{C},\ Y_0 = [W_0],\ k = 1$
    while $(||W_{k-1}^\top W_{k-1}||/||W_0^\top W_0|| > \varepsilon \text{ and } k < k_{max})$ **do**
      $\tilde{W}_k = (\alpha E + A)\left((\alpha E - A)^{-1}W_{k-1}\right)$
      $V_k = B_d(K_d W_{k-1})$
      $W_k = \tilde{W}_k - V_k$ ▷ $W_k = (A_d - B_d K_d)^k \hat{C}$
      $Y_k = [Y_{k-1}\ W_k]$
      $k = k + 1$
    end while
    $Z_0 = Z_{-1}$
    $Z_{-1} = Y_{k-1}$
  end while
  return Y_{k-1}
end procedure

Similarly, the solution to the filter algebraic Riccati equation may be obtained by using the control sided bilinear discretization of (2.24). With the low-rank Cholesky factors of the control and filter algebraic Riccati solutions, an approximate Riccati balancing transformation can be computed in a fashion similar to Algorithm 2.1, and the technique can be extended to singular descriptor systems [45].

3.2.2 Electric Machine: RBT Reduced Model

Using the electric machine model from Section 2.4.3, and normalized weights, an 8th order (4 stator,4 rotor) reduced model is obtained using approximate Riccati balanced truncation outlined above. Fig. 3.2, shows that the RBT model performs slightly better than even the unweighted EVV-LR-ADI (Chapter 2) based LBT model in the stator, but worse in the rotor. Table 3.1 provides quantitative errors, and shows that the Riccati model is the worst performer for rotor error, but best performer for stator error, and similar wall-time.

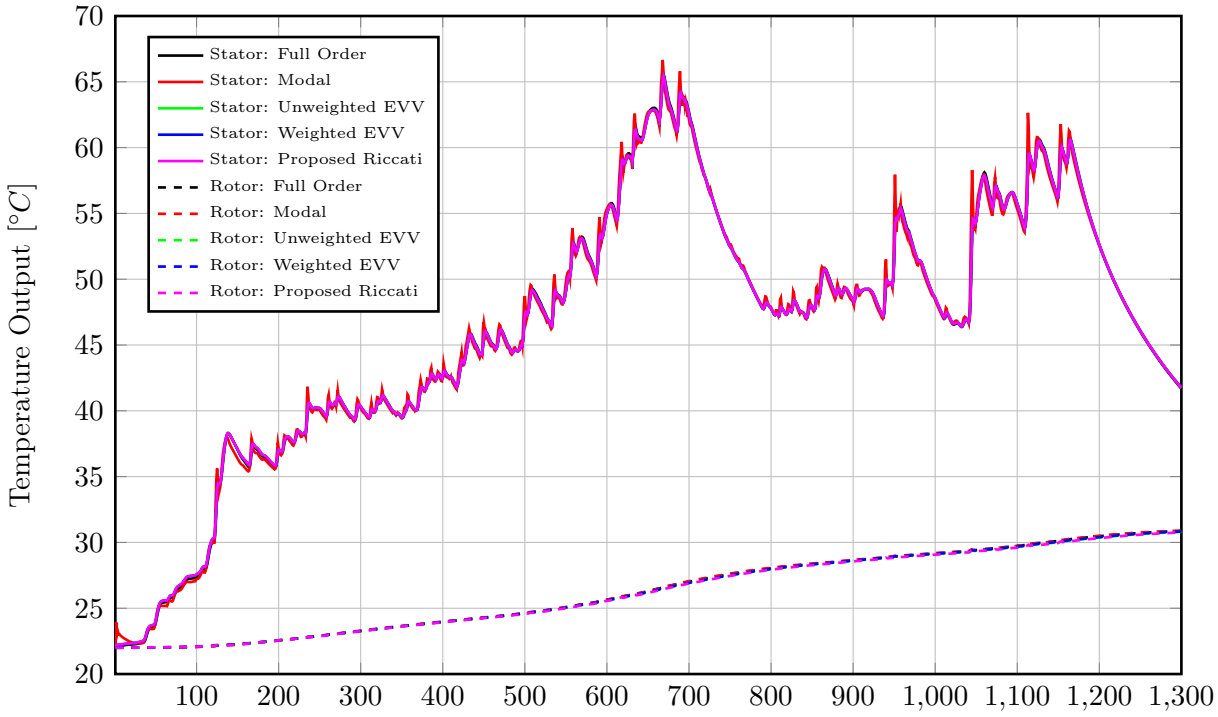

(a) Output

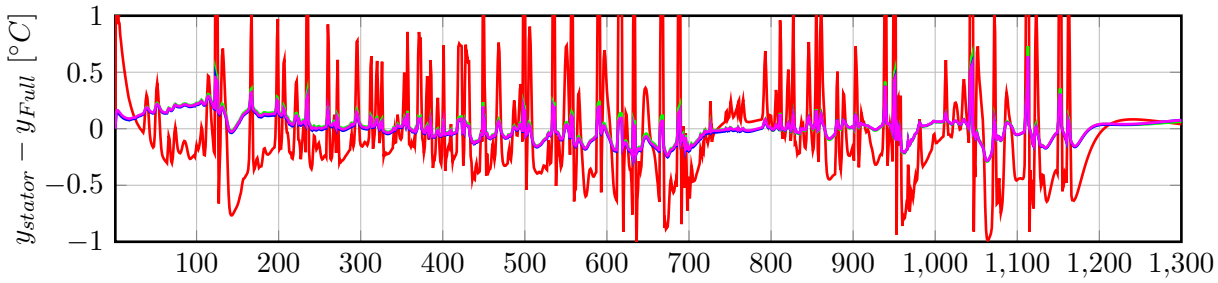

(b) Stator Error

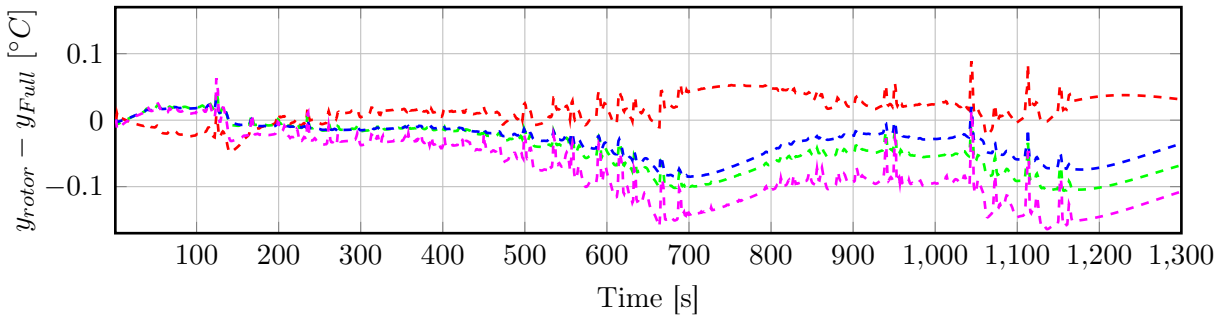

(c) Rotor Error

Figure 3.2: Outputs of the various models, and the errors between the full and 4th order reduced models for the locked rotor test.

Using the same setup as in Section 2.4.3, the simulations are re-run and the errors for the RBT reduced model are added to Table 2.1. The wall time results of Table 2.1 and 3.1 are different because MATLAB's built in `tic-toc` commands were used to obtain wall time, as such, different runs result in slightly different times.

Table 3.1: Reduced order model output error comparisons of locked rotor test ($\omega = 0$ RPM).

	Stator Max.	Rotor Max.	Stator Rel.	Rotor Rel.	Stator RMS	Rotor RMS	Wall Time [s]
Modal	5.062265	0.088559	0.097305	0.003014	0.560488	0.026249	0.183773
Unweighted EVV	0.695048	0.105179	0.015733	0.003834	0.114579	0.057626	0.148078
Weighted EVV	0.643097	0.085055	0.014763	0.003158	0.111175	0.040979	0.141497
Proposed Riccati	0.642324	0.163834	0.015147	0.006038	0.111805	0.090416	0.139837

3.3 Riccati Balanced Truncation for Conventional and Rate-Based Model Predictive Control (MPC)

Riccati balanced truncation can readily be performed on discrete time systems by obtaining a transformation that balances the solutions to the discrete control and filter algebraic Riccati equations, and truncating. The weighted discrete LQR problem is equivalent to finite time, unconstrained, linear quadratic MPC with a properly selected terminal penalty [120]. The dual problem of discrete LQE is Kalman filter (or unconstrained moving horizon estimator) with a properly selected terminal penalty.

Therefore unconstrained, discrete MPC/Kalman filter with properly selected terminal penalties is equivalent to the discrete LQG problem. This suggests that a reduced order model obtained by discrete Riccati balanced truncation is appropriate for reduced MPC law/Kalman filter compensator design.

3.3.1 Conventional MPC

The discrete time analog of LQR is concerned with selecting feedback control inputs, u_i, minimizing the cost

$$J_d = \sum_{i=t}^{\infty} y_i^\top Q y_i + u_i^\top R u_i \tag{3.25}$$

subject to linear dynamics, $Q \geq 0$, and $R > 0$. With a properly defined terminal state penalty matrix, P (which is the solution to the discrete algebraic Riccati equation), (3.25) can be recast as a finite horizon MPC problem when there are no constraints [121]. The finite horizon MPC problem is to select, u_i, to minimize

$$J_{MPC} = x_{t+N_p}^{\top} P x_{t+N_p} + \sum_{i=t}^{t+N_p-1} y_i^{\top} Q y_i + u_i^{\top} R u_i, \tag{3.26}$$

subject to dynamics, where N_p is the prediction horizon. Of the resulting sequence of controls, u_i, only u_t is applied, and then recalculated at each instant.

The connection between LQR and MPC motivates the use of RBT for the design of a reduced conventional MPC law. It is expected that a reduced MPC law/Kalman filter compensator designed with RBT reduced model will perform better than a reduced order model produced by open-loop methods.

Consider the design of full and reduced order compensators (conventional MPC with Kalman filter) given in Table 3.2 for the model in Table 3.3 (with the specified variable names) using unconstrained MPC designed with the parameters in Table 3.4. Table 3.3 provides the Riccati singular values for a model/compensator design with the parameters in Table 3.4, these singular values suggest the design of a 3rd order compensator. Fig. 3.3 shows the output and control responses of the reduced MPC/Kalman filter compensators designed with the various models for an initial condition of $x_0^{\top} = [-0.3431\ 1.6663\ -0.7668\ 2.6354\ -0.0169\ 0.3041\ 0.6843\ 0.0558]$. As expected, the performance of the RBT-based compensator is closest to the full order compensator. Moreover, the LBT-based reduced compensator exhibits poor performance and acts in an almost opposite manner than is expected.

Table 3.2: Compensators to be compared. The compensators are designed using the model provided in Table 3.3.

Compensator	**Type**
C_I	Designed with the full order model.
C_{II}	Designed with a 3rd order reduced model derived using LBT [13].
C_{III}	Designed with a 3rd order reduced model derived using RBT.

Table 3.3: Continuous-Time, linearized DAP model at the center of fuel/engine speed operating range.

$$
A = \begin{bmatrix}
-64.9506 & 61.3561 & -0.0002 & -0.5182 & 0 & 48.9016 & 0 & 0 \\
11.1492 & -29.9433 & 0.1853 & 0 & 0 & 0 & 0 & 0 \\
0 & 607.8534 & -9.8497 & 431.0396 & 0 & -3635.7872 & 0 & 0 \\
9.6121 & 0 & -0.139 & -45.3523 & 927.5554 & 2123.8713 & 38.8517 & 0 \\
-0.4816 & 0.5022 & 0 & -0.0042 & -4.5677 & 0.3907 & 0 & 0 \\
0.0047 & 0 & -0.0005 & -0.0837 & 8.9587 & -8.6892 & 0 & 0 \\
0.0095 & -0.01 & 0 & 0 & 0 & 0 & -4.5677 & 0.2942 \\
-0.0024 & 0 & 0 & -0.0042 & -4.6299 & 0.3961 & 16.0042 & -16.4312
\end{bmatrix}
$$

$$
B = \begin{bmatrix}
0 & 1.9438 \\
0 & 0 \\
-514.5376 & 0 \\
77.88 & -6.3636 \\
0 & 0.0128 \\
0.3073 & -0.0251 \\
0 & 0.0037 \\
0 & 0
\end{bmatrix}
\qquad
x = \begin{bmatrix}
p_{in} - p_{in,ss} \\
p_{pre} - p_{pre,ss} \\
\omega - \omega_{ss} \\
p_{ex} - p_{ex,ss} \\
\mathcal{F}_{in} - \mathcal{F}_{in,ss} \\
\rho_{ex} - \rho_{ex,ss} \\
\rho_{in} - \rho_{in,ss} \\
\mathcal{F}_{ex} - \mathcal{F}_{ex,ss}
\end{bmatrix},\ \mu_j = \begin{bmatrix}
2.9119 \\
0.60723 \\
0.12566 \\
0.038753 \\
0.01952 \\
0.0011816 \\
4.3578 \times 10^{-6} \\
6.7046 \times 10^{-8}
\end{bmatrix}
$$

$$
C = \begin{bmatrix}
1 & 0 & 0 & 0 & 0 & 0 & 0 & 0 \\
0 & 0.8273 & -0.0082 & 0 & 0 & 0 & 0 & 0
\end{bmatrix}
\qquad
u = \begin{bmatrix}
\text{VGT, } u_{VGT} \\
\text{EGR Flow, } \mathcal{W}_{ex,in}
\end{bmatrix}
$$

$$
D = \begin{bmatrix}
0 & 0 \\
0 & 0.1875
\end{bmatrix}
\qquad
y = \begin{bmatrix}
\text{Intake Pressure, } p_{in} \\
\text{EGR Rate, } \phi_{EGR}
\end{bmatrix}
$$

Table 3.4: Parameters used in the simulation of the controller performance.

N_p	1
T_s	0.016 $[s]$
Q	$\begin{bmatrix} 36 & -4.5 \\ -4.5 & 6 \end{bmatrix}$
R	$\begin{bmatrix} 4 & 0 \\ 0 & 1 \end{bmatrix}$
Λ	$I_{2\times 2}$
Γ	$I_{2\times 2}$

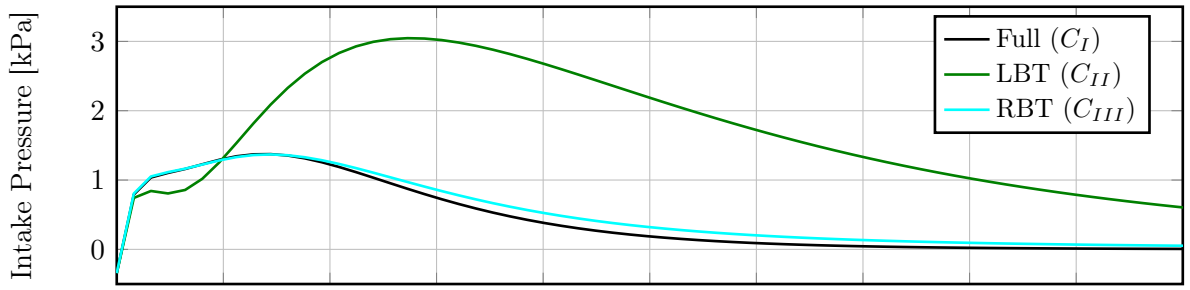

(a) Intake Pressure.

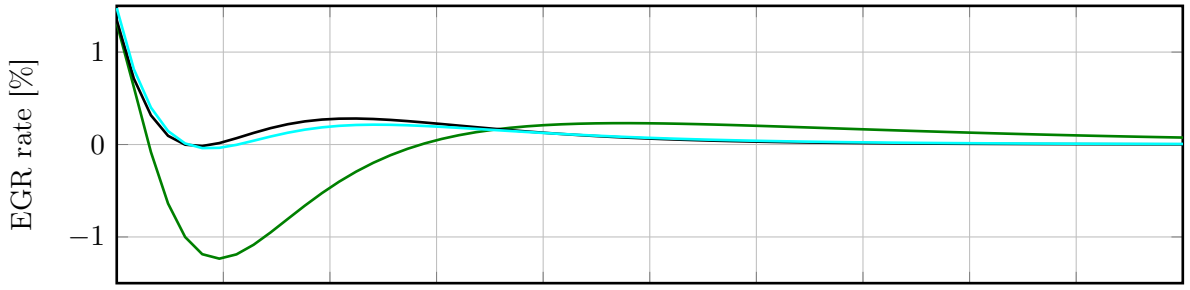

(b) EGR Rate.

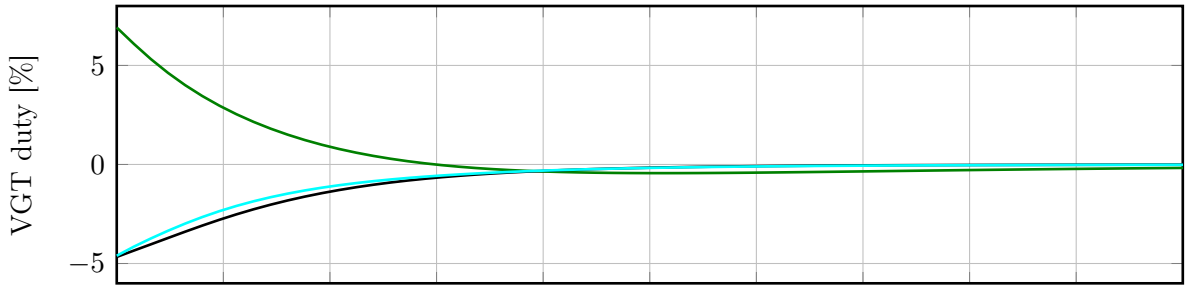

(c) VGT.

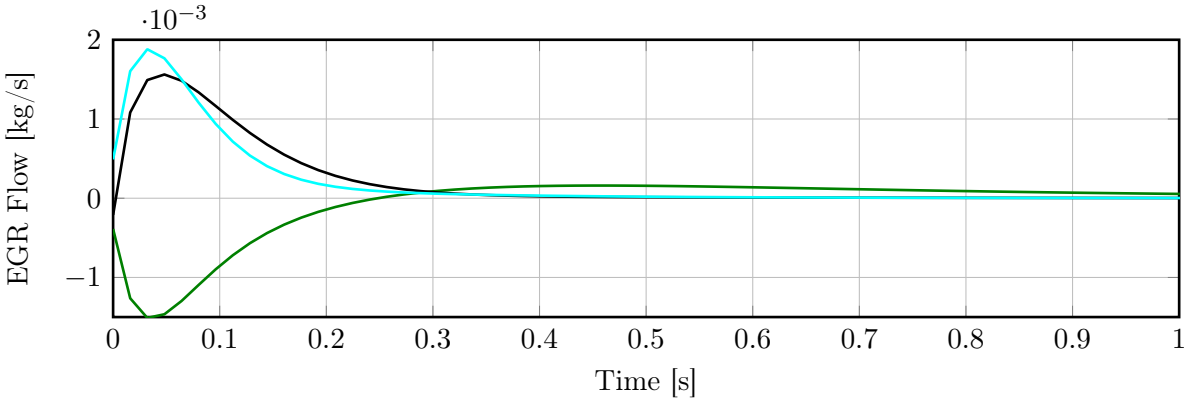

(d) EGR Flow.

Figure 3.3: Linear conventional MPC designed with 3rd order models, applied to the linear plant and compared to the compensator designed with the full order model.

While conventional MPC is well known and has a rich theory, it has shortcomings. When the control objective includes tracking, things such as reference controls and state are required. Further, without modification, modeling errors can manifest themselves as steady state errors. The lack of robustness to modeling errors and the extra knowledge required to mitigate the error makes conventional MPC cumbersome. This leads to using rate-based (velocity form) model predictive control.

3.3.2 Rate-Based MPC

One MPC methodology that has demonstrated less sensitivity to modeling error and can achieve zero steady-state tracking error without integral wind-up is rate-based (or velocity form) MPC [122, 123, 124, 125, 126]. Rate-based MPC uses differences in the state and control in its formulation, therefore does not require the knowledge of steady states and corresponding reference controls.

The rate-based formulation is derived by defining the augmented state $\bar{\mathbf{x}}_t$, output z_t, and input Δu_t as

$$\bar{\mathbf{x}}_t = \begin{bmatrix} x_t - x_{t-1} \\ y_{t-1} \end{bmatrix}, \tag{3.27a}$$

$$z_t = y_{t-1}, \tag{3.27b}$$

$$\text{and } \Delta u_t = u_t - u_{t-1}. \tag{3.27c}$$

With (3.27b) and (3.27c) the state-space equation becomes

$$\bar{\mathbf{x}}_{t+1} = \underbrace{\left[\begin{array}{c|c} A_d & 0 \\ \hline C_d & I_{p\times p} \end{array}\right]}_{\mathbf{A}_d} \bar{\mathbf{x}}_t + \underbrace{\left[\begin{array}{c} B_d \\ \hline D_d \end{array}\right]}_{\mathbf{B}_d} \Delta u_t, \tag{3.28a}$$

$$z_t = \underbrace{\begin{bmatrix} 0 & I_{p\times p} \end{bmatrix}}_{\mathbf{C}_d} \bar{\mathbf{x}}_t, \tag{3.28b}$$

where (A_d, B_d, C_d, D_d) is the discretization of the model, $I_{p\times p}$ is the identity matrix and has dimension equal to the number of outputs.

The augmented model (3.28) deviates from the proposed model of [124], which uses $z_t = y_t$ and y_t in the augmented state, because the addition of direct feedthrough would require knowing $D_d \Delta u_{t+1}$, resulting in a non-causal model. While not pursued in this dissertation, an alternative formulation to get y_t, instead of y_{t-1}, is to change y_{t-1} in (3.28) to $y_t = [C_d \; I]\bar{\mathbf{x}}_t + D_d \Delta u_t$.

General time varying input and output constraints, $u_i \in \mathcal{U}_i$ and $y_i \in \mathcal{Y}_i$, may be reformulated as

$$\bar{F}_i y_i \leq \bar{G}_i, \tag{3.29a}$$

$$\bar{V}_i \Delta u_i \leq \bar{W}_i, \tag{3.29b}$$

where $(\bar{F}_i, \bar{G}_i)$ and $(\bar{V}_i, \bar{W}_i)$, with $i \in \{t, t+1, \ldots, t+N_p-1\}$, define the linear constraints along the prediction window.

The rate-based receding horizon optimal control problem with prediction, control, and constraint horizon equal to N_p subject to a quadratic cost is [124]:

$$\left.\begin{aligned} \min_{\{\Delta u_i\}_{i=t}^{t+N_p-1}} \quad & \left(\bar{\mathbf{x}}_{t+N_p} - \begin{bmatrix} 0 \\ \bar{y}_t \end{bmatrix}\right)^\top P \left(\bar{\mathbf{x}}_{t+N_p} - \begin{bmatrix} 0 \\ \bar{y}_t \end{bmatrix}\right) \\ & + \sum_{i=t}^{t+N_p-1} (z_i - \bar{y}_{t,\infty})^\top Q (z_i - \bar{y}_{t,\infty}) \\ & + \sum_{i=t}^{t+N_p-1} \Delta u_i^\top R \Delta u_i, \\ & \text{subject to (3.28) and (3.29),} \end{aligned}\right\} \tag{3.30}$$

where $\bar{y}_{t,\infty}$ is the desired reference at time t. As in other MPC formulations, (3.30) is transformed into a constrained convex quadratic programming problem to solve for $\{\Delta u_i\}_{i=t}^{t+N_p-1}$ that can either be solved with explicit MPC [127] or using online MPC. Then as in (3.29), Δu_t is added to u_{t-1} to obtain u_t, the control to be applied at the specified time step. Just as in conventional MPC, the control delta must be recalculated at each time step.

As with conventional MPC, reduction of the number of states will decrease the computational complexity. To motivate the selection of the reduction procedure, consider the

transfer function of (3.28):

$$\begin{aligned} G_d(z) &= \left[\begin{array}{cc} 0 & I_{p\times p} \end{array}\right] \left(zI_{n+p\times n+p} - \left[\begin{array}{c|c} A_d & 0 \\ \hline C_d & I_{p\times p} \end{array}\right] \right)^{-1} \left[\begin{array}{c} B_d \\ \hline D_d \end{array}\right] \\ &= \frac{1}{z-1}\left(C_d(zI_{n\times n} - A_d)^{-1}B_d + D_d\right). \end{aligned}$$

Because it is desirable to retain the integrators, it is proposed to reduce $C_d(zI_{n\times n} - A_d)^{-1}B_d + D_d$. The reduced order rate-based compensator is then to be designed by reducing (3.1) to Σ_r by either RBT or LBT, augmenting Σ_r into $(\mathbf{A}_d, \mathbf{B}_d, \mathbf{C}_d)$, and then calculating an MPC law. At the same time, a reduced order rate-based Kalman filter is designed. The estimator is obtained by augmenting Σ_r as above, then solving (3.11) and forming (3.12) using the estimator model $(\mathbf{A}_d, \mathbf{B}_d, \mathbf{C}_d)$. The rate-based estimator takes the predictor-corrector form of (3.9) and is:

$$\hat{\hat{\mathbf{x}}}_{t|t-1} = \mathbf{A}_d\hat{\hat{\mathbf{x}}}_{t-1|t-1} + \mathbf{B}_d\Delta u_{t-1}, \tag{3.31}$$

$$\hat{\hat{\mathbf{x}}}_{t|t} = \hat{\hat{\mathbf{x}}}_{t|t-1} + \mathbf{L}(z_t - \mathbf{C}_d\hat{\hat{\mathbf{x}}}_{t|t-1}), \tag{3.32}$$

where $\mathbf{L}$ is the analogous gain to (3.12), and $\hat{\hat{\mathbf{x}}}_{t|t-1}$ denotes the state at time t given information at time $t-1$.

For a demonstration of the RBT-based reduced order model used in the design of compensator, the LQG compensator of Fig. 3.1 is replaced with a rate-based MPC/Kalman Filter compensator described above and is subject to the constraints at the operating point:

$$-60 \leq y_{t,1} \leq 40\ kPa, \tag{3.33a}$$

$$-6.8558 \leq y_{t,2} \leq 12.37\%, \tag{3.33b}$$

$$-25 \leq u_{t,1} \leq 15\%, \tag{3.33c}$$

$$-0.0242 \leq u_{t,2} \leq 0.0235\ \frac{kg}{s}, \tag{3.33d}$$

$$\text{with } u_i = u_{t-1} + \sum_{j=t}^{i} \Delta u_j \tag{3.33e}$$

along the prediction window.

Just as for conventional MPC, three different compensators, specified in Table 3.2, are designed using the linear model given in Table 3.3 and the parameters in Table 3.4. For the design of a reduced order compensator, the original model of Table 3.3 is reduced using the specified algorithm to a 3rd order model. The new model is placed in the augmented framework of (3.28), resulting in a 5th order compensator. For comparison, the full order model results in a 10th order compensator. Table 3.5 contains the augmented $\mathbf{A}$ and $\mathbf{B}$ with the discretized RBT reduced order model of Table 3.3.

Table 3.5: Zero-order hold discretized 3rd order model obtained using RBT at a sample time of $T_s = 0.016\ s$, and placed in the rate-based framework.

$$\mathbf{A}_d = \left[\begin{array}{ccc|cc} 0.993754 & 0.08691 & 0.009934 & 0 & 0 \\ -0.055662 & 0.809634 & -0.176618 & 0 & 0 \\ 0.01614 & 0.20642 & 0.460977 & 0 & 0 \\ \hline 0.503354 & -0.643326 & -0.474958 & 1 & 0 \\ -0.092951 & -0.152734 & -1.274626 & 0 & 1 \end{array}\right]$$

$$\mathbf{B}_d = \left[\begin{array}{cc} 0.032506 & -0.002053 \\ 0.053456 & -0.018327 \\ -0.030012 & -0.011977 \\ \hline 0 & 0 \\ 0 & 0.1875 \end{array}\right]$$

Fig. 3.4 provides the linear simulation results. Fig. 3.4(a) and 3.4(b) show the outputs have zero steady state error, except when constraints are active (between 5 and 6 seconds), and a small performance improvement by the RBT-based reduced compensator (C_{III}) in terms of tracking and disturbance rejection when compared to the LBT-based reduced compensator (C_{II}). The inputs, given in Fig. 3.4(c) and 3.4(d), demonstrate a small decrease in actuation provided by C_{III} when compared to C_{II}. While the linear results only show a small improvement in the inputs and outputs for this example, when applied to the nonlinear model in the following section, the differences between C_{II} and C_{III} will become more pronounced.

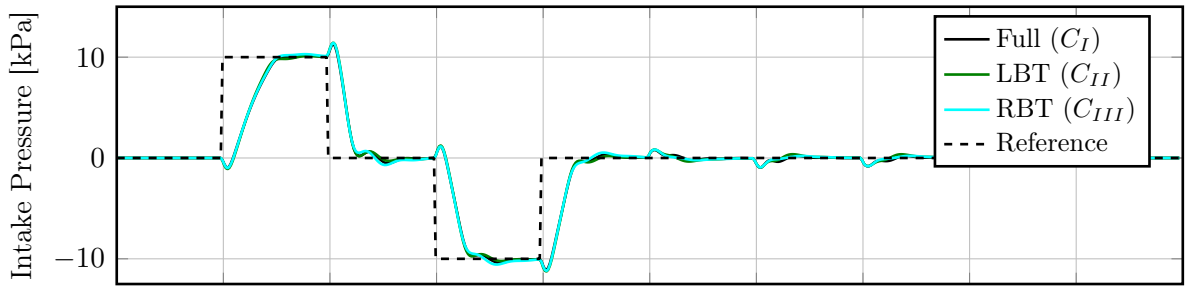

(a) Intake Pressure.

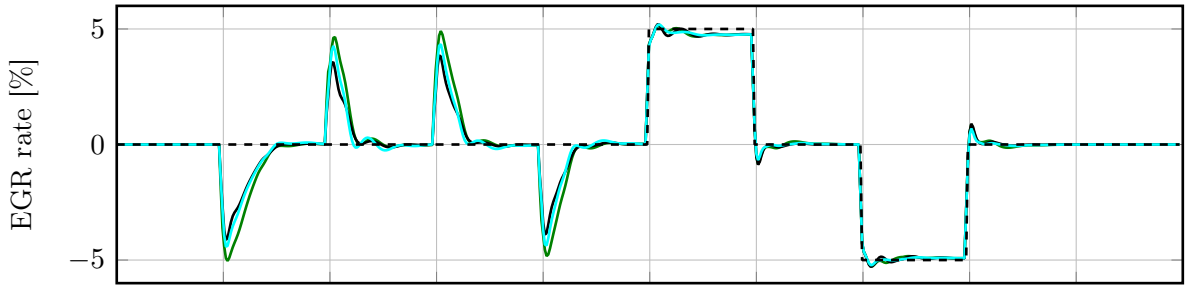

(b) EGR Rate.

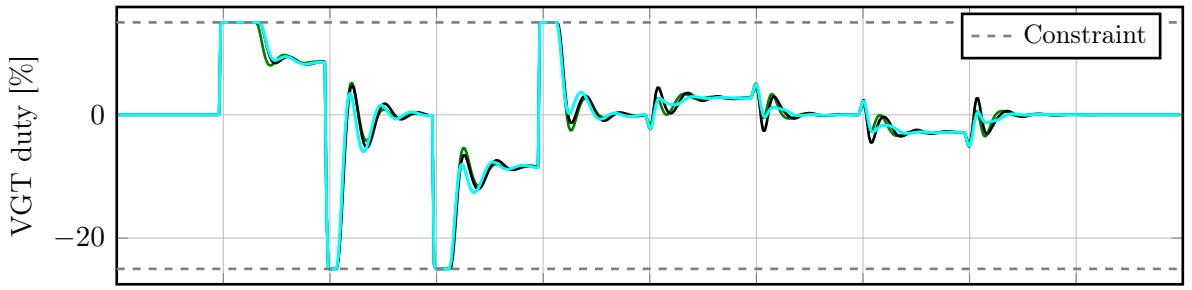

(c) VGT.

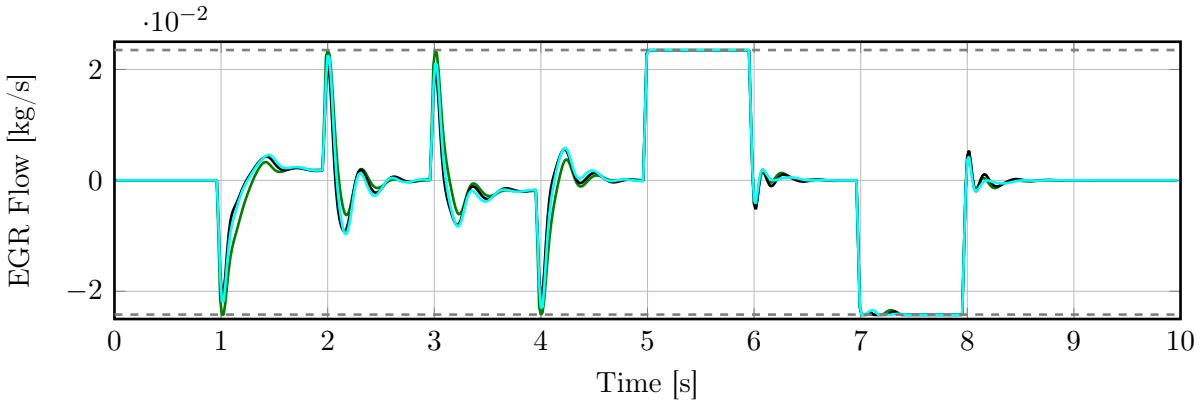

(d) EGR Flow.

Figure 3.4: Linear rate-based MPC designed with 3rd order models, applied to the linear plant and compared to the compensator designed with the full order model.

3.4 Real-Time Control of Diesel Engine Airpath

Diesel engines have a great fuel efficiency advantage for automotive applications, compared to their gasoline counterparts [128]. They, however, impose a special set of emission control challenges, particularly for nitrous oxide (NO_x) emissions [129]. One critical task, which has significant impact on diesel emission as well as drive performance, is the airpath control [130]. The main objective of the airpath control for diesel engines is to deliver air to meet drivers' demands, and at the same time to provide desired EGR (exhaust gas recirculation) to meet emission control requirements.

The diesel airpath (DAP) control system is illustrated in Fig. 3.5. The system under consideration has two control inputs: a linear actuator to change the vane angle of the variable geometry turbine (VGT), and the EGR flow to allow the right amount of EGR from the exhaust to intake manifold. The control objectives are often translated into desired intake manifold pressure and desired EGR by a high level controller. The airpath control problem can therefore be treated as a tracking problem. In achieving the desired intake manifold pressure and desired EGR, the airpath controller also has to consider several physical constraints on the inputs and outputs. This makes the model predictive control (MPC) framework a natural choice for the airpath control design.

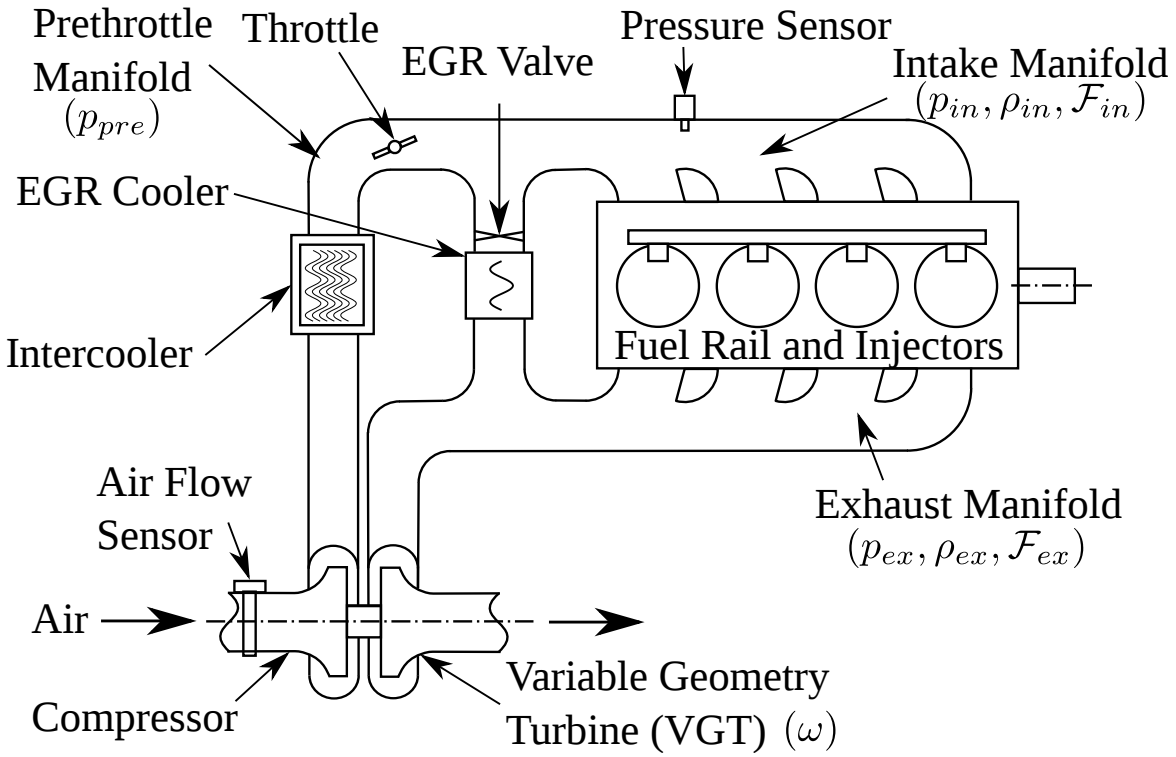

Figure 3.5: 8 state diesel engine airpath diagram. The symbols inside the parentheses indicate the state variables associated with the process.

The efficacy of MPC to the DAP problem was shown in [131]. Recently, MPC has been applied to an 8th order DAP model in [126] and [132]. To reduce computational complexity, an explicit model predictive controller (eMPC) using open-loop model order reduction [132] was demonstrated. The follow-up work [126] applied an explicit rate-based MPC controller [124] using a single reduced order model. However, in [126], [132], and [133], the open-loop model order reduction of [13] is used, which does not consider the control formulation in the reduction process. However, open-loop model order reduction using standard balanced realization and truncation has been shown to be unsuitable for design of robust stable feedback control [105].

In this section, a combined rate-based MPC and state estimator design is considered for the problem of airpath control. The 8th order model for the diesel airpath represents a challenge for both design and real-time implementation, given the limited engine control unit (ECU) computational/memory resources and fast control update. For the DAP control system shown in Fig. 3.5, direct feedthrough is present in the state space equation from the

input (e.g., EGR flow) to the output (EGR rate) [134]. Therefore the transfer function is not strictly proper and previously developed Riccati balanced truncation is necessary.

3.4.1 8 State Diesel Airpath Model

The derivation of the DAP model for control has been discussed extensively in [135], [136], and [137]. The dynamical equations for the engine components are derived through applications of the ideal gas law, conservation of mass, and conservation of energy in an adiabatic process. The equation for the turbine speed is a result from conservation of energy. The eight states present in this model are: three pressures, p, in the intake manifold, the pre-throttle volume, and the exhaust manifold; two densities, ρ, in the intake and exhaust manifold; two burn gas fractions, $\mathcal{F}$, in the intake and exhaust manifolds; and the VGT rotational speed, ω.

The burn gas fraction is defined as the ratio, by density, of the exhaust to the air in a specified volume.

For self-containedness and easy referencing, the equations of the 8th order DAP model from [136] are summarized here:

$$\dot{p}_{in} = \frac{\gamma\mathcal{R}}{\mathcal{V}_{in}}(\mathcal{W}_{c,in}\mathcal{T}_{c,in} + \mathcal{W}_{ex,in}\mathcal{T}_{ex} - \mathcal{W}_{in,eng}\mathcal{T}_{in} - \mathcal{W}_{in,ex}\mathcal{T}_{in} - \frac{\dot{\mathcal{Q}}_{in}}{c_p}), \tag{3.34a}$$

$$\dot{p}_{pre} = \frac{\mathcal{R}}{\mathcal{V}_{pre}}\frac{\mathcal{T}_c + \mathcal{T}_{ic}}{2}(\mathcal{W}_{c,in} - \mathcal{W}_{thr,in}), \tag{3.34b}$$

$$\dot{\omega} = \frac{30^2 c_p}{\pi^2 I_{tc}\omega}(\eta\mathcal{W}_{ex,tur}(\mathcal{T}_{ex} - \mathcal{T}_{tur}) - \mathcal{W}_{c,in}(\mathcal{T}_{c,in} - \mathcal{T}_{amb})), \tag{3.34c}$$

$$\dot{p}_{ex} = \frac{\gamma\mathcal{R}}{\mathcal{V}_{ex}}(\mathcal{W}_{eng,ex}\mathcal{T}_{eng,ex} - \mathcal{W}_{ex,tur}\mathcal{T}_{ex} - \mathcal{W}_{ex,in}\mathcal{T}_{ex} + \mathcal{W}_{in,ex}\mathcal{T}_{in} - \frac{\dot{\mathcal{Q}}_{ex}}{c_p}), \tag{3.34d}$$

$$\dot{\mathcal{F}}_{in} = \frac{\mathcal{W}_{ex,in}(\mathcal{F}_{ex} - \mathcal{F}_{in}) - \mathcal{W}_{c,in}\mathcal{F}_{in}}{\rho_{in}\mathcal{V}_{in}}, \tag{3.34e}$$

$$\dot{\rho}_{ex} = \frac{1}{\mathcal{V}_{ex}}(\mathcal{W}_{eng,ex} - \mathcal{W}_{ex,tur} - \mathcal{W}_{ex,in} + \mathcal{W}_{in,ex}), \tag{3.34f}$$

$$\dot{\rho}_{in} = \frac{1}{\mathcal{V}_{in}}(\mathcal{W}_{c,in} + \mathcal{W}_{in,ex} + \mathcal{W}_{in,eng}), \tag{3.34g}$$

$$\dot{\mathcal{F}}_{ex} = \frac{\mathcal{W}_{eng,ex}(\mathcal{F}_{eng,ex} - \mathcal{F}_{ex})}{\rho_{ex}\mathcal{V}_{ex}}. \tag{3.34h}$$

The definitions of the variables and subscripts used in (3.34) can be found in Table 3.6.

Table 3.6: Variable and subscript definitions.

Parameters	c_p	Specific heat, constant pressure
	η	Turbo charger mechanical efficiency
	γ	Heat capacity ratio
	I_{tc}	Inertia of compressor/turbine
	$\mathcal{R}$	Gas constant
	$\mathcal{V}$	Volumes
Variables	$\dot{\mathcal{Q}}$	Heat transfer rate
	$\mathcal{T}$	Temperature
	$\mathcal{W}_{1,2}$	Flow $\left(\frac{kg}{sm^3}\right)$ from 1 to 2
Subscripts	amb	Ambient
	c	Compressor
	eng	Engine
	ex	Exhaust
	ic	Intercooler
	in	Intake
	pre	Prethrottle
	thr	Throttle
	tur	Turbine

One control input is the VGT actuator (u_{VGT}), which controls the vane angle and dictates the speed of the turbine, and hence of the compressor, to regulate the airflow into the intake manifold. Another input is the EGR valve position (u_{EGR}), which controls the flow from the exhaust manifold to the intake manifold for effective NO_x treatment.

Despite the conceptually simple actuation of the EGR valve position, EGR flow ($\mathcal{W}_{ex,in}$) is chosen as the second control input so that DC-gain reversal can be avoided and a single MPC controller can be used [134]. $\mathcal{W}_{ex,in}$ is inverted using Eq. (12)-(14) from [132] to obtain u_{EGR}. This choice, however, has led to a direct feedthrough in the output equation of the state-space model.

Table 3.7 provides insight into how the inputs, u_{VGT} and u_{EGR}, enter the DAP model. In this model, throttle angle, engine speed (N), and fuel flow ($\mathcal{W}_f$) are treated as known disturbances. As is often desired for diesel engines, the throttle will be kept open as much as possible to reduce pumping losses (throttle closes when increased EGR flow capacity is required) [138].

Table 3.7: Variables, their dependencies, and source equations [136].

Variable	Dependent upon	Governing Laws
$\mathcal{T}_{ic}$	$\mathcal{T}_c$	Temperature Map
$\mathcal{T}_c$	$\mathcal{T}_{amb},\ p_{in},\ p_{ex},\ \eta$	Adiabatic $\mathcal{T}-\mathcal{V}$ relationship
$\mathcal{T}_{c,in}$	$p_{in},\ \omega$	Compressor Isentropic Efficiency Map
$\mathcal{T}_{in}$	$p_{in}=\rho_{in}R\mathcal{T}_{in}$	Ideal Gas Law
$\mathcal{T}_{ex}$	$p_{ex}=\rho_{ex}R\mathcal{T}_{ex}$	Ideal Gas Law
$\mathcal{T}_{tur}$	$p_{ex},\ \mathcal{T}_{ex},\ \omega,\ u_{VGT}$	Turbine Isentropic Efficiency Map
$\mathcal{W}_{c,in}$	$p_{in},\ \omega$	Compressor Flow Map
$\mathcal{W}_{thr,in}$	$p_{in},\ p_{pre}$	Mass Conservation
$\mathcal{W}_{in,eng}$	$\rho_{ex},\ N,\ \mathcal{T}_{in},\ p_{ex}$	Engine Volumetric Efficiency Map
$\mathcal{W}_{in,ex}$	$p_{in},\ p_{ex},\ \rho_{in},\ u_{EGR}$	Orifice Equation
$\mathcal{W}_{ex,in}$	$p_{in},\ p_{ex},\ \rho_{ex},\ u_{EGR}$	Orifice Equation
$\mathcal{W}_{ex,tur}$	$p_{ex},\ \rho_{ex},\ u_{VGT}$	Turbine Flow Map
$\mathcal{W}_{eng,ex}$	$\mathcal{W}_f+\mathcal{W}_{in,eng}$	Engine Mass Conservation
$\mathcal{T}_{eng,ex}$	$\mathcal{T}_{in},\ \mathcal{F}_{in},\ \mathcal{W}_f,\ \mathcal{W}_{in,eng}$	Engine Temperature Rise Map
$\mathcal{F}_{eng,ex}$	$\mathcal{F}_{in},\ \mathcal{W}_f,\ W_{in,eng}$	Stoichiometric Combustion Balance
$\dot{\mathcal{Q}}_{in}$	$\dot{\mathcal{Q}}_{in}=0$	Neglected
$\dot{\mathcal{Q}}_{ex}$	$\dot{\mathcal{Q}}_{ex}=0$	Neglected

3.4.2 Control Objective

The control objective in the following sections is to optimally track set-points for intake manifold pressure and EGR rate, subject to constraints, with a model predictive controller designed with a linear model in real-time. Because of the real-time requirement, the predictive controller will be designed with reduced order linear models.

The outputs of the system are therefore selected as the intake manifold pressure (p_{in}) and EGR rate (ϕ_{EGR}):

$$\phi_{EGR}=\frac{\mathcal{W}_{ex,in}}{\mathcal{W}_{ex,in}+\mathcal{W}_{in,eng}}. \tag{3.35}$$

To apply systematic model order reduction techniques for the system represented by (3.34), linearization is performed for the DAP model at the center of the nominal fuel/engine speed operating range [126]. Table 3.3 summarizes the ordering of inputs, outputs, and states. The inputs are ordered as $u=[u_{VGT}\ u_{EGR}]^\top$ and the outputs are ordered as $y=[p_{in}\ \phi_{EGR}]^\top$.

The tracking objective is combined with the objective to minimize actuator change, and is captured by rate-based MPC problem of (3.30) with a discretized (3.1).

Several conservative constraints for the nonlinear DAP control problem need to be enforced for initial tests. The set of constraints used in this section are given by (3.36):

$$\max\{\bar{y}_{t,1} - c_1, 0\} \leq \quad y_{t,1} \quad \leq 300\ kPa \tag{3.36a}$$

$$\max\{\bar{y}_{t,2} - c_2, 0\} \leq \quad y_{t,2} \quad \leq 50\% \tag{3.36b}$$

$$40\% \leq \quad u_{VGT} \quad \leq 80\% \tag{3.36c}$$

$$0 \leq \quad \mathcal{W}_{ex,in} \quad \leq f_{EGR}^{max}\ \frac{kg}{s} \tag{3.36d}$$

where c_1 and c_2 are positive constants. The EGR flow constraint, f_{EGR}^{max}, is a predefined function of operating conditions (i.e., a function of p_{ex}, p_{in}, and N) that prevents too much EGR flow from being demanded.

3.4.3 Diesel Airpath Simulation Results

To demonstrate the efficacy of a rate-based reduced compensator designed using linear RBT reduced order model, simulations over a "warm start" drive cycle using a Toyota proprietary DAP model and step responses on an experimental setup are presented. The simulation results consist of the plant controlled by a single rate-based compensator and by a gain scheduled rate-based compensator, using engine speed/fuel as the scheduling variables, designed using linearizations of the 8th order plant model, with linear constraints contained within (3.36).

The rate-based compensators consist of the control methodology of [133], an explicit MPC law calculated with the MPT toolbox [139] for output tracking control, and a rate-based Kalman filter. The observer takes the form of a steady-state Kalman filter of (3.31) and (3.32). The compensators are designed using either: the full order (C_I), LBT reduced order (C_{II}), or RBT reduced order (C_{III}) model.

An explicit MPC law takes the form of a linear piecewise affine control (PWA) law:

$$\Delta u_t = [H]_{kl}\hat{\tilde{\mathbf{x}}}_{t|t} + [k]_{kl} \text{ when } \{N, \mathcal{W}_f, \hat{\tilde{\mathbf{x}}}_t\} \in S_{kl}, \tag{3.37}$$

where S_{kl} denotes a convex polyhedron indexed by l in an engine speed/fuel zone indexed by

k, and $[H]_{kl}$ and $[k]_{kl}$ are a matrix and a vector of appropriate size, respectively, that define the PWA.

Single Zone Compensator Simulation Results

A single zone compensator consists of applying one compensator over the entire operating range (i.e., $k = 1$ in (3.37)). For the Toyota proprietary Simulink DAP model used in this study, the restricted operating range considered is engine speed between 750-3000 RPM, and fueling rate between 0-60 $\frac{mm^3}{str}$.

The reduced compensators are designed using a linearization of the Simulink model at the nominal engine speed/fuel operating condition of 1600 RPM/30 $\frac{mm^3}{str}$. The linearization is reduced from 8th to 3rd order, then placed into the augmented system (3.28), where a 5th order reduced compensator is derived. Contained in Fig. 3.6 is the operating range and a portion of the engine speed/fuel trajectory the New European Drive Cycle (NEDC) traverses. Fig. 3.6 also illustrates the partitioning of the operating space (by horizontal and vertical lines) and the operating points at which the linearizations were performed (circles) for the gain scheduled compensator design in the following subsection.

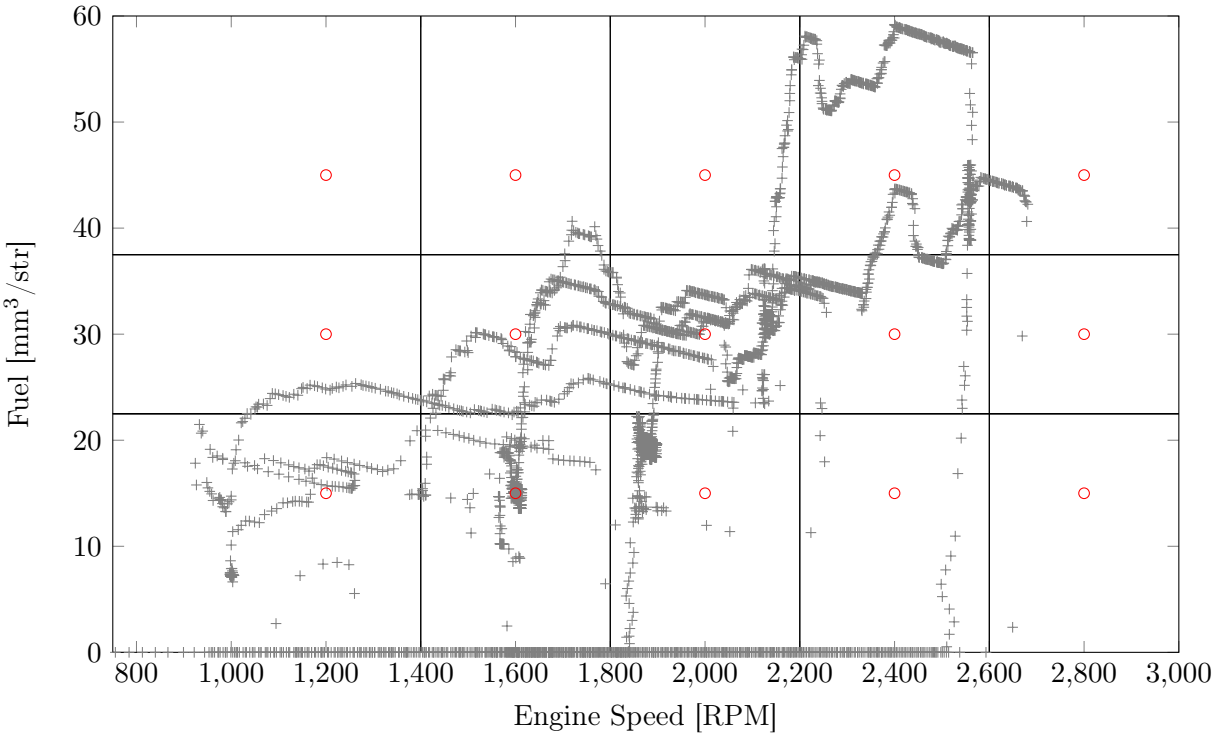

Figure 3.6: Partitioning of engine speed/fuel operating space. The circles denote a linearization point used in the gain scheduled MPC law. '+' indicates points visited by the trajectory when the engine is tested on the NEDC.

The weightings used for the compensator design are provided in Table 3.4. Resulting compensator ROM size, and FLOP count and projected timing estimates are provided in Table 3.8. The timing is predicted on a MPC5644A microcontroller, a moderately specified ECU [140], which has a clock speed of 150 MHz and permits 2 floating point operations per cycle. For the explicit MPC/Kalman filter compensator, Table 3.8 shows a roughly linear reduction in memory and computation.

Results of the output responses and inputs subject to a portion of the NEDC are provided in Fig. 3.7. The following observations are noteworthy:

- As seen in Fig. 3.7(a), 3.7(c), 3.7(e), and 3.7(g), the Full (C_I) and RBT (C_{III}) based compensators have similar performance.
- The LBT based compensator (C_{II}) results in regimes where asymptotic tracking is not achieved. This occurs when the fuel is greater than 45 $\frac{mm^3}{str}$.

- Other than a handful of areas where C_{III} has larger overshoot in the transient, it generally performs better in rise-time, settling time, and overshoot when compared to C_{II}.

- Table 3.8 shows that the 5th order reduced compensator (generated from the 3rd order model) results in over a 40% reduction in computation, which brings it into the realm of computational feasibility on the ECU with a 16 ms sample time.

Table 3.8: Compensator order, ROM size, and worst case FLOPs and computation time for a single zone and gain scheduled controller.

	Single Zone			**Gain Scheduled**		
Order	Size [B]	FLOPs	Time [μs]	Size [B]	FLOPs	Time [μs]
10	6012	3148	19.9	83556	3148	19.9
9	5020	2604	16.5	77192	2874	18.2
8	4648	2360	14.9	71012	2612	16.5
7	4788	2362	14.9	65520	2362	14.9
6	4396	2124	13.4	61076	2124	13.4
5	**4012**	**1898**	**12.0**	**56168**	**1898**	**12.0**
4	3636	1684	10.7	50904	1684	10.7
3	-	-	-	-	-	-

Table 3.9: $\mathcal{N}$ calculated by (3.38) and root mean square (RMS) error between reference and output subject to the portion of the NEDC between 850-1180 seconds.

	Single Zone		**Gain Scheduled**	
Model	$\mathcal{N}$ (10^5)	RMS	$\mathcal{N}$ (10^5)	RMS
C_I	1.3027	1.1070	1.1695	1.1179
C_{II}	2.6138	2.4160	1.5312	1.1582
C_{III}	1.4956	1.1204	1.3463	1.1256

Table 3.9 provides assessment of performance evaluated by (3.38),

$$\mathcal{N} = \sum_{n=1}^{N} (y_n - \bar{y}_{n,\infty})^\top Q (y_n - \bar{y}_{n,\infty}) + \Delta u_n^\top R \Delta u_n, \tag{3.38}$$

where N is the number of time steps used in the simulation, and the root mean square error between the reference and output. The table shows that the RBT (C_{III}) results in a smaller

$\mathcal{N}$, compared to LBT (C_{II}), when applied to the portion of the NEDC between 850-1180 seconds, showing the benefit of using the proposed closed-loop model reduction technique combined with the rate-based formulation.

Gain Scheduled Compensator Simulation Results

A gain scheduled linear compensator consists of partitioning an operating range into multiple zones, and designing a linear compensator for each zone. Gain scheduled MPC is common control technique for applying linear compensators to a nonlinear plant [141].

To control the DAP system, the operating space was partitioned into 15 zones (see Fig. 3.6), and a full or reduced order model was derived using the linearization at the specified point of the operating space.

Using the linearized model derived at the selected conditions, the design of the compensator in each zone was comprised of a rate-based MPC law and a rate-based Kalman filter. For the full order this resulted in a 10th order compensator (8 states + 2 ouputs), and for the reduced order compensators, this resulted in a 5th order compensator (3 states + 2 outputs).

The weightings for the controller in each zone, ($Q_k,\ R_k,\ \Lambda_k,\ \Gamma_k$), are taken to be the ($Q,\ R,\ \Lambda,\ \Gamma$) in Table 3.4. The FLOP count estimate calculates the worst case for zone evaluation ($\{N, \mathcal{W}_f\}$), polyhedra evaluation, control calculation, and compensator evaluation.

Results for the gain scheduled compensators subject to the NEDC are provided in Fig. 3.7 for comparison. The key things of Fig. 3.7(b), 3.7(d), 3.7(f), and 3.7(h) to note are:

- Overall, gain scheduling the compensators resulted in a better response for all compensators.

- Comparing Fig. 3.7(c) and 3.7(d), the gain scheduled MPC results in a smaller transient when fuel cuts occur during shift points.

- The gain scheduled RBT-based compensator (C_{III}) outperforms the LBT-based compensator (C_{II}) for all performance metrics (i.e., rise time, overshoot, and settling time), however, the benefit of RBT becomes less significant compared to the single zone case.

- The gain scheduled LBT-based compensator still has stability issues in the higher fuel regime ($> 45\frac{mm^3}{str}$).

Table 3.9 provides the performance measured by (3.38), and continues to show that the RBT (C_{III}) results in a smaller $\mathcal{N}$ when compared to LBT (C_{II}).

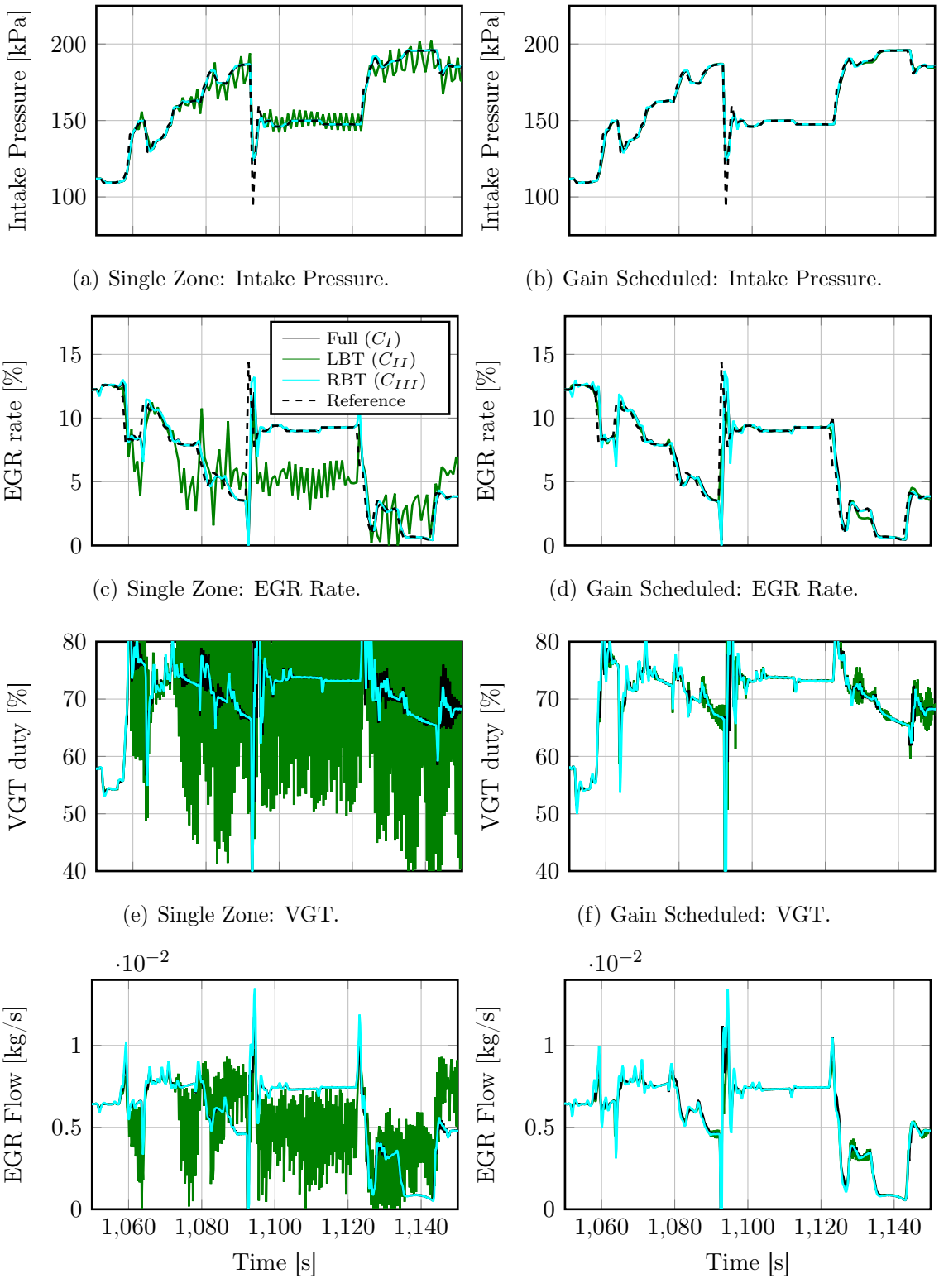

(a) Single Zone: Intake Pressure.

(b) Gain Scheduled: Intake Pressure.

(c) Single Zone: EGR Rate.

(d) Gain Scheduled: EGR Rate.

(e) Single Zone: VGT.

(f) Gain Scheduled: VGT.

(g) Single Zone: EGR Flow.

(h) Gain Scheduled: EGR Flow

Figure 3.7: Simulation results for single zone vs gain scheduled MPC subject to a portion of the NEDC.

3.4.4 Experimental Engine Results

Experiments to compare the reduced compensators on an experimental 3 liter, 4 cylinder diesel Toyota KD engine were carried out on a dynamometer at Toyota Motor Corporation's Higashi-Fuji facility. For engine safety, only small reference step changes were allowed. The reference steps were chosen to keep both intake pressure and EGR rate at the nominal value; then a 20 second step up followed by a step down command was applied to one reference at a time, pictured in Fig. 3.8(a) and 3.8(b).

A linear 7th order system, derived using system identification at 1600 RPM engine speed and 30 mm^3/str fueling rate was used for controller design. From this 7th order model, a 3rd order model was calculated using the method highlighted in Section 3.3.2, and the compensator was reduced from 9th to 5th order.

To decrease actuator motion and to reduce the effective feedback gain of the control, the weight on the control was increased relative to the output weight. Compensators were designed with Q and R weightings:

$$Q = I_{2\times 2},\ R = \mathrm{diag}(100, 10),$$

which places a higher weighting on intake pressure, but approximately equal emphasis on both actuator inputs due to scale. Fig. 3.8 provides the results for the two reduced compensators: C_{II} and C_{III}. It can be seen that C_{III} results in better performance in terms of overshoot and disturbance rejection (Fig. 3.8(a) and 3.8(b)), and the amount of control input (Fig. 3.8(c) and 3.8(d)).

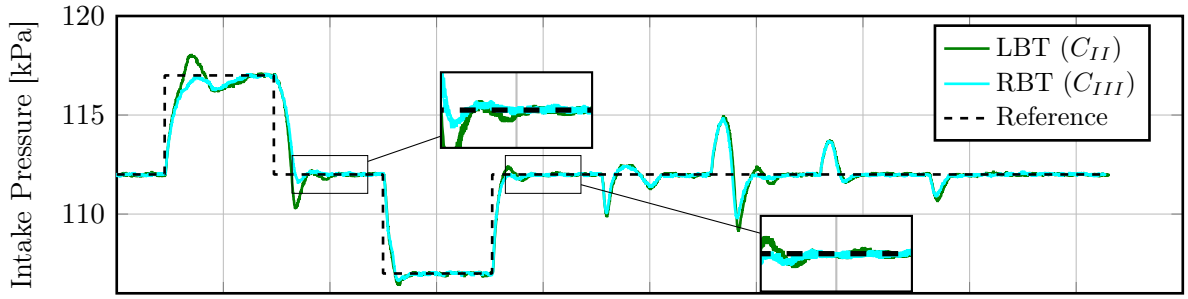

(a) Weighting I: Intake Pressure.

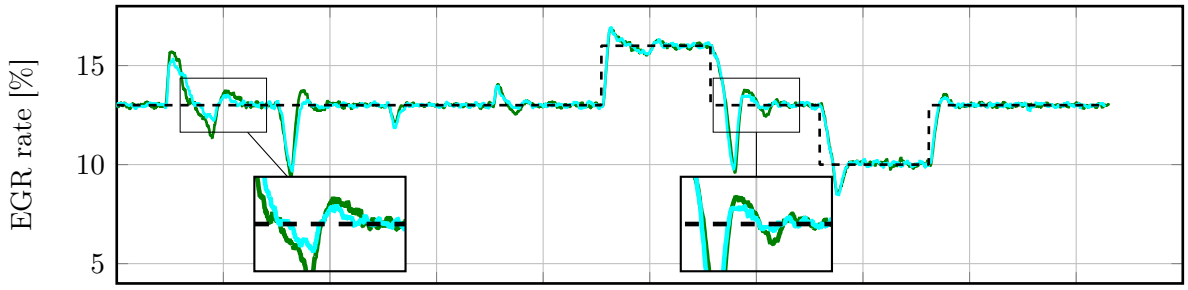

(b) Weighting I: EGR Rate.

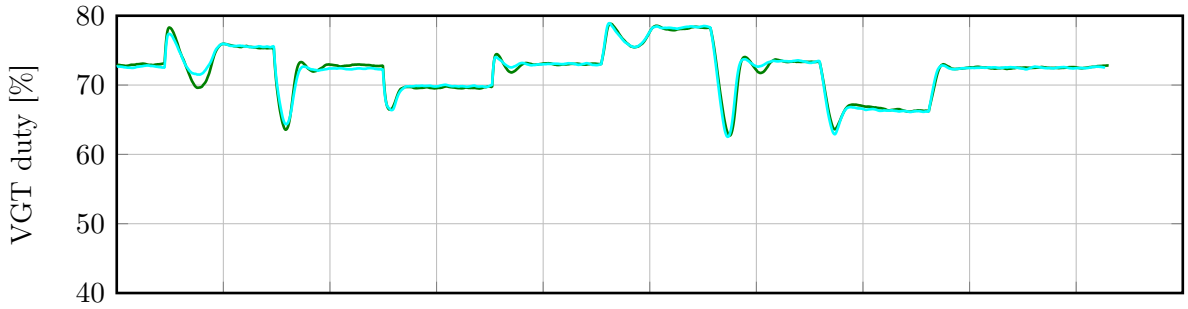

(c) Weighting I: VGT.

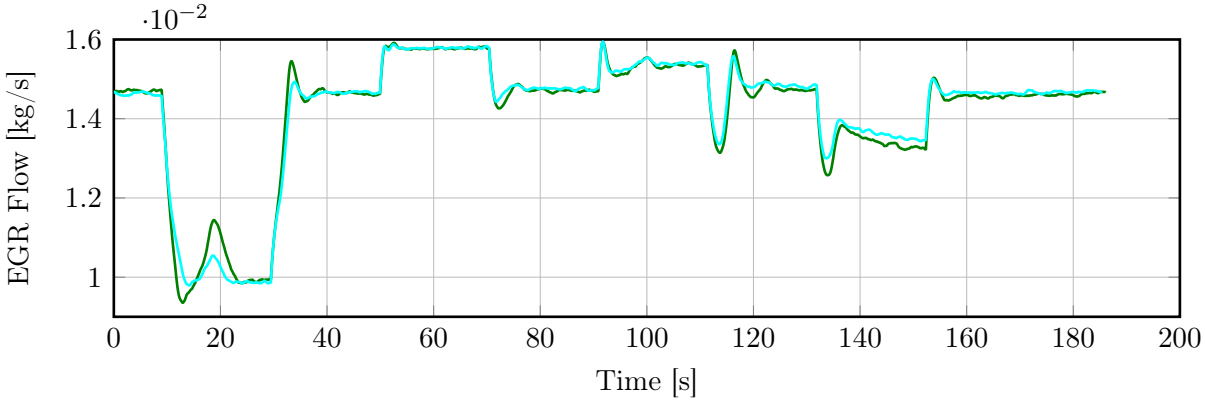

(d) Weighting I: EGR Flow.

Figure 3.8: Comparison of experimental results using different 3rd order models for controller design.

3.5 Conclusions

The chapter provides an extension of the closed-loop model order reduction given by [3] to account for the direct feedthrough from input to output, and non-normalized LQ weights in the optimized cost function and is called Riccati balanced truncation (RBT). An algorithm to compute approximate RBT of large scale descriptor systems is proposed using low-rank matrix square root factors of Riccati solutions. The link between unconstrained infinite time LQR and finite time MPC cost function was exploited to adapt closed-loop model order reduction to MPC through the use of a terminal state penalty.

A rate-based MPC law designed using RBT reduced model is used to control a nonlinear diesel airpath (DAP) model in real-time, demonstrating the benefit of using an estimator and MPC designed with the proposed closed-loop Riccati balanced truncation over the open-loop reduction technique.

The MPC controllers were applied to a linear plant with reference steps, a Toyota proprietary model running the New European Drive Cycle (NEDC), and to an experimental engine with reference steps. When compared to the popular Lyapunov balanced truncation applied to the DAP problem [133], the proposed reduction technique in the MPC/Kalman filter framework is shown to provide a simpler, more accurate and robust controller in terms of measurement-to-control, dynamic tracking, and disturbance rejection, while requiring less actuator movement. For the DAP system, this could translate to reduced emissions and particulate matter, as well as actuator wear and tear.

Chapter 4

Model Order Reduction for Constrained Linear Systems

To optimally control a hard constrained system in an effective manner in real-time, models are often required. An optimal control methodology that uses a model and can naturally account for constraints is model predictive control (MPC). For hard constrained linear systems, two techniques to calculate an MPC law are explicit MPC, a MPC law whose solution is a pre-computed piecewise linear control law [127], and on-line MPC (or implicit MPC), solving a constrained quadratic program at each step [142]. However, it has been demonstrated that model complexity often dictates the applicability of MPC to real-time systems, whether it be for explicit or on-line MPC [33, 38, 142].

Reducing MPC computational complexity often necessitates using model order reduction. Explicit MPC may have many piecewise terms, and removing a single state may result in reduction of both storage and computational complexity by several orders of magnitude (particularly for long prediction horizons and for systems with many states) [143]. Given a system with a prediction horizon N_p, m control inputs, and p outputs, reducing the number of states from n to r results in the complexity of an on-line MPC law obtained with a multi-stage interior point method going from $O(N_p(n+m+p)^3)$ to $O(N_p(r+m+p)^3)$ [38]. Therefore, various forms of MPC stand to lose much complexity by the reduction of the model.

However, reduced order models result in modeling errors [13]. These modeling errors

effect the constraint enforcement, stability, and feasibility of MPC [120, 144].

Over the past two decades MPC has matured to deal with model errors and disturbances using a variety of approaches that fall under the name robust MPC [145, 146, 147, 148, 149]. Some robust controller techniques include: constraint tightening [36, 150], transforming hard constraints into soft constraints [33, 151], and barrier functions [152].

For the purpose of handling hard constrained systems with controllers designed using reduced order models, the modeling errors recently have been treated as disturbances (both unknown and constant) and have been handled in command governor and robust MPC frameworks [34, 35, 36, 38]. While all techniques highlight the importance and possibility of reduced models for control, these techniques either incur some conservativeness, by decreasing the size of the admissible outputs and controls, or additional computational complexity.

Focusing on MPC, [36] proposed using tube MPC, and constraint tightening based on the error between a model and a reduced model obtained by truncation; [38] extends the idea to robust output feedback MPC and provides conditions of when robustness can be guaranteed for arbitrary models. However, no work has been reported on how to perform model order reduction for the control and estimation of constrained systems.

In this chapter, the "truncated states as disturbances" idea of [36] is employed to develop a reduced order output feedback MPC law with the framework of [146]. The results of [38] are used to provide robust stability, constraint satisfaction, and feasibility. Under the assumption that the reduced order model is obtained by residualization [17], the technique of [153] is used to provide tracking of a step reference. For consistency with Chapters 2 and 3, residualization is developed for continuous and discrete linear descriptor systems.

With knowledge of the controller and estimator (compensator), this chapter also proposes an optimization problem to yield a reduced order model, obtained from the full order model, for reduced compensator design that satisfies the hard constraints of the full order system. Employing robust output feedback MPC with a linear quadratic cost and a constant tube, and a reduced order model obtained by residualization, a solution methodology is proposed. A simple example is used to demonstrate that the proposed reduction problem can yield reduced controllers that are both more accurate and less conservative than those designed with models obtained using [3] and [13].

The chapter is structured as follows: Section 4.1 provides background on robust MPC. Section 4.2 forms the problem of MPC with reduced models, reduced tightened constraint sets, and some properties. Section 4.3 presents an optimization problem to be solved, proposes abstract and concrete formulations of a coupled reduction/constraint tightening problem. Section 4.4 demonstrates the efficacy of the proposed reduction to the design of a reduced MPC law using a simple tube. Finally, Section 4.5 provides conclusions of the chapter.

4.1 Constant Tube Robust MPC

This presentation of the background material follows that of [146] for constant tube robust output feedback MPC.

4.1.1 Nomenclature and Definitions

Given two sets $\mathcal{F},\ \mathcal{G} \in \mathbb{R}^q$, the Minkowski Sum is defined as $\mathcal{F} \oplus \mathcal{G} = \{x \in \mathbb{R}^q | x = a+b, a \in \mathcal{F},\ b \in \mathcal{G}\}$; and the Pontryagin difference is $\mathcal{F} \sim \mathcal{G} = \mathcal{F} \ominus \mathcal{G} = \{x \in \mathbb{R}^q | x + b \in \mathcal{F},\ b \in \mathcal{G}\}$. Given a matrix $K \in \mathbb{R}^{m \times q}$, and a set $\mathcal{F} \in \mathbb{R}^q$, matrix set multiplication is defined as: $K\mathcal{F} = \{x \in \mathbb{R}^m | x = Ka, a \in \mathcal{F}\}$. Provided with a scalar $\alpha \in \mathbb{R}$, $\alpha\mathcal{F} = \alpha I_{q \times q}\mathcal{F}$, where $I_{q \times q}$ is the identity matrix of dimension q. The distance between sets $\mathcal{F},\ \mathcal{G}$ is defined as $d(\mathcal{F}, \mathcal{G}) = \inf_{f \in \mathcal{F},\ g \in \mathcal{G}} ||f - g||$. The spectral radius, the maximum modulus of the eigenvalues, of a matrix $A \in \mathbb{R}^{n \times n}$ is given by $\rho(A)$, and A is said to be asymptotically stable if $\rho(A) < 1$.

Definition 4.1.1 (Positive Invariant Set)**.** *A set $\Omega \subset \mathbb{R}^n$ is a positively invariant set for $x_{t+1} = f(x_t)$ if $f(x_t) \in \Omega$ for all $x_t \in \Omega$.*

Definition 4.1.2 (Robust Positive Invariant Set)**.** *A set $\Omega \subset \mathbb{R}^n$ is a robust positively invariant (RPI) set for $x_{t+1} = f(x_t, w_t)$ if $f(x_t, w_t) \in \Omega$ for all $x_t \in \Omega$, $w_t \in \mathcal{W}$.*

Let $g(x_t)$ denote a feedback control law.

Definition 4.1.3 (Robust Stability)**.** *A set Ω is said to be robustly stable if given the $x_{t+1} = f(x_t, u_t, w_t)$, with $x_t \in \mathcal{X}$, $u_t = g(x_t) \in \mathcal{U}$, $w_t \in \mathcal{W}$; then $\lim_{t \to \infty} d(x_t, \Omega) = 0$.*

Definition 4.1.4 (Robust Constraint Fulfillment)**.** *If the system* $x_{t+1} = f(x_t, u_t, w_t)$*,* $y_t = h(x_t, u_t, v_t)$*, with* $x_t \in \mathcal{X}$*,* $u_t = g(x_t) \in \mathcal{U}$*,* $w_t \in \mathcal{W}$*,* $v_t \in \mathcal{V}$*, satisfies all hard constraints at each time instance; then the controller is said to satisfy constraints robustly.*

4.1.2 Output Feedback Robust MPC

The goal of robust output feedback MPC is to calculate a control law that robustly satisfies constraints and robustly stabilizes a system with input and output disturbances. Using a general MPC formulation, this is often achieved using a nominal model, an estimator, and robust positively invariant sets.

To build up the problem, assume that the minimal linear system with sufficiently small input and output disturbances, w_t and v_t, respectively, is provided

$$\Sigma : \begin{cases} x_{t+1} &= Ax_t + Bu_t + w_t, \\ y_t &= Cx_t + Du_t + v_t, \end{cases} \tag{4.1}$$

where $x_t \in \mathcal{X} \subset \mathbb{R}^n$, $u_t \in \mathcal{U} \subset \mathbb{R}^m$, $y \in \mathcal{Y} \subset \mathbb{R}^p$, $w_t \in \mathcal{W}$, $v_t \in \mathcal{V}$ for all t, and $\mathcal{X}, \mathcal{U}, \mathcal{Y}$, $\mathcal{W}$, $\mathcal{V}$ are all convex and compact sets that contain the origin.

Omitting the disturbances, the nominal system is given by

$$\bar{\Sigma} : \begin{cases} \bar{x}_{t+1} &= A\bar{x}_t + B\bar{u}_t, \\ \bar{y}_t &= C\bar{x}_t + D\bar{u}_t. \end{cases} \tag{4.2}$$

Given an output injection, $L \in \mathbb{R}^{n \times p}$, such that $\rho(A + LC) < 1$, the estimator is

$$\hat{\Sigma} : \begin{cases} \hat{x}_{t+1} &= A\hat{x}_t + B\hat{u}_t + L(y_t - \hat{y}_t), \\ \hat{y}_t &= C\hat{x}_t + D\hat{u}_t. \end{cases} \tag{4.3}$$

Define the errors between the estimated and nominal state, and actual and estimated state to be

$$e_t = \hat{x}_t - \bar{x}_t, \tag{4.4}$$

$$\tilde{x}_t = x_t - \hat{x}_t, \tag{4.5}$$

such that

$$x_t = \bar{x}_t + e_t + \tilde{x}_t.$$

Assume that there exist a feedback gain and output injection, $K \in \mathbb{R}^{m\times n}$ and $L \in \mathbb{R}^{n\times p}$, such that $\rho(A + BK) < 1$ and $\rho(A + LC) < 1$ (i.e., asymptotically stabilizing the nominal system). Separate the control u_t into feedforward and feedback parts:

$$u_t = \bar{u}_t + Ke_t \tag{4.6}$$

where $\bar{u}_t$ is calculated from the MPC law. Substituting $\hat{u}_t = u_t$,

$$\begin{aligned} e_{t+1} &= (A + BK)e_t + L(C\tilde{x}_t + v_t), && (4.7)\\ \tilde{x}_{t+1} &= (A + LC)\tilde{x} + w_t - Lv_t. && (4.8) \end{aligned}$$

Robust positively invariant sets $\bar{\mathcal{S}}$ and $\tilde{\mathcal{S}}$ are sought to bound the errors $e_t \in \bar{\mathcal{S}}$ and $\tilde{x}_t \in \tilde{\mathcal{S}}$, so that the original input, state, and output constraints may be tightened. Let

$$\begin{aligned} \tilde{\delta}_t &= w_t - Lv_t, && (4.9a)\\ \bar{\delta}_t &= LC\tilde{x}_t + Lv_t, && (4.9b) \end{aligned}$$

and define

$$\tilde{\Delta} = \mathcal{W} \oplus (-L\mathcal{V}). \tag{4.10}$$

Then because $\rho(A + LC) < 1$, and all sets are compact and contain the origin, there exist an RPI set, $\tilde{\mathcal{S}}$, that is compact, non-empty, and contains the origin, such that $\tilde{\mathcal{S}}$ satisfies

$$(A + LC)\tilde{\mathcal{S}} \oplus \tilde{\Delta} \subseteq \tilde{\mathcal{S}}. \tag{4.11}$$

Similarly define

$$\bar{\Delta} = LC\tilde{\mathcal{S}} \oplus L\mathcal{V}, \tag{4.12}$$

and because $\rho(A + BK) < 1$, and all sets are compact and contain the origin, there exist an

RPI sets, $\bar{\mathcal{S}}$, that is compact, non-empty, and contains the origin, such that $\bar{\mathcal{S}}$ satisfies

$$(A + BK)\bar{\mathcal{S}} \oplus \bar{\Delta} \subseteq \bar{\mathcal{S}}. \tag{4.13}$$

Define

$$\mathcal{S} = \tilde{\mathcal{S}} \oplus \bar{\mathcal{S}}, \tag{4.14}$$

then the following results naturally arise:

1. If $\tilde{x}_0 \in \tilde{\mathcal{S}}$, then $\tilde{x}_t \in \tilde{\mathcal{S}}$ and $x_t \in \hat{x}_t \oplus \tilde{\mathcal{S}}$ for all $t > 0$.
2. If $e_0 \in \bar{\mathcal{S}}$, then $e_t \in \bar{\mathcal{S}}$ and $\hat{x}_t \in \bar{x}_t \oplus \bar{\mathcal{S}}$ for all $t > 0$.
3. If $e_0 \in \bar{\mathcal{S}}$, $\tilde{x}_0 \in \tilde{\mathcal{S}}$, $\bar{\mathbf{u}} = \{\bar{u}_t\}_{t=0,1,\ldots}$, and $u_t \in \mathcal{U}$ is given by (4.6), then $x_t \in \hat{x}_t \oplus \tilde{\mathcal{S}} \subseteq \bar{x}_t \oplus \mathcal{S}$ for $t > 0$.

While $\tilde{\mathcal{S}}$ and $\bar{\mathcal{S}}$ are guaranteed to exist, they are dependent on the choice of K and L. Further, if $\bar{\mathcal{S}} \oplus \tilde{\mathcal{S}} \not\subset \mathcal{X}$, $K\bar{\mathcal{S}} \not\subset \mathcal{U}$, and/or $(C + DK)\mathcal{S} \not\subset \mathcal{Y}$, then the control will be infeasible. Linear programming problems exist to check if $\mathcal{W}$ and $\mathcal{V}$ are sufficiently small and a feasible tightened sets exist [154, Chapter 3].

With the RPI sets, the tightened input, state, and output constraints are, respectively:

$$\bar{\mathcal{U}} = \mathcal{U} \ominus K\bar{\mathcal{S}}, \tag{4.15a}$$

$$\bar{\mathcal{X}} = \mathcal{X} \ominus \mathcal{S}, \tag{4.15b}$$

$$\bar{\mathcal{Y}} = \mathcal{Y} \ominus (C + DK)\mathcal{S}. \tag{4.15c}$$

These tightened sets facilitate the output feedback robust MPC problem. Let N_p be the prediction horizon, define $\bar{\mathbf{x}}(\hat{x}_t) = \{\bar{x}_t, \ldots, \bar{x}_{t+N_p}\}$ to be the sequence of states generated by (4.2) subject to $\bar{\mathbf{u}}$ and $\bar{x}_t \in \hat{x}_t \oplus \tilde{\mathcal{S}}$. Then given the linear quadratic cost

$$J_f(\bar{\mathbf{x}}(\hat{x}_t), \bar{\mathbf{u}}) = \bar{x}_{t+N_p}^\top P \bar{x}_{t+N_p} + \sum_{i=t}^{t+N_p-1} \bar{y}_i^\top Q \bar{y}_i + \bar{u}_i^\top R \bar{u}_i, \tag{4.16}$$

where $Q = Q^\top \geq 0$, $R = R^\top > 0$, $P = P^\top \geq 0$, the MPC law is determined by the solution to

$$\begin{aligned}(\bar{x}_t^*, \bar{\mathbf{u}}^*) = \arg\min_{\{\bar{x}_t, \bar{\mathbf{u}}\}} \quad & J_f(\bar{\mathbf{x}}(\hat{x}_t), \bar{\mathbf{u}}). \\ s.t \quad & (4.2),\ \bar{u}_i \in \bar{\mathcal{U}},\ \bar{y}_i \in \bar{\mathcal{Y}} \\ & \bar{x}_t \in \hat{x}_t \oplus \tilde{\mathcal{S}}, \bar{x}_j \in \bar{\mathcal{X}},\ j \in \{t+1, \ldots, t+N_p\}\end{aligned} \tag{4.17}$$

and the control at time t is calculated by (4.6).

As previously mentioned, if n is high order, the MPC problem may not be calculable in real-time. In order to meet the real-time requirement, an MPC law derived from a reduced order model may be used. A reduced order model, however, will introduce modeling error, and modeling error can cause a variety of issues in this form of MPC: suboptimal control policy, steady state error, and constraint violation. A suboptimal control policy cannot be overcome, however, constraint violation may be handled in a robust MPC framework.

4.2 Reduced Output Feedback MPC

Reduced order output feedback MPC law (ROOFMPC) is concerned with controlling the full order model with a output feedback MPC law designed with a reduced order model. The ROOFMPC law is represented by $g(\hat{x}_{r,t})$, where $\hat{x}_{r,t}$ is the estimated reduced state. $g(\hat{x}_{r,t})$ should satisfy similar requirements presented in [155] for robust MPC, with small modifications:

R1 Σ controlled by $u_t = g(\hat{x}_{r,t})$, should satisfy constraints $\mathcal{U}$, $\mathcal{X}$, and $\mathcal{Y}$ at all time $t \geq 0$, and

R2 $\lim_{t\to\infty} g(\hat{x}_{r,t}) - K_{f,t}x_t = 0$, where $K_{f,t}$ is the unconstrained MPC gain that minimizes J_f [141].

Satisfaction of R1 yields a control law that does not destabilize the system, and satisfaction of R2 provides an MPC law that tends to the desired control and target.

This approach follows that of [36] with the difference that constant tube MPC, the robust output feedback MPC framework of [146] presented in the previous section, and arbitrary

convex polytope state constraints are employed. Assume that Σ has been transformed by $\mathscr{T}$, partitioned, and rearranged into

$$\Sigma : \begin{cases} x_{r,t+1} &= A_r x_{r,t} + B_r u_t + ((A_{11} - A_r)x_{r,t} + A_{12}\theta_t + (B_1 - B_r)u_t), \\ \theta_{t+1} &= A_{21}x_{r,t} + A_{22}\theta_t + B_2 u_t, \\ y_t &= C_r x_{r,t} + D_r u_t + ((C_1 - C_r)x_{r,t} + C_2\theta_t + (D - D_r)u_t), \end{cases} \tag{4.18}$$

with the additional assumptions that A_{22} is stable, and the nominal reduced order system (4.19) is minimal:

$$\bar{\Sigma}_r : \begin{cases} \bar{x}_{r,t+1} &= A_r \bar{x}_{r,t} + B_r \bar{u}_t, \\ \bar{y}_{r,t} &= C_r \bar{x}_{r,t} + D_r \bar{u}_t. \end{cases} \tag{4.19}$$

Define

$$w_t = (A_{11} - A_r)x_{r,t} + A_{12}\theta_t + (B_1 - B_r)u_t, \tag{4.20a}$$

$$v_t = (C_1 - C_r)x_{r,t} + C_2\theta_t + (D - D_r)u_t, \tag{4.20b}$$

and note that all of the constraints, $\mathcal{U}$, $\mathcal{X}$, and $\mathcal{Y}$ may be put into the general form: $\mathcal{P} = \{(x,u)|[E_x \ E_u][x^\top \ u^\top]^\top \leq F\}$, with the proper basis selected for $x = [x_{r,t}^\top, \theta_t^\top]^\top$. The "disturbance" sets are defined by the affine map

$$\mathcal{W} = \begin{bmatrix} A_{11} - A_r & A_{12} & B_1 - B_r \end{bmatrix} \mathcal{P} \tag{4.21}$$

$$\mathcal{V} = \begin{bmatrix} C_1 - C_r & C_2 & D - D_r \end{bmatrix} \mathcal{P} \tag{4.22}$$

Form error and estimator dynamics of $\tilde{\Sigma}$ with $[K \ 0]$, $[L^\top 0^\top]^\top$ as in (4.7) and (4.8), respectively:

$$\tilde{\Sigma} : \begin{cases} \begin{bmatrix} x_{r,t+1} \\ \theta_{t+1} \end{bmatrix} = \begin{bmatrix} A_r & 0 \\ A_{21} & A_{22} \end{bmatrix} \begin{bmatrix} x_{r,t} \\ \theta_t \end{bmatrix} + \begin{bmatrix} B_r \\ B_2 \end{bmatrix} u_t + \begin{bmatrix} I_{r\times r} \\ 0 \end{bmatrix} w_t, \\ y_t = C_r x_{r,t} + D_r u_t + v_t, \end{cases} \tag{4.23}$$

with $u_t = Kx_{r,t}$, and calculate the associated RPI sets $\tilde{\mathcal{S}}$, $\bar{\mathcal{S}}$, and $\mathcal{S}$. Following the assumptions that A_{22} and $\bar{\Sigma}_r$ are stable, and all the sets are compact and contain the origin, $\tilde{\mathcal{S}}$, then $\bar{\mathcal{S}}$,

and $\mathcal{S}$ are guaranteed to exist [156].

Let $\mathcal{F} = \{f \in \mathbb{R}^n | E_f f \leq F\}$, define the projection operator, $\text{Proj}_r(\mathcal{F}) = \{f_r \in \mathbb{R}^r | E_f [I_{r\times r}^\top \ 0^\top]^\top f_r \leq F\}$. Assuming that $\mathcal{U}$ and $\mathcal{X}$ are not dependent (i.e., the combined constraints are represented by the Cartesian product $\mathcal{X} \times \mathcal{U}$), the constant tube constraints then become:

$$\bar{\mathcal{U}}_r = \mathcal{U} \ominus K\text{Proj}_r(\bar{\mathcal{S}}), \tag{4.24a}$$

$$\bar{\mathcal{X}}_r = \text{Proj}_r(\mathcal{P} \ominus \mathcal{S}), \tag{4.24b}$$

$$\bar{\mathcal{Y}}_r = \mathcal{Y} \ominus ((C_r + D_r K)\text{Proj}_r(\mathcal{S})). \tag{4.24c}$$

To define the MPC problem, let $\bar{\mathbf{u}}$ be a sequence of controls, $\bar{\mathbf{x}}_r(\hat{x}_t) = \{\bar{x}_{r,t}, \ldots, \bar{x}_{r,t+N_p}\}$ be the response of nominal reduced order model, (4.19), subject to $\bar{\mathbf{u}}$ and $\bar{x}_{r,t} \in \hat{x}_{r,t} \oplus \text{Proj}_r(\tilde{\mathcal{S}})$. Select the linear quadratic cost for tracking

$$\begin{aligned} J_r(\bar{\mathbf{x}}_r(\hat{x}_{r,t}), \bar{\mathbf{u}}) &= (\bar{x}_{r,t+N_p} - \bar{x}_{r,t,\infty})^\top P(\bar{x}_{r,t+N_p} - \bar{x}_{r,t,\infty}) \\ &+ \sum_{i=t}^{t+N_p-1} (\bar{y}_i - \bar{y}_{t,\infty})^\top Q(\bar{y}_i - \bar{y}_{t,\infty}) + (\bar{u}_i - \bar{u}_{t,\infty})^\top R(\bar{u}_i - \bar{u}_{t,\infty}), \end{aligned} \tag{4.25}$$

where $\bar{y}_{t,\infty}$ is the reference, $\bar{u}_{t,\infty}$ is the control required to achieve the reference (of the nominal system), and $\bar{x}_{r,t,\infty}$ is the corresponding steady state of the nominal reduced order model. The tracking ROOFMPC law is determined by the solution to

$$\begin{aligned} (\bar{x}^*_{r,t}, \bar{\mathbf{u}}^*) = \arg \min_{\{\bar{x}_{r,t}, \bar{\mathbf{u}}\}} \quad & J_r(\bar{\mathbf{x}}(\hat{x}_{r,t}), \bar{\mathbf{u}}), \\ s.t \quad & (4.2),\ \bar{u}_i \in \bar{\mathcal{U}}_r,\ \bar{y}_i \in \bar{\mathcal{Y}}_r \\ & \bar{x}_{r,t} \in \hat{x}_{r,t} \oplus \text{Proj}_r(\tilde{\mathcal{S}}), \bar{x}_{r,j} \in \bar{\mathcal{X}}_r,\ j \in \{t+1, \ldots, t+N_p\} \end{aligned} \tag{4.26}$$

where the control at time t is calculated by (4.6).

With the robust MPC formulation and the constraint tightening technique proposed for reduced order models, and the assumptions of [38] for the controller and adapting it to the above scenario, Theorem 4.2.1 and 4.2.2 state the conditions required for robust constraint

satisfaction, stability, and feasibility assuming $\bar{y}_{t,\infty} = 0$ (i.e. a regulating problem). Theorem 4.2.3 provides asymptotic tracking of reference steps subject to standard assumptions.

Theorem 4.2.1 (Robust Constraint Satisfaction)**.** *Suppose $\bar{y}_{t,\infty} = 0$, $x_0 \in \mathcal{X}$, $y_0 \in \mathcal{Y}$, the initial system, observer, and nominal system states are in $\mathrm{Proj}_r(\mathcal{P})$ and the reduced state satisfies $\tilde{x}_{r,0} = x_{r,0} - \hat{x}_{r,0} \in \mathrm{Proj}_r(\tilde{\mathcal{S}})$ and $e_{r,0} = \hat{x}_{r,0} - \bar{x}_{r,0} \in \mathrm{Proj}_r(\bar{\mathcal{S}})$. Then $x_{r,0} \in \bar{x}_{r,0} \oplus \mathrm{Proj}_r(\mathcal{S})$. If, in addition, initial state $\bar{x}_{r,0}$ and the control sequence $\bar{\mathbf{u}} = \{\bar{u}_0, \ldots, \bar{u}_{N_p-1}\}$ of the nominal system satisfy the tighter constraints $\bar{y}_{r,t} \in \mathcal{Y} \ominus ((C_r + D_r K)\mathrm{Proj}_r(\mathcal{S})) = \bar{\mathcal{Y}}_r$ and $\bar{u}_t \in \mathcal{U} \ominus K\mathrm{Proj}_r(\bar{\mathcal{S}})$ for all $t > 0$, then the output y_t and control u_t from (4.1) of Σ satisfy the original constraints $\mathcal{U}$, $\mathcal{X}$, and $\mathcal{Y}$, for all $t > 0$ and admissible truncated states.*

Proof. See Appendix A.3.1 for the proof. □

Theorem 4.2.2 (Robust Stability)**.** *Suppose $\bar{y}_{t,\infty} = 0$, $x_0 \in \mathcal{X}$, $y_0 \in \mathcal{Y}$, $\bar{x}_{r,t+i|t}$ (the predicted state from $\bar{x}_{r,t}$) is bounded given the control sequence $\bar{\mathbf{u}}$, then the set $\mathrm{Proj}_r(\bar{\mathcal{S}}) \times \mathrm{Proj}_r(\tilde{\mathcal{S}})$ is robustly exponentially stable for Σ controlled with the ROOFMPC law/estimator with a region of attraction $(\mathrm{Proj}_r(\bar{\mathcal{X}}_r) \oplus \mathrm{Proj}_r(\bar{\mathcal{S}})) \times \mathrm{Proj}_r(\tilde{\mathcal{S}})$ and any state $x_{r,0} = \hat{x}_{r,0} + \tilde{x}_{r,0}$ such that $(\hat{x}_{r,0}, \tilde{x}_{r,0}) \in \bar{\mathcal{Y}}_r \oplus (C_r + D_r K)\mathrm{Proj}_r(\bar{\mathcal{S}})$ is robustly steered to $\mathrm{Proj}_r(\mathcal{S})$ exponentially fast while satisfying input, state, and output constraints.*

Proof. See Appendix A.3.2 for the proof. □

Just like [146], if the assumptions continue to hold the ROOFMPC problem of (4.26) is recursively feasible.

Remark 4.2.1. *The condition $e_0 = \hat{x}_0 - \bar{x}_0 \in \mathrm{Proj}_r(\bar{\mathcal{S}})$ may be challenging to satisfy at the beginning, and can prove to be problematic to the stability of the reduced compensator.*

4.2.1 Residualization of Linear Descriptor Systems

If $\bar{y}_{t,\infty} \neq 0$, i.e. a tracking problem, the reduced order model should match the DC-gain of the full order model, otherwise R2 cannot be satisfied. This means that the residualization reduced order model must be used.

Residualization uses the notion of singular perturbations of a system [17, 157]. Singular perturbations is often implemented by transforming and partitioning the system into slow

and fast states. Assuming the fast states tend rapidly to a steady state, the fast states are approximated using an algebraic relation and are solved for as functions of the slow states [58].

For model order reduction, the slow-fast separation is not necessarily a good design paradigm, and a transformation, $\mathscr{T}$, calculated from quantities such as gramians or Riccati solutions, like in Algorithms 2.1 or 3.1, respectively, is employed. For consistency with Chapter 2 and 3, Algorithm 4.1 provides residualized reduced order model of a realization transformed by $\mathscr{T}$ for continuous and discrete time linear descriptor systems (under certain conditions). Appendix B contains constructive derivations of singular perturbations of continuous and discrete time descriptor systems.

Algorithm 4.1 Residualization of a linear system with a transformation, $\mathscr{T}$.

1: **procedure** LINEAR_SING_PERTURB($\mathscr{T}, (\tilde{E}, \tilde{A}, \tilde{B}, \tilde{C}, \tilde{D}), x_0, r$)
Require: $\mathscr{T}$ invertible
2: Apply the similarity transformation $\mathfrak{T}$

$$\Sigma_{\mathcal{L}} : (E, A, B, C, D) = (\mathscr{T}^{-1}\tilde{E}\mathscr{T}, \mathscr{T}^{-1}\tilde{A}\mathscr{T}, \mathscr{T}^{-1}\tilde{B}, \tilde{C}\mathscr{T}, \tilde{D})$$

3: Partition $\Sigma_{\mathcal{L}}$ as in (2.7)
4: Define

$$W = \begin{bmatrix} I_{r\times r} & 0 \end{bmatrix}$$

5: **if** (E, A, B, C, D) is a continuous time system, **then**
6: Assume E_{11} and $E_{21}E_{11}^{-1}A_{12} - A_{22}$ are invertible.
7: Residualize

$$\begin{aligned}
E_r &= E_{11}, && (4.27a)\\
A_r &= A_{11} + A_{12}(E_{21}E_{11}^{-1}A_{12} - A_{22})^{-1}(A_{21} - E_{21}E_{11}^{-1}A_{11}), && (4.27b)\\
B_r &= B_1 + A_{12}(E_{21}E_{11}^{-1}A_{12} - A_{22})^{-1}(B_2 - E_{21}E_{11}^{-1}B_1), && (4.27c)\\
C_r &= C_1 + C_2(E_{21}E_{11}^{-1}A_{12} - A_{22})^{-1}(A_{21} - E_{21}E_{11}^{-1}A_{11}), && (4.27d)\\
D_r &= D + C_2(E_{21}E_{11}^{-1}A_{12} - A_{22})^{-1}(B_2 - E_{21}E_{11}^{-1}B_1). && (4.27e)
\end{aligned}$$

8: **else**
9: Assume $E_{22} - A_{22}$ and $E_{11} + (A_{12} - E_{12})(E_{22} - A_{22})^{-1}E_{21}$ are invertible.
10: Residualize

$$\begin{aligned}
E_r &= E_{11} + (A_{12} - E_{12})(E_{22} - A_{22})^{-1}E_{21}, && (4.28a)\\
A_r &= A_{11} + (A_{12} - E_{12})(E_{22} - A_{22})^{-1}A_{21}, && (4.28b)\\
B_r &= B_1 + (A_{12} - E_{12})(E_{22} - A_{22})^{-1}B_2, && (4.28c)\\
C_r &= C_1 + C_2(E_{22} - A_{22})^{-1}(A_{21} - E_{21}E_r^{-1}A_r), && (4.28d)\\
D_r &= D + C_2(E_{22} - A_{22})^{-1}(B_2 - E_{21}E_r^{-1}B_r). && (4.28e)
\end{aligned}$$

11: **end if**
12: Define

$$\begin{aligned}
&\Sigma_r : (E_r, A_r, B_r, C_r, D_r), && (4.29a)\\
&x_r(0) = W\mathscr{T}^{-1}x_0. && (4.29b)
\end{aligned}$$

return Σ_r, $x_r(0)$
13: **end procedure**

Let $G_c(s)$, $G_d(z)$, $G_{r,c}(s)$, and $G_{r,d}(z)$ be the continuous and discrete time transfer functions, and their reductions, respectively. Singular perturbation guarantees $G_c(0) = G_{r,c}(0)$

($G_d(1) = G_{r,d}(1)$ in discrete time), or that the steady state of the full and reduced order models are equal (for both continuous and discrete models), which is crucial for applications such as step tracking.

Other properties of Algorithm 4.1 are: if Σ is asymptotically stable, so is the reduction, and the reduction satisfies the same error bound of the transfer function in continuous time [17, 26]:

$$||G_c(s) - G_{r,c}(s)||_\infty \leq 2 \sum_{i=r+1}^{n} \sigma_i, \tag{4.30}$$

where σ_i are the Hankel Singular Values. Error bounds can exist for discrete systems, however, their derivation is often dependent upon a continuous time model and the discretization method used [17].

Focusing on ordinary ($E = I_{n\times n}$) difference equations, the singular perturbation truncation from Algorithm 4.1 is [17]:

$$\begin{aligned} A_r &= A_{11} + A_{12}(I - A_{22})^{-1}A_{21}, && \text{(4.31a)} \\ B_r &= B_1 + A_{12}(I - A_{22})^{-1}B_2, && \text{(4.31b)} \\ C_r &= C_1 + C_2(I - A_{22})^{-1}A_{21}, && \text{(4.31c)} \\ D_r &= D + C_2(I - A_{22})^{-1}B_2. && \text{(4.31d)} \end{aligned}$$

With a reduced order model that matches the steady state of the full order model, and the assumptions of [153] (with a relaxation of the terminal output error in the cost), the following tracking result is obtained.

Theorem 4.2.3 (Asymptotic Tracking)**.** *Define $K_{r,f}$ to be the MPC gain [158], and assume $\rho(A_r + LC_r) < 1$, $\rho(A_r + B_rK) < 1$, and $\rho(A_r + B_rK_{r,f}) < 1$. If there exists some t and*

1. *$x_t \in \mathcal{X}$, $y_t \in \mathcal{Y}$;*
2. *$e_{r,t} \in \text{Proj}_r(\bar{\mathcal{S}})$ and $\tilde{x}_{r,t} \in \text{Proj}_r(\tilde{\mathcal{S}})$;*
3. *$\bar{u}_{t,\infty} \in \bar{\mathcal{U}}_r$, $\bar{x}_{r,t,\infty} \in \bar{\mathcal{X}}_r$, and $\bar{y}_{t,\infty} \in \bar{\mathcal{Y}}_r$;*

4. $\bar{y}_{t,\infty} \in colspan\{C_r(I-(A_r+B_rK_{r,f}))^{-1}B_r+D_r\}$,

then

$$\lim_{t\to\infty} y_t = \bar{y}_{t,\infty}. \tag{4.32}$$

Proof. See Appendix A.3.3 for the proof. □

Remark 4.2.2. *If the step response steady states of* Σ_r *and* Σ *are not equal, e.g. if residualization is not used, then a command governor is required to ensure step response tracking [35, 153]. Further, a combination of reduced MPC and command governor may be used to further reduce the conservativeness of the constraint.*

4.3 Constraint Conscious Model Order Reduction Formulation

4.3.1 General Formulation

The primary focus of model order reduction is to find a reduced order model, Σ_r, that best approximates an aspect of a high dimensional model, Σ. The reduction criterion is typically captured by minimizing some norm or function involving the error between the full and reduced order models, $\mathscr{E}(\Sigma, \Sigma_r)$. Some of the best understood results rely on parameterizing the reduction by a "balancing transformation," $\mathscr{T}$, that places the model in some canonical form before a truncation occurs.

However, it may be the case that the selection of $\mathscr{T}$ results in too conservative, or restrictive, admissible control and/or output constraints, $\mathcal{U}_r$ and $\mathcal{Y}_r$, to be of any practical use.

Therefore, it is proposed that a model reduction problem for constrained systems should consider both model accuracy and constraint conservativeness. Let $\mathscr{C}$ denote a measure of constraint conservativeness, and assume the following are known:

1. a model, Σ, and its constraint sets $(\mathcal{U}, \mathcal{X}, \mathcal{Y})$;

2. a reduction technique to obtain the reduced order model, Σ_r;

3. a robust control/estimation methodology, including a way to modify constraints subject to known model errors; and

4. a measure of modeling errors between Σ and Σ_r.

Then the general model reduction problem for constrained systems is formulated as determining a reduced order model, Σ_r, and the constraint sets $(\bar{\mathcal{U}}_r, \bar{\mathcal{X}}_r, \bar{\mathcal{Y}}_r)$ that ensure the desired performance of the robust control/estimation methodology, and solves the following problem:

$$\min_{\Sigma_r} \quad \mathscr{E}(\Sigma, \Sigma_r) + \lambda \mathcal{C}(\mathcal{U}, \mathcal{X}, \mathcal{Y}, \bar{\mathcal{U}}_r, \bar{\mathcal{X}}_r, \bar{\mathcal{Y}}_r), \tag{4.33}$$

where λ is the weighting of the constraint conservativeness.

Such broad optimizations problems are not new to the field of model order reduction, and have been used to great effect for a wide variety of problems [159, 160, 161].

4.3.2 Constraint Conservativeness Function

To select tube constraints, it is desirable to use as much of the original admissible region, $\mathcal{F}$, as possible, e.g., given the tightened constraint $\mathcal{F}_r \subseteq \mathcal{F}$, $\mathcal{F}_r = \mathcal{F}$ is ideal. For analysis, this motivates the construction of a constraint conservativeness function, $\mathscr{C}$,

Definition 4.3.1 (Constraint Conservativeness Function)**.** *Let $\mathfrak{M}$ be a σ-algebra of measurable sets in $\mathbb{R}^q$ [162]. Given sets $\mathcal{F}_r$, $\mathcal{F} \in \mathfrak{M}$, such that $\mathcal{F}_r \subseteq \mathcal{F}$, a constraint conservativeness function satisfies the following*

1. *$\mathscr{C}(\mathcal{F}, \mathcal{F}_r) \in [0, 1]$.*

2. *If $\mathcal{F}_r = \mathcal{F}$, then $\mathscr{C}(\mathcal{F}, \mathcal{F}_r) = 0$.*

3. *$\mathscr{C}(\mathcal{F}, \mathcal{F}_r) = 1$ if*

   (a) *$\mathcal{F}$ is unbounded and $\mathcal{F}_r$ is bounded.*

   (b) *$\mathcal{F}$ is bounded and $\mathcal{F}_r$ has measure zero.*

Given two measurable sets, $\mathcal{F}_1$ and $\mathcal{F}_2$, both in $\mathcal{F}$, if $\mathscr{C}(\mathcal{F}, \mathcal{F}_1) \leq \mathscr{C}(\mathcal{F}, \mathcal{F}_2)$; then $\mathcal{F}_2$ is said to be more conservative than a set $\mathcal{F}_1$.

Definition 4.3.2 (Characteristic Conservativeness Function)**.** *Let $\mathfrak{M}$ be a σ-algebra of measurable sets in $\mathbb{R}^q$, and assume that sets $\mathcal{F},\ \mathcal{G} \in \mathfrak{M}$. Define the characteristic conservativeness function between two sets $\mathcal{G}$ and $\mathcal{F}$, with $\mathcal{G} \subseteq \mathcal{F}$, to be*

$$\mu_{\mathcal{F}}(\mathcal{G}) = \lim_{\delta \to \infty} \frac{1}{|\mathcal{F} \cap \mathcal{B}(\bar{f}, \delta)|} \int_{\mathcal{B}(\bar{f}, r)} |1_{\mathcal{F}}(f) - 1_{\mathcal{G}}(f)| df, \tag{4.34}$$

where $\mathcal{B}(\bar{f}, \delta)$ is a ball of radius δ centered at a $\bar{f} \in \mathcal{F}$, $1_{\mathcal{F}}(f)$ is the characteristic function of the set $\mathcal{F}$, and $|\mathcal{F}| = \int_{\mathbb{R}^q} 1_{\mathcal{F}}(f) df$.

For this chapter, it is assumed that all the sets are compact and bounded. This yields a simpler way to calculate μ.

Theorem 4.3.1. *For $\mathcal{G} \in \mathfrak{M}$ and bounded $\mathcal{F} \in \mathfrak{M}$, with $\mathcal{G} \subseteq \mathcal{F}$,*

$$\mu_{\mathcal{F}}(\mathcal{G}) = 1 - \frac{|\mathcal{G}|}{|\mathcal{F}|}. \tag{4.35}$$

Proof. See Appendix A.3.4 for the proof. □

For either high dimensional problems where the majority of the volume is contained near the boundary, or systems where the states have vastly different scales, it may be more appropriate to replace the characteristic function with a positive measurable function to serve as a weighting or scaling along a dimension.

4.3.3 Reduction Formulation For Output Feedback MPC

The end goal of this chapter is to use a reduced MPC law, given by (4.26), to track a step reference. To tailor the reduction problem to the control problem, the following design variables are present: how to obtain the reduced order model, Σ_r; $\mathscr{C}$, the constraint conservativeness function; how to modify the constraints for the reduced problem; λ, the constraint conservativeness weight; and LQ cost weightings/noise covariances.

With the MPC formulation, the selected truncation technique will be to transform by a similarity transformation, $\mathscr{T}$, and truncate using singular perturbations of Algorithm 4.1

for Σ_r. For the constraint conservativeness, define

$$\mathcal{Z} = (\mathcal{U}, \text{Proj}_r(\mathscr{T}^{-1}\mathcal{X}), \mathcal{Y}), \tag{4.36a}$$

$$\mathcal{Z}_r = (\bar{\mathcal{U}}_r, \bar{\mathcal{X}}_r, \bar{\mathcal{Y}}_r), \tag{4.36b}$$

and select $\mathscr{C} = \mu_{\mathcal{Z}}(\mathcal{Z}_r)$, the characteristic conservativeness function of (4.34). The MPC problem uses constant tube tightened MPC, and the sets are obtained as in (4.24). The RPI sets used to define $\mathcal{Z}_r$ are calculated using the technique of [156] with closed-loop dynamics defined with the feedback and output injection matrices, K and L, of the reduced order model.

The calculation of the RPI sets requires repeated computations and sums of $((A_r + B_rK)^i)^\top w_t$ in a "support function." Using the notation of [156] for the constraints, f_i, ideally, $f_i^\top((A_r+B_rK)^s)w = 0$, for all f_i and $w \in \mathcal{W}$ to restrict the number of computations; however, this is generally not possible. To limit the number of computations, instead it is proposed to select stabilizing K and L such that $||A_r + B_rK||_2$ and $||A_r + LC_r||_2$ are minimized.

Provided with transfer functions G and G_r of Σ and Σ_r, respectively, the tightened constraints sets are determined by the model error between Σ and Σ_r from (4.24), and the selected model reduction problem is

$$\mathscr{T}^\star = \arg \min_{\mathscr{T} \in GL_n(\mathbb{R})} \quad ||G - G_r||_\infty + \lambda \mu_{\mathcal{Z}}(\mathcal{Z}_r), \tag{4.37}$$

where $GL_n(\mathbb{R})$ is the general linear group (the group of invertible matrices) [163].

Remark 4.3.1. *There are a variety of other control/estimator/constraint methodologies that may be used. E.g., the constraint tightening of Section 4.2 may be extended using the dynamics of the truncated states, homothetic tubes [164], parametrized tubes [165], state dependent tubes [154], etc.*

In the following section, MPC and estimator weights will be selected, and different conservativeness weights and constraints will be used to demonstrate the efficacy of the proposed approach.

4.4 Single-Input, Single-Output Example

To demonstrate the efficacy of the model reduction formulation, and the dependence upon the parameters, for the design of reduced order robust MPC law, an example problem is presented. The example activates input, state, and output constraints Table 4.1 gives the model, linear quadratic design parameters, constraints, and output normal constraint parameter. Table 4.2 provides the 4 models that will be used to design the reduced robust MPC law to control the model: the full order and three reduced order using the techniques of [13], RBT (Chapter 3), and the proposed reduction formulation.

Table 4.1: The model, constraints, and parameters.

$A = \begin{bmatrix} -0.7352 & 0.2695 \\ -0.3808 & -0.1172 \end{bmatrix}$	$B = \begin{bmatrix} 0.1855 \\ 1.7664 \end{bmatrix}$
$C = \begin{bmatrix} -0.8832 & 0.8832 \end{bmatrix}$	$D = 0$
$Q = 1, \quad R = 1$	$\Gamma = 1, \quad \Lambda = 1$
$N_p = 5$	$\lambda = \{1, 1000\}\|\|G - G_r\|\|_\infty$
$-1 \leq u_t \leq 1$	$-1 \leq y_t \leq 1$
$\begin{bmatrix} -0.8832 & 0.8832 \\ 0.8832 & -0.8832 \\ 0.707107 & 0.707107 \\ -0.707107 & -0.707107 \end{bmatrix} x_t \leq \begin{bmatrix} 1 \\ 1 \\ \beta \\ \beta \end{bmatrix}$	$\beta = \{1, 2\}$

Table 4.2: Models to compare MPC and Kalman filter performance.

Name	**Model**
Full	Full order model (using nominal MPC)
LBT	LBT reduced order model ([13])
RBT	RBT reduced order model (Chapter 3)
Proposed	Proposed reduced order model

MATLAB's fmincon is used to find a $\mathscr{T}$ minimizing (4.37), and all polytope set manipulations are performed with the MPT toolbox [139].

λ is chosen to be either $\lambda_1 = 1||G(z) - G_{r,LBT}||_\infty$, the error between the full and LBT reduced order model, and $\lambda_2 = 1000||G(z) - G_{r,LBT}||_\infty$. The dependence of λ on the error provides appropriate scaling between the model error and the constraint conservativeness.

Table 4.3 provides the modeling error, and the weighted constraint conservativeness of the various reduced order models. Notable trends of Table 4.3: when emphasis is placed on constraint conservativeness, the proposed technique always performs the best; and when emphasis is placed on model accuracy, the proposed technique is the most accurate.

Table 4.3: Cost components parameterized by selected β and λ.

		$\beta = 1$		$\beta = 2$	
	Name	$\|\|G - G_r\|\|_\infty$	$\mu_z(\mathcal{Z}_r)$	$\|\|G - G_r\|\|_\infty$	$\mu_z(\mathcal{Z}_r)$
$\lambda_1 = 1\|\|G - G_{r,LBT}\|\|_\infty$	LBT	0.9025	0.8863	0.9025	0.8863
	RBT	0.7910	0.7231	0.7910	0.7231
	Proposed	0.7548	0.6818	0.7941	0.6127
$\lambda_2 = 1000\|\|G - G_{r,LBT}\|\|_\infty$	LBT	0.9025	0.4738	0.9025	0.4738
	RBT	0.7910	0.3817	0.7910	0.3817
	Proposed	0.7865	0.3420	0.8153	0.3216

Figs. 4.1 and 4.2 provide the control response, output response, and the tightened nominal constraints (dashed lines) of the full order model of Table 4.1 controlled with the compensator designed from Table 4.2, for different β and λ. Fig. 4.1 shows the case where $\beta = 1$, and a state constraint is reached limiting the input and output performance. Fig. 4.2 shows the case when $\beta = 2$, and no state constraints are activated, but nominal input and output constraints are.

In all cases, it is seen that:

1. nominal constraints are satisfied,

2. tracking is achieved when the conditions of Theorem 4.2.3 are satisfied, and

3. the proposed reduction technique works the best.

Figs. 4.1 and 4.2 suggest that when model accuracy is valued over conservativeness of the constraints, the performance and conservativeness of the reduced MPC laws are very similar. However, Figs. 4.1 and 4.2 suggest that when conservativeness of the constraints is heavily penalized (meaning larger control/output constraint sets are desired), the proposed methodology is far superior.

Between Table 4.3 and Figs. 4.1 and 4.2, it is seen that trade-offs can be made between model accuracy and the degree of the constraint conservativeness. This supports the notion that open-loop model accuracy should not necessarily be the most important aspect of model order reduction for constrained systems, since less accurate open-loop models may result in better closed-loop performance and less conservative constraints.

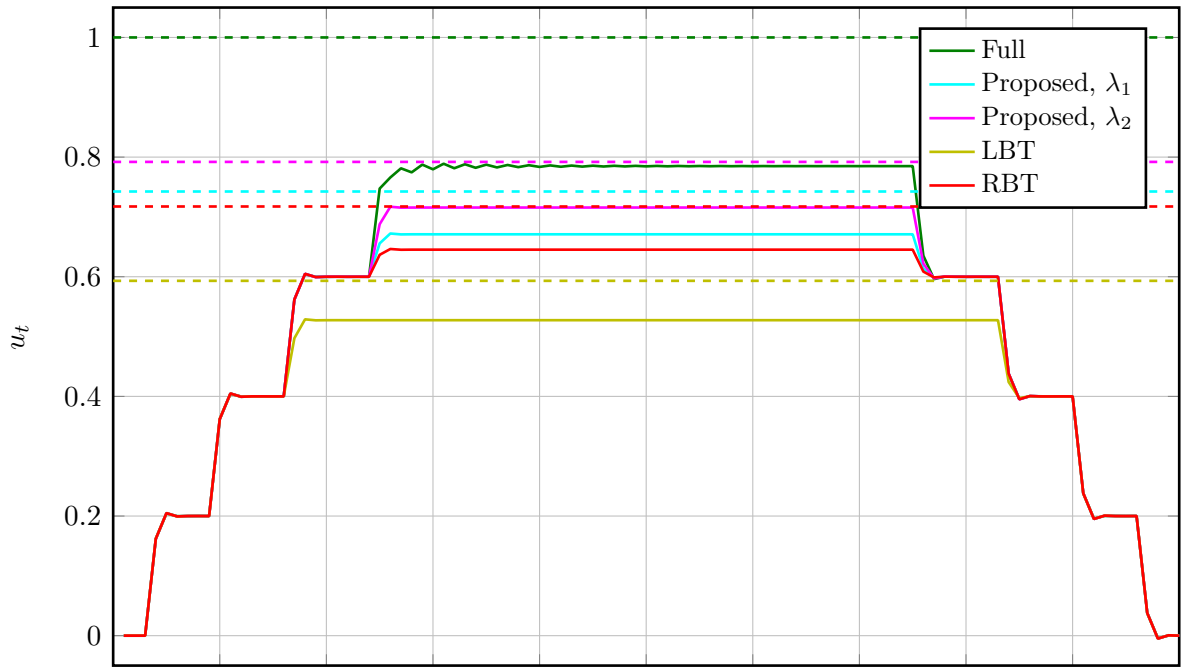

(a) Control Input

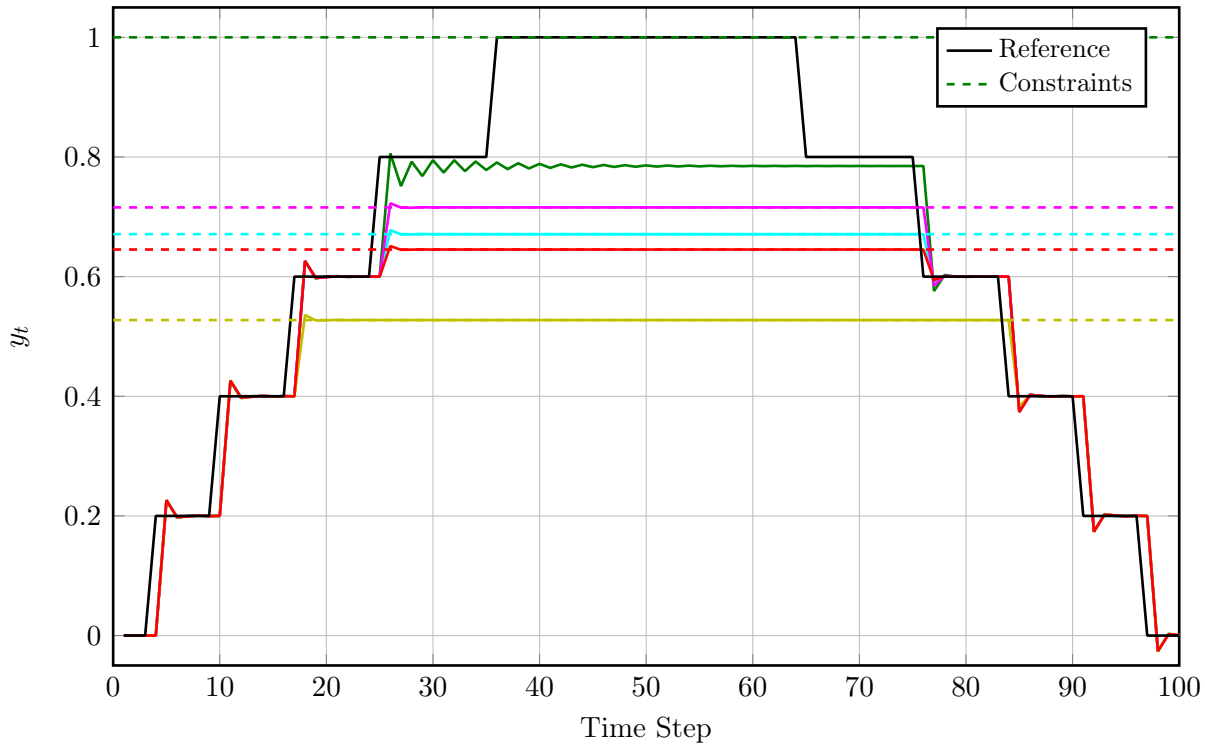

(b) Output

Figure 4.1: Output, estimated reduced state, and control response of the full order MPC to the LBT, RBT, and proposed reduced MPC law with $\beta = 1$.

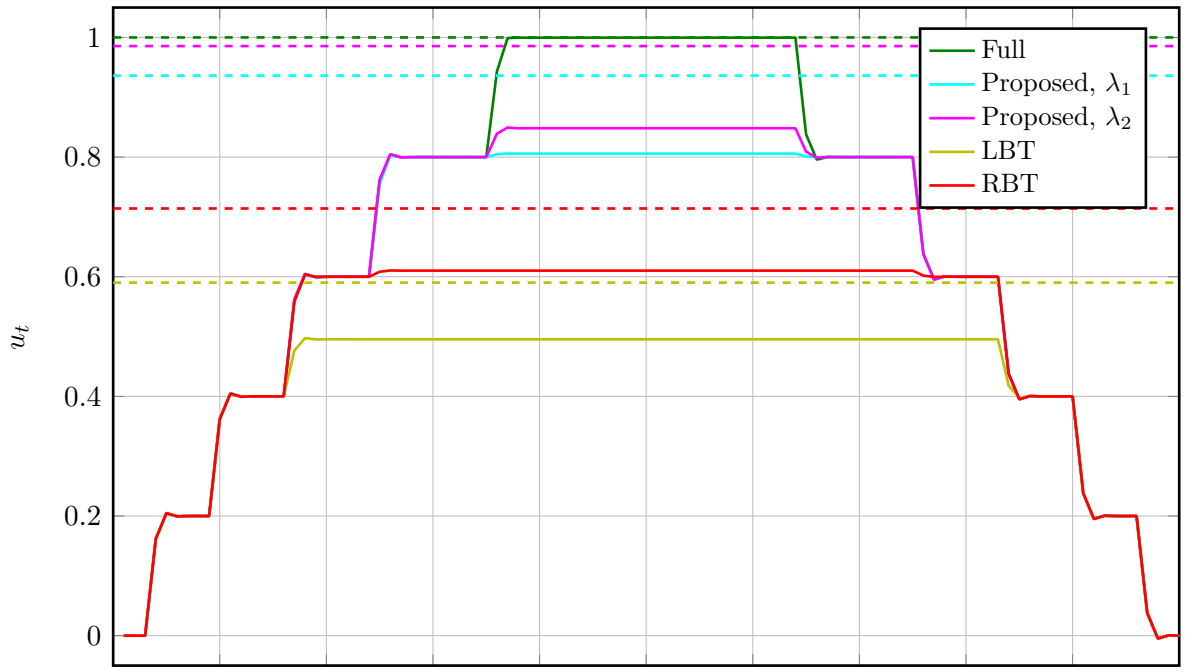

(a) Control Input

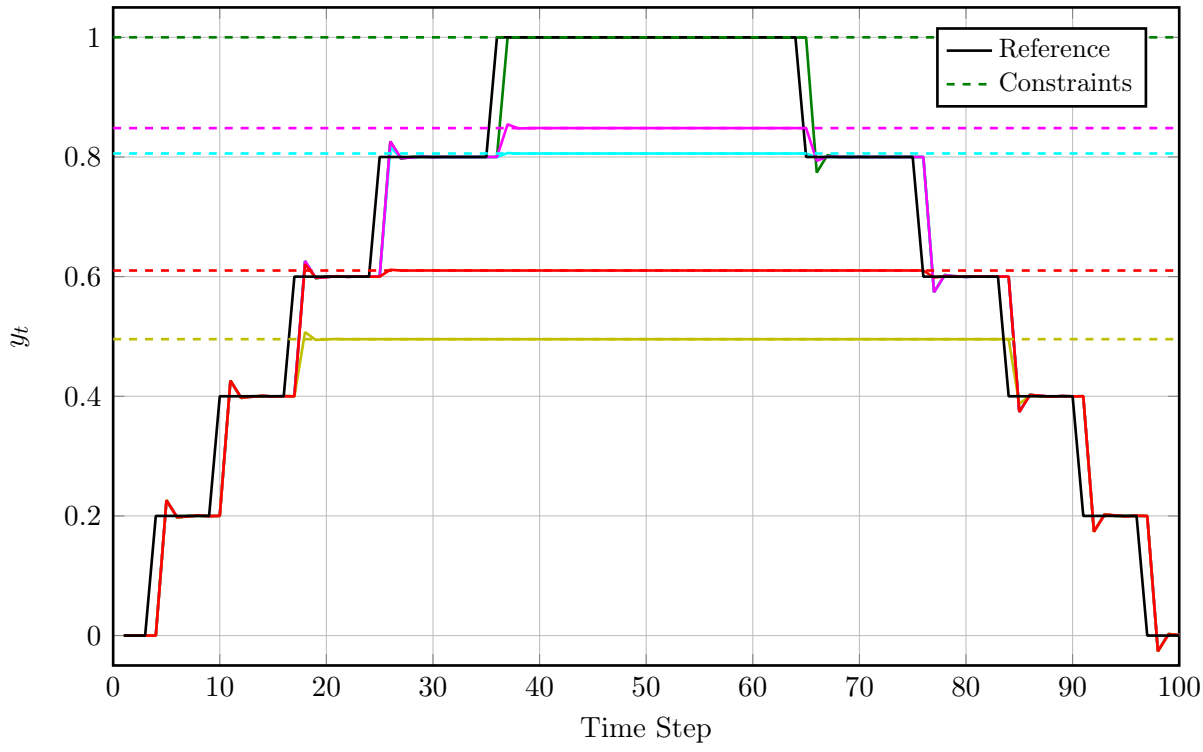

(b) Output

Figure 4.2: Output, estimated reduced state, and control response of the full order MPC to the LBT, RBT, and proposed reduced MPC law with $\beta = 2$.

4.5 Conclusions

In this chapter, the "truncated states as noise" idea of [36] was modified and used in the robust model predictive control (MPC) framework of [146] to yield a reduced order output feedback MPC (ROOFMPC) law that was shown to be robustly stable, feasible, and satisfy constraints. With standard assumptions, it was also shown that the reduced MPC law can track step references contained within the tightened constraints. A novel reduction problem was developed that balances the trade-off between model accuracy and constraint conservativeness. Employing the tightening algorithm specified by the ROOFMPC law, and residualization truncation, a solution to the novel reduction problem was proposed. A low order problem was used to demonstrate the efficacy of the technique. The demonstrated efficacy of the technique, even to a low order problem, shows the potential benefits of a model order reduction formulation that simultaneously considers modeling error and constraint conservativeness. Moreover, the results suggest that open-loop model accuracy should not necessarily be the most important aspect of model order reduction for constrained systems.

While the proposed model reduction formulation was applied to a linear system, using a constant tube methodology and open-loop error measure, the abstract problem formulation is readily amenable to nonlinear systems, time varying constraints, closed-loop error measures, and any combination in between.

Chapter 5

Open-Loop Nonlinear Model Order Reduction

The research effort described in this chapter was was initially motivated by the need to apply model predictive control (MPC) for nonlinear systems. MPC is a popular control technique, because of its simple and amenable nature to controlling constrained multi-input, multi-output (MIMO) systems. It works by selecting inputs that optimize future trajectories subject to a specified cost function with state and input constraints. For a linear system, most MPC may be cast as a quadratic programming problem and effective solvers are readily available [158]. However, for nonlinear systems, this is no longer true, and the nonlinear optimization problem has to be solved numerically at each time step, typically incurring a high computational cost.

While a variety of solution techniques exist for nonlinear optimization, e.g., sequential quadratic programming (SQP) and other Newton-type algorithms [166], and more recently, integrated pertubation analysis and SQP [167], the applicability of nonlinear MPC (NMPC) on given computing hardware is often limited to systems with low order or slow dynamics and abundant computational resources.

For systems with fast dynamics and limited computational resources, such as those encountered in automotive applications, linear MPC (LMPC) has been used in most of the published work because real-time nonlinear optimization required for NMPC is most often intractable for systems with even a moderate number of states (e.g., > 4) [71, 168]. For

most nonlinear system applications, scheduling must be employed to adjust the model used in LMPC according to different operating conditions; which drastically increases the design and calibration complexity [6].

One possible way to make NMPC more applicable to real-time systems is to reduce computational complexity of the prediction model. One approach to reduce complexity is to reduce the number of states in the model through model order reduction (MOR). Unlike MOR for linear systems, which has been well developed, methods for nonlinear MOR (NMOR) are far less explored. While there are a number of approaches proposed in the literature that exploit specific nonlinearities (e.g., piecewise affine nonlinear, bilinear, and systems with a large scale linear system with a small subset of nonlinear states), the most common approach appears to be balanced truncation with Galerkin projection [48, 169, 170].

Balanced truncation relies on transforming states so that they are in a balanced representation where the states are ordered by how much energy they transfer from input to output. In this balanced form, states that contribute little from input to output are truncated. As a direct extension of MOR of a linear system [13], Galerkin projection uses the controllability and observability gramians to build a balanced representation and "insignificant" states are truncated to derive a reduced order nonlinear system. The controllability and observability gramians, on the other hand, can be constructed by either linearizing the system around the design point and then calculating the gramians of the linearized model, or using empirical gramians, which use properly generated trajectories/experimental data to numerically establish the controllability and observability gramians [69, 70].

For nonlinear models, a variety of systematic open-loop nonlinear reduction techniques exist for different purposes: reduction along a trajectory [50, 171], maintaining structure or properties of the original model [47, 62], nonlinear frequency matching [49], nonlinear moment matching [25, 64], global reduction of affine-input nonlinear systems [67, 172], and balanced truncation at a fixed design point [46, 70, 72], to mention a few. For nonlinear automotive engine models, reduced order modeling using time scale separation [173, 174] and balanced model reduction techniques [171] have been applied to achieve different goals.

For diesel engine airpath control addressed in this chapter, the empirical gramian based balanced truncation for NMOR is pursued because it can capture some information about the

nonlinearity, and data needed for calculation is easily accessible/implementable. However, several problems have been encountered in applying the empirical gramian based approach [70] to the diesel airpath (DAP) model, these include: challenges in generating valid trajectories due to input and state constraints, and difficulty in approximating the input-to-output relationship when outputs (intake manifold pressure and exhaust gas recirculation (EGR) rate) have different scales and different performance requirements.

To address these issues, a modified empirical gramian formulation is proposed that uses different probe directions than those of [69], significantly simplifying the empirical gramian, and incorporates weighting factors in gramian calculations to accommodate different control design goals in deriving a reduced order nonlinear model for NMPC of the DAP. The application of the proposed empirical gramian formulation to the DAP control system demonstrates the advantage of the proposed approach.

This chapter is structured as follows: Section 5.1 covers linear system gramians and empirical gramians along with their use in balanced truncation model order reduction. Section 5.2 presents the modified empirical gramian formulation. Section 5.3 applies the proposed gramian formulation to reduce a 9 state diesel airpath model, and compares the open- and NMPC closed-loop responses of the reduced order models obtained using the different gramians and the full order model. Section 5.4 concludes with a summary of the results.

5.1 Galerkin Projection Model Order Reduction for Nonlinear Systems

As stated in Chapter 2, an alternate definition of the gramians may be obtained through improper integrals. Consider the asymptotically stable, ordinary linear system ($E = I_{n\times n}$) represented by $\Sigma_{\mathcal{L}}$:

$$\Sigma_{\mathcal{L}} : \begin{cases} \dot{x} &= Ax + Bu, \\ y &= Cx + Du, \end{cases} \tag{5.1}$$

with $A \in \mathbb{R}^{n\times n}$, $B \in \mathbb{R}^{n\times m}$, $C \in \mathbb{R}^{p\times n}$, $D \in \mathbb{R}^{p\times m}$. The linear controllability gramian, P, and observability gramian, Π, are respectively defined as:

$$P = \int_0^\infty e^{A\tau} B B^\top e^{A^\top \tau} d\tau, \tag{5.2a}$$

$$\Pi = \int_0^\infty e^{A^\top \tau} C^\top C e^{A\tau} d\tau. \tag{5.2b}$$

If $\Sigma_{\mathcal{L}}$ is completely controllable and observable, then from (5.2), it can be shown that P and Π satisfy the Lyapunov equations [175] of (2.5).

In [69], alternate gramian definitions to (5.2) were developed using empirically obtained covariance matrices about a design/equilibrium point (the control and state where $\dot{x} = 0$). Let (x_e, u_e) be the design/equilibrium point of a nonlinear system

$$\Sigma : \begin{cases} \dot{x} = f(x,u), \\ y = h(x,u), \end{cases} \tag{5.3}$$

with $x \in \mathbb{R}^n$, $u \in \mathbb{R}^m$, and $y \in \mathbb{R}^p$, under the following assumptions:

*A*5.1**:** the nonlinear model, (5.3), is known;

*A*5.2**:** the output and state responses of (5.3) are $L^2[0,\infty)$-integrable about an asymptotically stable equilibrium point, (x_e,u_e); and

*A*5.3**:** that an asymptotically stable linear representation of (5.3), (A, B, C, D), exists about the equilibrium point.

To calculate the empirical controllability gramian using response data, a set of input probe directions, $c_i T_j e_k$, are used to vary the control, u^{ijk}, where c_i, T_j, and e_k are selected from the following sets:

$$T_{\mathcal{C}}^m = \{T_1, \ldots, T_{r_c} | T_l T_l^\top = I_{m\times m}, l = 1, \ldots, r_c\}, \tag{5.4a}$$

$$M_{\mathcal{C}} = \{c_1, \ldots, c_{s_c} | c_i \in \mathbb{R}^+, i = 1, \ldots, s_c\}, \text{ and} \tag{5.4b}$$

$$E_{\mathcal{C}}^m = \{e_1, \ldots, e_m | \text{standard basis in } \mathbb{R}^m\}. \tag{5.4c}$$

$T_{\mathcal{C}}^m$ is a set of orthogonal matrices of dimension m, whose columns will define excitation directions, c_i in $M_{\mathcal{C}}$ are positive perturbation sizes, and r_c and s_c are the number of elements in these two sets, respectively. Each perturbation size is applied to each excitation direction to build a set of probe directions.

Using assumptions $A5.1$ and $A5.2$, the empirical controllability gramian is calculated as

$$\bar{W}_{\mathcal{C}} = \sum_{i=1}^{m}\sum_{j=1}^{r_c}\sum_{k=1}^{s_c}\frac{1}{r_c s_c c_i^2}\int_0^\infty \Phi(\tau)d\tau, \tag{5.5}$$

where

$$\Phi(\tau) = (x^{ijk}(\tau) - x_{ss}^{ijk})(x^{ijk}(\tau) - x_{ss}^{ijk})^\top. \tag{5.6}$$

and $x^{ijk}(t)$, with the initial condition $x(0) = x_e$, is the impulse response to

$$u^{ijk}(t) = c_i T_j e_k \delta(t) + u_e, \tag{5.7}$$

where $\delta(t)$ is the Dirac delta function, u_e is the design point corresponding to x_e, and x_{ss}^{ijk} corresponds to the steady state with input $u^{ijk}(t)$.

Similarly, an empirical observability gramian is defined, but now the initial condition is perturbed and covariance matrices are built using the output. Using similar set definitions:

$$T_{\mathcal{O}}^n = \{T_1, \ldots, T_{r_o} | T_l T_l^\top = I_{n\times n}, l = 1, \ldots, r_o\}, \tag{5.8a}$$

$$M_{\mathcal{O}} = \{c_1, \ldots, c_{s_o} | c_k \in \mathbb{R}^+, k = 1, \ldots, s_o\}, \text{ and} \tag{5.8b}$$

$$E_{\mathcal{O}}^n = \{e_1, \ldots, e_n | \text{standard basis in } \mathbb{R}^n\}, \tag{5.8c}$$

the empirical observability gramian is calculated as

$$\bar{W}_{\mathcal{O}} = \sum_{k=1}^{r_o}\sum_{l=1}^{s_o}\frac{1}{r_o s_o c_l^2}\int_0^\infty T_k \Psi^{kl}(\tau) T_k^\top d\tau, \tag{5.9}$$

with

$$[\Psi^{kl}]_{ij}(\tau) = (y^{ikl}(\tau) - y_{ss}^{ikl})^\top (y^{jkl}(\tau) - y_{ss}^{jkl}), \tag{5.10}$$

where $\Psi^{kl} \in \mathbb{R}^{n\times n}$, $[\cdot]_{ij}$ denotes the element in the matrix, $y^{ikl}(t)$ is the response of the

system with the initial condition being perturbed to

$$x^{ikl}(0) = c_k T_l e_i + x_e, \tag{5.11}$$

the input is fixed as u_e, and y_{ss} is the steady state output.

Remark 5.1.1. *For a linear system, one can set $r_c = s_c = r_o = s_o = 1$ to recover $P = \bar{W}_{\mathcal{C}}$ and $\Pi = \bar{W}_{\mathcal{O}}$. Because superposition and homogeneity are applicable to solutions of linear systems, so no extra information can be gathered by probing the system in additional directions. However, superposition and homogeneity no longer hold for nonlinear systems, therefore adding probe directions could result in more information and different gramians.*

In [70], it was noted that nonlinear systems are not amenable to using the Dirac $\delta(t)$, and instead empirical gramians were developed with step responses. The control perturbation for the controllability gramian then becomes

$$u^{ijk}(t) = c_i T_j e_k 1(t) + u_e. \tag{5.12}$$

With the modification of the signal used to define the controllability gramian given by (5.12), [70] proceeds to show that for a linear system $A\bar{W}_{\mathcal{C}}A^\top = P$. Assumption $A5.3$ is necessary for P to have non-zero singular values. Finally, a caution was stated that the reader should interpret the results with care when trajectories leave the region of attraction of an equilibrium point.

With these considerations in mind, the empirically obtained gramians may be used in conjunction with balanced truncation to reduce the order of the nonlinear system. Instead of a similarity transformation as used in linear model order reduction, a linear affine transformation in conjunction with balanced truncation is employed [176].

Algorithm 5.1 captures how to calculate the balancing transformation, $\mathscr{T}$. To yield the truncated reduced nonlinear system, Σ_r, using the empirically defined balancing transformation, Algorithm 5.2 is provided with the selected reduced order, transformation, model, and parameters.

Algorithm 5.1 Empirical gramian defined balancing transformation.

procedure EMPIRICALBASEDBT(Σ,$\{T_{\mathcal{C}}^m, M_{\mathcal{C}}, E_{\mathcal{C}}^m\}$,$\{T_{\mathcal{O}}^n, M_{\mathcal{O}}, E_{\mathcal{O}}^n\}$, (x_e, u_e), x_0, r)

Calculate (5.5) and (5.9) for positive definite $\bar{W}_{\mathcal{C}}$ and $\bar{W}_{\mathcal{O}}$, respectively.

Calculate the Cholesky factors (matrix square root factors) of $\bar{W}_{\mathcal{C}} = XX^\top$, $\bar{W}_{\mathcal{O}} = YY^\top$.

Calculate the singular value decomposition (SVD) of $Y^\top X = GMH^\top$, where M is a positive definite diagonal matrix and G and H are orthogonal matrices.

Form the balancing transformation

$$\mathscr{T} = XHM^{-1/2}. \tag{5.13}$$

return $\mathscr{T}$

end procedure

Serving as a nonlinear generalization of Algorithm 3.2, Algorithm 5.2 provides the truncated nonlinear reduced order model.

Algorithm 5.2 Nonlinear MOR with a transformation $\mathscr{T}$.

procedure NONLINEAR_TRUNCATION($\mathscr{T}, \Sigma, (x_e, u_e), x_0, r$)

Define submersion and immersion matrices

$$W = \begin{bmatrix} I_{r\times r} & 0 \end{bmatrix}, \tag{5.14a}$$

$$V = \begin{bmatrix} I_{r\times r} \\ 0 \end{bmatrix}. \tag{5.14b}$$

Define the offset from the equilibrium point x_e to be

$$z = (I - \mathscr{T}VW\mathscr{T}^{-1})x_e. \tag{5.15}$$

Truncate the nonlinear model for Σ_r:

$$\Sigma_r : \begin{cases} \dot{x}_r &= W\mathscr{T}^{-1}f(\mathscr{T}Vx_r + z, u), \\ y_r &= h(\mathscr{T}Vx_r + z, u), \\ x_r(0) &= W\mathscr{T}^{-1}x_0. \end{cases} \tag{5.16}$$

return Σ_r

end procedure

The reduced state of Algorithm 5.2 can be immersed into the higher dimensional state using the linear affine transformation

$$\tilde{x} = \mathscr{T}Vx_r + z, \tag{5.17}$$

and with a properly selected $\mathscr{T}$, it is expected that $\tilde{x} \approx x$ in some neighborhood of the design point x_e.

Another common approach to obtain a nonlinear reduced order model is to linearize (5.3), calculate the linear gramians P and Π of (5.2), replace the empirical gramians with the linear gramians in Algorithm 5.1 to obtain a $\mathscr{T}$, and use Algorithm 5.2 for the reduced order model. Both approaches will be used in Section 5.3.

Remark 5.1.2. *While Algorithm 5.1 leads to a reduced order model, it may not always result in a reduced complexity model as the reduced states still are evaluated using the nonlinear function, f, of the full order model, and a simplified representation may not exist [176]. Techniques such as Discrete Empirical Interpolation exist to decrease the cost of nonlinear function evaluation [177, 178].*

5.2 Modified Empirical Gramian Formulations

The empirical gramians of [70], defined by (5.5) and (5.9), have potential drawbacks:

1. calculating an empirical gramian requires computing all combinations of elements from the T (excitation directions), M (perturbation sizes), and E (selection) sets;

2. for systems with constraints, the combinations of $c_i T_j e_k$ (the *probe directions*) may result in constraint violation in some directions; and

3. when outputs have different scales, more weighting could inadvertently be put on the larger output.

To elaborate on the first two points, consider a simple example with $M_{\mathfrak{C}} = \{c_1, c_2, c_3, c_4\}$. Empirical gramians are generated using probe directions along the surface of spheres (dictated by the choice of orthogonal T_l matrices shown in Fig. 5.1(a)). Consider the probe directions about u_e, where the input is constrained by the solid box. In this case $c_3 T_1 e_1$ and $c_4 T_1 e_1$ lie outside the constraint. There are two immediate ways to address this: one is to constrain the input in the direction $T_1 e_1$ so that $c_2 T_1 e_1$, $c_3 T_1 e_1$, and $c_4 T_1 e_1$ all result in the same probing signal. Another is to eliminate the c_i's from the set if any $c_i T_j e_k$ violates the

input constraints. Both cases will result in either additional weights being placed in certain probe directions or reduced information being gathered.

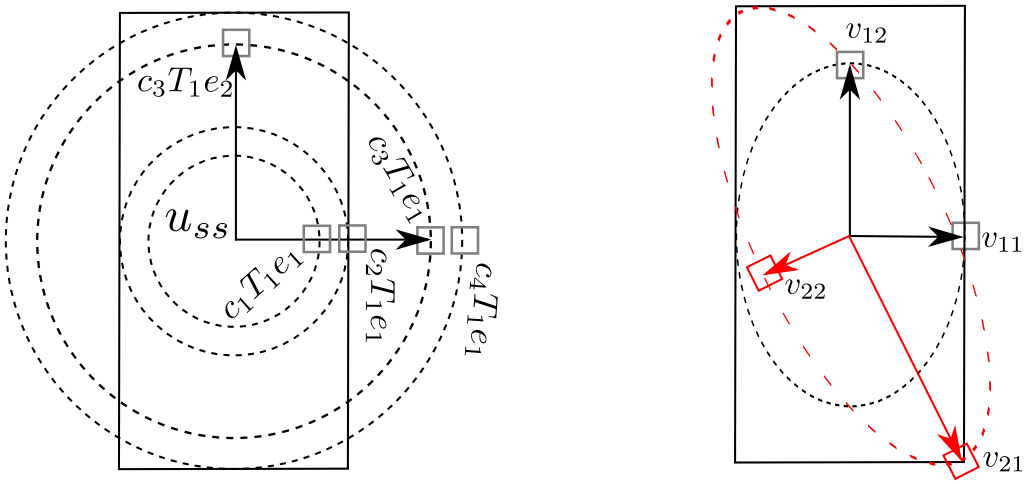

(a) $\bar{W}$, probe directions for the empirical gramians of [69, 70].

(b) W, probe directions of the proposed modified empirical gramian formulation of (5.22) and (5.28).

Figure 5.1: Depictions of the probe directions in the empirical gramians experiments.

To address the potential drawbacks, new formulations of the empirical gramians are proposed that combine the T-, M-, and E- sets to probe with different amplitudes along directions, as in Fig. 5.1(b), so that input and state constraints can be easily accommodated, particularly for the case when the associated constraints have different magnitudes.

For the new weighted controllability gramian formulation, sets of orthogonal vectors, v_{il}, are selected to form a matrix $V_l^{\mathcal{C}}$, using the positive definite weighting R.

$$V_l^{\mathcal{C}} = \begin{bmatrix} v_{1l} & \cdots & v_{ml} \end{bmatrix} \in \mathbb{R}^{m \times m}, \tag{5.18}$$

where

$$\tilde{v}_{il}^{\top} \tilde{v}_{jl} = ||\tilde{v}_{il}||^2 \delta_{ij}, \tag{5.19a}$$

$$R = E_l E_l^{\top}, \tag{5.19b}$$

$$v_{il} = E_l \tilde{v}_{il}, \tag{5.19c}$$

with δ_{ij} denoting the Kronecker delta, defined as:

$$\delta_{ij} = \begin{cases} 1 & \text{if } i = j, \\ 0 & \text{otherwise,} \end{cases} \tag{5.20}$$

and E_l being the Cholesky factor (or matrix square root factor) of R. The matrices, $V_l^{\mathcal{C}}$, form the set

$$V_{\mathcal{C}}^m \;=\; \{V_1^{\mathcal{C}}, \ldots, V_{r_c}^{\mathcal{C}}\},$$

with $v_{i_1 j_1} \neq v_{i_2 j_2}$ unless $i_1 = i_2$ and $j_1 = j_2$.

Definition 5.2.1. *Let v_{ij} be defined as above, define the control probe directions to be*

$$u^{ij}(t) = v_{ij} 1(t) + u_e, \tag{5.21}$$

$x^{ij}(t)$ to be the solution of Σ subject to u^{ij} as the input, x_e as the initial condition, and x_{ss}^{ij} be to steady-state of Σ to u^{ij}. The modified empirical controllability covariance matrix is

$$W_{\mathcal{C}} = \sum_{i=1}^{m} \sum_{j=1}^{r_c} \frac{1}{r_c ||\tilde{v}_{ij}||^2} \int_0^\infty \Phi^{ij}(t) dt, \tag{5.22}$$

with

$$\Phi^{ij}(t) = (x^{ij}(t) - x_{ss}^{ij})(x^{ij}(t) - x_{ss}^{ij})^\top. \tag{5.23}$$

Theorem 5.2.1. *For a completely controllable, asymptotically stable linear system, Σ_L, $AW_{\mathcal{C}}A^\top = \hat{P}$, where $\hat{P}$ is the weighted linear controllability gramian that solves*

$$A\hat{P} + \hat{P}A^\top + BRB^\top = 0. \tag{5.24}$$

Proof. See Appendix A.4.1 for the proof. □

Similarly, the observability gramian requires orthogonal vectors, w_{il}, in W_l,

$$V_l^{\mathcal{O}} = \begin{bmatrix} w_{1l} & \cdots & w_{nl} \end{bmatrix} \in \mathbb{R}^{n \times n} \tag{5.25}$$

with

$$w_{il}^{\top} w_{jl} = ||w_{il}||^2 \delta_{ij}. \tag{5.26}$$

The set of initial condition probe directions then becomes

$$V_{\mathcal{O}}^{n} \quad = \quad \{V_1^{\mathcal{O}}, \ldots, V_{r_o}^{\mathcal{O}}\},$$

and $w_{i_i j_1} \neq w_{i_2 j_2}$ unless $i_1 = i_2$ and $j_1 = j_2$.

Definition 5.2.2. *Let w_{ij} be defined as above, define the initial condition probe direction of Σ to be*

$$x^{al}(0) = w_{al} + x_e, \tag{5.27}$$

and y_{ss}^{al} to be the corresponding steady state output. The empirical observability gramian then becomes

$$W_{\mathcal{O}} = \sum_{l=1}^{r_o} \frac{1}{r_o} V_l^{\mathcal{O}} \left[\int_0^{\infty} \Lambda_l^{-1} \Psi_l(t) \Lambda_l^{-1} \, dt \right] (V_l^{\mathcal{O}})^{\top}, \tag{5.28}$$

where

$$\Lambda_l = \mathrm{diag}(||w_{1l}||_2^2, \ldots, ||w_{nl}||_2^2), \tag{5.29}$$

and

$$[\Psi_l(t)]_{ab} = (y^{al}(t) - y_{ss}^{al})^{\top} Q (y^{bl}(t) - y_{ss}^{bl}). \tag{5.30}$$

Remark 5.2.1. *While one most often has seen the gramian with $Q = I_{p \times p}$, non-identity Q generalizes the result and allows for different emphasis to be placed on the outputs.*

Theorem 5.2.2. *For a completely observable, asymptotically stable linear system, $W_{\mathcal{O}} = \hat{\Pi}$, where $\hat{\Pi}$ is the weighted linear observability gramian satisfying*

$$A\hat{\Pi} + \hat{\Pi} A^{\top} + C^{\top} Q C = 0. \tag{5.31}$$

Proof. See Appendix A.4.2 for the proof. □

To obtain the reduced order model using the modified empirical gramian formulation, $W_{\mathcal{C}}$ and $W_{\mathcal{O}}$ are substituted for $\bar{W}_{\mathcal{C}}$ and $\bar{W}_{\mathcal{O}}$ in Algorithm 5.1 to calculate a $\mathscr{T}$, and Algorithm 5.2 is used to truncate the nonlinear model.

Some important points to note:

1. The proposed formulation of the empirical gramians eliminates using the combination of each excitation direction with each perturbation size. If properly selected, this can reduce the number of experiments required to form an empirical gramian.

2. Assuming $R = I_{m\times m}$ and $Q = I_{p\times p}$, when $V_{\mathcal{C}}^m$ is equal to the combination of all possible $T_{\mathcal{C}}^m$ and $M_{\mathcal{C}}$, and $V_{\mathcal{O}}^n$ is equal to the combination of all possible $T_{\mathcal{O}}^n$ and $M_{\mathcal{O}}$ of [70], (5.22) and (5.28) are equivalent to the empirical gramians of (5.5) and (5.9). Therefore, the gramians of [70] are special cases of the proposed formulations.

3. One still should interpret the results of an empirical gramian with care when trajectories leave the region of attraction of an equilibrium point.

4. Empirical gramians, and the modified framework, can be generalized to discrete time systems by using sums instead of integrals, like in [179].

Remark 5.2.2. *There also exist an efficient solver for empirical gramians, cross gramians, and sensitivity gramians [180].*

In the following section, the linear, empirical, and modified emperical gramians will be used to define a balancing transformation for NMOR. Their performance will be evaluated in open-loop matching, and closed-loop NMPC tracking of intake pressure and EGR rate.

5.3 Nonlinear Model Order Reduction and MPC for a 9 State Diesel Airpath System

In contrast to Chapter 3, a 9 state diesel airpath model is used in this section. The main objective remains the same, and that is to deliver air to meet drivers' demands, and at the same time provide desired EGR rate to meet emission control requirements.

5.3.1 Model

Fig. 5.2 provides an illustration of the 9 state DAP system. The DAP model under consideration has two control inputs, nine states, and two outputs. The inputs are the

variable geometry turbine (VGT), u_{VGT}, and the EGR valve, u_{EGR}. u_{VGT} is a linear actuator that changes the vane angle to dictate the speed of the turbine, and hence of the compressor, to regulate the airflow into the intake manifold. u_{EGR} changes the valve opening to control the flow from the exhaust manifold to the intake manifold for effective NO_x treatment. In this model, throttle percent closed (θ), engine speed (N), and fuel flow ($\mathcal{W}_{fuel}$) are treated as known disturbances.

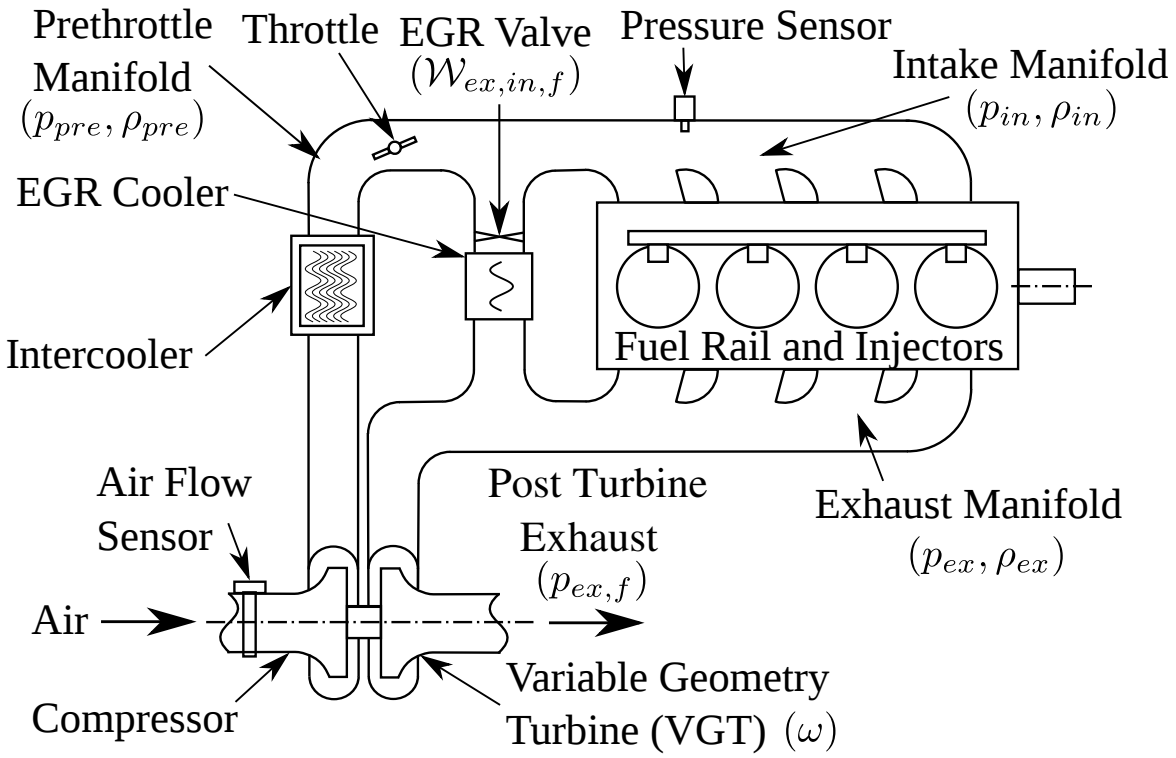

Figure 5.2: 9 state diesel engine airpath diagram. The symbols inside the parentheses indicate the state variables associated with the process.

The derivation of the DAP model for control has been discussed in [136]. The dynamical equations for the engine components are derived through applications of the ideal gas law, conservation of mass, and conservation of energy (Table 3.7 provides a summary). The equation for the turbine speed is a result from conservation of energy. The DAP model used in this chapter is different from that used in Chapter 3: the burn gas fractions are removed, pre-throttle air density is added, and two filter states are added for estimation of post-turbine exhaust pressure, $p_{ex,f}$, and the EGR flow from exhaust $\mathcal{W}_{ex,in,f}$. The six remaining states present in this model are: pressures, p, and densities, ρ, in the intake manifold, the

pre-throttle volume, and the exhaust manifold; and the VGT rotational speed, ω.

The equations of the 9th order DAP model are summarized here for easy reference:

$$\dot{p}_{pre} = \gamma\mathcal{R}\frac{\mathcal{W}_{c,in}\mathcal{T}_c - \mathcal{W}_{thr,in}\mathcal{T}_{pre}}{\mathcal{V}_{pre}} \tag{5.32a}$$

$$\dot{\rho}_{pre} = \frac{\mathcal{W}_{c,in} - \mathcal{W}_{thr,in}}{\mathcal{V}_{pre}} \tag{5.32b}$$

$$\dot{p}_{in} = \frac{\gamma\mathcal{R}}{\mathcal{V}_{in}}(\mathcal{W}_{c,in}\mathcal{T}_{c,in} + \mathcal{W}_{ex,in}\mathcal{T}_{ex} - \mathcal{W}_{in,eng}\mathcal{T}_{in} - \mathcal{W}_{in,ex}\mathcal{T}_{in} - \frac{\dot{\mathcal{Q}}_{in}}{c_p}), \tag{5.32c}$$

$$\dot{\rho}_{in} = \frac{1}{\mathcal{V}_{in}}(\mathcal{W}_{c,in} + \mathcal{W}_{in,ex} + \mathcal{W}_{in,eng}), \tag{5.32d}$$

$$\dot{p}_{ex} = \frac{\gamma\mathcal{R}}{\mathcal{V}_{ex}}(\mathcal{W}_{eng,ex}\mathcal{T}_{eng,ex} - \mathcal{W}_{ex,tur}\mathcal{T}_{ex} - \mathcal{W}_{ex,in}\mathcal{T}_{ex} + \mathcal{W}_{in,ex}\mathcal{T}_{in} - \frac{\dot{\mathcal{Q}}_{ex}}{c_p}), \tag{5.32e}$$

$$\dot{\rho}_{ex} = \frac{1}{\mathcal{V}_{ex}}(\mathcal{W}_{eng,ex} - \mathcal{W}_{ex,tur} - \mathcal{W}_{ex,in} + \mathcal{W}_{in,ex}), \tag{5.32f}$$

$$\dot{\omega} = \frac{30^2 c_p}{\pi^2 I_{tc}\omega}(\eta\mathcal{W}_{ex,tur}(\mathcal{T}_{ex} - \mathcal{T}_{tur}) - \mathcal{W}_{c,in}(\mathcal{T}_{c,in} - \mathcal{T}_{amb})), \tag{5.32g}$$

$$\dot{p}_{ex,f} = f_1 p_{ex,f} + f_2 p_{ex}, \tag{5.32h}$$

$$\dot{\mathcal{W}}_{ex,in,f} = f_3\mathcal{W}_{ex,in,f} + f_4\mathcal{W}_{stat}, \tag{5.32i}$$

where $\mathcal{W}_{stat}$ is the static EGR valve flow. $f_\bullet$ are the filter coefficients, and Table 3.6 gives definitions of the remaining variables and subscripts.

The outputs of the system are selected as intake pressure, p_{in}, and the fractional rate of EGR, or EGR rate, entering the intake manifold. EGR rate is defined as

$$\phi_{EGR} = \frac{\mathcal{W}_{ex,in,f}}{\mathcal{W}_{ex,in,f} + \mathcal{W}_{in,eng}}, \tag{5.33}$$

and the outputs will be ordered as

$$y = [p_{in}\ \phi_{EGR}]^\top. \tag{5.34}$$

In the following subsections, nonlinear model order reduction will be attempted to derive a lower order model to facilitate NMPC design. In the process, the nonlinear model (5.32) will be used as a virtual engine test bench that generates data for the gramian calculation.

5.3.2 DAP Nonlinear Model Order Reduction

Nonlinear model order reduction is attempted for the DAP model (5.32), using the proposed empirical gramian formulation. Nonlinear MPC is then designed using the reduced order model and evaluated with the full order model as the plant.

To compare the results with other model reduction approaches, two other reduced order nonlinear models are derived as summarized in Table 5.1. Moreover, NMPC using the full order model for prediction is also included.

Table 5.1: Gramians and the parameters used to calculate a balancing transformation.

Model	**Description**	**Parameters**
LG	4th order nonlinear model derived from Algorithm 5.1 with the linear gramians, (5.2a) and weighted observability gramian.	(x_e, u_e), $Q = \text{diag}(1, 100)$
EG Trad	4th order nonlinear model derived with Algorithm 5.1 with the empirical gramians of [70].	(x_e, u_e), $T_{\mathcal{C}}^2 = I_{2\times 2}$, $T_{\mathcal{O}}^9 = I_{9\times 9}$, $M_{\mathcal{C}} = \{2.5, 7\}$, $M_{\mathcal{C}} = \{1\}$.
EG Mod	4th order nonlinear model derived with Algorithm 5.1 and the modified empirical gramians (5.22) and (5.28).	(x_e, u_e), $Q = \text{diag}(1, 100)$, $R = I_{2\times 2}$, $v_{il} = 0.1\|u_i\|e_i$, $w_{jl} = 0.1\|x_j\|e_j$

For the EG Trad model, the parameters chosen result in 4 control and 9 initial condition probe directions; for the control directions, 10% perturbations were selected, but the initial condition perturbation size was limited to 1 due to physical definition and limitation of the variables associated with densities. However, the EG Mod model requires only 2 control and 9 initial condition probe directions but spans 10% perturbations in each input/state.

The operating condition selected for design was $N = 167\ rad/s$, $\mathcal{W}_{fuel} = 1.33\ g/s$, $\theta = 6\%$ closed, $u_{VGT} = 70\%$ closed, $u_{EGR} = 25\%$ open, and represents a nominal operating condition. The resulting steady state used for the design, x_e, is calculated by simulating the model until the norm of the derivative is less than 1×10^{-8}. For the LG and EG Mod gramians, the output weight, $Q = \text{diag}(1, 100)$, was chosen to reflect the desire for greater EGR rate accuracy.

5.3.3 Open-Loop Results

The output response of the three 4th order models given in Table 5.1 were tested to evaluate the model reduction performance and compare with the full order model in open-loop. The input sequence was designed to excite several operating regimes of the model.

Fig. 5.3 provides the output responses of p_{in} (Fig. 5.3(a)) and ϕ_{EGR} (Fig. 5.3(b)) to the control inputs of Fig. 5.3(c). Fig. 5.3(a) and 5.3(b) show that over even moderate deviations of the inputs, the nonlinear reduced order models derived using linearized model gramian (LG) and empirical gramian of [70] (EG Trad) are unstable. However, "EG Mod," the model derived with the modified empirical gramian proposed in this chapter, remains stable and performs considerably better with a maximum error of 5 kPa in intake pressure, and 9% EGR rate over the input sequence compared to the full order.

In [70] it is stated that for the empirical gramian, perturbing only once in each direction leads to insufficient information for the gramians. Given the simulation results of Fig. 5.3, even with two perturbations along each excitation direction, the EG Trad does not result in viable reduced order model. However, EG Mod used only a single probe direction in each input/state to derive a viable reduced order model. This suggests the modified empirical gramian could have another advantage of requiring fewer tests if experimental data is used for calculation.

5.3.4 MPC Applied to the DAP

To use the NMPC framework, the reduced order DAP models of Table 5.1 were discretized with a sampling time of 1 ms using the forward Euler scheme. Due to non-minimum phase behavior, a longer prediction horizon is necessary [181], in this example the prediction horizon, $N_p = 1000$, or a 1 second horizon; however, a longer prediction horizon increases the number of decision variables and hence the complexity of the controller.

To bring the controller into the realm of computational feasibility for a simulation, input-velocity - input move blocking MPC is employed to reduce the number of decision variables [182]. Input velocity MPC uses control deltas, $\Delta u_i = u_i - u_{i-1}$, and error between the output, y_i, and the reference, $\bar{y}_{t,\infty}$. This contrasts conventional and rate-based MPC of Chapter 3.3,

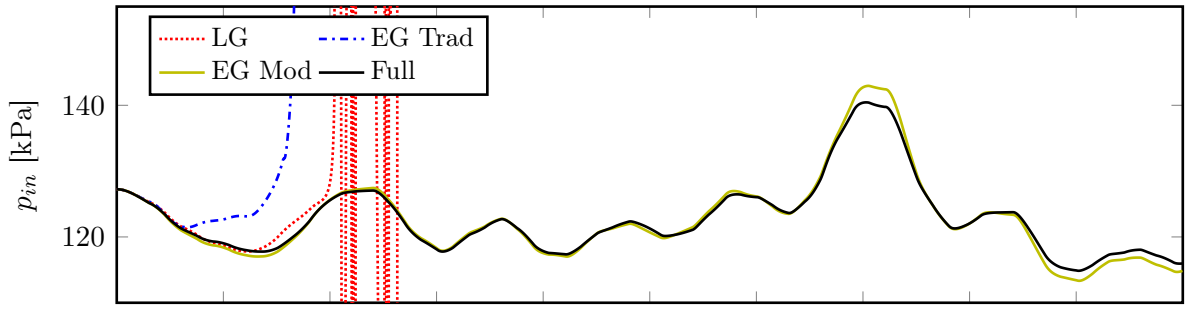

(a) Open-loop intake pressure response.

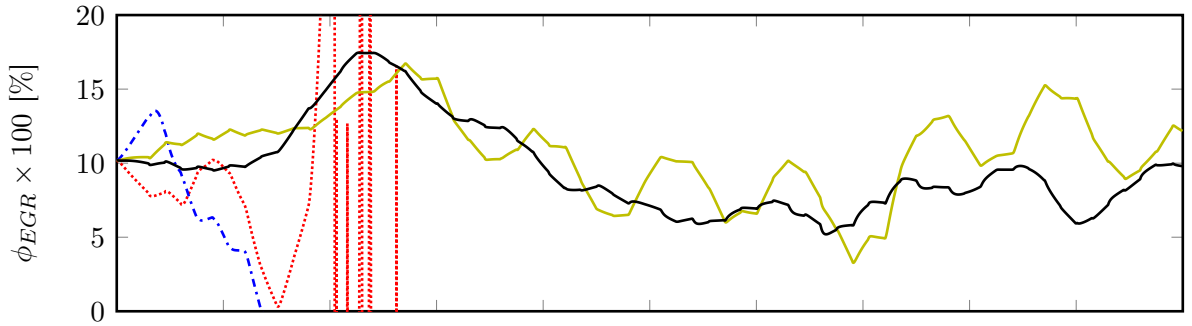

(b) Open-loop EGR Rate response.

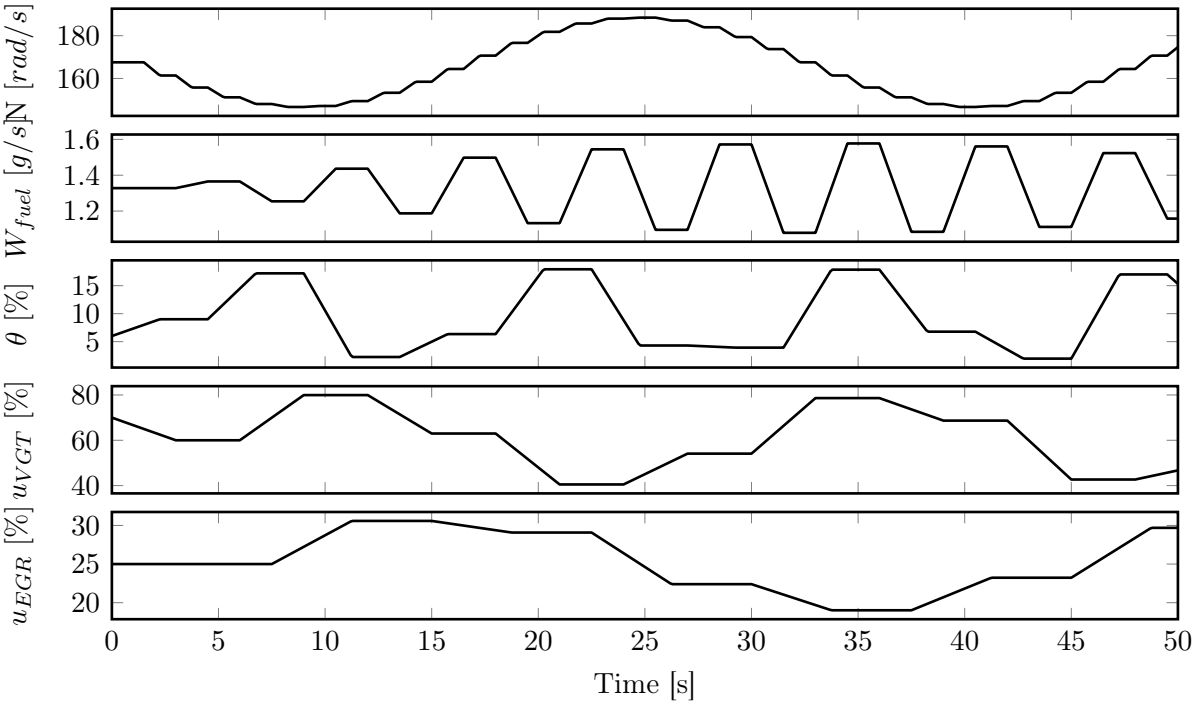

(c) Open-loop inputs.

Figure 5.3: Open-loop response comparison of the full order model and the 4th order models derived using different gramians subject to inputs that excite different operating conditions.

because no terminal penalty exists and no state augmentation is necessary. Move blocking MPC solves for control inputs at different intervals, and is given by the following optimization problem:

$$\left.\begin{aligned} \min_{\{\Delta\hat{u}_i\}_{i\in\mathcal{B}}} \quad & \sum_{i=t}^{t+N_p} (y_i - \bar{y}_{t,\infty})^\top Q (y_i - \bar{y}_{t,\infty}) + \Delta u_i^\top R \Delta u_i, \\ s.t. \quad & \text{Eq. (5.3)}, \\ & u_i \in \mathcal{U} \\ & u_i = u_{i-1} + \Delta u_i, \\ & \Delta u_i = \Delta\hat{u}_i, \text{ if } i \in \mathcal{B}, \\ & \Delta u_i = 0, \text{ if } i \notin \mathcal{B}, \end{aligned}\right\} \tag{5.35}$$

where $\mathcal{U}$ denote the input constraints, $\mathcal{B} = \{t, t+t_1, \ldots, t+t_k\}$, and t_j denotes times when the control is allowed to change. For the examples presented, $t_j = 32j$ was selected, bringing the number of decision variables from 2000 to 64.

For the simulations, the cost function weightings were selected as $Q = \text{diag}([1\ 100])$ and $R = I_{2\times 2}$, the same as the Q and R used for empirical gramian design, to reflect a design that places more emphasis on the EGR rate.

Fig. 5.4 presents the results of the NMPC tracking step references using four different models for design: full order, LG, EG Trad, and EG Mod. The results show

- All the controllers stabilize the system, but performance is vastly different.
- In Fig. 5.4(a) and 5.4(b), the EG Mod reduced order model results in the smallest errors, when compared to the full order response.
- In Fig. 5.4(c) and 5.4(d), the EG Mod controls are the closest match to the optimal controls generated using the full order model.

Table 5.2 contains the total time required to calculate the control for the simulation on an Intel i5-2430M processor with MATLAB's fmincon solver. While the present NMPC controller is not real-time feasible, it demonstrates that the model order reduction results in about a 20% decrease in computation time for the DAP model.

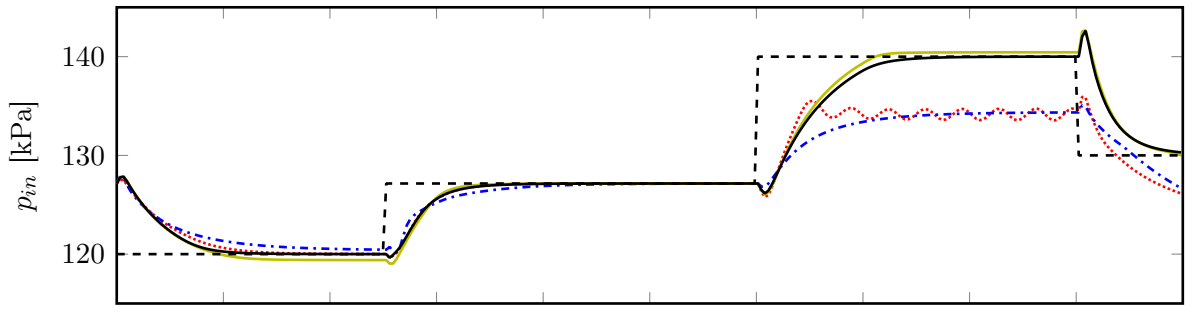

(a) Intake pressure tracking using NMPC law.

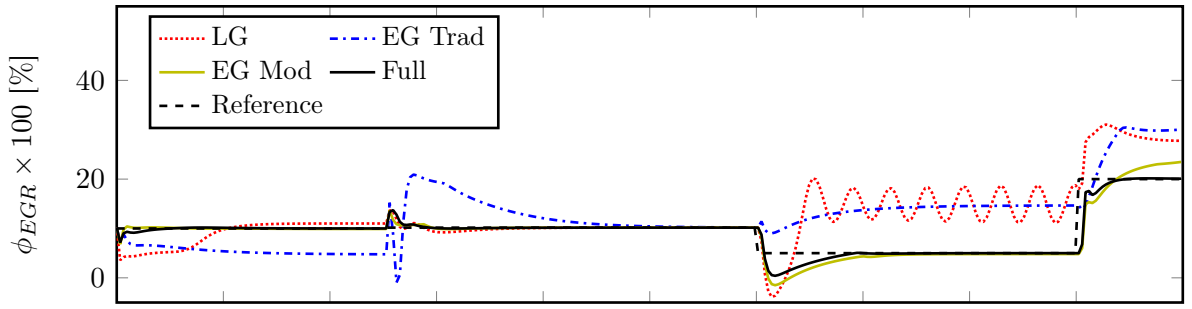

(b) EGR Rate tracking using NMPC law.

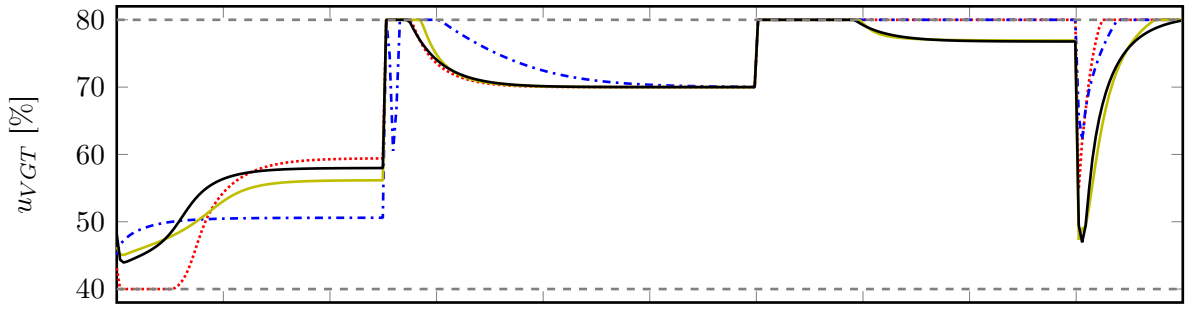

(c) VGT control input.

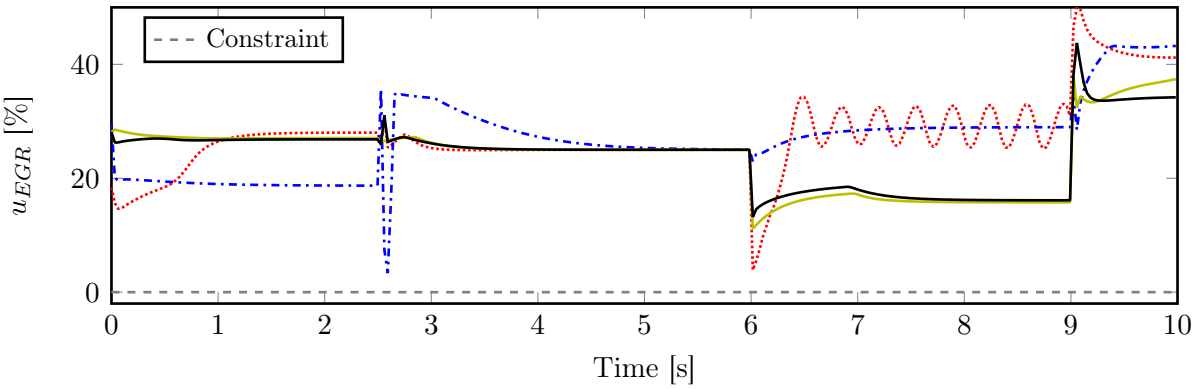

(d) EGR Valve control input.

Figure 5.4: NMPC tracking responses. The modified empirical gramian-based reduced order model results in similar output and control responses.

Table 5.2: Total NMPC calculation times over 10 second simulation for different models.

Model	Full	LG	EG Trad	EG Mod
Time [s]	2697.4	2098.7	2052.8	2151.7

5.4 Conclusions

In this chapter, modified definitions of the empirical gramians were presented. The modified empirical gramians allows one to select the probing input signals with different amplitudes and directions, therefore making it easier to address the case of constraints on the input and state. Further, output weighted gramians were employed to show the improvement in open- and closed-loop accuracy to a goal oriented model order reduction. Open-loop and closed-loop NMPC simulations were provided, demonstrating that the reduced order model derived using the modified empirical gramian resulted in superior performance to both a reduced order model derived with a linear gramian and the empirical gramian of [70]. Finally, the reduced order models demonstrated a decrease in control calculation time.

Chapter 6

Closed-Loop Nonlinear Model Order Reduction

The work presented in this chapter considers closed-loop model order reduction for nonlinear systems from the perspective of closed-loop performance matching, assuming that linear quadratic (LQ) optimal control and estimation (separately designed) are employed. This design framework captures many well known compensation techniques, e.g., LQG, MPC/moving horizon estimator (MHE), and finite horizon LQR/Kalman filter.

LQ methods for linear systems depend on the solutions of an algebraic, differential/difference, or operator Riccati equations [107, 183] (occasionally called closed-loop gramians in the algebraic case [184]). These Riccati solutions provide information about subspaces that are easy to control and estimate relative to an LQ cost. For the purpose of reduction, easy to control and estimate states are unimportant to compensator design and can be truncated [3]. For nonlinear systems, however, the general Hamilton-Jacobi-Bellman equation must be solved [175], and the concept of a Riccati solution breaks down for model reduction. Affine input nonlinear systems have the notion of past and future energy functions and a excellent theoretical foundation [60, 61, 185], however, the practical use remains a challenge because of the global existence and non-uniqueness of continuous functions that solve nonlinear partial differential equations [66, 186]. Therefore, it is proposed to use an empirical approach to calculate control and filter Riccati covariance matrices using controlled inputs/outputs and state estimation information.

Combining the results of Chapter 3 and 5, the notion of linear quadratic balanced truncation, and closed-loop gramian balanced truncation, is extended to nonlinear systems using empirically obtained Riccati covariance matrices. Balanced truncation using the covariance matrices is leveraged to provide a control specific reduced order model and the efficacy of the proposed approach is demonstrated with a spatially discretized catalytic rod example.

The chapter is organized as follows: in Section 6.1 a brief overview of MOR is provided and the goal of closed-loop model order reduction is discussed. In Section 6.2 the empirical Riccati covariance matrices are defined and a reduction procedure is provided to derive a nonlinear reduced order model for LQ compensator design. Section 6.3 provides an example to demonstrate the utility of the proposed approach, a spatially discretized model of a catalytic rod is controlled with an MPC/extended Kalman filter (EKF) compensator designed with the proposed reduction technique, and compared against the full order compensator and compensators derived with other common gramian and Riccati-based reduced order models. Finally, the chapter is recapped in Section 6.4 and an open problem stated.

6.1 Reduced Control and Estimator Problem

Inspired by the closed-loop model order reduction results for linear systems of Chapter 3, systematic approaches to perform model order reduction for nonlinear systems that focus on closed-loop performance are sought. To state the model order reduction problem for nonlinear compensator design, assume a model for the system, Σ, under feedback control $u = c(x)$, is in the general ordinary differential equation form:

$$\Sigma : \begin{cases} \dot{x} &= f(x,u), \\ y &= h(x,u), \\ u &= c(x), \end{cases} \tag{6.1}$$

where the state $x \in \mathcal{X} \subset \mathbb{R}^n$, input $u \in \mathcal{U} \subset \mathbb{R}^m$, and output $y \in \mathcal{Y} \subset \mathbb{R}^p$ are constrained with sets $(\mathcal{X}, \mathcal{U}, \mathcal{Y})$. (6.1) has an equilibrium (x_e, u_e, y_e). Moreover, assume an estimator

model of the same dimension is known:

$$\hat{\Sigma}: \begin{cases} \dot{\hat{x}} &= \hat{f}(\hat{x}, u, y), \\ \hat{y} &= h(\hat{x}, u), \\ \hat{x}_0 &= x_e. \end{cases} \tag{6.2}$$

Assuming that the controller and estimator are designed independent of one another using LQ design methodologies, the work presented here pursues a reduced order model for controller design, with closed-loop performance that matches that of the full order controller while the computational complexity is substantially reduced.

6.2 Empirical Riccati Covariance Matrices and the Reduced Order Model

In [46], the authors use minimum energy control and the output energy of the free response of a linear system and the relationship to the linear controllability and observability gramians, respectively, to motivate the definitions of an empirical gramian. The same approach is taken here to define the Riccati covariance matrices, but instead the LQ regulator (LQR) and LQ estimation (LQE) problem will be related to the control and filter Riccati solutions, respectively.

The following assumptions are made to ensure the existence and boundedness of the covariance matrices presented in the following subsections:

*A*6.1**:** $u = c(x)$ is an asymptotically stabilizing controller,

*A*6.2**:** $u - u_e$ is $L^2[0, \infty)$-integrable,

*A*6.3**:** the resulting output, $y(t) - y_e$, of a system subject to $c(x)$ is $L^2[0, \infty)$-integrable,

*A*6.4**:** the estimated state converges asymptotically to $\hat{x}_{ss}$, and

*A*6.5**:** $\hat{x} - \hat{x}_{ss}$ is $L^2[0, \infty)$-integrable.

In general, the separation principle does not hold for nonlinear systems. This makes it necessary to also assume that the compensator ($u = c(\hat{x})$) asymptotically stabilizes both Σ and $\hat{\Sigma}$.

6.2.1 Empirical Control Riccati Covariance Matrix

To motivate the empirical Riccati covariance matrix for nonlinear systems, we start with the formulation for linear systems. Given a linear system, $\Sigma_{\mathcal{L}}$, LQ weights Q and R with a cross term S, and an asymptotically stabilizing controller $u = -Kx$, the control cost function is defined as

$$\begin{aligned} J_{\mathcal{L}}(x_0, K) &= \int_0^\infty y^\top(t)Qy(t) + 2y^\top(t)Su(t) + u^\top(t)Ru(t)dt, \\ &= x_0^\top \bar{P} x_0 < \infty, \end{aligned} \tag{6.3}$$

where $\bar{P}$ is a symmetric positive definite matrix known as the closed-loop control gramian, and is dependent upon K. In a special case when K is the LQR gain, $\bar{P}$ is the solution to the control Riccati equation.

For a simpler exposition, assume $S = 0$ and there is no direct feedthrough, $D = 0$, then $J_{\mathcal{L}}$ can be separated into control and output cost components:

$$x_0^\top \bar{P}_u x_0 = \int_0^\infty u^\top(t)Ru(t)dt, \tag{6.4a}$$

$$x_0^\top \bar{P}_y x_0 = \int_0^\infty x^\top(t)C^\top QCx(t)dt, \tag{6.4b}$$

where $\bar{P}_u$ and $\bar{P}_y$ satisfy the Lyapunov equations

$$(A - BK)^\top \bar{P}_u + \bar{P}_u(A - BK) = -K^\top RK, \tag{6.5a}$$

$$(A - BK)^\top \bar{P}_y + \bar{P}_y(A - BK) = -C^\top QC, \tag{6.5b}$$

then $\bar{P}$ can be calculated from algebraic Lyapunov equations

$$\bar{P} = \bar{P}_u + \bar{P}_y. \tag{6.6}$$

$\bar{P}_u$ in (6.5a) can be easily established by recognizing

$$\begin{aligned} \bar{P}_u &= \int_0^\infty e^{(A-BK)^\top t} K^\top R K e^{(A-BK)t} dt, \\ (A-BK)^\top \bar{P}_u + \bar{P}_u (A-BK) &= \int_0^\infty \frac{d}{dt}\left\{ e^{(A-BK)^\top t} K^\top R K e^{(A-BK)t} \right\} dt, \\ &= -K^\top R K. \end{aligned}$$

Likewise the equation for $\bar{P}_y$ in (6.5a) can be established.

Moreover, the quantities $\bar{P}_u$, $\bar{P}_y$, and $\bar{P}$ can be obtained experimentally by calculating covariances of the output, y, and input, u, responses to different initial conditions. To perform the calculation, experiments are built that perturb the initial condition about the equilibrium, x_e, as follows:

Select the probe directions to be orthogonal vectors, $w_{il} \in \mathbb{R}^n$, such that

$$w_{il}^\top w_{jl} = ||w_{il}||^2 \delta_{ij}, \tag{6.7}$$

$$w_{il} + x_e \in \mathcal{X} \tag{6.8}$$

where δ_{ij} denotes the Kronecker delta, defined as:

$$\delta_{ij} = \begin{cases} 1 & \text{if } i = j, \\ 0 & \text{otherwise,} \end{cases} \tag{6.9}$$

with $i = 1, \ldots, n$, $l = 1, \ldots, r_o$ and r_o denotes the number of experimental sets, and $w_{i_1 j_1} \neq w_{i_2 j_2}$ unless $i_1 = i_2$ and $j_1 = j_2$. Define the matrix $V_l^{\mathcal{O}}$ as

$$V_l^{\mathcal{O}} = \begin{bmatrix} w_{1l} & \cdots & w_{nl} \end{bmatrix} \in \mathbb{R}^{n \times n}. \tag{6.10}$$

Definition 6.2.1. *Let $x^{il}(0) = w_{il} + x_e$, x^{il}, u^{il}, and y^{il} be the corresponding responses of (6.1); then with assumptions A6.1-A6.3, the empirical control Riccati covariance matrix is finite and defined as*

$$P = \frac{1}{r_o} \sum_{l=1}^{r_o} \int_0^\infty V_l^{\mathcal{O}} \Omega_l^{-1} \Psi_l(t) \Omega_l^{-1} (V_l^{\mathcal{O}})^\top dt \tag{6.11}$$

where

$$[\Psi_l(t)]_{ij} = \begin{bmatrix} y^{il} - y^{il}_{ss} \\ u^{il} - u^{il}_{ss} \end{bmatrix}^\top \begin{bmatrix} Q & S \\ S^\top & R \end{bmatrix} \begin{bmatrix} y^{jl} - y^{jl}_{ss} \\ u^{jl} - u^{jl}_{ss} \end{bmatrix}, \tag{6.12}$$

$$\Omega_l = \text{diag}(||w_{1l}||^2, \ldots, ||w_{nl}||^2), \tag{6.13}$$

and y_{ss} and u_{ss} are the steady state output and control.

The relation between the empirically defined matrix P of (6.11) and algebraic Riccati solution is established by the following theorem:

Theorem 6.2.1. *With $S = 0$ and $D = 0$, if Σ is linear, minimal, and stabilized by a feedback gain K, then $P = \bar{P}$ satisfies the closed-loop Lyapunov equation*

$$(A - BK)^\top P + P(A - BK) = -C^\top QC - K^\top RK. \tag{6.14}$$

If K is selected as the optimal LQ gain, $K = R^{-1}B^\top P$, then P satisfies the algebraic Riccati equation (ARE)

$$A^\top P + PA + C^\top QC - PBR^{-1}B^\top P = 0. \tag{6.15}$$

Proof. See Appendix A.5.1 for the proof. □

6.2.2 Empirical Filter Riccati Covariance Matrix

The dual to the control problem is that of estimation. It is common to formulate the estimation problem with the dual system $\Sigma^*_{\mathcal{L}} = (-A^\top, -C^\top, B^\top, D^\top)$, with weights Γ and Λ and a cross term N. If L is a stabilizing estimator of $\Sigma^*_{\mathcal{L}}$, the estimation cost function is

$$\begin{aligned} J^*_{\mathcal{L}}(x^*_0, L) &= \int_{-\infty}^{0} y^{*\top}(t)\Gamma y^*(t) + 2y^{*\top}(t)Nu^*(t) + u^{*\top}(t)\Lambda u^*(t)dt, \\ &= x^{*\top}_0 \Pi^{-1} x^*_0, \end{aligned} \tag{6.16}$$

and with $N = 0$ and $D = 0$,

$$\Pi = \Pi_{u^*} + \Pi_{y^*}, \tag{6.17}$$

which are defined analogously to (6.4a). Π is a symmetric positive definite matrix known as the closed-loop observability gramian (in a special case when L is the LQE gain, Π is the filter Riccati solution). This formulation, however, presents two conceptual problems: how to measure the dual states and how to go forward in time? To make the problem tractable, the LQE formulation is used:

$$\min_{\hat{x}} \ \mathbb{E}[(\hat{x}-x)^\top(\hat{x}-x)|y], \tag{6.18}$$

subject to linear dynamics $\Sigma_{\mathcal{L}}$, and additive zero mean Gaussian noises on the input (v) and output (w) with covariances,

$$\begin{aligned}\mathbb{E}[v(t)v^\top(t)] &= \Gamma,\\ \mathbb{E}[w(t)w^\top(t)] &= \Lambda,\\ \mathbb{E}[w(t)v^\top(t)] &= N,\end{aligned}$$

where $\mathbb{E}$ denotes the expectation. Using the LQE formulation, an algebraic Riccati equation arises, and its solution is Π [107, Chapter 7].

Similar to the empirical control Riccati covariance matrix, Π can be calculated through estimator responses to control and output experiments.

Select the probe directions to be orthogonal vectors $\tilde{v}_{il} \in \mathbb{R}^{m+p}$, such that

$$(\tilde{v}_{il})^\top \tilde{v}_{jl} = ||\tilde{v}_{il}||^2 \delta_{ij}, \tag{6.19a}$$

$$E_l E_l^\top = \begin{bmatrix} \Gamma & -N \\ -N^\top & \Lambda \end{bmatrix}, \tag{6.19b}$$

$$v_{il} = E_l \tilde{v}_{il}, \tag{6.19c}$$

$$\begin{bmatrix} u^{il} \\ y^{il} \end{bmatrix} = v_{il} + \begin{bmatrix} u_e \\ y_e \end{bmatrix}, \tag{6.19d}$$

with $i = 1, \ldots, m+p$, $l = 1, \ldots, r_c$, where r_c denotes the number of experimental sets, and $\tilde{v}_{i_1 j_1} \neq \tilde{v}_{i_2 j_2}$ unless $i_1 = i_2$ and $j_1 = j_2$.

Definition 6.2.2. *Select $\tilde{v}_{il}$ such that $[I_{m\times m}\ 0_{m\times p}]v_{il} + u_e \in \mathcal{U}$, $[0_{p\times m}\ I_{p\times p}]v_{il} + y_e \in \mathcal{Y}$, where I and 0 are identity and zero matrices of specified dimension. Then with assumptions A6.4*

and A6.5, the empirical filter Riccati covariance matrix is finite and defined to be:

$$\tilde{\Pi} = \sum_{i=1}^{m+p} \sum_{l=1}^{r_c} \frac{1}{r_c ||\tilde{v}_{il}||^2} \int_0^\infty \Phi^{il}(t) dt, \tag{6.20}$$

where

$$\Phi^{il}(t) \;=\; \left(\hat{x}^{il}(t) - \hat{x}^{il}_{ss}\right)\left(\hat{x}^{il}(t) - \hat{x}^{il}_{ss}\right)^\top, \tag{6.21}$$

and $\hat{x}^{il}(t)$ ($\hat{x}^{il}_{ss}$) is the solution (steady state) of (6.2) with the perturbed control and output.

The relation between the empirically defined matrix $\tilde{\Pi}$ of (6.20) and algebraic Riccati solution is established by the following theorem:

Theorem 6.2.2. *With $N = 0$ and $D = 0$, if $\hat{\Sigma}$ is linear, minimal, and stabilized with estimation gain L, let*

$$\Pi = (A - LC)\tilde{\Pi}(A - LC)^\top, \tag{6.22}$$

then Π satisfies the closed-loop Lyapunov equation

$$(A - LC)\Pi + \Pi(A - LC)^\top = -B\Gamma B^\top - L\Lambda L^\top. \tag{6.23}$$

If L is selected as the optimal LQ gain, $L = \Pi C^\top \Lambda^{-1}$, then Π satisfies the algebraic Riccati equation

$$A\Pi + \Pi A^\top + B\Gamma B^\top - \Pi C^\top \Lambda^{-1} C\Pi = 0. \tag{6.24}$$

Proof. See Appendix A.5.2 for the proof. □

Remark 6.2.1. *Theorem 6.2.1 and 6.2.2 hold true when the cross term in the cost function (6.3) and/or (6.16) is not zero ($S \neq 0$, $N \neq 0$), and/or when direct feedthrough is present ($D \neq 0$). This is achieved by adding cross term Lyapunov equations,*

$$\begin{aligned}
(A - BK)^\top \bar{P}_c + \bar{P}_c(A - BK) &= C^\top SK + K^\top S^\top C, \\
(A - LC)^\top \bar{\Pi}_{c^*} + \bar{\Pi}_{c^*}(A - LC) &= BNL^\top + LN^\top B^\top
\end{aligned}$$

so that

$$\begin{aligned}\bar{P} &= \bar{P}_u + \bar{P}_y + \bar{P}_c,\\ \bar{\Pi} &= \bar{\Pi}_{u^*} + \bar{\Pi}_{y^*} + \bar{\Pi}_{c^*},\end{aligned}$$

and modifying the LQ problem and optimal gain, respectively.

Just as for the empirical controllability/observability covariance matrices: care must be taken to assure that the state will stay within the domain of attraction of the controller $c(x)$ and estimator, and the empirical Riccati covariance matrices are dependent upon the selection of the probe directions w_{il} and $\tilde{v}_{il}$.

While the equivalence of the empirical Riccati solution is established for linear systems, the calculation of P and $\tilde{\Pi}$ in the form of (6.11) and (6.20), respectively, is extended for nonlinear systems whose Riccati-like quantities cannot be analytically derived, and this forms the key idea of the proposed reduction method.

Remark 6.2.2. *Empirical Riccati covariance matrices can be defined for discrete time systems by using sums instead of integrals. Because the empirical gramian framework was used, small modifications can be made to software such as [180] for rapid implementation.*

6.2.3 Model Order Reduction Algorithm

The measure of how easy it is to control and estimate a subspace, and hence its contribution to an LQ cost, is given by the empirical Riccati singular values (ERSVs) and follows that of [3].

Definition 6.2.3 (Empirical Riccati Singular Values)**.** *Given the covariance matrices P, $\tilde{\Pi}$ from* (6.11)*,* (6.20)*, respectively, the ERSVs are defined as $\mu_j = \sqrt{\lambda_j(P\tilde{\Pi})}$. $\lambda_j(\cdot)$ denotes the eigenvalues of the matrix ordered from the largest to the smallest.*

A small ERSV corresponds to a subspace that is easy to control and estimate, thereby having little impact on the cost and not important for compensator design. To select the order r of the reduced order model, one often chooses r such that $\mu_r \gg \mu_{r+1}$.

The notion of an internally balanced representation is employed for model order reduction:

Definition 6.2.4 (Empirical Riccati Balanced)**.** Σ *is said to be internally balanced when* $P = \tilde{\Pi} = M$*.* $M = \text{diag}(\mu_1, \ldots, \mu_n)$ *with* $\mu_1 \geq \mu_2 \geq \ldots \geq \mu_n$*, where* n *is the order of the system.*

To derive the reduced order model of order r, the model is transformed to an internally balanced representation and the $n - r$ last states are truncated. The balancing transformation, $\mathscr{T}$, is given by Algorithm 6.1. $\mathscr{T}$, the reduced order, the model and parameters are provided to Algorithm 5.2 to yield a reduced order model for compensator design.

Algorithm 6.1 NMOR using empirical Riccati balanced truncation.

1: **procedure** EMPIRICAL_RBT($P, \tilde{\Pi}, f, h, (x_e, u_e), x_0, r$)
2: Calculate (6.11) and (6.20) for positive definite empirical Riccati covariance matrices P and $\tilde{\Pi}$, respectively.
3: Calculate the Cholesky factors of $P = XX^\top$, $\tilde{\Pi} = YY^\top$.
4: Calculate the singular value decomposition (SVD) of $Y^\top X = GMH^\top$, where M is a positive definite diagonal matrix and G and H are orthogonal matrices.
5: Form the balancing transformation

$$\mathscr{T} = M^{1/2} G^\top Y^{-1}. \tag{6.25}$$

return $\mathscr{T}$
6: **end procedure**

In [70], it is noted that for a linear system, the difference between a controllability gramian and the controllability covariance matrix, W_C, is the contragredient transformation of $W_{\mathcal{C}}$ by A (for the filter Riccati covariance matrix, this is $\tilde{\Pi}$ and $A - LC$). For the purposes of step tracking, covariance matrix based reduction is expected to yield a better reduction because it uses a step input, not an impulse input like in the case of the gramian. Likewise, it is expected that the filter Riccati covariance matrix will yield a better reduced order model for compensator design when compared to the filter Riccati solution.

Remark 6.2.3. *This reduction technique provides a generalization to the work in [30], not only to the case of cross-term weight, but to nonlinear systems.*

Remark 6.2.4. *Beside the different balancing transformation, there are two key differences between the proposed approach and empirical gramians. One is the inclusion of feedback*

control in the empirical observability gramian framework to calculate the empirical control Riccati covariance matrix. The other is the use of estimator dynamics to calculate the empirical filter Riccati covariance matrix, whereas the original system dynamics are used in calculating the empirical controllability gramian.

6.3 Empirical Riccati MOR Applied to a Catalytic Rod

6.3.1 Catalytic Rod Model and Discretizations

An exothermic catalytic rod with reaction rate independent of the concentration is a thin rod in a reactor that transforms a chemical species A to species B inside the rod. The 1-D, non-dimensional model of the temperature distribution along the catalytic rod with constant temperature at the endpoints, and is given by

$$\frac{\partial x}{\partial t} = \frac{\partial^2 x}{\partial z^2} - \beta_T e^{-\gamma} + \beta_T e^{-\frac{\gamma}{1+x}} + \beta_U (b(z)u - x) \tag{6.26}$$

subject to boundary conditions $x(0,t) = 0$, $x(\pi,t) = 0$ and initial condition $x(z,0) = x_0(z)$. β_T is the dimensionless heat of reaction, β_U is the dimensionless heat transfer coefficient, γ is the dimensionless activation energy, $x(z,t)$ is the dimensionless temperature along the rod, z denotes the position along the rod from the entrance of species A to the exit of species B, and u is the dimensionless temperature of the surrounding cooling medium. Typical values for the model are $\beta_T = 50$, $\beta_U = 2$, and $\gamma = 4$. Greater details of the catalytic rod model can be found in [187, Section 4.3].

Given these parameters, a non-zero initial condition will evolve into a stable steady state, denoted $x_e(z)$, with an undesirable "hot-spot" in the center of the rod. Using the knowledge that a hot-spot occurs in the center, a distributed measurement, $y(t)$, along the rod of length π is taken with emphasis placed at the center,

$$y(t) = \frac{1}{0.1\pi\sqrt{2\pi}} \int_0^\pi e^{-\frac{(z-\frac{\pi}{2})^2}{0.02\pi^2}} x(z,t) dz, \tag{6.27}$$

and the cooling medium enters from the endpoints, providing the input distribution:

$$b(z) = \frac{1}{\pi}(\cos(z) + 1). \tag{6.28}$$

The control objective, therefore, is to optimally regulate the dimensionless temperature to zero using output feedback subject to constraints on the control and state. The control objective, nonlinearity, and constraints, naturally lead to the use of model predictive control (MPC) with an extended Kalman filter (EKF) for state estimation. While MPC is intuitive for constrained optimal control problems, it is computationally expensive. To reduce complexity, and thereby the computational cost, the model will be spatially discretized into a system of ordinary differential equations (ODEs) using the method of lines with a uniform gridding of z into $N+2$ states ($z^j = j\Delta z,\ j \in 0, 1, \ldots, N+1$), resulting in $\frac{dx(z^j,t)}{dt} = f_j(x(z^j,t), u(t))$ and $y(t) = \sum_j \mathscr{C}_j x(z^j,t)$. The ODEs will be reduced using four different techniques, the reduced models will be temporally (time) discretized with a forward Euler scheme to $x_{t+1}(z^j) = x_t(z^j) + \Delta t f_j(x_t(z^j), u_t)$ and $y_t = \mathscr{C} x_t$, and the resulting discrete time reduced order models will be used for compensator design. The discrete time compensator is then applied to the continuous time, spatially discretized model.

6.3.2 MPC/Extended Kalman Filter Compensator Formulation

The optimal control problem to regulate the dimensionless temperature x to zero using output feedback is captured with the LQ cost:

$$J = x_{t+N_p}^\top P_d x_{t+N_p} + \sum_{i=t}^{t+N_p-1} (\mathscr{C} x_i)^\top Q_d \mathscr{C} x_i + R_d u_i^2, \tag{6.29}$$

where $x_t = \hat{x}_t$, the vector of states estimated by the EKF, $x_i,\ i \in \{t+1, t+N_p\}$ are predicted using $x_{t+1}(z^j)$, N_p is the prediction horizon, P_d is the solution to the linear discrete control algebraic Riccati equation associated with the discretized Q_d and R_d weights, $\mathscr{C}$, $[\mathscr{B}]_j = \Delta t \beta_U b(z^j)$, and the linearization $[A_d]_{ji} = \frac{\partial x_{t+1}(z^j)}{\partial x_t^i}|_{(x_e(z),u=0)}$:

$$P_d = A_d^\top P_d A_d + \mathscr{C}^\top Q_d \mathscr{C} - (A_d P_d \mathscr{B})^\top (R_d + \mathscr{B}^\top P_d \mathscr{B})^{-1} (A_d P_d \mathscr{B}). \tag{6.30}$$

This cost is selected because in a small neighborhood of the equilibrium, where no constraints are active, this approximately becomes a linear, infinite horizon LQR problem.

The MPC problem is formulated to minimize J subject to the spatially discretized dynamics, input, and constraints on the state:

$$\begin{aligned} \min_{\{u_i\}_{i=t}^{t+N_p-1}} \quad & J, \\ s.t. \quad & x_{i+1} = x_i + \Delta t f(x_i, u_i), \\ & x_t = \hat{x}_t,\ u_i \leq 1,\ -0.9 \leq x_i. \end{aligned} \tag{6.31}$$

Per the standard MPC formulation, (6.31) is solved at each time step, t, and u_t is applied to the continuous time/spatially discretized model for Δt in a sample and hold fashion. In the case of a reduced order model Σ_r, being used to design the MPC law, $\hat{x}_t$ is replaced with the immersed estimated reduced state $\mathscr{T}V\hat{\hat{x}}_{r,t}$, and redundant state constraints are identified and eliminated.

6.3.3 Simulation Results

To demonstrate the efficacy of the proposed control specific reduction procedure, the performances of compensators designed with the models from Table 6.1 are compared.

Table 6.1: Models used for compensator design.

M_1:	the full order, spatially discretized, continuous time model
M_2:	reduced, 2nd order model based on Riccati balanced truncation using a linearization of $\frac{dx(t,z^j)}{dt}\|_{(x_e(z),u=0)}$ [71]
M_3:	reduced, 2nd order model based on empirical control/filter Riccati covariance matrix designed at $(x_e(z), u = 0)$ (proposed)
M_4:	reduced, 2nd order model based on gramian balanced truncation using a linearization of $\frac{dx(t,z^j)}{dt}\|_{(x_e(z),u=0)}$ [13]
M_5:	reduced, 2nd order model based on empirical controllability/observability covariance matrix designed at $(x_e(z), u = 0)$ [72]

The probe directions for the empirical controllability/observability and control/filter Riccati covariances matrices were taken to be $w_{kl}(0) = 0.25e_k$, $v_{kl} = 0.25e_k$, where e_k is the k^{th} unit vector of the respective search space.

To obtain the simulation results, the rod length is discretized into 51 segments ($N = 50$), $N_p = 1$, $\Delta t = 0.005$, $Q = 50$, $R = 1$, $S = 0$, and the input and output covariances for the EKF are selected to be $\Gamma = 1$, $\Lambda = 0.05$, and $N = 0$, respectively. Sequential quadratic programming [166] is used to calculate the MPC law, and sparse data types are used where appropriate.

Fig. 6.1 displays various responses: the open-loop output of the specified model, closed-loop output with a compensator designed with specified model, the specified model's estimated output and generated control. Table 6.2 provides measures of computational time obtained with MATLAB's tic-toc and weighted ℓ^2 performance.

Fig. 6.1 and Table 6.2 show that the closed-loop reduction methods have worse open-loop performance, but significantly better closed-loop performance. The reduced order model computation is approximately equal for all methods and result in $\approx 88\%$ improvement over the full order model.

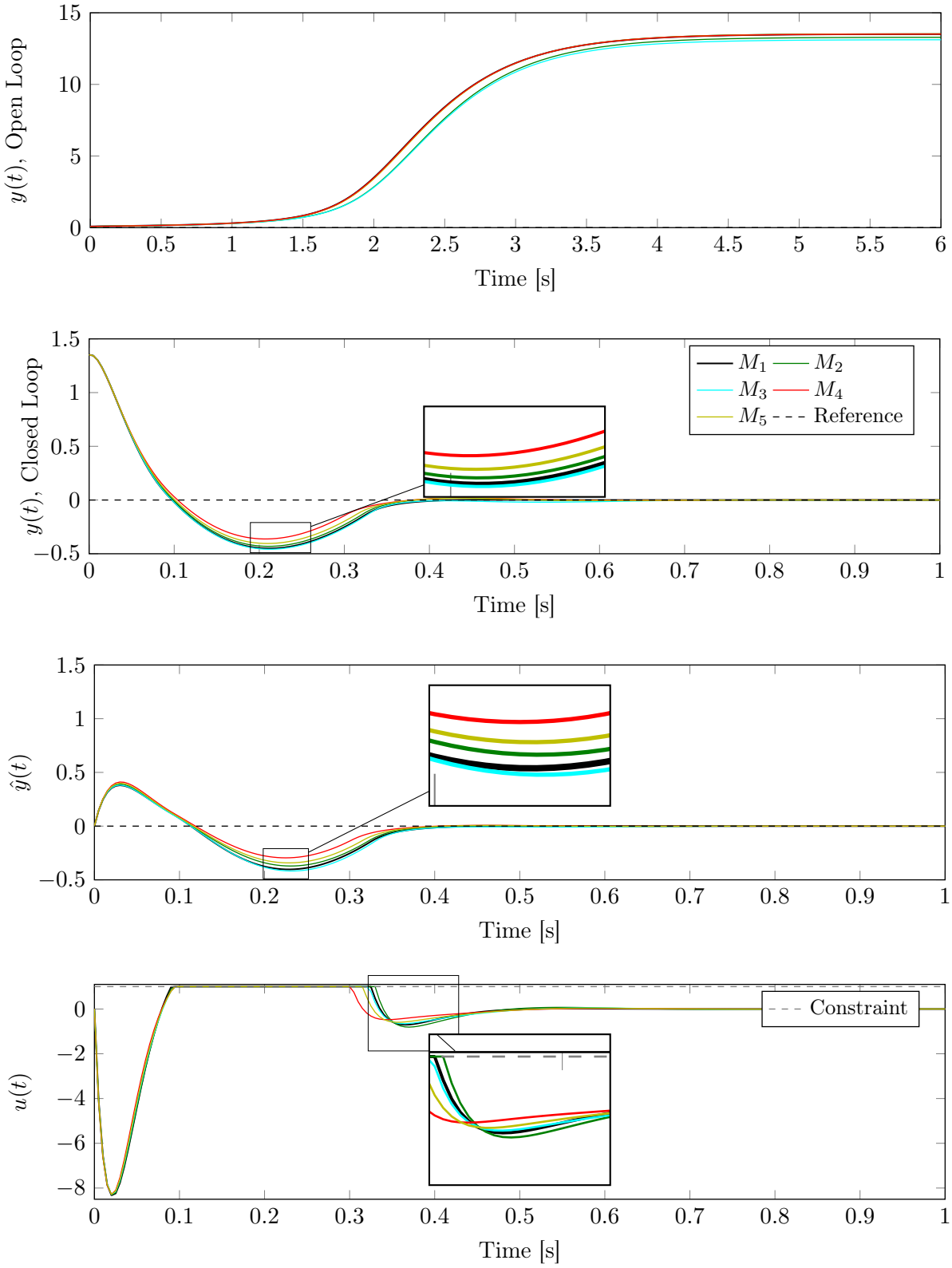

Figure 6.1: A comparison of control, open-loop, closed-loop, and estimated output for compensators generated with the full and reduced order models.

Table 6.2: Table of performance metrics comparing computation time and weighted ℓ^2 error.

	M_1	M_2	M_3	M_4	M_5
Control Computation Time (s)	100.99	11.95	12.04	11.91	12.02
Estimation Computation Time (s)	12.98	1.02	1.02	1.02	1.02
Total Time (s)	113.97	12.97	13.06	12.93	13.04
Error: $\sum_{t=0}^{1} Q(y_t - y_{r,t})^2 + R(u_t - u_{r,t})^2$	-	0.7597	0.4004	7.8950	2.2566

6.4 Conclusions

In this chapter, an empirical approach following that used to obtain empirical Gramians is proposed to calculate control and filter Riccati covariance matrices from selected weights, controller, and estimator. A new model order reduction approach based on empirical Riccati covariance matrices is developed and demonstrated on a catalytic rod model. A spatially discretized model with 50 states was then reduced to the second order using 4 different techniques, and the reduced compensator performances were compared to that of the compensator designed with the full 50 state model. It was found that the proposed reduction resulted in a compensator whose performance was closer to that of the full order compensator. In terms of computational complexity, the reduced order model lead to an 88% reduction in control computation time with negligible loss of performance.

Chapter 7

Conclusions

The aim of this dissertation is the development of frameworks and numerical tools to decrease computational complexity of simulation, condition monitoring, and control of linear and nonlinear systems using systematic model order reduction techniques. Two challenges to obtaining reduced order models are selecting the reduction methodology, and then obtaining quantities/transformations to perform the state removal. In this dissertation, new algorithms to obtain approximations of large scale gramian and Riccati solutions of linear descriptor systems are developed, the LQG balanced truncation methodology is generalized and re-purposed for model predictive control/Kalman filtering, a new reduction problem and solution methodology are proposed for the design of a reduced order compensator of a constrained system, and a new formulation of empirical gramians are proposed and modified to yield Riccati covariance matrices.

For the selected purposes of the reductions, the efficacy of the techniques were demonstrated on a variety of toy, challenging, and real world problems.

7.1 Contributions

The major contributions of this dissertation are:

1. *Novel techniques to efficiently calculate, and aid in calculating low-rank matrix square root factors to approximate a gramian and Riccati solution, for the purpose of model order reduction of large scale linear systems.*

First, bilinear discretizations of descriptor systems were developed, and their eigenvalues/vectors found. The eigenvalues/vector information was used to guide a low-rank alternating direction implicit method to obtain an accurate low-rank matrix square root factor for a gramian or Riccati solution approximation.

Then, it was noted that convergence could be slow, creating a need to increase the rank of the approximation or to re-calculate the entire gramian. To deal with both problems, a novel up/downdating technique was proposed. The up/downdating technique facilitates:

(a) "condensing" a slowly converging low-rank matrix square root factor to decrease the memory footprint,

(b) exploitation of the linearity of a gramian to the constant term, allowing component/parallelized calculation of gramians of multi-input, multi-output (MIMO) systems, and

(c) a posteriori weighting of gramians.

It was found that these components only need to be calculated a single time, and could be combined to yield (in the most general form) a weighted gramian approximation for the purpose of approximate balanced truncation. This enables faster calculation/design of an approximate reduced order model when compared to prior methods that require the direct computation of the weighted gramian approximation.

The methods were applied to random systems to demonstrate computational feasibility and accuracy, and an electric machine model for the purpose of condition monitoring. For large, random systems, the proposed technique resulted in faster and more accurate calculation of the gramian than the the generalized Bartels-Stewart algorithm. For the electric machine problem, the combined model was reduced from over 100,000 states to 8 while performing better than the state-of-the-art modal truncation.

2. *Extending Linear Quadratic Gaussian (LQG) balanced truncation and using it in conjunction with model predictive control.*

LQG balanced truncation typically used the normalized LQG formulation with no direct feedthrough or cross-term. Chapter 3 developed the generalization to the non-normalized LQG, with cross-term, of a system with direct feedthrough, denoted Riccati balanced truncation (RBT).

A way of calculating low-rank matrix square root factors of the Riccati solutions for large scale systems was developed using the Newton-Kleinman iteration and the novel techniques to calculate low-rank matrix square root factors of the gramians for large scale systems. It was noted how to perform approximate RBT. An approximate RBT reduced electric machine model was obtained and compared in open-loop, and it too performed better than state-of-the-art modal truncation while still being acceptable for condition monitoring.

In discrete time, the LQG problem was linked to a compensator comprised of an MPC law, with an appropriately selected terminal penalty, and a Kalman filter estimator. It was then shown that LQG balanced truncation presented a more robust reduced order model for compensator design than the popular Lyapunov balanced truncation on a variety of MPC formulations for a linear diesel airpath (DAP) model.

The full and reduced linear DAP model was then placed into rate-based and gain scheduled rate-based compensators and applied to control a nonlinear DAP model and experimental engine. In all cases, the proposed technique resulted in a compensator that was more robust than the Lyapunov balanced truncation compensator, and a compensator whose performance was closer to the optimal full order compensator.

3. *A novel methodology for obtaining a reduced order model for design of control and estimation of constrained systems.*

   In Chapter 4, model order reduction for constrained systems is formulated as an optimization problem. Using a robust MPC framework, by treating the incurred modeling error as a disturbance, the conservativeness of a constant constraint tube is defined. The optimization problem is selected to minimize the sum of model error between a full and reduced order model in some norm, and the measure of constraint conservativeness.

   Constraint satisfaction, feasibility, and stability of the reduced order model fall out of

the robust MPC theory, while asymptotic tracking of step responses is shown using the work of [35, 153] coupled with the choice of a reduced order model obtained using balanced residualization.

A low-dimensional example is used to demonstrate that not only can more accurate reduced order models be found, but there exists reduced order models that decrease the conservativeness of the tightened reduced constraints. This decreased conservativeness enables larger admissible control, state, and output constraint sets.

4. *Generalizing and simplifying the empirical gramian calculation and extending it to empirical Riccati covariance matrices, both for nonlinear model order reduction.*

   Prior to this work, empirical gramians required state and output responses subject to every possible combination of selected orthogonal direction and scale of input and state perturbations. Chapter 5 presented a simplified form that not only requires less computation, but is easily generalized to the weighted gramian case. The simplified empirical gramian, calculated using fewer "experiments," yields a more accurate reduced order DAP model than the conventional empirical gramian. The reduced DAP models are then shown to result in decreased MPC computation time, and the reduced DAP model obtained using the proposed simplified empirical gramian demonstrates greater accuracy in the closed-loop.

   Using the modified empirical gramian formulation, and the notion of a closed-loop gramian, Chapter 6 develops empirical Riccati covariance matrices for the purpose of obtaining a reduced order model for nonlinear controller/estimator design. It is found that for linear systems, this approach yields closed-loop gramian balanced truncation, which encapsulated LQG balanced truncation, for closed-loop model order reduction. The empirical Riccati covariance matrices are applied to generate a reduced order compensator of a catalytic rod goverened by a spatially and temporally discretized partial differential equation. Of the reduction methods tested, the reduced compensator obtained using the proposed empirical Riccati covariance matrices was the closest to the optimal full order compensator.

7.2 Future Work

There are many challenges in the field of model, control-oriented, and control order reduction of linear, nonlinear, and constrained systems. The immediate extensions of the research presented in this dissertation are:

1. MOR for large scale linear systems (Chapters 2 and 3):

   (a) *Error bounds of approximate downdating.*

   Can error bounds akin to Theorem 2.3.1 be calculated when approximate downdating, and mixtures of up/downdating are applied?

   (b) *Error bounds between the full order model, a ROM obtained by balanced truncation with exact gramians, and the reduced order model obtained by approximate Lyapunov balanced truncation.*

   For some approximate balanced truncation techniques, error bounds between the various full and reduced order models can be computed [80]. Can error bounds be computed using the up/downdating methodology proposed in this dissertation?

   (c) *Order selection to perform approximate up/downdating.*

   How, or in what order, should the up/downdating be performed to result in the "best" reduced order model?

2. MOR for constrained systems (Chapter 4):

   (a) *Computationally efficient polytopic set manipulations and approximations to decrease constraint conservativeness.*

   The largest challenge, from the author's point of view, of applying the methodology to high order systems is set manipulation. For high dimensional polytope sets, $n \geq 6$, manipulation becomes intractable both in terms of computation and storage because of combinatoric growth of vertices [188]. Having a way to either decrease the complexity of set manipulation, or approximating invariant sets, could lead to decreased constraint conservativeness.

(b) *Selection, and efficient calculation, of K and L gains for the reduced MPC framework.*

In Chapter 4, K and L were selected to minimize $||A_r + B_r K||_2$ and $||A_r + LC_r||_2$, respectively, because it provided a guaranteed performance bound if $|| \cdot ||_2 < 1$. However, this methodology does not consider the invariant sets $\tilde{S}$, $\bar{S}$, and S because of added computational costs and limitations of set manipulation. The question becomes how to select K and L to yield invariant sets to satisfy some objective, e.g. minimum volume S?

(c) *Implementing tube and state-dependent constraint methodologies in the reduced MPC framework, and accounting for input and output disturbances.*

While a constant tube robust control approach was used, there are a plethora of other techniques that could provide a less conservative controller/estimator, as well as be better suited for MPC. Specific examples include: homothetic or parametrized constraint tubes [164, 165] and state-dependent "disturbances" and constraints [154, 189, 190].

Additionally, if input and output disturbances are characterized, it can be readily included in the robust framework and used on a physical system.

(d) *Application of the model reduction problem to constrained nonlinear systems.*

The proposed reduction problem of this chapter is general: it requires model error between a full and reduced order system, and a measure of constraint conservativeness. Given a reduction technique and the appropriate invariant sets for a nonlinear system, a methodology could be readily developed and applied to nonlinear systems.

3. Empirical gramians and Riccati Covariance Matrices (Chapters 5 and 6):

(a) *Approximate balanced truncation for large-scale systems.*

For large linear systems, it is known that the Hankel singular values tend to decay rapidly. Does the same hold true for nonlinear systems and empirical gramians/Riccati covariance matrices?

If it does hold true, can the approximate balanced truncation methodology using low-rank matrix square roots factors of covariance matrices be applied to nonlinear systems?

(b) *Stability, robustness, and error measures of reduced order nonlinear models by balanced truncation.*

For linear systems there are ways to analyze stability, robustness, and modeling error. What techniques can be applied to nonlinear reduced order models, and what results can be obtained?

(c) *Balanced residualization of nonlinear systems.*

All the nonlinear reduced order models in this dissertation were obtained by balanced truncation. How does the performance vary when singular perturbation truncation is applied to a balanced nonlinear model [191]?

(d) *Reducing the nonlinear reduced order model evaluation complexity with Discrete Empirical Interpolation (DEI) model order reduction [177, 178].*

Truncation and residualization of nonlinear models does not necessarily decrease computational complexity. However, there exist methods to approximate the nonlinear model with a "reduced basis of functions" to decrease the complexity of the nonlinear model evaluation. How can this be coupled with empirical covariance matrix-based balanced truncation?

(e) *Optimal selection of probe directions.*

For systems with strong nonlinearities, the empirical covariance matrices are heavily dependent upon the probe directions. How should probe directions be chosen to yield a reduced order model for the desired purpose?

Appendices

APPENDIX A

Proofs

A.1 Chapter 2

A.1.1 Proof of Theorem 2.2.1

Proof. The discrete controllability ALE is given by (2.18b). Substituting (2.24a)-(2.24d) into (2.18b) yields

$$(\alpha E - A)^{-1}\left((\alpha E - A)P_d(\alpha E - A)^\top - (\alpha E + A)P_d(\alpha E + A) - 2\alpha BB^\top\right)(\alpha E - A)^{-\top} = 0.$$

Expanding terms with P_d and simplifying, this becomes

$$-2\alpha(\alpha E - A)^{-1}(AP_dE^\top + EP_dA^\top + BB^\top)(\alpha E - A)^{-\top} = 0,$$

and since $\alpha E - A$ is regular, P_d must solve the continuous controllability ALE:

$$AP_dE^\top + EP_dA^\top + BB^\top = 0.$$

Because it was assumed Σ is r-controllable, the solution P_d is unique and $P_d = P$ [84]. □

A.1.2 Proof of Theorem 2.2.2

Proof. Since $\lambda E - A$ is assumed to be regular, (E, A) may be placed into Weierstrass canonical form [192]. In the Weierstrass canonical form, it is trivial to see that $\lambda_{dc,i} = \frac{\alpha+\lambda_{c,i}}{\alpha-\lambda_{c,i}}$.

To show $V_d = V_c$, note that $\lambda_{c,i} = \alpha\frac{\lambda_{dc,i}-1}{\lambda_{dc,i}+1}$, then

$$(\lambda_{dc,i}I - (\alpha E - A)^{-1}(\alpha E + A))V_{dc,i} = (\alpha E - A)^{-1}(\lambda_{dc,i}(\alpha E - A) - (\alpha E + A))V_{dc,i} = 0,$$

resulting in

$$(\alpha E - A)^{-1}(\lambda_{c,i}E - A)V_{dc,i} = 0 \Rightarrow V_{dc,i} = V_{c,i}.$$

□

A.1.3 Proof of Theorem 2.2.3

Proof. The discrete observability ALE is given by (2.19b). Substituting (2.27a)-(2.27d) into (2.19b) yields

$$(\alpha E - A)^{-\top}\left((\alpha E - A)^{\top}\Pi_d(\alpha E - A) - (\alpha E + A)^{\top}\Pi_d(\alpha E + A) - 2\alpha C^{\top}C\right)(\alpha E - A)^{-1} = 0.$$

Expanding terms with Π_d and simplifying, this becomes

$$-2\alpha(\alpha E - A)^{-\top}(A^{\top}\Pi_d E + E^{\top}\Pi_d A + C^{\top}C)(\alpha E - A)^{-1} = 0,$$

and since $\alpha E - A$ is regular, Π_d must solve the continuous observability ALE:

$$A^{\top}\Pi_d E + E^{\top}\Pi_d A + C^{\top}C = 0.$$

Because it was assumed Σ is r-observable, the solution Π_d is unique and $\Pi_d = \Pi$ [84]. □

A.1.4 Proof of Theorem 2.2.4

Proof. Since $\lambda E - A$ is assumed to be regular, (E, A) may be placed into Weierstrass canonical form [192]. In the Weierstrass canonical form, it is trivial to see that $\lambda_{d,i} = \frac{\alpha+\lambda_{c,i}}{\alpha-\lambda_{c,i}}$.

For the eigenvectors of the discretized system, note that $\lambda_{c,i} = \alpha\frac{\lambda_{d,i}-1}{\lambda_{d,i}+1}$, then

$$(\lambda_{d,i}I - (\alpha E + A)(\alpha E - A)^{-1})V_{d,i} = (\lambda_{d,i}(\alpha E - A) - (\alpha E + A))(\alpha E - A)^{-1}V_{d,i} = 0,$$

resulting in

$$(\lambda_{c,i}E - A)(\alpha E - A)^{-1}V_{d,i} = 0.$$

Since $(\lambda_{c,i}E - A)(\alpha E - A)^{-1}V_{d,i} = 0$, $(\alpha E - A)^{-1}V_{d,i}$ must be an eigenvector of the continuous pencil, or

$$(\alpha E - A)^{-1}V_{d,i} = V_{c,i} \Rightarrow V_{d,i} = (\alpha E - A)V_{c,i},$$

and massaging $\alpha E - A$ into $(\alpha - \lambda_{c,i})E + (\lambda_{c,i}E - A)$ yields

$$V_{d,i} = (\alpha - \lambda_{c,i})EV_{c,i}.$$

However, $\alpha > 0$, $\mathrm{Re}\{\lambda_{c,i}\} < 0$, therefore $(\alpha - \lambda_{c,i}) \neq 0$, and because an eigenvector scaled by a non-zero constant is still an eigenvector,

$$V_{d,i} = EV_{c,i}.$$

□

A.1.5 Proof of Theorem 2.2.5

Proof. **Stability** Σ stable means that the eigenvalues of the pencil $\lambda E - A$ exist on the open left half plane. The open left half plane gets mapped by the bilinear transform to the open disc [88] and there can be no $\alpha > 0$ such that $|\lambda_{d,i}| \geq 1$, therefore the discretizations are stable [193].

Controllability (Observability) If Σ is stable and r-controllable (r-observable), then the

generalized controllability (observability) gramian has full rank [84].

Since the controllability (observability) gramian of Σ and its discretization are equal and have full rank, the discretizations are controllable (observable) [194, Theorem 6.1].

□

A.1.6 Proof of Theorem 2.3.1

Proof. The induced 2-norm error between a matrix, F and its j-rank SVD approximation (where μ_i is the i-th singular value) [40]

$$F_j = \sum_{i=1}^{j} \mu_i u_i v_i^\top, \tag{A.1}$$

is

$$||F - F_j||_2 = \mu_{j+1}. \tag{A.2}$$

The rest of the proof proceeds by induction. Recall K has singular values σ_i, therefore $KK^\top$ has singular values σ_i^2. The case of $s = 1$ is readily covered by (A.2),

$$\left\| \tilde{K}_1 \tilde{K}_1^\top - K_0 K_0^\top - K_1 K_1^\top \right\|_2 \leq \sigma_{q+1,1}^2.$$

The case of $s = 2$,

$$\begin{aligned}
\left\| \tilde{K}_2 \tilde{K}_2^\top - \sum_{i=0}^{2} K_i K_i^\top \right\|_2 &= \left\| \tilde{K}_2 \tilde{K}_2^\top - \tilde{K}_1 \tilde{K}_1^\top + \tilde{K}_1 \tilde{K}_1^\top - \sum_{i=0}^{2} K_i K_i^\top \right\|_2, \\
&= \left\| \tilde{K}_2 \tilde{K}_2^\top - \tilde{K}_1 \tilde{K}_1^\top + \tilde{K}_1 \tilde{K}_1^\top - K_0 K_0^\top - K_1 K_1^\top - K_2 K_2^\top \right\|_2, \\
&\leq \left\| \tilde{K}_1 \tilde{K}_1^\top - (K_0 K_0^\top + K_1 K_1^\top) \right\|_2 \\
&\quad + \left\| \tilde{K}_2 \tilde{K}_2^\top - (\tilde{K}_1 \tilde{K}_1^\top + K_2 K_2^\top) \right\|_2, \\
&= \sigma_{q+1,1}^2 + \sigma_{q+1,2}^2.
\end{aligned}$$

It is assumed that the inequality (2.40) holds for $s = l - 1$, then the $s = l$ case must be

shown.

$$\begin{aligned}
\left\| \tilde{K}_l \tilde{K}_l^\top - \sum_{i=0}^{l} K_i K_i^\top \right\|_2 &= \left\| \tilde{K}_l \tilde{K}_l^\top - \sum_{i=1}^{l-1} \tilde{K}_i \tilde{K}_i^\top + \sum_{i=1}^{l-1} \tilde{K}_i \tilde{K}_i^\top - \sum_{i=0}^{l} K_i K_i^\top \right\|_2, \\
&= \left\| \tilde{K}_l \tilde{K}_l^\top - \tilde{K}_{l-1} \tilde{K}_{l-1}^\top - K_l K_l^\top + \cdots \right. \\
&\qquad \left. + \tilde{K}_1 \tilde{K}_1^\top - K_0 K_0^\top - K_1 K_1^\top \right\|_2, \\
&\leq \left\| \tilde{K}_1 \tilde{K}_1^\top - (K_0 K_0^\top + K_1 K_1^\top) \right\|_2 + \\
&\qquad \cdots + \left\| \tilde{K}_l \tilde{K}_l^\top - (\tilde{K}_{l-1} \tilde{K}_{l-1}^\top + K_l K_l^\top) \right\|_2, \\
&= \sum_{i=1}^{l} \sigma_{q+1,i}^2,
\end{aligned}$$

since $||\tilde{K}_l \tilde{K}_l^\top - (\tilde{K}_{l-1} \tilde{K}_{l-1}^\top + K_l K_l^\top)|| = \sigma_{q+1,l}^2$ and $||\tilde{K}_{l-1} \tilde{K}_{l-1}^\top - \sum_{i=0}^{l-1} K_i K_i^\top|| \leq \sum_{i=1}^{l-1} \sigma_{q+1,i}^2$ from the induction assumption.

□

A.2 Chapter 3

A.2.1 Proof of Theorem 3.1.1

Proof. Substituting (3.13) into (3.15) and recalling $\Pi = YY^\top$,

$$\bar{\Pi} = M^{1/2} U^\top Y^{-1} Y Y^\top Y^{-\top} U M^{1/2} = M.$$

Similarly, for $\bar{P}$, recall $Y^\top X = UMV^\top$,

$$\begin{aligned}
\bar{P} &= M^{-1/2} U^\top Y^\top X X^\top Y U M^{-1/2} \\
&= M^{-1/2} U^\top U M V^\top V M U^\top U M^{-1/2} = M.
\end{aligned}$$

□

A.3 Chapter 4

A.3.1 Proof of Theorem 4.2.1

Proof. This is a straightforward application of the definitions of the various RPI sets and the fact that $\text{Proj}_r(\mathcal{P}) \subseteq \mathcal{P}$.

□

A.3.2 Proof of Theorem 4.2.2

Proof. Since there exists a T such that $x_T \in \mathcal{X}$, $y_T \in \mathcal{Y}$, $\tilde{x}_{r,t} \in \text{Proj}_r(\tilde{S})$, $\tilde{x}_t \in \text{Proj}_r(\tilde{S})$ for all $t > T$ because $\text{Proj}_r(\tilde{S})$ is an RPI set of the reduced estimator dynamics. It follows from [145], that (4.26) with the estimated state the problem is robustly exponentially stable.

Since the constraints are always satisfied along the prediction horizon, the problem remains feasible for any admissible truncated state $\bar{x}_{r,t}$, or that the problem is recursively feasible. □

A.3.3 Proof of Theorem 4.2.3

Proof. From the construction of $\bar{\mathcal{U}}_r$, $\bar{\mathcal{X}}_r$, and $\bar{\mathcal{Y}}_r$,

$$\lim_{t\to\infty} y_t - \bar{y}_{t,\infty} \in (C_r + D_r K)\mathcal{S}, \tag{A.3}$$

from robust stability. $\lim_{t\to\infty} K_{r,f}\bar{x}_{r,t} - K_f x_t = 0$, $\bar{x}_{r,t,\infty} \in \bar{\mathcal{X}}_r$ combined with $\rho(A_r + LC_r) < 1$ implies the estimated states converge [153]:

$$\lim_{t\to\infty} \bar{x}_{r,t} - \hat{x}_{r,t} = 0.$$

Finally, if $\bar{y}_{t,\infty} \in \text{colspan}\{C_r(I - (A_r + B_r K_{r,f}))^{-1} B_r + D_r\}$, then by the final value theorem, $y_t = y_\infty$. This condition is particularly important for underactuated systems. □

A.3.4 Proof of Theorem 4.3.1

Proof. Since $\mathcal{G} \subseteq \mathcal{F}$, $1_{\mathcal{G}}(f) \leq 1_{\mathcal{F}}(f)$ for all $f \in \mathbb{R}^q$, the integral is always positive, and the absolute value can be dropped. Because $\mathcal{G}$ and $\mathcal{F}$ are measurable, $|\mathcal{G}|$ and $|\mathcal{F}|$ are defined. With $\mathcal{F}$ being bounded,

$$\begin{aligned} \mu_{\mathcal{F}}(\mathcal{G}) &= \frac{1}{|\mathcal{F}|}\int_{\mathcal{F}} 1_{\mathcal{F}}(f) - 1_{\mathcal{G}}(f)df = \frac{1}{|\mathcal{F}|}\left(\int_{\mathcal{F}} 1df - \int_{\mathcal{G}} 1df\right) \\ &= \frac{|\mathcal{F}| - |\mathcal{G}|}{|\mathcal{F}|} = 1 - \frac{|\mathcal{G}|}{|\mathcal{F}|}. \end{aligned}$$

□

A.4 Chapter 5

A.4.1 Proof of Theorem 5.2.1

Proof. Provided with the fact

$$I_{m\times m} = \sum_{i=1}^{m} \frac{\tilde{v}_{ij}\tilde{v}_{ij}^{\top}}{\tilde{v}_{ij}^{\top}\tilde{v}_{ij}}, \tag{A.4}$$

the proof follows that of Section 2.1.2 of [70] with a slight modification for R,

$$\hat{P} = \int_0^{\infty} e^{A\tau}BRB^{\top}e^{A^{\top}\tau}d\tau, \tag{A.5}$$

which becomes the weighted linear controllability gramian, (5.24) [175]. □

A.4.2 Proof of Theorem 5.2.2

Proof. The proof follows that of Section 2.2 of [70] with a slight modification for Q,

$$\hat{\Pi} = \int_0^{\infty} e^{A^{\top}\tau}C^{\top}QCe^{A\tau}d\tau, \tag{A.6}$$

which becomes the weighted linear observability gramian, (5.31) [175]. □

A.5 Chapter 6

A.5.1 Proof of Theorem 6.2.1

Proof. (6.14) occurs by construction of (6.11) from (6.4a), and (6.15) follows by the substitution of $K = R^{-1}B^\top P$ into (6.14). □

A.5.2 Proof of Theorem 6.2.2

Proof. Consider the following fact:

$$\sum_{a=1}^{m+p} \frac{\tilde{v}_{al}\tilde{v}_{al}^\top}{\tilde{v}_{al}^\top \tilde{v}_{al}} = I_{(m+p)\times(m+p)},$$

(6.23) can be established by construction of the dual to (6.20) from (6.4a), and (6.24) follows by the substitution of $L = \Pi C^\top \Lambda^{-1}$ into (6.23). □

APPENDIX B

Singular Perturbations of Descriptor Systems

The author has only seen singular perturbations of descriptor systems when it is explicitly assumed that E_{22} is nilpotent or imposes an algebraic constraint [195]. What follows are theorems/derivations for continuous and discrete time systems where E_{22} may not be singular.

B.1 Continuous Time

Theorem B.1.1. *Given a continuous descriptor system, (E, A, B, C, D), that is conformably partitioned into states to keep (x_1) and states to truncate (x_2), assume E_{11} and $E_{21}E_{11}^{-1}A_{12} - A_{22}$ are invertible.*

Define

$$\tilde{A}_{22} = E_{21}E_{11}^{-1}A_{12} - A_{22} \tag{B.1a}$$

$$\tilde{A}_{21} = A_{21} - E_{21}E_{11}^{-1}A_{11} \tag{B.1b}$$

$$\tilde{B}_2 = B_2 - E_{21}E_{11}^{-1}B_1, \tag{B.1c}$$

then the singularly perturbed reduced order model is

$$
\begin{aligned}
E_r &= E_{11}, && \text{(B.2a)}\\
A_r &= A_{11} + A_{12}\tilde{A}_{22}^{-1}\tilde{A}_{21}, && \text{(B.2b)}\\
B_r &= B_1 + A_{12}\tilde{A}_{22}^{-1}\tilde{B}_2, && \text{(B.2c)}\\
C_r &= C_1 + C_2\tilde{A}_{22}^{-1}\tilde{A}_{21}, && \text{(B.2d)}\\
D_r &= D + C_2\tilde{A}_{22}^{-1}\tilde{B}_2. && \text{(B.2e)}
\end{aligned}
$$

Proof. Conformably partition (E, A, B, C, D) into

$$
\begin{aligned}
\begin{bmatrix} E_{11} & E_{12} \\ E_{21} & E_{22} \end{bmatrix} \begin{bmatrix} \dot{x}_1 \\ \dot{x}_2 \end{bmatrix} &= \begin{bmatrix} A_{11} & A_{12} \\ A_{21} & A_{22} \end{bmatrix} \begin{bmatrix} x_1 \\ x_2 \end{bmatrix} + \begin{bmatrix} B_1 \\ B_2 \end{bmatrix} u,\\
y &= \begin{bmatrix} C_1 & C_2 \end{bmatrix} \begin{bmatrix} x_1 \\ x_2 \end{bmatrix} + Du.
\end{aligned} \qquad \text{(B.3)}
$$

For the continuous system, $\dot{x}_2 = 0$ is taken to be the singular "condition," which implies

$$E_{21}\dot{x}_1 = A_{21}x_1 + A_{22}x_2 + B_2u. \qquad \text{(B.4)}$$

Now $\dot{x}_1$,

$$\dot{x}_1 = E_{11}^{-1}(A_{11}x_1 + A_{12}x_2 + B_1u), \qquad \text{(B.5)}$$

is substituted into (B.4) to yield

$$E_{21}E_{11}^{-1}(A_{11}x_1 + A_{12}x_2 + B_1u) = A_{21}x_1 + A_{22}x_2 + B_2u,$$

which gives

$$x_2 = (E_{21}E_{11}A_{12} - A_{22})^{-1}\left((A_{21} - E_{21}E_{11}^{-1}A_{11})x_1 + (B_2 - E_{21}E_{11}^{-1}B_1)u\right). \qquad \text{(B.6)}$$

To shorten the longhand computation, chunk

$$\tilde{A}_{22} = E_{21}E_{11}^{-1}A_{12} - A_{22} \tag{B.7a}$$

$$\tilde{A}_{21} = A_{21} - E_{21}E_{11}^{-1}A_{11} \tag{B.7b}$$

$$\tilde{B}_2 = B_2 - E_{21}E_{11}^{-1}B_1, \tag{B.7c}$$

At this point, all the assumptions required for singular perturbations becomes clear: E_{11} and $E_{22}E_{11}^{-1}A_{12} - A_{22}$ must be invertible, which in the ordinary case reduces to A_{22} invertible.

Substituting everything into (B.4), the reduced order model becomes

$$E_r = E_{11}, \tag{B.8a}$$

$$A_r = A_{11} + A_{12}\tilde{A}_{22}^{-1}\tilde{A}_{21}, \tag{B.8b}$$

$$B_r = B_1 + A_{12}\tilde{A}_{22}^{-1}\tilde{B}_2, \tag{B.8c}$$

$$C_r = C_1 + C_2\tilde{A}_{22}^{-1}\tilde{A}_{21}, \tag{B.8d}$$

$$D_r = D + C_2\tilde{A}_{22}^{-1}\tilde{B}_2. \tag{B.8e}$$

□

B.2 Discrete Time

Theorem B.2.1. *Given a discrete descriptor system, (E, A, B, C, D), that is conformably partitioned into states to keep (x_t^1) and states to truncate (x_t^2), assume $E_{22} - A_{22}$ and $E_{11} + (A_{12} - E_{12})(E_{22} - A_{22})^{-1}E_{21}$ are invertible.*

Then the singularly perturbed reduced order model is

$$
\begin{aligned}
E_r &= E_{11} + (A_{12} - E_{12})(E_{22} - A_{22})^{-1}E_{21}, && \text{(B.9a)}\\
A_r &= A_{11} + (A_{12} - E_{12})(E_{22} - A_{22})^{-1}A_{21}, && \text{(B.9b)}\\
B_r &= B_1 + (A_{12} - E_{12})(E_{22} - A_{22})^{-1}B_2, && \text{(B.9c)}\\
C_r &= C_1 + C_2(E_{22} - A_{22})^{-1}(A_{21} - E_{21}E_r^{-1}A_r), && \text{(B.9d)}\\
D_r &= D + C_2(E_{22} - A_{22})^{-1}(B_2 - E_{21}E_r^{-1}B_r). && \text{(B.9e)}
\end{aligned}
$$

Proof. Conformably partition (E, A, B, C, D) to get

$$
\begin{aligned}
\begin{bmatrix} E_{11} & E_{12} \\ E_{21} & E_{22} \end{bmatrix} \begin{bmatrix} x_{t+1}^1 \\ x_{t+1}^2 \end{bmatrix} &= \begin{bmatrix} A_{11} & A_{12} \\ A_{21} & A_{22} \end{bmatrix} \begin{bmatrix} x_t^1 \\ x_t^2 \end{bmatrix} + \begin{bmatrix} B_1 \\ B_2 \end{bmatrix} u, \\
y &= \begin{bmatrix} C_1 & C_2 \end{bmatrix} \begin{bmatrix} x_t^1 \\ x_t^2 \end{bmatrix} + Du.
\end{aligned} \qquad \text{(B.10)}
$$

The singular condition for discrete systems is

$$x_{t+1}^2 = x_t^2, \qquad \text{(B.11)}$$

Substituting into $E_{21}x_{t+1}^1 + E_{22}x_{t+1}^2$ yields

$$x_t^2 = (E_{22} - A_{22})^{-1}(A_{21}x_t^1 + B_2u - E_{21}x_{t+1}^1), \qquad \text{(B.12)}$$

making x_t^2 appear non-causal. At this point it becomes apparent that $E_{22} - A_{22}$ has to be assumed to be invertible.

Define

$$F = (A_{12} - E_{12})(E_{22} - A_{22})^{-1}, \qquad \text{(B.13)}$$

then substituting (B.12) into $E_{11}x_{t+1}^1 + E_{12}x_t^2$ and manipulating, provides the causal

$$(E_{11} + FE_{21})x_{t+1}^1 = (A_{11} + FA_{21})x_t^1 + (B_1 + FB_2)u. \qquad \text{(B.14)}$$

This yields that (E_r, A_r, B_r) of the reduced order model may be defined

$$E_r = E_{11} + (A_{12} - E_{12})(E_{22} - A_{22})^{-1}E_{21}, \tag{B.15a}$$

$$A_r = A_{11} + (A_{12} - E_{12})(E_{22} - A_{22})^{-1}A_{21}, \tag{B.15b}$$

$$B_r = B_1 + (A_{12} - E_{12})(E_{22} - A_{22})^{-1}B_2. \tag{B.15c}$$

The output, however, appears non-causal with the substition of x_t^2,

$$y_t = C_1 x_t^1 + C_2(E_{22} - A_{22})^{-1}(A_{21}x_t^1 + B_2 u - E_{21}x_{t+1}^1) + Du,$$

but can be taken care of by assuming E_r is invertible to get

$$x_{t+1}^1 = E_r^{-1}(A_r x_t^1 + B_r u),$$

which when substituted into y_t yields

$$C_r = C_1 + C_2(E_{22} - A_{22})^{-1}(A_{21} - E_{21}E_r^{-1}A_r), \tag{B.16a}$$

$$D_r = D + C_2(E_{22} - A_{22})^{-1}(B_2 - E_{21}E_r^{-1}B_r). \tag{B.16b}$$

□

Bibliography

[1] S. Tan and L. He. *Advanced Model Order Reduction Techniques in VLSI Design*. Cambridge University Press, 2007.

[2] K. Zhou. "Computationally-efficient finite-element-based thermal and electromagnetic models of electric machines". PhD thesis. University of Michigan, 2015.

[3] E. Jonckheere and L. Silverman. "A new set of invariants for linear systems–Application to reduced order compensator design". In: *Automatic Control, IEEE Transactions on* 28.10 (Oct. 1983), pp. 953–964.

[4] T. Penzl. "Algorithms for model reduction of large dynamical systems". In: *Linear Algebra and its Applications* 415.2-3 (2006), pp. 322–343.

[5] W. Marquardt. "Nonlinear model reduction for optimization based control of transient chemical processes". In: *in Proceedings of the Sixth International Conference on Chemical Process Control, Tucson, AZ*, pp. 12–42.

[6] K. J. Åström and B. Wittenmark. *Adaptive Control*. 2nd. Mineola, NY: Dover Publications, Inc, 2008.

[7] P. A. Ioannou and J. Sun. *Robust Adaptive Control*. Upper Saddle River, NJ: Prentice Hall, 1996.

[8] T. Ogunfunmi. *Adaptive Nonlinear System Identification*. New York, NY: Springer, 2007.

[9] G. Obinata and B. D. Anderson. *Model Reduction For Control System Design*. London: Springer-Verlag, 2001.

[10] A. Antoulas, D. Sorensen, and S. Gugercin. "A survey of model reduction methods for large-scale systems". In: *Contemporary mathematics* 280 (2001), pp. 193–220.

[11] A. C. Antoulas. *Approximation of Large-Scale Dynamical Systems*. Vol. 6. SIAM, 2005.

[12] W. Schilders, H. van der Vorst, and J. Rommes. *Model Order Reduction: Theory, Research Aspects and Applications*. European Consortium for Mathematics in Industry. Springer London, Limited, 2008.

[13] B. Moore. "Principal component analysis in linear systems: Controllability, observability, and model reduction". In: *Automatic Control, IEEE Transactions on* 26.1 (Feb. 1981), pp. 17–32.

[14] H. Sandberg and A. Rantzer. "Balanced truncation of linear time-varying systems". In: *IEEE Transactions on Automatic Control* 49.2 (Feb. 2004), pp. 217–229.

[15] J. Theis, P. Seiler, and H. Werner. "LPV Model Order Reduction by Parameter-Varying Oblique Projection". In: *IEEE Transactions on Control Systems Technology* (2017).

[16] J. M. Scherpen. "Balancing for nonlinear systems". In: *Systems & Control Letters* 21.2 (1993), pp. 143–153.

[17] Y. Liu and B. D. O. Anderson. "Singular perturbation approximation of balanced systems". In: *Decision and Control, 1989., Proceedings of the 28th IEEE Conference on*. 1989, 1355–1360 vol.2.

[18] P. C. Hughes and R. Skelton. "Modal truncation for flexible spacecraft". In: *Journal of Guidance and Control* 4.3 (1981), pp. 291–297.

[19] D. Enns. "Model reduction with balanced realizations: An error bound and a frequency weighted generalization". In: *Decision and Control, 1984. The 23rd IEEE Conference on*. Vol. 23. Dec. 1984, pp. 127–132.

[20] D. F. Enns. "Model Reduction for Control Systems Design". PhD thesis. Department of Aeronautics and Astronautics, Stanford University, 1984.

[21] C.-A. Lin, T.-Y. Chiu, et al. "Model-reduction via frequency weighted balanced realization". In: *Control-Theory and Advanced Technology* 8.2 (1992), pp. 341–351.

[22] V. Sreeram and B. Anderson. "Frequency weighted balanced reduction technique: A generalization and an error bound". In: *Decision and Control, 1995., Proceedings of the 34th IEEE Conference on*. Vol. 4. IEEE. 1995, pp. 3576–3581.

[23] B. Anderson and Y. Liu. "Controller reduction: concepts and approaches". In: *Automatic Control, IEEE Transactions on* 34.8 (Aug. 1989), pp. 802–812.

[24] D. G. Meyer. "Fractional balanced reduction: Model reduction via fractional representation". In: *IEEE Transactions on Automatic Control* 35.12 (1990), pp. 1341–1345.

[25] A. Astolfi. "Model Reduction by Moment Matching for Linear and Nonlinear Systems". In: *IEEE Transactions on Automatic Control* 55.10 (Oct. 2010), pp. 2321–2336.

[26] K. Glover. "All optimal Hankel-norm approximations of linear multivariable systems and their L^∞-error bounds". In: *International Journal of Control* 39.6 (1984), pp. 1115–1193.

[27] K. Willcox and J. Peraire. "Balanced model reduction via the proper orthogonal decomposition". In: *AIAA journal* 40.11 (2002), pp. 2323–2330.

[28] E. Verriest. "Suboptimal LQG-design via balanced realizations". In: *Decision and Control including the Symposium on Adaptive Processes, 1981 20th IEEE Conference on*. Vol. 20. IEEE. 1981, pp. 686–687.

[29] D. Mustafa and K. Glover. "Controller reduction by H_∞-balanced truncation". In: *Automatic Control, IEEE Transactions on* 36.6 (June 1991), pp. 668–682.

[30] J. Davis and R. Skelton. "Another balanced controller reduction algorithm". In: *Systems & control letters* 4.2 (1984), pp. 79–83.

[31] Y. Liu, B. D. Anderson, and U.-L. Ly. "Coprime factorization controller reduction with Bezout identity induced frequency weighting". In: *Automatica* 26.2 (1990), pp. 233–249.

[32] D. McFarlane, K. Glover, and M. Vidyasagar. "Reduced-order controller design using coprime factor model reduction". In: *IEEE Transactions on Automatic Control* 35.3 (1990), pp. 369–373.

[33] S. Hovland and J. Gravdahl. "Complexity reduction in explicit MPC through model reduction". In: *Proceedings of the 17th World Congress*. 2008, pp. 7711–7716.

[34] U. Kalabić et al. "Reduced order reference governor". In: *Decision and Control (CDC), 2012 IEEE 51st Annual Conference on*. IEEE. 2012, pp. 3245–3251.

[35] U. V. Kalabić, I. V. Kolmanovsky, and E. G. Gilbert. "Reduced order extended command governor". In: *Automatica* 50.5 (2014), pp. 1466–1472.

[36] P. Sopasakis, D. Bernardini, and A. Bemporad. "Constrained model predictive control based on reduced-order models". In: *Decision and Control (CDC), 2013 IEEE 52nd Annual Conference on*. Dec. 2013, pp. 7071–7076.

[37] M. Löhning et al. "Model predictive control using reduced order models: Guaranteed stability for constrained linear systems". In: *Journal of Process Control* 24.11 (2014), pp. 1647–1659.

[38] M. Kögel and R. Findeisen. "Robust output feedback model predictive control using reduced order models". In: *IFAC-PapersOnLine* 48.8 (2015). 9th {IFAC} Symposium on Advanced Control of Chemical Processes {ADCHEM} 2015Whistler, Canada, 7-10 June 7- 10, 2015, pp. 1008–1014.

[39] T. Penzl. "Numerical solution of generalized Lyapunov equations". In: *Advances in Computational Mathematics* 8.1 (1998), pp. 33–48.

[40] L. N. Trefethen and D. Bau. *Numerical Linear Algebra*. Philadelphia, PA: Society for Industrial and Applied Mathematics, 1997.

[41] M. S. Tombs and I. Postlethwaite. "Truncated balanced realization of a stable non-minimal state-space system". In: *International Journal of Control* 46.4 (1987), pp. 1319–1330.

[42] T. Stykel. "Gramian-based model reduction for descriptor systems". In: *Mathematics of Control, Signals, and Systems (MCSS)* 16.4 (2004), pp. 297–319.

[43] T. Penzl. "A Cyclic Low-Rank Smith Method for Large Sparse Lyapunov Equations". In: *SIAM Journal on Scientific Computing* 21.4 (1999), p. 1401.

[44] P. Kürschner. "Efficient Low-Rank Solution of Large-Scale Matrix Equations". PhD thesis. Shaker Verlag Aachen, 2016.

[45] P. Benner and T. Stykel. "Model order reduction for differential-algebraic equations: a survey". In: *Surveys in Differential-Algebraic Equations IV*. Springer, 2017, pp. 107–160.

[46] S. Lall, J. E. Marsden, and S. Glavaŝki. "A subspace approach to balanced truncation for model reduction of nonlinear control systems". In: *International Journal of Robust and Nonlinear Control* 12.6 (2002), pp. 519–535.

[47] S. Lall, P. Krysl, and J. E. Marsden. "Structure-preserving model reduction for mechanical systems". In: *Physica D: Nonlinear Phenomena* 184.1 (2003), pp. 304–318.

[48] B. Besselink, N. van de Wouw, and H. Nijmeijer. "Model reduction of nonlinear systems with bounded incremental L^2 gain". In: *Decision and Control and European Control Conference (CDC-ECC), 2011 50th IEEE Conference on*. IEEE. 2011, pp. 7170–7175.

[49] P. Li and L. T. Pileggi. "Compact reduced-order modeling of weakly nonlinear analog and RF circuits". In: *IEEE Transactions on Computer-Aided Design of Integrated Circuits and Systems* 24.2 (Feb. 2005), pp. 184–203.

[50] M. J. Rewienski. "A trajectory piecewise-linear approach to model order reduction of nonlinear dynamical systems". PhD thesis. Massachusetts Institute of Technology, 2003.

[51] O. Nilsson and A. Rantzer. "A novel approach to balanced truncation of nonlinear systems". In: *Control Conference (ECC), 2009 European*. Aug. 2009, pp. 1559–1564.

[52] W. S. Gray and E. I. Verriest. "Balancing Non-Linear Systems Near Attracting Invariant Manifolds". In: *Proceedings of the 1999 ECC, Karlsruhe, Germany* (1999).

[53] W. S. Gray and E. I. Verriest. "Balanced realizations near stable invariant manifolds". In: *Automatica* 42.4 (2006), pp. 653–659.

[54] J. Theis, P. Seiler, and H. Werner. "Model order reduction by parameter-varying oblique projection". In: *2016 American Control Conference (ACC)*. July 2016, pp. 4586–4591.

[55] E. I. Verriest. "Nonlinear balancing and Mayer-Lie interpolation". In: *System Theory, 2004. Proceedings of the Thirty-Sixth Southeastern Symposium on*. 2004, pp. 180–184.

[56] A. J. Krener. "Reduced Order Modeling of Nonlinear Control Systems". In: *Analysis and Design of Nonlinear Control Systems*. Springer, 2008, pp. 41–62.

[57] J. M. Scherpen and W. S. Gray. "On singular value functions and Hankel operators for nonlinear systems". In: *American Control Conference, 1999. Proceedings of the 1999*. Vol. 4. IEEE. 1999, pp. 2360–2364.

[58] A. Isidori. *Nonlinear Control Systems*. 3rd. London, UK: Springer, 2002.

[59] A. Bloch. *Nonholonomic Mechanics and Control*. New York, NY: Springer, 2003.

[60] J. M. A. Scherpen and A. Van der Schaft. "Normalized coprime factorizations and balancing for unstable nonlinear systems". In: *International Journal of Control* 60.6 (1994), pp. 1193–1222.

[61] J. M. Scherpen. "H_∞ balancing for nonlinear systems". In: *International Journal of Robust and Nonlinear Control* 6.7 (1996), pp. 645–668.

[62] A. Astolfi. "Model reduction by moment matching for nonlinear systems". In: *Decision and Control, 2008. CDC 2008. 47th IEEE Conference on*. IEEE. 2008, pp. 4873–4878.

[63] J. Scherpen. “Balanced Realizations, Model Order Reduction, and the Hankel Operator”. In: *The Control Handbook. Control System Advanced Methods*. Ed. by W. S. Levine. Boca Raton, FL: CRC Press, 2011.

[64] G. Scarciotti and A. Astolfi. “Model reduction by moment matching for nonlinear time-delay systems”. In: *Decision and Control (CDC), 2014 IEEE 53rd Annual Conference on*. IEEE. 2014, pp. 3642–3647.

[65] T. C. Ionescu and A. Astolfi. “Nonlinear Moment Matching-Based Model Order Reduction”. In: *IEEE Transactions on Automatic Control* 61.10 (Oct. 2016), pp. 2837–2847.

[66] W. S. Gray and E. I. Verriest. “Algebraically defined Gramians for nonlinear systems”. In: *Proceedings of the 45th IEEE Conference on Decision and Control*. IEEE. 2006, pp. 3730–3735.

[67] E. Verriest. “Time variant balancing and nonlinear balanced realizations”. In: *Model Order Reduction: Theory, Research Aspects and Applications*. Springer, 2008, pp. 213–250.

[68] C. Himpe and M. Ohlberger. “Cross-gramian-based combined state and parameter reduction for large-scale control systems”. In: *Mathematical Problems in Engineering* 2014 (2014).

[69] S. Lall, J. E. Marsden, and S. Glavaški. “Empirical model reduction of controlled nonlinear systems”. In: *Proceedings of the IFAC World Congress*. International Federation of Automatic Control. 1999, p. 473–478.

[70] J. Hahn, T. F. Edgar, and W. Marquardt. “Controllability and observability covariance matrices for the analysis and order reduction of stable nonlinear systems”. In: *Journal of Process Control* 13.2 (2003), pp. 115–127.

[71] R. Choroszucha, J. Sun, and K. Butts. “Closed-loop model order reduction and MPC for diesel engine airpath control”. In: *American Control Conference (ACC), 2015*. IEEE. 2015, pp. 3279–3284.

[72] R. Choroszucha, J. Sun, and K. Butts. “Nonlinear Model Order Reduction for Predictive Control of the Diesel Engine Airpath”. In: *American Control Conference (ACC), 2016*. 2016.

[73] R. B. Choroszucha and J. Sun. “Empirical Riccati covariance matrices for closed-loop model order reduction of nonlinear systems by balanced truncation”. In: *2017 American Control Conference (ACC)*. May 2017, pp. 3476–3482.

[74] F. Tröltzsch. *Optimal Control of Partial Differential Equations*. Graduate Studies in Mathematics 112. American Mathematical Society, 2010.

[75] S. Brenner and R. Scott. *The Mathematical Theory of Finite Element Methods*. Vol. 15. Springer Science & Business Media, 2007.

[76] P. Benner. “Solving large-scale control problems”. In: *IEEE control systems* 24.1 (2004), pp. 44–59.

[77] A. Laub et al. “Computation of system balancing transformations and other applications of simultaneous diagonalization algorithms”. In: *Automatic Control, IEEE Transactions on* 32.2 (1987), pp. 115–122.

[78] A. C. Antoulas, D. C. Sorensen, and Y. Zhou. “On the decay rate of Hankel singular values and related issues”. In: *Systems & Control Letters* 46.5 (2002), pp. 323–342.

[79] J.-R. Li. “Model reduction of large linear systems via low rank system gramians”. PhD thesis. Massachusetts Institute of Technology, 2000.

[80] S. Gugercin and J.-R. Li. “Smith-type methods for balanced truncation of large sparse systems”. In: *Dimension reduction of large-scale systems*. Springer, 2005, pp. 49–82.

[81] S. Gugercin, D. C. Sorensen, and A. C. Antoulas. “A modified low-rank Smith method for large-scale Lyapunov equations”. In: *Numerical Algorithms* 32.1 (2003), pp. 27–55.

[82] L. Dai. *Singular Control Systems*. Springer-Verlag New York, Inc., 1989.

[83] G.-R. Duan. *Analysis and Design of Descriptor Linear Systems*. Vol. 23. Springer Science & Business Media, 2010.

[84] T. Stykel. “Stability and inertia theorems for generalized Lyapunov equations”. In: *Linear Algebra and its Applications* 355.1 (2002), pp. 297–314.

[85] R. Smith. “Matrix Equation XA+BX=C”. In: *SIAM Journal on Applied Mathematics* 16.1 (1968), pp. 198–201.

[86] S. Gugercin and A. Antoulas. “A survey of model reduction by balanced truncation and some new results”. In: *International Journal of Control* 77.8 (2004), pp. 748–766.

[87] T. Stykel. “Low-rank iterative methods for projected generalized Lyapunov equations”. In: *Electron. Trans. Numer. Anal* 30.1 (2008), pp. 187–202.

[88] J. W. Brown and R. V. Churchill. *Complex Variables and Applications*. 7th. Boston, MA: McGraw Hill, 2003.

[89] B. M. Chen, Z. Lin, and Y. Shamash. *Linear Systems Theory: A Structural Decomposition Approach*. Springer Science & Business Media, 2004.

[90] P. R. Kumar and P. Varaiya. *Stochastic Systems: Estimation, Identification, and Adaptive Control*. SIAM, 2015.

[91] G. H. Golub and C. F. Van Loan. *Matrix Computations*. Vol. 3. JHU Press, 2012.

[92] Y. Zhou. “Numerical methods for large scale matrix equations with applications in LTI system model reduction”. PhD thesis. Rice University, 2002.

[93] L. Eldén and H. Park. “Block downdating of least squares solutions”. In: *SIAM Journal on Matrix Analysis and Applications* 15.3 (1994), pp. 1018–1034.

[94] F. Arrigo and M. Benzi. “Updating and downdating techniques for optimizing network communicability”. In: *SIAM Journal on Scientific Computing* 38.1 (2016), B25–B49.

[95] M. Biggs, A. Ghodsi, and S. Vavasis. “Nonnegative Matrix Factorization via Rank-one Downdate”. In: *Proceedings of the 25th International Conference on Machine Learning*. ICML ’08. Helsinki, Finland: ACM, 2008, pp. 64–71.

[96] L. Deng. "Multiple-rank updates to matrix factorizations for nonlinear analysis and circuit design". PhD thesis. PhD thesis, Stanford University, 2010.

[97] E. N. Atkinson. "Computing ATA-BTB=LTDL using generalized hyperbolic transformations". In: *Linear Algebra and its Applications* 194 (1993), pp. 135–147.

[98] V. Mehrmann and T. Stykel. "Balanced truncation model reduction for large-scale systems in descriptor form". In: *Dimension Reduction of Large-Scale Systems*. Springer, 2005, pp. 83–115.

[99] J. Pries and H. Hofmann. "Magnetic and thermal scaling of electric machines". In: *International Journal of Vehicle Design* 61.1-4 (2012), pp. 219–232.

[100] J. Pries. "Computationally Efficient Steady-State Simulation Algorithms for Finite-Element Models of Electric Machines". PhD thesis. University of Michigan, 2015.

[101] R. Haberman. *Applied Partial Differential Equations*. 4th. Upper Saddle River, NJ: Pearson - Prentice Hall, 2004.

[102] T. K. Lee et al. "Hybrid electric vehicle supervisory control design reflecting estimated lithium-ion battery electrochemical dynamics". In: *Proceedings of the 2011 American Control Conference*. June 2011, pp. 388–395.

[103] N. Jaljal, J.-F. Trigeol, and P. Lagonotte. "Reduced thermal model of an induction machine for real-time thermal monitoring". In: *IEEE Transactions on Industrial Electronics* 55.10 (2008), pp. 3535–3542.

[104] R. J. LeVeque. *Finite Difference Methods for Ordinary and Partial Differential Equations: Steady-State and Time-Dependent Problems*. Philadelphia, PA: Society for Industrial and Applied Mathematics, 2007.

[105] E. Jonckheere, M. Safonov, and L.M.Silverman. "Topology induced by the Hankel norm in the space of transfer matrices". In: *Decision and Control including the Symposium on Adaptive Processes, 1981 20th IEEE Conference on*. Vol. 20. Dec. 1981, pp. 118–119.

[106] P. Opdenacker and E. A. Jonckheere. "LQG balancing and reduced LQG compensation of symmetric passive systems". In: *International Journal of Control* 41.1 (1985), pp. 73–109.

[107] B. Anderson and J. Moore. *Optimal Control: Linear Quadratic Methods*. Prentice-Hall, Inc., 1990.

[108] T. Richardson and R. Kwong. "On positive definite solutions to the algebraic Riccati equation". In: *Systems & Control Letters* 7.2 (1986), pp. 99–104.

[109] R. E. Skelton and A. Yousuff. "Component cost analysis of large scale systems". In: *International Journal of Control* 37.2 (1983), pp. 285–304.

[110] L. Pernebo and L. Silverman. "Model reduction via balanced state space representations". In: *Automatic Control, IEEE Transactions on* 27.2 (1982), pp. 382–387.

[111] M. Opmeer. "Model reduction for controller design for infinite-dimensional systems". PhD thesis. University of Groningen, 2006.

[112] M. R. Opmeer. "LQG balancing for continuous-time infinite-dimensional systems". In: *SIAM Journal on Control and Optimization* 46.5 (2007), pp. 1831–1848.

[113] R. Saragih and Y. Soeharyadi. "Reduced-order Model Based on H_∞-Balancing for Infinite-Dimensional Systems". In: *Applied Mathematical Sciences* 7.9 (2013), pp. 405–418.

[114] P. Benner and J. Heiland. "LQG-balanced truncation low-order controller for stabilization of laminar flows". In: *Active Flow and Combustion Control 2014*. Springer, 2015, pp. 365–379.

[115] A. Laub. "A Schur method for solving algebraic Riccati equations". In: *IEEE Transactions on automatic control* 24.6 (1979), pp. 913–921.

[116] S. Bittani, A. Laub, and J. Willems, eds. *The Riccati Equation*. Springer-Verlag New York, Inc., 1991.

[117] P. Benner and Z. Bujanović. "On the solution of large-scale algebraic Riccati equations by using low-dimensional invariant subspaces". In: *Linear Algebra and its Applications* 488 (2016), pp. 430–459.

[118] V. Mehrmann. *The Autonomous Linear Quadratic Control Problem*. Lecture Notes In Control and Information Sciences 163. Berlin, Germany: Springer-Verlag, 1991.

[119] K. L. Hitz and B. D. O. Anderson. "Iterative method of computing the limiting solution of the matrix Riccati differential equation". In: *Electrical Engineers, Proceedings of the Institution of* 119.9 (Sept. 1972), pp. 1402–1406.

[120] D. Mayne et al. "Constrained model predictive control: Stability and optimality". In: *Automatica* 36.6 (2000), pp. 789–814.

[121] P. Scokaert and J. Rawlings. "Constrained linear quadratic regulation". In: *Automatic Control, IEEE Transactions on* 43.8 (1998), pp. 1163–1169.

[122] G. Pannocchia and J. B. Rawlings. "The velocity algorithm LQR: a survey". In: (2001).

[123] L. Wang. "A Tutorial on Model Predictive Control: Using a Linear Velocity-Form Model". In: *Developments in Chemical Engineering and Mineral Processing* 12.5-6 (2004), pp. 573–614.

[124] L. Wang. *Model Predictive Control System Design and Implementation Using MATLAB*. Springer, 2009.

[125] G. Betti, M. Farina, and R. Scattolini. "An MPC algorithm for offset-free tracking of constant reference signals". In: *2012 IEEE 51st IEEE Conference on Decision and Control (CDC)*. Dec. 2012, pp. 5182–5187.

[126] M. Huang et al. "Rate-Based Model Predictive Control of Diesel Engines". In: *7th IFAC Symposium on Advances in Automotive Control* 7 (2013), pp. 177–182.

[127] A. Bemporad et al. "The explicit linear quadratic regulator for constrained systems". In: *Automatica* 38.1 (2002), pp. 3–20.

[128] J. L. Sullivan et al. "CO2 Emission Benefit of Diesel (versus Gasoline) Powered Vehicles". In: *Environmental Science & Technology* 38.12 (2004), pp. 3217–3223.

[129] M. Zheng, G. T. Reader, and J. Hawley. "Diesel engine exhaust gas recirculation - a review on advanced and novel concepts". In: *Energy Conversion and Management* 45.6 (2004), pp. 883–900.

[130] P. Ortner et al. "MPC for a diesel engine air path using an explicit approach for constraint systems". In: *Computer Aided Control System Design, 2006 IEEE International Conference on Control Applications, 2006 IEEE International Symposium on Intelligent Control, 2006 IEEE*. Oct. 2006, pp. 2760–2765.

[131] P. Ortner and L. del Re. "Predictive Control of a Diesel Engine Air Path". In: *Control Systems Technology, IEEE Transactions on* 15.3 (2007), pp. 449–456.

[132] M. Huang et al. "Towards combining nonlinear and predictive control of diesel engines". In: *American Control Conference (ACC), 2013*. IEEE. 2013, pp. 2846–2853.

[133] M. Huang et al. "Rate-Based Model Predictive Controller for Diesel Engine Air Path: Design and Experimental Evaluation". In: *IEEE Transactions on Control Systems Technology* PP.99 (2016), pp. 1–14.

[134] T. Jimbo et al. "Predictive control for high-EGR SI engines without misfire via flow-based design". In: *Decision and Control (CDC), 2012 IEEE 51st Annual Conference on*. 2012, pp. 3771–3776.

[135] M. Kao and J. J. Moskwa. "Turbocharged diesel engine modeling for nonlinear engine control and state estimation". In: *Journal of dynamic systems, measurement, and control* 117.1 (1995), pp. 20–30.

[136] I. Kolmanovsky et al. "Issues in modelling and control of intake flow in variable geometry turbocharged engines". In: *Chapman and Hall CRC research notes in mathematics* (1999), pp. 436–445.

[137] C. F. Taylor. *The Internal-Combustion Engine in Theory and Practice: Combustion, Fuels, Materials, Design*. Vol. 2. MIT press, 1985.

[138] J. B. Heywood. *Internal Combustion Engine Fundamentals*. Vol. 930. Mcgraw-Hill New York, 1988.

[139] M. Herceg et al. "Multi-Parametric Toolbox 3.0". In: *Proc. of the European Control Conference*. `http://control.ee.ethz.ch/~mpt`. Zürich, Switzerland, July 2013, pp. 502–510.

[140] *MPC5644A Data Sheet: Advance Information (Rev.7)*. Freescale Semiconductor, 2012.

[141] E. F. Camacho and C. Bordons. *Model Predictive Control*. Vol. 2. Springer London, 2004.

[142] Y. Wang and S. Boyd. "Fast Model Predictive Control Using Online Optimization". In: *Control Systems Technology, IEEE Transactions on* 18.2 (Mar. 2010), pp. 267–278.

[143] S. Hovland, J. Gravdahl, and K. Willcox. "Explicit Model Predictive Control for Large-Scale Systems Via Model Reduction". In: *Journal of Guidance, Control, and Dynamics* 31.4 (2008).

[144] E. C. Kerrigan. "Robust constraint satisfaction: Invariant sets and predictive control". PhD thesis. PhD thesis, Cambridge, 2000.

[145] D. Q. Mayne, M. M. Seron, and S. Raković. "Robust model predictive control of constrained linear systems with bounded disturbances". In: *Automatica* 41.2 (2005), pp. 219–224.

[146] D. Q. Mayne et al. "Robust output feedback model predictive control of constrained linear systems". In: *Automatica* 42.7 (2006), pp. 1217–1222.

[147] C. Panos et al. "Dynamic optimization and robust explicit model predictive control of hydrogen storage tank". In: *Computers & Chemical Engineering* 34.9 (2010), pp. 1341–1347.

[148] K. Kouramas, C. Panos, and E. Pistikopoulos. "Algorithm for robust explicit/multi-parametric MPC in embedded control systems". In: *Proceedings of the 18th IFAC World Congress, Milan, Italy*. 2011.

[149] G. C. Goodwin et al. "Robust model predictive control: reflections and opportunities". In: *Journal of Control and Decision* 1.2 (2014), pp. 115–148.

[150] F. Tahir and I. Jaimoukha. "Robust feedback model predictive control of constrained uncertain systems". In: *Journal of Process Control* 23.2 (2013), pp. 189–200.

[151] S. Hovland et al. "Stability of model predictive control based on reduced-order models". In: *Decision and Control, 2008. CDC 2008. 47th IEEE Conference on*. IEEE. 2008, pp. 4067–4072.

[152] R. Fletcher. *Practical Methods of Optimization*. 2nd. India: Wiley, 2006.

[153] D. Limon et al. "Robust tube-based {MPC} for tracking of constrained linear systems with additive disturbances". In: *Journal of Process Control* 20.3 (2010), pp. 248–260.

[154] S. Rakovic. "Robust control of constrained discrete time systems: Characterization and implementation". PhD thesis. University of London, 2005.

[155] L. Chisci, J. Rossiter, and G. Zappa. "Systems with persistent disturbances: predictive control with restricted constraints". In: *Automatica* 37.7 (2001), pp. 1019–1028.

[156] S. V. Rakovic et al. "Invariant approximations of the minimal robust positively invariant set". In: *IEEE Transactions on Automatic Control* 50.3 (2005), pp. 406–410.

[157] P. V. Kokotovic, R. O'malley, and P. Sannuti. "Singular perturbations and order reduction in control theory - An overview". In: *Automatica* 12.2 (1976), pp. 123–132.

[158] E. F. Camacho and C. B. Alba. *Model Predictive Control*. Springer Science & Business Media, 2013.

[159] D. Hyland and D. Bernstein. "The optimal projection equations for model reduction and the relationships among the methods of Wilson, Skelton, and Moore". In: *IEEE Transactions on Automatic Control* 30.12 (1985), pp. 1201–1211.

[160] W.-Y. Yan and J. Lam. "An approximate approach to H/sup 2/optimal model reduction". In: *IEEE Transactions on Automatic Control* 44.7 (1999), pp. 1341–1358.

[161] T. Bui-Thanh, K. Willcox, and O. Ghattas. "Model reduction for large-scale systems with high-dimensional parametric input space". In: *SIAM Journal on Scientific Computing* 30.6 (2008), pp. 3270–3288.

[162] G. B. Folland. *Real Analysis: Modern Techniques and Their Applications*. 2nd. Singapore: Wiley, 1999.

[163] C. W. Curtis. *Linear Algebra: An Introductory Approach*. New York, NY: Springer, 1984.

[164] S. V. Raković et al. "Homothetic tube model predictive control". In: *Automatica* 48.8 (2012), pp. 1631–1638.

[165] S. V. Rakovic et al. "Parameterized tube model predictive control". In: *IEEE Transactions on Automatic Control* 57.11 (2012), pp. 2746–2761.

[166] M. Diehl, H. J. Ferreau, and N. Haverbeke. "Efficient numerical methods for nonlinear MPC and moving horizon estimation". In: *Nonlinear model predictive control*. Springer, 2009, pp. 391–417.

[167] R. Ghaemi, J. Sun, and I. V. Kolmanovsky. "An integrated perturbation analysis and sequential quadratic programming approach for model predictive control". In: *Automatica* 45.10 (2009), pp. 2412–2418.

[168] L. Del Re et al. *Automotive model predictive control: models, methods and applications*. Vol. 402. Springer, 2010.

[169] A. Birouche, B. Mourllion, and M. Basset. "Model order-reduction for discrete-time switched linear systems". In: *International Journal of Systems Science* 43.9 (2012), pp. 1753–1763. eprint: `http://dx.doi.org/10.1080/00207721.2011.554911`.

[170] P. Benner and T. Damm. "Lyapunov equations, energy functionals, and model order reduction of bilinear and stochastic systems". In: *SIAM journal on control and optimization* 49.2 (2011), pp. 686–711.

[171] O. Nilsson. "On modeling and nonlinear model reduction in automotive systems". PhD thesis. Lund University, 2009.

[172] K. Fujimoto and J. M. Scherpen. "Nonlinear balanced realization based on singular value analysis of Hankel operators". In: *Decision and Control, 2003. Proceedings. 42nd IEEE Conference on*. Vol. 6. IEEE. 2003, pp. 6072–6077.

[173] T. Broomhead et al. "Model Reduction of Diesel Mean Value Engine Models". In: *SAE 2015 World Congress & Exhibition*. SAE International, Apr. 2015.

[174] T. J. Broomhead. "A Model Based Approach to the Control of Diesel Generators". In: (2016).

[175] F. Lewis, D. Vrabie, and V. Syrmos. *Optimal Control*. Wiley, 2013.

[176] M. Schlegel et al. "Projection based model reduction for dynamic optimization". In: *AIChE Annual Meeting. Indianapolis*. 2002.

[177] S. Chaturantabut and D. C. Sorensen. "Discrete Empirical Interpolation for nonlinear model reduction". In: *Proceedings of the 48h IEEE Conference on Decision and Control (CDC) held jointly with 2009 28th Chinese Control Conference*. Dec. 2009, pp. 4316–4321.

[178] S. Chaturantabut and D. C. Sorensen. "Nonlinear model reduction via discrete empirical interpolation". In: *SIAM Journal on Scientific Computing* 32.5 (2010), pp. 2737–2764.

[179] J. Hahn and T. F. Edgar. "A gramian based approach to nonlinearity quantification and model classification". In: *Industrial & engineering chemistry research* 40.24 (2001), pp. 5724–5731.

[180] C. Himpe and M. Ohlberger. "A Unified Software Framework for Empirical Gramians". In: *Journal of Mathematics* 2013 (2013), pp. 1–6.

[181] M. Soroush and H. M. Soroush. "Long-prediction-horizon nonlinear model predictive control". In: ed. by B. Kouvaritakis and M. Cannon. IET, 2001. Chap. 9, pp. 189–202.

[182] Y. Gao et al. "Robust nonlinear predictive control for semiautonomous ground vehicles". In: *American Control Conference (ACC), 2014*. June 2014, pp. 4913–4918.

[183] M. Krstic and A. Smyshlyaev. *Boundary Control of PDEs: A Course on Backstepping Designs*. Vol. 16. Siam, 2008.

[184] K. Yasuda and R. E. Skelton. "Assigning controllability and observability Gramians in feedback control". In: *Journal of Guidance, Control, and Dynamics* 14.5 (1991), pp. 878–885.

[185] L. Pavel and F. W. Fairman. "Controller Reduction for Nonlinear Plants - an L_2 Approach". In: *International Journal of Robust and Nonlinear Control* 7.5 (1997), pp. 475–505.

[186] J. Sjöberg. "Optimal control and model reduction of nonlinear DAE models". PhD thesis. Institutionen för systemteknik, 2008.

[187] P. D. Christofides. *Nonlinear and Robust Control of PDE Systems: Methods and Applications to Transport-Reaction Processes*. Boston, MA: Birkhauser, 2000.

[188] F. Blanchini and S. Miani. *Set-theoretic methods in control*. Springer Science & Business Media, 2007.

[189] R. Ghaemi, I. V. Kolmanovsky, and J. Sun. "Robust control of linear systems with disturbances bounded in a state dependent set". In: *IEEE Transactions on Automatic Control* 56.7 (2011), pp. 1740–1745.

[190] F. Scibilia, S. Olaru, and M. Hovd. "On feasible sets for MPC and their approximations". In: *Automatica* 47.1 (2011), pp. 133–139.

[191] N. Fenichel. "Geometric singular perturbation theory for ordinary differential equations". In: *Journal of Differential Equations* 31.1 (1979), pp. 53–98.

[192] G. I. Kalogeropoulos et al. "The Weierstrass Canonical Form of a Regular Matrix Pencil: Numerical Issues and Computational Techniques." In: *Numerical Analysis and Its Applications*. Springer. 2008, pp. 322–329.

[193] C. L. Phillips and H. T. Nagle. *Digital Control System Analysis and Design*. Prentice Hall Press, 2007.

[194] C. K. Chui and G. Chen. *Discrete H_∞ Optimization: With Applications in Signal Processing and Control Systems*. Vol. 26. Springer Science & Business Media, 2012.

[195] Y. Y. Wang, S. J. Shi, and Z. J. Zhang. "A descriptor-system approach to singular perturbation of linear regulators". In: *IEEE Transactions on Automatic Control* 33.4 (Apr. 1988), pp. 370–373.